WET GAS METERING

by

RICHARD STEVEN BEng MSc

A THESIS SUBMITTED FOR THE DEGREEE OF
DOCTOR OF PHILOSOPHY

UNIVERSITY OF STRATHCLYDE
DEPARTMENT OF MECHANICAL ENGINEERING
GLASGOW, UK
APRIL 2001

Abstract

Wet Gas Metering is becoming increasingly important to the Oil and Gas Industry. In this research a wet gas flow is defined as a liquid / gas two-phase flow that has a gas mass content greater then 50 %. The Venturi Meter is a favoured wet gas meter in the Oil and Gas Industry. However, industry's understanding of wet gas flow phenomena in such a meter is limited and is therefore forced to accept large metering errors when existing correlations are used to take account of the liquid presence. Furthermore, these correlations all require an input value for the liquid flowrate. This information is not readily available to natural gas production engineers. This research extensively discusses the current wet gas metering situation and then uses new independent data from the NEL Wet Gas Loop to compare the performance of existing correlations when used with a Venturi Meter. This new data is examined to determine parameters that effect the meter reading and then new correlations are presented. One new correlation offered uses the additional information from a downstream pressure tapping in conjunction with the traditional upstream pressure reading and the Venturi pressure differential to predict the gas flowrate without knowledge of the liquid flowrate.

In Memory of My Friend

Colin Dickie

Contents

Abstract

Acknowledgements

Contents

Nomenclature

<u>Nomenclature</u>

<u>English Language Symbols</u>

A The area of the Venturi Meter inlet.

A_t The area of the Venturi Meter throat.

d The Root Mean Fractional Deviation.

d   The Orifice Plate Meter throat diameter.

D   The Orifice Plate Meter inlet pipe diameter.

DP2/DPtp   The ratio of the two-phase upstream to downstream differential pressure and the two-phase upstream to throat differential pressure.

Eu The Euler Number.

Fr_g The Gas Densiometric Froude Number.

g The gravitational constant.

K_g and K_l The gas and liquid flow coefficients. (Excludes the velocity of approach.)

K_g^* The gas flow coefficient for the throat to downstream flow. (Includes the velocity of approach.)

M The gradient of the best linear fit line on a Murdock Graph.

$\dot{m}_g$ The gas mass flowrate.

$\dot{m}_{uncorrected}$ The mass flowrate erroneously predicted by a Differential Pressure Meter if no correction is included for the effect of liquid presence in a gas flow.

$\dot{m}_{g(experimental)}$ The gas mass flowrate measured by the dry gas reference turbine meter.

$\dot{m}_{g(predicted)}$ The gas mass flowrate predicted by the particular correlation in question is used to correct for the effect of the liquid presence.

$\dot{m}_l$ The liquid mass flowrate.

$\dot{m}_{uncorrected}$ The mass flowrate erroneously predicted by a Differential Pressure Meter if no correction is included for the effect of liquid presence in a gas flow.

P The Pressure

$\dot{Q}_g$ The gas volumetric flowrate.

$\dot{Q}_l$ The liquid volumetric flowrate.

$\dot{Q}_{tp}$ The two-phase volumetric flowrate.

Re_g The superficial gas flow Reynolds Number.

Re_l The superficial liquid flow Reynolds Number.

U_g The average gas velocity.

U_l The average liquid velocity.

U_{sg} The superficial gas velocity.

U_{sl} The superficial liquid velocity.

We The Weber Number.

x The flow quality, i.e. the ratio of the gas mass flow to the total mass flow.

Y_g The gas expansibility coefficient.

Greek Language Symbols

ΔP_2 The dry gas upstream to downstream differential pressure.

$\Delta P2$ The wet gas upstream to downstream differential pressure.
         pressure tappings.

ΔP_g The superficial gas differential pressure between the upstream and throat pressure tappings.

ΔP_g^* The superficial gas flow differential pressure between the throat and downstream tapping.

ΔP_l The superficial liquid differential pressure between the upstream and throat pressure tappings.

ΔP_{ol} The liquid differential pressure between the upstream and throat pressure tappings which would be read if all the two-phase flow mass flowed as liquid.

ΔP_t	The dry gas upstream to throat differential pressure.
ΔP_{tp}	The two-phase differential pressure between the upstream and throat pressure tappings.
ΔP_{tp}^{*}	The two-phase differential pressure between the throat and downstream
μ_g	The gas viscosity.
μ_l	The liquid viscosity.
v_g	The specific volume of the gas flow.
$v_{homogenous}$	The specific volume of a homogenous two-phase flow.
v_l	The specific volume of the liquid flow.
$\rho_{homogenous}$	The density of a homogenous flow.
ρ_g and ρ_l	The gas flow and liquid flow densities respectively.
σ_l	The liquid surface tension.

"Wet Gas Metering" is a subject that is becoming increasingly important to the Oil and Gas Industry. The term "wet gas" has no official definition but the companies in the natural gas production industry all agree that the term denotes a relatively small amount of liquid in a production natural gas flow. Such flows are becoming increasingly common in this industry due to the following two reasons. Firstly, as a dry natural gas well ages the flow conditions slowly change and these changes, which invariably include a reduction in line pressure, result in the heavier hydrocarbon gases condensing in the pipeline. Therefore, as many gas wells world-wide are now coming to the later stages of their production life wet gas metering is becoming increasingly important. Secondly, with the industry eager to maximise the return on the off-shore platform investment, many natural gas producers (often called "operators") are developing "marginal" fields (i.e. fields that produce two-phase flows of natural gas with sea water and / or natural gas condensate from the outset). These marginal fields are having their wet natural gas production flows combined with the main wells dry or wet natural gas production flow upstream of the separator facilities. Hence, here again there is a demand for wet gas metering.

The excepted dry natural gas production metering standards of the operators is to meter the gas flowrate to within 1%. There is no single accepted way to meter wet gas flows but currently none of the available wet gas metering systems can achieve this standard. Of the various meters available to industry the natural gas production industry based in the North Sea strongly favours the use of Differential Pressure Meter and Ultrasonic Meter types. Traditionally, the Orifice Plate Meter was used by the industry for all two-phase flows but more recently the Venturi Meter has become the Differential Pressure Meter of choice while the Transient Time Ultrasonic Meter has been developed as a viable alternative. There is considerable rivalry between the manufacturers of these meter types but so far neither of these meter types has shown a distinct advantage over the other. What is clear is that both meter types offer a far from perfect solution to the industrial problem of wet natural gas metering. A great deal of development needs to be carried out on all existing wet gas meters if the metering standards desired by the industry are to be met (i.e. the same standards as

dry natural gas metering). Hence, this topic offers great scope for an industrial relevant PhD.

One of the greatest problems in wet natural gas metering is the lack of knowledge of the liquid content in wet natural gas flows. All the published papers that discuss methods of correcting either the Differential Pressure Meter or the Ultrasonic Meter errors caused by the liquid presence require the quantity of liquid flowing to be initially known in order to calculate the gas mass flowrate. So far, no wet gas metering technique for any meter type comes anywhere near the industry's desired standards for metering the liquid and gas phase flowrates simultaneously.

Traditionally, the greatest difficulty in developing any wet natural gas metering technique was the lack of any suitable test apparatus. That is, with the operators not willing to allow meter tests on actual production flows, due to the potential financial penalties involved with any resulting production delays, meter manufacturers have to test meters on wet gas test loops. A major problem with this was that the test equipment available round the world was unable to replicate the flow conditions found in wet natural gas production lines. These conditions vary widely from well to well. Wet gas production wells exist round the world for pressures of 5 Bar to in excess of 1000 Bar, 250 K to in excess of 400K, gas flow rates of 500 m^3/hr to in excess of 3000 m^3/hr and typical pipe diameters at the natural gas metering skids are four, six and eight inch pipes. The Oil and Gas Industry encounters the full range of two phase flow qualities but typically "wet gas" flows are considered to have a greater mass of gas flowing than liquid. Furthermore, it should be noted that just as there is no one common set of flow conditions for natural gas production there is also no one common position for the placement of the meter in production installations. Due to various production difficulties meters are often installed in any convenient length of pipe regardless of the dry gas metering standards. Hence, there is no one typical flow condition and metering position which a test rig should attempt to replicate. However, prior to this research the available wet gas test rigs were only capable of reaching the lower ends of this desired flow condition range.

At the outset of this project the NEL was in the process of designing a Wet Gas Loop to improve this situation and allow meters to be tested in wet gas conditions that more closely resembled those found in actual wet natural gas production flows.

The proposed project offered by the NEL was to initially aid with the design of this Wet Gas Loop and then to conduct any experimental wet gas metering research (with use of the Wet Gas Loop) that the researcher saw fit.

During the design of the NEL Wet Gas Loop the meter manufacturer ISA Controls Ltd. subsequently sponsored this research project by the supply of a six-inch Venturi (of beta ratio 0.55) manufactured to the standard specification of the operators. This standard Venturi Meter included the downstream pressure tapping common in Venturi Meters manufactured for the natural gas industry in recent years. Henceforth, the project was aimed at investigating and improving the performance of Venturi Meters in wet gas flows.

The project objectives were therefore set as follows. Firstly, the project would aid the design of the new NEL Wet Gas Loop while an in-depth review of wet gas metering technology was conducted. This review was to identify the existing Differential Pressure Meter wet gas correlations. Then with the new independent wet gas data obtained by this research during the commissioning of the NEL Wet Gas Loop the first independent comparison of these existing correlations would be made. Trends in the data were to be searched for and a new improved wet gas correlation would be created specific to the industrially popular six inch, 0.55 Beta ratio Venturi Meter. Finally, with all the existing Differential Pressure Meter correlations requiring the liquid flowrate to be initially known in order to find the gas flowrate, an investigation into weather the extra information gained from a downstream pressure tapping could allow the gas flowrate to be calculated without prior knowledge of the liquid flowrate was to be conducted.

Therefore, this thesis first discusses the background history of wet gas metering before going on to describe the new NEL Wet Gas Loop. The wet gas Venturi Meter tests are then discussed before the results are used to compare the performances of all the existing Differential Pressure Meter two-phase correlations that were judged by this project to be of relevance to wet natural gas metering. Then careful examination of this new independent data for any physical phenomena of note that should be accounted for in the forming of new correlations was undertaken. A new correlation is then developed. Finally, the problem of metering the gas flowrate when the liquid flowrate is unknown is discussed and a method for achieving this goal is offered

which makes use of the upstream to downstream differential pressure reading across the Venturi Meter as well as the traditional upstream to throat differential pressure reading.

2.1) The Industrial Necessity for Improved Wet Gas Metering Performance

Wet Gas Metering is a topic that has become more important to industry in recent years. However, the term "Wet Gas" does not have an accepted definition throughout the different industries which deal with two-phase or multi-phase flows and indeed there is even ambiguity between different organisations within the same industry! The loose definition that is agreed on is that "Wet Gas" states the existence of relatively small volumes of liquid in a gas flow.

Even though a general need for two-phase flow measurement has been required since the last century it is only in the last thirty years that any comprehensive attempts have been made to form a measurement method that would be universally accepted. Up until the early 1960's (when the flow of liquid-gas mixtures was common place) there was no accepted methods published that an engineer could use. All that could be done was to treat the two-phase flow as homogenous (i.e. take the mean density of the mixture) and use single-phase measurement methods. This practice is neither theoretically correct nor accurate over the full range of two-phase flows.

Since the early 1960's there has been a number of papers published on two-phase pipe flow measurement that have been accepted by industry. However, the fact that two-phase flow takes into account such a wide range of conditions (e.g. flow quality, line pressures, pipe diameter and inclination, fluid properties etc.) means that the various preferred correlations have specific ranges and restrictions on their use. Therefore, for practical industrial purposes extrapolations and / or assumptions are often required that have little or no scientific backing. Furthermore, most correlations published to date all have the same serious shortcoming that restricts their use. That is, they assume from the outset that either the total mass flow or the flow quality (the gas mass flow to total mass flow ratio) is known and the correlation then gives the required unknown parameter. This is satisfactory for situations such as closed loop cycles were the total mass of the flows combined phases is known (e.g. steam/water in a power station), but there are cases when neither of these parameters are known (e.g.

geothermal wells or wet natural gas pipelines) and for these cases a method of determining one of these parameters is required before the correlations can be used.

It is in the North Sea Oil and Gas Industry that serious consideration is now being given to improving the methods for measuring wet gas flow. The two main reasons for this increasing interest are as follows:

Firstly, some gas fields that started operational life producing natural gas with no condensate have now degraded and a small amount of gas condensate is now adding to any existing liquid (i.e. water) in the pipeline. If no water was initially present a dry gas metering condition has now become a wet gas metering condition. If water was initially present then the presence of condensates means that the total amount of liquid in the pipeline may exceed the design condition for that platform and the existing separator may therefore become undersized. This is a common non-standard condition in an unprocessed natural gas measurement operation between well-heads and the processing plants. Since it is important that the actual amount of gas produced by a well is known for fiscal metering purposes (various gas wells owned by different companies selling gas at different rates use communal pipelines to shore) and so that the well owner can make an informed decision on the well's productivity a reliable method of measuring the wet gas flow is greatly desired.

Secondly, several small marginal gas fields (i.e. small fields which would produce wet gas from the outset) are known to exist in the North Sea. Whereas it is traditionally the case that each main or satellite platform should have its own facilities it is clear that these small marginal fields would need to share facilities with existing platforms in order to be financially viable. This is due to these new reserves being small and therefore not profitable if each needs its own platform. By sharing facilities with existing gas fields costs can be greatly reduced and marginal fields made worthy of development while increasing the life and therefore the profitability of older existing platforms. However, as the current method of measuring gas flows from a wet gas well is to pass the flow through a separator on the platform and then to a single-phase gas meter a problem arises when two separate wells have their flows mixed prior to the separator. That is, what proportion of the gas comes from each well? This is important information when the two wells belong to the same

organisation and they want to assess the productivity of the individual wells in order to make an informed decision on their individual profitability or perhaps one of the wells has a dedicated customer. This is a buyer that has a legal right to purchase the gas from a particular well at a set price. Furthermore if the wells do not belong to the same organisation an accurate measurement of their individual flows before their mixing upstream of the communal separator is vital. This is therefore one of the reasons why improvements in the accuracy of wet gas metering is important to the Oil and Gas Industry. It was stated by Nederveen (of NAM[1]) [1] that if the need for bulk separators on off shore platforms was removed then significant savings could be made. Each such bulk separator is estimated to cost £20 million during its life span but as they are currently an integral part of platform design the actual savings possible is as yet unknown. (NAM went on to say that an accurate wet gas meter could also do away with on shore separators at wet gas fields, a saving of $500,000 each). It is clear however that the potential saving could reduce the capital cost of developing a marginal well enough to make the well financially viable.

Currently, due to the engineers present inability to measure wet gas flow as accurately as single-phase flow, the wells that do already share facilities have greater uncertainties in their gas flow measurements. An example of a current situation in which there is an overall increase in gas measurement uncertainty due to the requirement to meter upstream of the separator is given by Stobie [2]. Similar schematic diagrams to those of Stobie are offered on page 7 which clearly show the need for more reliable wet gas meters. Figure 2.1 shows the traditional case of one separator for one well. It is in this case that separator undersizing would lead to the requirement for wet gas metering at the sales meter. Figure 2.2 shows what happens if a new marginal well (well 2) is operated by use of the infrastructure of an existing well (well 1). It is clear that in this situation, to find the percentage of gas from each well, metering must take place before the communal pipeline to the separator.

It is therefore necessary for all parties involved in the North Sea Gas Industry to accept that everyone will have a greater exposure to metering errors in these wet gas metering situations but this is the only way to develop otherwise uneconomic

---

[1] "NAM" stands for Nederlandse Aardoliemaatschappij, the Dutch natural gas production company.

reserves. Therefore any improvement in the accuracy of wet gas metering will reduce this exposure to greater metering errors and make the sharing of off-shore facilities more attractive to all the relevant parties.

Traditional Situation
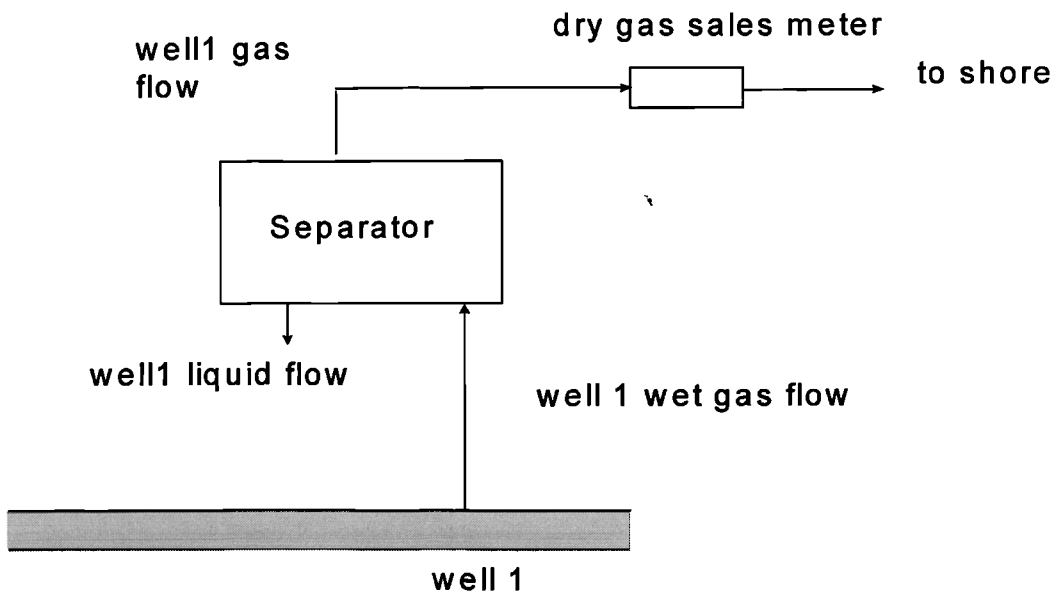
Figure 2.1 The Traditional Single Well / Single Separator Case.

Marginal Field (Well 2) Addition
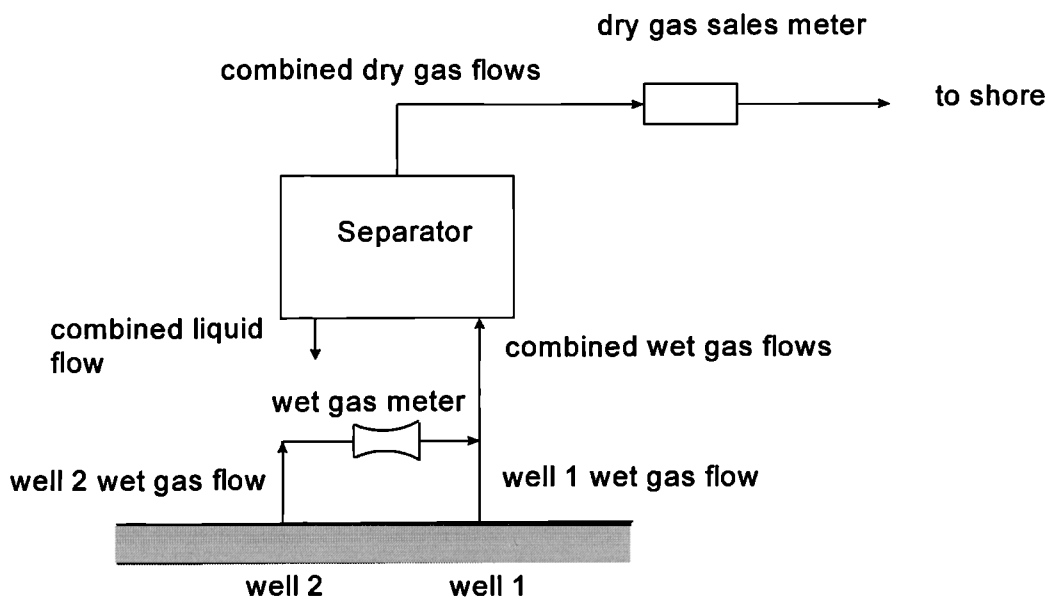
Figure 2.2 The Combined Well / Single Separator Case.

2.2) How is "Wet Gas" Defined by Industry?

The first step in investigating Wet Gas Metering is to understand what the various Oil and Gas Companies, Academics and Meter Manufacturers consider "Wet Gas" to be. There is no standard definition for the term "Wet Gas" that is accepted by industry. As stated earlier the only general agreement seems to be that the term "Wet Gas" states the existence of a relatively small volume of liquid in a gas flow. As a result of this there are a number of definitions which can be used by (or imposed on) an engineer.

Much of the work published on the subject of Two-Phase Measurement to date does not mention the term "Wet Gas" specifically. Indeed correlations currently used in conjunction with differential pressure meters to measure flows that the pipeline operators would all call wet gas flows, were not derived with "Wet Gas " specifically in mind but a much wider range of flow conditions. Some of the more recent papers published by the Oil & Gas companies state what liquid content is being found in the various wells but the bulk of the academic papers simply state the range of beta (β) values tested (i.e. gas volume flowrate to total volume flowrate) with no mention of why this range was selected.

In a paper on the practicalities of Wet Gas Metering in the North Sea Stobie[2] of Phillips Petroleum addressed this problem. He quotes one gas pipeline operator as saying "if gas has one pound mass of liquid per one million cubic feet of gas per day at standard atmospheric conditions (mmscfd)[2] or more then it is wet". This means that at standard atmospheric conditions the volume ratio of liquid flow to total flow ($1-\beta$), is $1.4*10^{-8}$. He goes on to say that other pipeline users say that the gas is wet if there is more than five barrels of liquid (1 barrel = 42 US gallons) to one mmscfd of gas, which is a liquid volume to total volume ratio ($1-\beta$) of 0.000028 and that a recent wet gas ultrasonic meter project defined wet gas as one where the liquid content was more than "0.1% by volume". At standard atmospheric conditions this represents some 180 barrels of liquid per mmscfd or in other words 5600 cubic feet of liquid per mmscfd.

---

[2] The standard unit for gas flow in the Oil & Gas Industry is one million cubic feet at standard atmospheric conditions per day, (mmscfd).

However, Stobie claims that from the general trend of wet gas definitions this quantity of liquid per quantity of gas seems far too high to be considered a reasonable wet gas definition and is more like a standard multi-phase flow. The final word given was that he believes the gas to be wet if it contains ten barrels or more of liquid per mmscfd, which is a liquid volume to total volume $(1-\beta)$ value of 0.000056 at standard atmospheric conditions.

Of the papers published that talk of the actual liquid quantity (or "loading") found in the gas pipelines of the Oil & Gas Industry there are...

a) Washington [3] states "... the range of liquid/gas ratios found in most producing gas fields is limited to 500 cubic metres of liquid to 1 mmscfd of gas". This is a liquid to gas ratio (LGR) of $5*10^{-4}$. The beta ratio (β) is 99.95% and therefore liquid volume to total volume $(1-\beta)$ is 0.05% at standard atmospheric conditions.

b) Jamieson [4], lists a "high liquid loading" as 91.5 cubic metres of liquid to 1 mmscmd (i.e. a liquid volume flowrate to total volume flowrate of 0.009% at standard atmospheric conditions) and a "medium liquid loading" as 73.4 cubic metres to 1mmscmd (i.e. a liquid volume flowrate to total volume flowrate of 0.007% at standard atmospheric conditions).

c) Nederveen et al. [1] "...typical NAM conditions are 8-10 MPa and a LGR lower than 200 cubic metres per 1 mmscfd." Also "In normal production a gas well will rarely exceed a liquid/ gas ratio of 400 cubic metres of liquid per 1mmscfd of gas." However, NAM also tell of a need to measure wet gas at smaller liquid flows when they say "... because of undersizing of the separation equipment on one of the satellites liquid is carried over into the export gas resulting in a LGR of 15 to 20 cubic metres per 1 mmscfd of gas".

d) Another published paper that discusses the range of Wet Gas directly is by R. de Leeuw [5]. Here the author states the typical conditions found at Coevorden (a wet gas field in The Netherlands) as "...natural gas at pressures of around 90 bar and liquid fractions of up to 4% by volume...". So the liquid volume flowrate to total volume flowrate at the line pressure is 3.846%. There is not enough information given on the particular gas properties to calculate the equivalent ratio for the gas at standard atmospheric conditions. However, it can be seen from the test envelope that the range

tested was a liquid volume flowrate to total volume flowrate $(1-\beta)$ from 0.1% down to 0%.

Of the papers published about work done on wet gas using test apparatus the papers that directly refer to the relevant range are the following:

e) Wilson [6, 3]) refers to an Ultrasonic Wet Gas Development Project set up to develop an Ultrasonic Meter that is commercially acceptable for dry gas flows into an acceptable wet gas meter for "humid gas containing small, < 0.1% by volume, free liquids". At the operating line pressure this is an approximate liquid volume to total volume of 0.01%.

f) McCrometer [7 ,8], the manufacturer of the V-Cone Meter, tested their meter for wet gas performance and chose a range of up to 5% of liquid by mass. As the test fluids were water and air and the test pressures were given it can be calculated that the tests were done for the range of liquid volume flowrate to total volume flowrate $(100-\beta)$% of 0 % to 0.0458% at standard atmospheric conditions. This therefore indicates the range McCrometer considers to be "Wet Gas".

In general however, most of the published papers that deal with the problem of small amounts of liquid in a gas flow do not give any definition of wet gas and nor do they give any reasons for their chosen range. The majority of the papers listed as references use steam/water or air/water as the working fluids and the ratios of liquid to gas are given in terms of quality "x" (the gas mass flow to the total mass flow). The problem for the engineer investigating "wet gas" conditions is that the ranges of quality in these papers are often too low to be considered "wet gas". It could therefore be deduced from this literature review, conducted in 1998, that the Oil & Gas Industry consider the relevant range of liquid volume flowrate to total volume flowrate $(1-\beta)$ for investigating wet gas effects on fluid meters in use in the North Sea Gas Fields to be around 0.005 % $\leq$ $(100-\beta)$ % $\leq$ 0.05%, with most of the normal operations being at the lower end of this range.

However, in the last two years some operators have been declaring "wet gas" to include two-phase flows of much greater liquid content. In particular Shell Expro now internally define wet gas to be all two-phase flows of Gas Volume Fractions greater than 95% (i.e. GVF>95%). They claim that for natural gas well conditions this

loosely equates to a maximum liquid content of equal mass flows of liquid and gas. With all the above information taken into account it was decided that this research would define "Wet Gas" to be all two-phase flows with a Gas Volume Fraction greater than 95% at actual conditions. It is noted however, that most of the actual wet gas flows in the natural gas production industry are in the upper end of this range.

2.3) Wet Gas Fluid Types

So far the type of liquid flowing in the pipeline has not been discussed. In reality each well has an unique combination of liquids. The mix is made up of salt water (drawn into the pipe from the well), gas condensate (i.e. both hydrocarbon liquids drawn in from the well with the natural gas and condensate formed by the heavier hydrocarbon gases condensing in the pipeline due to the pressure drop) and a liquid injected into the pipeline to prevent the formation of hydrates (usually glycol or methanol). Nederveen [1] states that there are no significant differences between the effects of water and condensate on the differential pressure meter. Conformation of this would make the work of wet gas meter researchers much easier but although all the liquids can be considered incompressible their different fluid properties suggest it is possible that different flow patterns can exist for the different fluid combinations at similar flow conditions (i.e. line pressure and temperature, pipe diameter, gas flowrates etc.). This author therefore considers it more accurate to say that for a given flow pattern there are no significant differences between the effects of different liquid flows. For this reason, during the design of the NEL Wet Gas Loop, this author made a study of the possible test fluids to ensure a similar flow pattern to that which exists in real natural gas production lines (see Appendix 1).

12

2.4) The Current Metering Situation on Wet Natural Gas Fields

In order to review the current state of wet gas metering in industry it is necessary to understand the current methods used to measure single phase natural gas flows and some of the practical problems that arise on the gas field location.

The types of meters being currently used in the North Sea Oil and Gas Industry to measure unprocessed natural gas flows are the two differential pressure devices: Orifice Plates and Venturi Meters, and more recently Ultrasonic Meters. (Other meter types such as Coriolis, Vortex and Turbine Meters are not considered by the operators for unprocessed natural gas production metering and hence there is virtually no literature on these meters performance in unprocessed natural gas production flows.) The vast majority of the work done on general two-phase metering using differential pressure devices has been on Orifice Plate Meters (with only a little of this work using data in the wet gas range) and only in the last few years has any useful work on Venturi Meters in wet gas existed at all. Although both are still used, the industry now tends towards the more expensive Venturi Meter, probably because orifice plates are more susceptible to damage by either the intermittent "slugs" in the pipeline or pressure pulses and not so much for the reduction of total head loss the Venturi offers over the Orifice Plate. In reviewing the methods currently in use to attempt to meter wet natural gas flows it is necessary to understand the fundamental principles behind the design and applications of single phase natural gas meters as all the methods for wet natural gas corrections start from here. It is assumed here the reader understands single-phase metering technologies.

2.4.1) Differential Pressure Meters and the Production of Dry Natural Gas

Of the four Differential Pressure Meters available only the Orifice Plate and Venturi Meter are in widespread use for unprocessed natural gas metering. The V-Cone (a patented device designed and manufactured by McCrometer Ltd.) is not in general use due to it being a relatively new meter on the market and it is therefore largely untested (and not considered) by many industries. The reason for the exclusion

of the Nozzle Meter is not stated in any Oil and Gas Industry papers. It appears to be a tradition amongst operators to ignore the nozzle meter.

The Orifice Meter is the original DP Meter and has always been used by industry and as in every heavy industry once something is tried and tested the design mentally sticks. It is also the case that a huge amount of research has been carried out and much data has been collected for Orifice Plate Meters. Hence the cheap and simple Orifice Plate is still in use. However, dry or wet natural gas wells never flow smoothly all the time and periodic slugs (liquid plugs in a gas flow) and pressure pulses can strike the Orifice Plate causing substantial damage. In fact Ting [12] examines the operational ability of bent Orifice Plates. It is a common practice in the Oil and Gas Industry to remove Orifice Plates to check for damage every month or so when the meter is easily accessible. (It should be noted here that these slugs and pressure pulses are the reason Turbine Meters are not used in unprocessed natural gas production lines. Ting and Jones Jr. [13] state that "the damage to turbine meters in this service would be unacceptable" hereby explaining why these accurate single-phase meters are not used offshore for unprocessed natural gas measurement applications. This is unfortunate as these authors found the turbine meter more accurate in wet gas metering than the Orifice Plate Meter.) However, although the Orifice Plate is sturdier than the turbine meter it is still susceptible to damage and the awkwardness of access to the meter for repair in many offshore installations means a sturdier meter than the Orifice Plate Meter is desirable. The Nozzle and Venturi Meters are both considered sturdier due to their geometrical shape, the full force of the oncoming slug or pressure pulse is assumed to be largely deflected by the converging inlet. (Incidentally, unlike Orifice Meters the Oil and Gas Industry does not check the condition of their Venturis, once they are installed they are left.) Thus, for sturdier meters the choice is only between Nozzles and Venturis. However, another characteristic between the different DP Meters is their difference in total head (pressure) loss.

The Orifice Meter, being the simplest (and therefore cheapest) meter to manufacture, is associated with a relatively large total head loss due to the uncontrolled nature of the flow. The relatively large re-circulation zones both upstream and downstream of the orifice plate causes large viscous forces and hence a

relatively large amount of energy dissipation. The Nozzle Meter is far more difficult and expensive to manufacture but has a smaller head loss than the Orifice Plate Meter due to the control of the flow at the inlet (i.e. there is no re-circulation zone upstream of the nozzle). The Venturi Meter is the most difficult and expensive meter to manufacture but has by far the smallest head loss due to the diffuser vastly reducing the re-circulation downstream of the pressure tappings. This head loss is not of real importance to the Oil and Gas Industry until the total head available is not enough to drive the gas alone. Then the expenditure of pumping makes head loss extremely important. In practice in the North Sea Oil and Gas Industry the well pressures are so high the pressure drop differences are often irrelevant. It appears that the Orifice Plate Meter is used by tradition and more recently the Venturi Meter has been increasingly used to increase the sturdiness of the meters. The Nozzle Meter is not used, again due to tradition rather than due to any practical reasons. Interestingly enough however, some engineers are now beginning to believe that under some flow conditions the nozzle may have a distinct advantage over the more expensive and favoured Venturi. The Venturi Standards (ISO 5167-1 i.e. [9]) state that the converging duct and the throat section must be blended by a specified radius "R_2" (where $R_2 = 3.625d$ +/- $0.125d$). This is not as smooth as a nozzle entrance to the throat which is smoothly blended so that for lower Reynolds Number flows the Venturi can have separation and a re-circulation zone at the pressure tapping points in the throat that the Nozzle does not. This means there could be a greater error in a Venturi Meter than a Nozzle Meter. Hence, this is a reason for attaining much more detailed data on Venturis to get accurate values of discharge coefficients over a range of flow conditions. However, it should be noted here that, at the higher Reynolds Number flows typical of natural gas flows, flow separation in the Venturi is not considered a great problem. As it is a problem more prevalent at lower Reynolds Number gas flows, Venturis are seen to be as suitable as Nozzles at these high Reynolds Numbers and they have the added advantage of allowing extra pressure readings to be made in the diffuser. It will be shown by the following research that this extra information is of great advantage to the wet gas flow metering engineer.

For all DP Meters there are some operational problems that are common to them all. It should be noted that none of the wet gas papers published mention the fact that there are errors involved in even single phase gas flow measurements (e.g. it has been known for some time that there is an error caused by different diameters of pressure tappings in single phase flow as they have different effects on the flow near them. Such phenomena are discussed by Shaw [14]. However, although no paper has yet explicitly stated it, it is clear that all the investigators of wet gas metering assume that the single phase gas measurement of that particular meter is the true actual gas flow in order that a distinction between wet gas errors and other errors can be made.

Hence, it can be concluded that due to the practicalities of the flow conditions that exist in natural gas production pipelines and due to the metering traditions of the operators the current favoured differential pressure meter is the Orifice Plate with a slow change now occurring to the Venturi. The proper use of Venturis to meter dry gas flows involves complying to the ISO standards [9]. It must be stated here that these standards are not always possible to meet in off-shore applications. Space and weight on off-shore installations are extremely costly and metering although considered important, is not seen as the most critical consideration by the operators. It is therefore a fact that meters often get stuck in the pipeline at any convenient free pipe length regardless of the ISO standards. Therefore, these meters can suffer from adverse performance by being directly downstream of pipe bends, valves etc. It will later be explained how these problems are further exacerbated when considering wet gas metering. In fact, it is found that all the dry natural gas metering problems still exist when it comes to metering wet gas and more problems are added by the presence of the liquid.

2.4.2) <u>Ultrasonic Meters and the Production of Dry Natural Gas</u>

A more recently developed meter for use in industrial flow metering market and which has shown promise in single-phase and two-phase flow metering tests is the Ultrasonic Meter. The first Ultrasonic Meters (USM's) were available in the 1950's and manufacturers are now producing fourth or fifth generation products. Unlike

Differential Pressure Meters there is a wide range of designs available. This is due to the fact that the basic principles of these meters allow a wide variety of ideas to be developed, many in isolation from others due to commercial rivalry. However, the general concepts of these meters are the same and it is assumed here the reader has a general knowledge of these meters single phase operation principles.

In the last few decades various meter designs have come on the market and new concepts are still being developed. One of the most common and successful designs is that of the "transient-time" meter. It is this meter type that has recently undergone a series of tests organised as a joint industry project entitled "The Ultraflow Wet Gas Development Project", to determine its performance in wet natural gas flows. Currently no other ultrasonic meter has undergone any wet gas flow testing. For this reason only the transient-time ultrasonic meter operation in natural gas flows is discussed in this section.

These "transient-time" Ultrasonic Meters appear to be giving good results for dry natural gas production flows when they are installed in the pipework at a suitable distance from disturbances. In this way Ultrasonic Meters are advertised as the future of natural gas metering by their manufacturers as they appear to give similar accuracy to the Venturi Meters and have other advantages over other meter types. To start with they are non-intrusive. Other advantages claimed for dry natural gas applications include a turn-down of many ultrasonic meters claimed to be up to 400:1, which is far superior to both the standard Differential Pressure Meters and the turbine meter which usually have no more than 10:1 turndown. However the accuracy of these ultrasonic meters at the limits of these ranges are not mentioned. Due to the rapid response time of USM's they are good for metering transient or pulsating flows and in the event of flow reversal (e.g. possible in times of platform maintenance) the ultrasonic meter continues to operate unlike most flow meters. It is also true that multi-path ultrasonic meters build up a picture of the velocity profile and therefore the behaviour of the flow. Other types of meter do not give this additional information. Finally, the fact that the acoustic velocity of a gas is dependent on both the gas temperature and the gas composition means that by measuring acoustic velocity continuously any change in the gas temperature and / or composition is immediately noticed by the operators.

However, these significant advantages of Ultrasonic Meters in dry natural gas are offset by some significant problems when they are used in practice to meter dry natural gas in the actual production environment. The first of these problems is similar to one suffered by the Venturi. The same problem of poor meter location effects the Ultrasonic Meter. If the meter is too close to bends, valves or other obstructions, the resulting swirl / turbulence can seriously effect the accuracy of the mathematical techniques used to find the velocity profile and therefore the flowrate. Furthermore, there is a question mark over the strength of the bonding material used in the manufacture of the Ultrasonic transducers. Testing has shown the transducers to fail at temperatures in excess of $150^{0}C$ and when there is a sudden pressure fluctuation (a fairly common occurrence in production pipelines). A final serious problem is that the signals read by the meter are very susceptible to background noise from other components in or close to the line. These can degrade the strength of the signal and sometimes the signal can be lost completely. That is, in positions such as the "Christmas tree[3]" at the well head or on an off-shore platform, any systems close by, such as valves, can create enough noise to render the ultrasonic meter unusable. However, although the technical challenges facing development engineers attempting to overcome these problems seems substantial the development of these meters continues and it is clear that if the fore-mentioned problems can be solved the Ultrasonic Meter would have a strong claim to being at least the most capable single phase meter in the market.

Compared to the Differential Pressure Meters, with the meters ideally installed, the Ultrasonic Meter manufacturers claim an uncertainty of ± 0.5% for their ultrasonic meters in dry natural gas flows and as the meter uses a velocity based measurement it does not have the restrictions at high Reynolds number as do DP Meters. The un-calibrated Orifice Meter that conforms to ISO 5167-1 is assumed to have an uncertainty of ± 0.5%. The Venturi manufacturers tend to claim uncertainties in the order of ± 1% after calibration (although in reality it may be higher).

---

[3] The "Christmas Tree" is a term used that represents the sub-sea valve arrangement at the point where the pipeline from the production well exits from the sea floor.

It is with this background and rivalry in dry natural gas metering applications that these two meter types started to be applied to wet gas development. It will be shown in the next section how wet gas flows brought more problems to each of the meter types and has led to further advantages and disadvantages appearing during comparisons of the two meters.

2.4.3) Common Practical Problems in the Off-Shore Metering of Wet Gas

Like all practical applications of theoretical ideas the actual use of Venturis and Ultrasonic Meters on offshore platforms for measuring wet gas flow uncovers several practical problems.

2.4.3.1) Practical Problems with Flow Conditioners

It is stated in most fluid metering textbooks that all differential pressure meters greatly benefit from good flow conditions, i.e. a fully developed velocity profile and no swirl. In order to be assured of this an upstream length of twenty pipe diameters and a downstream length of ten pipe diameters is often suggested. The problem here is that on a platform offshore space and weight are very expensive (approximately £1 million / cubic foot) so the idea of having more pipework than the minimum necessary to remove the gas for metering purposes is not appealing. A common solution in other industries for such a problem is to introduce a "flow conditioner", a device that alters the flow to the desired condition for metering. Such devices are discussed in ISO 5167-1:1997 [9]. It is generally true that what is good for single-phase flow measurement is good for two-phase flow or multi-phase flow measurement. However it was found in practice offshore that these devices cannot be used as the pressure drop across the device can be enough to cause any water in the flow to sublimate and the water crystals (or "hydrates") can then block the passages of the conditioner making the velocity profile worse rather than better. It should also be noted that the effectiveness of these devices is reduced by placing them too close to the nearest upstream obstruction as often the swirl and local velocities of the flow

is too much for the conditioner to cope. Thus even without the problem of conditioner partial blockage the usefulness of these devices for improving flow conditions in the short straight upstream length of pipe is limited. Due to the first problem Stobie [2] suggests that these flow conditioners should not be used if there is any chance of ice crystals forming unless a way of suppressing this formation can be introduced. Injecting chemicals like glycol or methanol can achieve this. If this injection is not done and a conditioner is installed, then the wet gas metering engineer has to deal with measuring flows with unknown velocity profiles and swirl velocities as well as unknown two-phase flow patterns. (However, as stated earlier even with this injection / conditioner there could still be problems.) Jamieson and Dickinson [4] suggested that, to avoid complicating the measurement system, any chemical injection points required for any reason should only be installed downstream of the meter. Naturally the above case would contradict that.

For the case of sub-sea meters, Venturi Meters are usually installed in the well pipe line in a position that has a minimum swirl in the flow. To achieve this the meter is upstream of the choke and the "Christmas tree" is designed and installed to have no out of plane bends upstream of the meter.

2.4.3.2) Practical Problems with Flow Patterns

The two-phase flow pattern directly affects the meter's performance in a way which is not yet fully understood. In fact this is one of the main problems in wet gas flow metering. Just as engineers dealing with single-phase pipe flow know it is important to know whether the flow is laminar or turbulent and if any secondary flow effects, such as separation and re-circulation zones are present, engineers dealing with two-phase flows know this information is equally important but in addition the flow pattern (or "flow regime") must also be known.

It must be noted that the pipework configuration in the vicinity of the meter has a direct effect on the flow pattern. That is, the choice of meter position, e.g. whether it is at a high or low point on the pipework, or close to bends, can effect the local flow pattern and therefore the meter reading. In fact, knowing a particular flows flow

pattern is one of the greatest problems faced by engineers attempting to meter wet natural gas and with meters often installed in non-standard positions, in reality the flow patterns will not be fully developed as the flow enters the meter but will be in transition. As it is clearly not practical for a researcher to investigate every possible combination of flow conditions and upstream non-standard pipework the best a researcher can do is attempt to predict the likely flow patterns for the case of typical flow conditions with typical fluids and pipework that allows the flow pattern to be fully developed at the inlet to the meter.

The "flow pattern" is a way of describing the way the phases are dispersed in the pipe relative to each other. All two-phase flow text books offer lengthy descriptions of flow patterns and definitions for particular types of common patterns. A word of warning must be given that as yet there are no officially recognised definitions for these flow patterns and as a result the same physical flow pattern can be called by different names by different researchers. However there is now reasonable agreement for most basic types of flow pattern and it is only in the areas of transition between these that ambiguities still exist.

The commonly accepted definitions for two phase flow patterns are usually given in the literature for horizontal and vertical flows separately due to gravity having a significant effect on the flow pattern due to the high density difference between the phases. As this project deals with horizontal pipeline metering, only the typical definitions of horizontal flow patterns are discussed here. These definitions are based upon visual interpretation of engineers investigating two phase flows. The standard flow pattern diagrams visually showing well defined flow patterns are shown in Figure 2.3.

It should be noted that in reality the boundaries between these flow patterns are very difficult to judge. In fact, when viewing a two phase flow it can be (but not always) extremely difficult to decide which of the particular definitions fit best as often the flow seems to be in continuous transition between them.
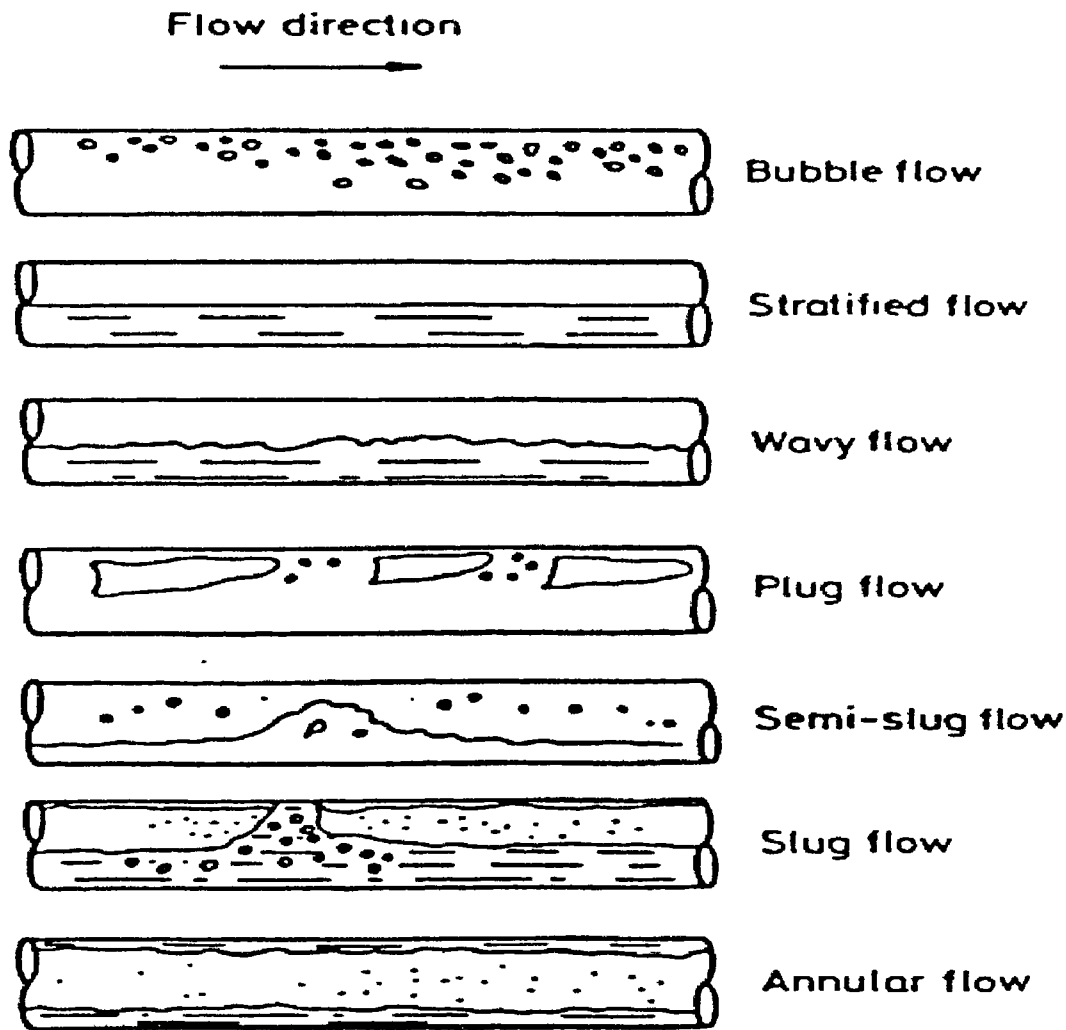
Figure 2.3 - Flow Regimes in horizontal two-phase flow

The situation for wet gas is slightly simpler than the more generalised situation discussed above but it is still far from simple. Due to the fact that there is less liquid flowing than gas (see earlier definition of "wet gas"), some flow patterns are far more likely to occur than others, e.g. "bubble flow" will not occur due to the lack of liquid mass flow.

The phenomena that dictate which particular flow pattern exist in each different set of circumstances are extremely complex. To date there is no purely mathematical method for predicting with great certainty what flow pattern will occur at a set location in the pipe (say an entrance to a flow meter). To give some indication of the complexity of the interaction between the phases in two-phase flows the following

description of only some of the phenomena an engineer would have to deal with to successfully mathematically model the flow (and hence estimate the flow pattern) are now given. Annular / Dispersed flow is chosen as an example. This flow can be seen to have a liquid film flowing on the wall of the pipe with gravity causing the film to be thicker at the base while the gas flow comes through the centre of the pipe with droplets of liquid suspended or "entrained" in the gas flow (see Figure 2.3). The localised thickness of this annular liquid ring depends on factors such as the liquid and gas mass flowrates, the density of the fluids of each phase (i.e. a measure of the buoyancy force), the pipe inside bore, the viscosity and surface tension of the liquid as this parameter partly dictates the amount of liquid that will be removed from the film and entrained in the gas. The amount of liquid entrainment is dictated by such factors as the liquid surface tension as this largely determines the drop size and therefore the droplet weight and therefore the associated buoyancy force (which is also partially determined by the line pressure) and by the complex disturbances at the phase interface between the liquid film and gas core. Of course, when a drop leaves the liquid film it may well be "atomised" (i.e. split into many smaller droplets by the drag force of the gas) and allowance has to be made for drops being reabsorbed into the annular film. To accurately calculate the flow in the pipe all these relationships would have to be modelled along with the liquid shear at the wall and the liquid / gas shear at the phase interface and all this is still assuming the flow has no mass transfer between its phases and the pipe geometry remains constant with no obstructions to the flow such as an intrusive flow meter.

It is therefore not surprising that no general mathematical model has yet been created that can accurately predict flow patterns. Academia and Industry currently use "Flow Pattern Maps" to obtain predictions of flow patterns at given conditions. These are of great importance to the engineer as knowledge of the flow pattern largely dictates what method of analysis or correlation should be used to predict the flow behaviour. These are maps that have mostly been formed by plotting many experimental data points and then fitting the various flow patterns into regions. Naturally such a technique does not give exact results and the boundaries between any

two regions are not rigid but more blended together to give a transition region (similar to the observations of actual flow pattern transitions).

Of the flow pattern maps available in the literature many are for horizontal flow. However, like many of the correlations that exist for two-phase flow these maps were formed from data taken from experimental ranges that do not cover the full spectrum of conditions that industry desires. In particular, the Oil and Gas Industry needs maps that can deal with complex natural gas mixture flows at very high pressures and flowrates. Many maps were made for specific purposes so these maps fit closer to the desired range being examined by that industry. This also meant the maps could be presented in the form most suitable to that application (i.e. the functions on each axis could be chosen to be the most convenient). Examples of earlier maps are the "Baker Map" modified by Scott which has been used by the Chemical Industry as it was one of the first maps to include correlations that took different fluid properties into account (although much of its data was from experiments in air and water) and the Hoogendoorn Map which used data from air / water and air / oil and was used extensively by the Oil and Gas Industry. A more modern map exists in the form of the Taitel and Duckler Map [56]. The major difference this map has with respect to the previous maps is that it is only semi-empirical. There is a general acceptance in academia that this map is the most accurate of the general flow maps. More recently still R. de Leeuw of Shell Expro [5] published a paper that gave an unspecified flow map with an actual natural gas field data range (from the Coevorden field in The Netherlands) and a high pressure Nitrogen / Diesel Oil test range plotted on it. This is rare data on multi-phase flow patterns of wet natural gas at high pressure (90 bar) in actual well conditions.   .

Only a few papers in the literature offer information on the actual flow patterns found by engineers on site at a natural gas field. These are de Leeuw [5] who states that at Coevorden stratified and annular flows were found, Washington (Ref. 3) states that "at normal gas pipeline velocities the liquid travels either as a small film around the circumference of the pipe (annular or stratified flow) or as a rivulet in the bottom of the pipe if mounted horizontally". Ting of Chevron Petroleum [13] does not explicitly say what flow pattern he wished to examine (i.e. that which Chevron believe

exists in their natural gas pipelines) but it can be deduced from the paper that he was attempting to create a mist or annular dispersed flow by the design of the rig used. However, the vast majority of papers published do not mention the flow pattern, the test rigs simply inject the chosen liquid at a sufficient distance upstream and this author assumes these experimenters consider this distance to be enough to assure equilibrium between the phases at the test piece. There is evidence for this being sound practice (see Washington's comments in [3]). However, no mention is made of these equilibrium flow patterns being the same as exist at the field measurement points.

The Taitel & Duckler and the Shell Flow Pattern Maps are used in this thesis to predict the probable flow patterns that exist in the field and the flow patterns that should be achieved by the National Engineering Laboratory Wet Gas Loop.

The final word on the flow patterns that could exist at a flow meter is that it must be realised that an intrusive meter can and probably will change the flow pattern of the flow through it. This point is considered of great importance to understanding the performance of such a meter. Only by knowing the local conditions at the pressure tapping points can the significance of the readings be properly understood and the hope for a fully theoretical prediction method for flowrates be realised (rather than the current correlation methods).

2.4.3.3) Practical Problems in Finding the Fluid Properties

It was stated earlier that one of the aims of improving wet gas metering performance was to allow the removal of the bulk separator from the platforms. It should be noted however, that a test separator is required to obtain gas and liquid samples from the flow so that chemical analysis can estimate the fluid properties. Of course, this test separator is relatively small compared to the bulk separator.

All two-phase flow correlations currently in use for differential pressure meters assume that the gas composition and either the liquid flowrate or flow quality are known from the outset. At present, it is only possible to measure wet gas flows to the desired accuracy by using separators. Shell Expro use a Venturi installation to

measure the gas flow from the separator and a Coriolis Meter to measure liquid mass flow and density. Facilities are usually provided for taking samples of both gas and liquid. The liquid samples are analysed on-shore and the composition found. The gas sample can also be analysed on-shore but Shell Expro prefer a gas chromatograph to be on-line to monitor the gas composition of the sample and AGA8 to calculate the gas density. (As the practical problems with wet natural gas metering are being discussed here it is important to note that Shell Expro do not consider installing and operating a gas chromatograph on an unmanned off-shore platform as a simple operation. Jamieson and Dickinson [4] state the practical problems and that it took a nine month trial to prove the feasibility of the system). The total well stream composition obtained from a well test is fed into a flash calculation so that the gas density, liquid density and gas mass fraction can be calculated when the line pressure and temperature change. In this way the practical problem of determining the fluid properties is achieved. Naturally there are uncertainties in these calculations that contribute to the overall uncertainty of the metering system. (Jamieson and Dickinson [4] suggested that it is possible to significantly reduce these uncertainties by increasing the frequency of use of the gas chromatograph for each pipeline.) The test separator cannot therefore be removed, like the bulk separator, with the successful development of a wet gas meter. However, it is significantly smaller and cheaper than the bulk separator and unlike the bulk separator, if it malfunctions there is no need for the platform to be immediately shut down, maintenance can wait for the next convenient down time with the last reliable readings being taken as correct. Any error this assumption creates will almost certainly be much smaller than the cost of carrying out unscheduled maintenance. Shell state that in practice the conditions of a well do not change rapidly and therefore for practical purposes the gas mass fraction only needs to be assessed annually (see Refs. 4, 5 and 43). It should be pointed out however that this last point does not apply to new wells. There is a significant change in the quality of flows in the initial stages of production before a well settles into its steady state.

2.4.3.4) Practical Problems in Meter Survivability

One of the important practical abilities an offshore wet gas meter must have is the ability to survive adverse conditions that periodically occur in all such natural gas flows. These are caused by situations such as a large amount of liquid that has collected downstream of the meter in a low point in the pipework being suddenly pushed forward by the gas and "flooding" the meter (a condition called "slugging") or on start up after a period of no flow where it is inevitable that sea water has entered the pipe. Occasionally there can be a spike in line pressure due to unpredictable phenomena in the well itself. The meter must survive these situations, ideally while it continues to give readings and if it does shut down / fail to give readings in these adverse conditions it is imperative that it can self start again when conditions return to normal. This is because, if they are stationed on unmanned platforms or sub-sea or in awkward positions in manned platforms, the cost of maintenance and repair can be considerable (often due more to the downtime of the whole facility and the associated drop in production than the meter costs).

It has been noted earlier that offshore facilities are noisy facilities (i.e. a high level of acoustic interference exists) and hence a lot of background "noise" can exist around an Ultrasonic Meter. It is of great importance when using these meters to reduce the "noise" as much as possible, a problem that does not exist for differential pressure meters. Hence, when using ultrasonics it is necessary to keep all restrictions in the pipeline far away or else the signals will be destroyed and the meter will be rendered useless.

2.4.3.5) Practical Problems in Finding the Liquid Content in the Gas Flow

Nearly all the research to date that deals with the metering of wet gas flows does so from the starting assumption that the total mass flow or the flow quality is known. It is from this starting point that the available wet gas metering techniques estimate the gas flowrate. In other words the metering engineer needs to know the liquid content of the flow in order to derive the gas flowrate from the meter readings.

It is always assumed that the properties of each component in the flow are known. These assumptions cannot be taken for granted when dealing with natural gas wells. Currently, the total mass flow and quality is found by using a bulk separator to separate the phases for single-phase measurement and the fluid properties are found either by measuring the line pressure and temperature and taking samples from a test separator to shore (where AGA 8 will calculate the properties) or by use of an on line gas chromatograph. (See Jamieson & Dickinson [4] for more details). Therefore, in order for an existing wet gas correlation to be successfully applied a method of finding the phase properties and the liquid content must exist but the advantage of having an accurate correlation is entirely lost if the need for the bulk separator is still there. In promising to solve this problem the Shell Tracer Method is of great significance to the development of wet gas metering.

The patented "Tracer Dilution Technique" as supplied to industry by SGS Redwood in the U.K and Petrotech a.s. in Norway operates along the following lines. After sampling the flow to ascertain the flows components (i.e. by use of a test separator) suitable tracer chemicals are injected at a precise rate into the pipeline. A suitable tracer is one which is readily absorbed by one and only one of the flow components. de Leeuw [43] gives an explanation of the suitable choice of tracers and fluorescent dyes are selected. A sample of the flow is taken at a sufficiently long distance downstream of the injection point to ensure complete mixing. The tracer method is used for single-phase flows, and ISO 2975 "Measurement of Water Flow in Closed Conduits-Tracer Methods" states that to be assured of less than 1% tracer variation a mixing length of approximately 150 pipe diameters is required. No such standard exists for multi-phase flow (this therefore includes wet gas flows) but Shell suggest that the mixing length should be similar. By then separating the different flow components and analysing the quantity of the tracer chemical in that sample the flow rate of that component can be found. In this way the water and condensate flow rates can be determined. The equation for each liquid compound present is:

$$Q = \frac{C_o}{C_s} \cdot q$$

where Q = liquid flowrate of that compound

q = quantity of tracer per unit time

C_o = concentration of the tracer solution injected into the stream.

C_s = concentration of the sample taken downstream of injection point.

As the industry knows from experience that the liquid content of a stable established natural gas well changes very gradually, periodic checks once or twice a year are suggested as sufficient by de Leeuw [5, 43]. For new wells, where the conditions change more rapidly, or wells where conditions are suspected of having changed more regular tracer tests would be needed.

However, de Leeuw states that field trials of this tracer dilution method have shown that the total uncertainty of the tracer technique is about 8 %. This significant uncertainty is carried into all the differential pressure meter correlations (de Leeuw quotes accuracy of 2% to 4% for his correlation when using this tracer technique). Furthermore, it would be ideal to have a system that gave continuously updated readings so that any change in the conditions would not go unnoticed until the next liquid content check. Even though the current tracer method is a major advance in multi-phase technology and seems to be the best system available it is not the ideal answer to the problem. More development of the technique would be beneficial as would any other research into methods of determining the liquid content in an unprocessed natural gas pipeline.

Two other methods that researchers have considered for measuring the liquid content are the use of a densitometer or a "clamp on" ultrasonic meter. Neither is as yet accepted for use in unprocessed natural gas production lines. However, for completeness in this literature review a brief discussion is given below.

The densitometer system consists of a gamma ray source that is attached to the top of the pipe, while at the base of the pipe a photomultiplier detector is attached. The system is calibrated with an empty pipe to examine the effect of the steel

pipework and then with the pipe full of liquid. Such systems are used regularly to measure single phase densities. It has been suggested by some researchers that this system could be used to measure liquid content in a two-phase pipeline. However, there are considerable difficulties in applying this technology to two-phase flow systems (including wet gas flows). One of these difficulties is of course the problem of the effect of flow patterns. Hall [57] describes how the NEL's investigation into this systems was conducted during Ultrasonic Wet Gas tests in the NEL's Wet Gas System. The conclusions were that a vertical chord could predict the height in the pipe of a stratified liquid flow and that this information could possibly be used to measure the liquid flowrate. However, it is made clear by Hall that this will only work for stratified flows, annular dispersed flows (such as exist in actual wet natural gas production lines) cannot as yet have their liquid content estimated in this way. This is therefore not as yet practical for industrial use.

Clamp on Ultrasonic Meters have been considered for the measurement of liquid content in a two-phase flow by Schlumberger (unpublished confidential work) and by Vedapuri and Gopal of Ohio University [60]. In this research a clamp-on ultrasonic meter was developed to measure the height and velocity of the liquid in a stratified flow with limited success. No mention of mist / dispersed flow is made and therefore this technology is not as yet practical for use in actual wet natural gas production lines.

It should also be mentioned that some operators install gamma ray densitometers in the wet natural gas production lines to help in the estimation of liquid content. These devices are designed to measure the density of a single phase liquid flow but some engineers have suggested that the difference in signal absorption between gas and liquid can help estimate the quantity of liquid flowing. The principle is to find the density measured by the densitometer for the two-phase flow (ρ_γ) and knowing the gas and liquid densities (ρ_g and ρ_l) find the function (f) that gives the Liquid Volume Fraction (LVF) i.e.:

$$LVF = f\left(\frac{\rho_\gamma - \rho_g}{\rho_l - \rho_g}\right)$$

However, no technical paper could be found discussing any research into this topic.

With these practical wet natural gas metering difficulties discussed it is now relevant to discuss the published wet gas metering research concerning Differential Pressure Meters and Ultrasonic Meters.

2.5) Published Work on Wet Gas Metering

The literature on the topics of "Wet Gas Metering" and the more general "Two-Phase Metering" can be broadly split into two categories. That is, the practical investigations that use test facility and actual field data to form useable metering correlations from relatively simplified mathematical models of the flow and the far more complex academically based investigations which attempt to model the flow to a higher level of accuracy. It is found that the greater the degree of complexity that is included in such a mathematical model the less practical use the model has. Hence there is a distinct split in the literature. Either a paper is of direct relevance to a wet gas metering engineer as its findings can be applied directly to the metering of production flows or it is of academic interest only because, for the models to give meaningful results they require information that is not available to the metering engineer. (For example, liquid film thickness, liquid droplet size etc.). As this current research is industrially based this literature review is biased towards the more practical papers. However, after detailed discussion of the practical papers in section (2.5.1) a short summary of the more academic papers is presented in section (2.5.2).

2.5.1) Meter Research Directly Applicable to Industry

2.5.1.1) Two Phase Differential Pressure Meter Research

The majority of the published literature on Wet Gas Flow Metering deals with the performance of the Orifice Plate Meter. More recently researchers have given greater emphasis to the Venturi Meter although much of this research has consisted of taking Venturi Meter readings and then applying them to the existing Orifice Plate Meter correlations to check their suitability. McCrometer have published a report on their limited research into the V-Cone Meters performance in wet gas flows but virtually no work has been published dealing with wet gas effects on Nozzle Meters.

Most of the literature that gives information on the effects of wet gas on differential pressure meters installed in horizontal pipelines is not restricted to just wet gas conditions. On the contrary, the majority of papers deal with the more general problem of two-phase flow and they have experimental ranges and conditions that determine whether they are relevant to wet natural gas flows at field conditions or not. It is common for a paper to be of restricted benefit to wet natural gas horizontal flow research due to some flow condition being unsuitable, e.g. vertically up or down flow, the flow quality being too low or the pipe diameter not being large enough to have similarity with natural gas pipelines from gas fields.

A study of the methods used by researchers in the field of general two-phase flow metering shows that several different approaches have been taken. These are:

a) Assume the two-phase flow to be a single-phase flow and create a suitable expression for the two-phase density using the flow quality, x, (i.e. the ratio of gas mass flow to total flow) to replace the single-phase density in the standard single-phase flow equation. An example of this is given in the Homogenous Flow Model in Section 2.5.1.1.1.1.

b) When assuming homogenous flow the quality, x, can be replaced in the single-phase flow equation by some factor Φ where $\Phi = f(x)$ and is obtained from experimental data. An example of this is the James correlation [20] where

$\Phi = x^{1.5}$. However, this correlation is not suitable for use with wet gas due to the experimental ranges used.

c) When separated flow is assumed each phase can be treated as if it flows alone. Using a modified Lockhart-Martinelli factor 'X' and experimental data a correlation can be formed. An example is the Murdock Equation (see Section 2.5.1.1.1.2).

d) When separated flow is assumed the single-phase gas flow equation can be used with a correcting blockage factor (sometimes denoted 'BF'). This BF is the correction that takes account of the area restriction on the gas flow due to the liquid presence. Its value is found from experimental data. An example is the Smith & Leang correlation [33] discussed in Section 2.5.1.1.1.4.

2.5.1.1.1) The Orifice Meter and Wet Gas Flows

A comprehensive summary of two-phase flow effects on Orifice Plate Meters is given by Lin in "Two-Phase Flow Measurement with Orifices" [21] published in 1986. Since little recent work on Orifice Plates in Wet Gas has been carried out it is still the most current review of two-phase orifice correlations. In fact, only Ting and Jones [13] have published any further investigations since Lin's publication.

Lin first explains that with a standard orifice plate, the information gained by that device when situated in two-phase flow (i.e. the pressure drop, the one parameter measured) restricts the correlation to giving an expression that relates the total mass flow and the flows quality. Lin calls this a "One-Parametric Two-Phase Flow Measurement". In order to actually find the values of the total mass flow and flow quality one of these values has to be known at the outset or an extra piece of information must be obtained from the flow. Lin calls this a "Two-Parametric Two-Phase Flow Measurement". The vast majority of Differential Pressure Meter correlations are "one parametric" two-phase flow correlations.

Lin discusses fourteen different research papers dealing with "one parametric" two-phase flow Orifice Plate Metering. However, not all of these are of significance to the metering of wet natural gas flow at a field location. Five are of significance and

these are The Homogenous Model, The Murdock correlation, The Chisholm correlation, The Smith and Leang correlation and The Lin correlation.

Ting [12, 13, 35, 36 and 52] offers no correlation in his papers but discusses data obtained from experimental apparatus and natural gas fields. Each of the above correlations will be discussed separately. In individual ways even these correlations have some limitations regarding this research project. The remaining nine correlations listed by Lin are less suitable when considering horizontal wet natural gas flow metering in field conditions than the five listed above, for different reasons which are as follows:

a) The Hoopes correlation [22] was derived with relatively low pressures
(0.62 bar $\leq$ P $\leq$12.41 bar) and low qualities (x $\leq$ 0.34).

b) The James correlation [20] was derived with relatively low pressures
(5.1 bar $\leq$ P $\leq$ 18.7 bar) and a low quality (x $\leq$ 0.56).

c) The Bizon correlation [23] was derived with a low quality (x $\leq$ 0.5) and a small pipe diameter (diameter of 1").

d) The Marriott paper [24] is not available to the British Library and therefore the flow conditions are unknown.

e) The Collins & Gacesa correlation [25] was derived for vertical up flow in small diameter pipes (diameter $\leq$ 3") with a relatively low flow quality (x $\leq$ 0.9).

f) The Kremlevskii & Dyudina correlation [26] was derived with low pressures
(P $\leq$ 4 bar).

g) The Davies & Daniel correlation [27] was derived with a low pressure (6 bar), small pipe diameter (diameter = 0.375") and very low qualities (0.00017 $\leq$ x $\leq$ 0.18).

h) The Lorenzi and Muzzio correlation [28] was derived with very low pressures
(P $\leq$ 1.49 bar).

i) The Matter et al. correlation [29] was derived from a low pressure (P = 2.44 bar), and a small pipe diameter ($\cong$ 2").

One of the main difficulties in investigating two-phase flow (including wet gas flow) through a meter is predicting the flow pattern. There is still no method that is

100% accurate in predicting flow patterns. For recent wet natural gas research the Taitel & Duckler semi-empirical method and the Shell Expro Flow Pattern Map are the two most widely accepted prediction methods. However, many of the Orifice Plate Meter two-phase correlations were formed before these prediction methods existed. (Of course it should be noted that for all that there are better methods available to predict flow patterns for fully developed flows there is still no good method of predicting flow patterns in transition through components such as DP Meters. A better prediction of the upstream flow pattern can now be made but there is no advance in predicting the flow pattern through the meters.)

This means that different investigators simply chose to model the flow pattern they assumed existed in the Orifice Plate Meter. There were two schools of thought. Firstly, it was thought by some that as the Orifice Plate has a lot of associated turbulence a large amount of mixing must take place and hence dispersed / mist flow would result which could be modelled as a homogenous flow. However, the other view was that an Orifice Plate Meter that had separated flow upstream of the meter would continue to have separated flow through the meter (i.e. the turbulence caused by the Orifice Plate causes mixing within the single phases only and any liquid entrainment rate into the gas flow is negligible).This belief rises from the fact that as the densities of liquids and gases are of a different magnitude up until the line pressure becomes extremely high (like well head pressures which are hundreds of bar) the gravity effect is predominant and so entrainment levels are minimal.

Note that both the homogenous and separated models assume thermal equilibrium through the meter. However, also note that the homogenous model also assumes "no slip", i.e. the phase velocities are equal, while the separated flow does not have this restriction. The following is a discussion of the five existing correlations suitable for application to wet gas flow metering.

2.5.1.1.1.1) <u>Homogenous Flow Model Correlation</u>

The homogenous flow model is one of the oldest methods of modelling two-phase flow. Whereas the other correlations have full derivations given in their respective

papers the author found no derivation for the homogenous equation as applied to wet gas and hence (unlike the other correlations to be discussed) it is derived in full below.

The basis of the homogenous flow model correlation concept is to treat the two-phase flow as if it were a single-phase flow by introducing an expression for the combined densities so that the single-phase Orifice Plate Meter equation can be used.

i.e.
$$\dot{m}_{total} = KYA_t \sqrt{2\rho \, \Delta P} \qquad (2.1)$$

where K and Y are the discharge coefficient (including the velocity of approach factor) and expansibility terms respectively for the psuedo-single phase flow. The homogeneous model assumes these values to be approximately equal to their gas counter-parts. The derivation of such a density is as follows:

Let v denote 'specific volume'. Then,

$$\upsilon_{\text{hom }ogenous} = \frac{Volume_{total}}{Mass_{total}} = \frac{\left(V_l + V_g\right)}{\left(M_l + M_g\right)} \qquad (2.2)$$

where, for a steady flow, V_l & V_g are the liquid and gas volumes in a unit length of pipe respectively and M_l & M_g are the liquid and gas masses in that same unit length of pipe respectively at any instant in time. Therefore:

$$\upsilon_{\text{hom }ogenous} = \frac{V_l}{M_{total}} + \frac{V_g}{M_{total}} \qquad (2.3)$$

By definition
$$x = \frac{M_g}{M_{total}} \qquad (2.4)$$

and hence
$$(1-x) = \frac{M_l}{M_{total}} \qquad (2.5)$$

36

where 'x' is the mass quality,

Hence
$$\upsilon_{\text{hom}ogenous} = \frac{V_g}{\left(\dfrac{M_g}{x}\right)} + \frac{V_l}{\left(\dfrac{M_l}{1-x}\right)}$$
(2.6)

$$\therefore \quad \upsilon_{\text{hom}ogenous} = x\upsilon_g + (1-x)\upsilon_l = \frac{1}{\rho_{\text{hom}ogenous}}$$
(2.7)

or,
$$\frac{1}{\rho_{\text{hom}ogenous}} = \frac{x}{\rho_g} + \frac{(1-x)}{\rho_l}$$
(2.8)

where, $\rho_{\text{hom}ogenous}$ is the homogeneous density and subscripts 'l' and 'g' refer to liquid and gas respectively. Substituting this homogenous value for density into the single-phase Orifice Plate Meter equation gives:

$$\dot{m}_{total} = KYA_t \sqrt{2\rho_{\text{hom}ogenous}\Delta P_{tp}}$$
(2.9)

which can be rearranged to give:

$$\Delta P_{tp} = \frac{\dot{m}_{total}^2 \left(\dfrac{\rho_g}{\rho_l} + x\left(1 - \dfrac{\rho_g}{\rho_l}\right)\right)}{2\rho_g \left(KYA_t\right)^2}$$
(2.10)

where subscript 'tp' indicates 'two-phase flow', i.e. ΔP_{tp} is the pressure drop across the meter in two-phase flow and $\dot{m}_{total}$ is the total two-phase mass flow rate. It is clear from equation (2.10) that for a single-phase gas flow (x = 1) or a single-phase liquid flow (x = 0) the equation reduces to that of equation (2.1) with $\rho_{homogenous}$ becoming ρ_g or ρ_l respectively (and Y becoming unity for the liquid flow). Equation (2.10) can be used directly to obtain a value of the total mass flowrate by reading ΔP_{tp} from the DP meter, using the values of the gas expansion coefficient Y_g and the gas discharge

coefficient, K_g, (as it is assumed that these parameters are approximately equal to Y and K), the meter throat area, A_t, and calculating the densities from the upstream conditions and fluid properties. As the quality (x) is assumed known the individual phase mass flows can be obtained using equations (2.4) and (2.5). A form of the equation often used by researchers is obtained in the following way:

If the total mass flow flowed as gas the flow equation would be:

$$\dot{m}_{total} = K_g Y_g A_t \sqrt{2\rho_g \Delta P_g} \qquad (2.1a)$$

Dividing the two-phase pressure drop (equation 2.10) by the single-phase 'gas' pressure drop attained from equation 2.1a, gives:

$$\frac{\Delta P_{tp}}{\Delta P_g} = x + ((1-x)(\frac{\upsilon_l}{\upsilon_g})) \qquad (2.11)$$

It should be noted that Lin [21] chose to use the liquid as the single phase. This intuitively suggests that he was considering the measurement of bubbly flow.

To use equation (2.11) the reading ΔP_{tp} would be taken from the meter and from knowledge of the flow quality (x) and the fluid properties (in this case the specific volumes) a value for ΔP_g can be obtained assuming the specific volumes are known from the pressure and temperature measurements and knowledge of the fluid properties. As ΔP_g represents the pressure drop that would occur if the total mass flow of the two-phase flow was flowing as a gas this value can be used in the single-phase flow equation for gas to find the actual total mass flowrate. As it is assumed that the flow quality is known the gas and liquid flowrates are then simply calculated.

$$\dot{m}_g = x \dot{m}_{total} \qquad (2.4)$$

$$\dot{m}_g = (1-x) \dot{m}_{total} \qquad (2.5)$$

With some algebraic manipulation the above series of equations give a final expression for the total mass flow:

$$m_{total} = \frac{K_g Y_g A_t \sqrt{2\rho_g \Delta P_{tp}}}{\sqrt{\dfrac{\rho_g}{\rho_l} + x\left(1 - \dfrac{\rho_g}{\rho_l}\right)}} \qquad (2.12)$$

However, it is now generally regarded necessary to take more account of the flow pattern and it is with this statement that Murdock starts his paper [30].

2.5.1.1.1.2) The Murdock Correlation

The paper published by Murdock in 1962 [30] dealt with the general problem of measuring two-phase flows accurately. The correlation Murdock offered was formed from a wide range of data points and therefore it was valid for a wide range of flow conditions. Murdock based his work on Orifice Plate Meters designed to the ASME standards of the time.

The data points were obtained from two separate sources. These were the U.S. Naval Boiler and Turbine Laboratory and W.H.Osborne of the Champlin Oil & Refining Co. The first set of data was for steam/water only while Osborne's data had air/water, gas/water, gas/salt water and gas/distillate fluid combinations. Along with this varied collection of fluids, the data points used by Murdock covered a wide range of flow conditions. The range of the ninety data points used was:

1.01 bar ≤ P ≤ 63 bar (not 40 bar as stated by Lin [21])

0.025 bar ≤ ΔP ≤ 1.25 bar

0.11 ≤ x ≤ 0.98

63.35 mm ≤ D ≤ 101.6 mm

25.4 mm ≤ d ≤ 31.8 mm

0.2602 ≤ β ≤ 0.5

54 ≤ Re_l ≤ 46,600

13,000 ≤ Re_g ≤ 1,270,000

Murdock's method was to consider the two-phase flow to be two separate flows flowing through an Orifice Plate Meter individually. Hence each phase's data was treated as if that phase alone was present.

For the gas phase the gas Reynolds No. was used to find the value of the chosen meter flow coefficient by using the ASME standards [11]. Using the known value of gas flowrate and making certain assumptions, values for the gas expansion factor, Y_g, the pressure differential, ΔP, across the standard meter can be estimated. This value for the pressure differential is that which would exist if the gas flowed alone through the orifice and hence a subscript 'g' can be added, ΔP_g. (Note that this value is the pressure drop across the DP meter of the gas phase flowing alone and not the pressure drop that would occur if the total mass flow flowed as a gas).

The standard Orifice Plate Equation:

$$\dot{m}_{gas} = K_g Y_g A_t \sqrt{2\rho_g . \Delta P_g}$$

(2.1b)

gives

$$\Delta P_g = \frac{1}{2\rho_g} \left(\frac{\dot{m}_{gas}}{Y_g K_g A_t} \right)^2$$

Where $\dot{m}_{gas}$, A_t, ρ_g are known from experimental data and K_g is obtained from knowledge of Re_g. By assumptions about Y_g, ΔP_g can be calculated.

Likewise, the liquid Reynolds No. can be used to obtain the flow coefficient (K_l) for that liquid flow flowing alone through the meter from the ASME standards. As the liquid expansion factor is approximately unity the liquid flow pressure differential across the Orifice Plate Meter can be calculated directly from the single-phase Orifice Plate Flow Equation.

$$\dot{m}_l = K_l Y_l A_t \sqrt{2\rho_l \Delta P_l}$$

(2.1c)

which gives

$$\Delta P_l = \frac{1}{2\rho_l} \left(\frac{\dot{m}_{liquid}}{Y_l K_l A_t} \right)^2$$

Where $\dot{m}_{liquid}$, A_t, ρ_l are known from experimental data and K_l is obtained from knowledge of Re_l. Y_l is unity therefore ΔP_g can be calculated directly.

The actual pressure differential measured by the meter in two-phase flow is given in ninety data points (ΔP_{tp}). These ninety points were given in the report [30] as raw data and plotted on a graph reproduced here as Figure 2.4. It is from these points on this graph that Murdock fitted a line and formed his correlation. Murdock gave his correlation in two forms:

1) In terms of the two-phase flow pressure drop to the single-phase pressure drop if the gas phase flowed alone through the meter.

$$\frac{\sqrt{\Delta P_{tp}}}{\sqrt{\Delta P_g}} = 1.26 \frac{\sqrt{\Delta P_l}}{\sqrt{\Delta P_g}} + 1 \qquad (2.13)$$

ΔP_{tp} = The actual two-phase pressure drop across the meter.

ΔP_g = The pressure drop across the meter if the gas phase flowed alone.

ΔP_l = The pressure drop across the meter if the liquid phase flowed alone.

And:

2) In terms of the total mass flowrate:

$$\dot{m}_{total} = \frac{K_g Y_g A_t \sqrt{2\rho_g \Delta P_{tp}}}{x + 1.26(1-x)\left(\dfrac{K_g Y_g}{K_l}\right)\sqrt{\dfrac{\rho_g}{\rho_l}}} \qquad (2.14)$$

where

$\dot{m}_{total}$ = The total mass flow (kg/s)

K_g = The Flow Coefficient if gas flows alone.

K_l = The Flow Coefficient if liquid flows alone.

Y_g = Gas Expansion Factor.

A = Area of meter throat. (m^2)

ΔP_{tp} = The two-phase pressure drop across the meter. (N/ m^2)

ρ_g = The gas density. (kg/ m^3)

ρ_l = The liquid density. (kg/ m^3)

x = The mass quality.

Murdocks full derivation is presented by this author in Ref. 58. It must be noted here that the term $\sqrt{\Delta P_l}\big/\sqrt{\Delta P_g}$ in equation (2.13) represents the ratio of the square root of the pressure drop across the meter if that quantity of liquid that exists in the two-phase flow flows alone to the square root of the pressure drop across the meter if that quantity of gas that exists in the two-phase flow flows alone. This is a similar term to the Lockhart Martinelli parameter (denoted as 'X') first defined in the 1940's while they were investigating isothermal, two-phase, two-component flow in horizontal tubes. Originally Lockhart and Martinelli defined 'X' as the ratio of the two phases friction pressure drops if the phases flowed alone in a straight horizontal pipe. However, two-phase metering investigators have since used 'X' as the ratio of the two phases acceleration pressure drops across a flow meter if the phases flowed alone, i.e. when considering two-phase flows it is common to denote 'X' as the ratio of the momentum pressure drop but still call this parameter the Lockhart-Martinelli parameter. Therefore, although Murdock did not do so, equation (2.13) is now most often written as equation (2.15).

$$\frac{\sqrt{\Delta P_{tp}}}{\sqrt{\Delta P_g}} = 1 + 1.26\,X \qquad\qquad (2.15)$$

The result was a correlation model that gives a prediction of the gas flowrate for any two-phase flow with parameters lying within the stated experimental ranges. Murdock claimed these equations gave an uncertainty of ± 1.5%. It should be noted here that even though the largest uncertainty is ± 1.5% across the range of conditions there is clearly a fair spread of data points either side of the fitted line in the region of high
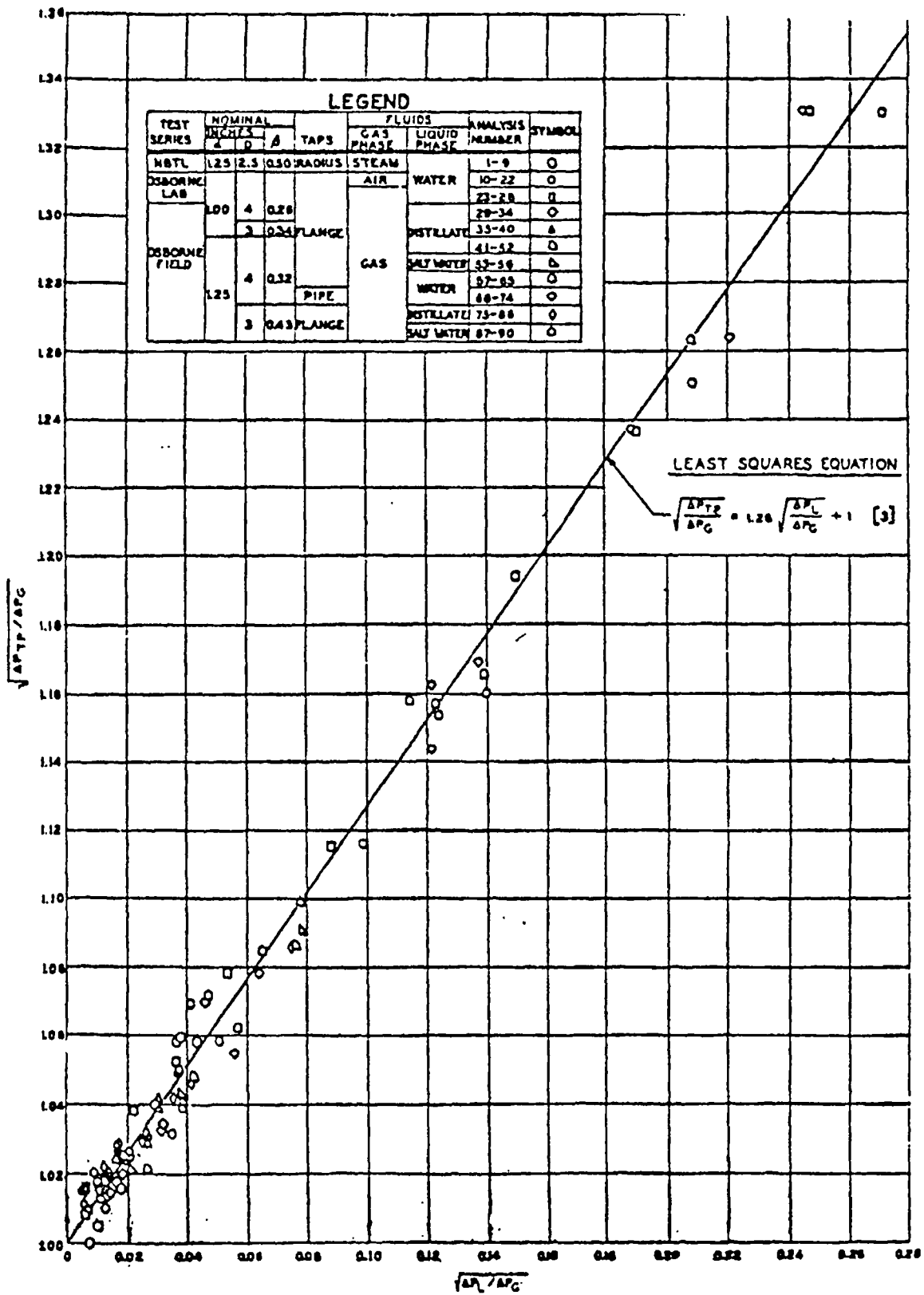
Figure 2.4. The Murdock Graph.

quality flows (i.e. low values of $\sqrt{\Delta P_l / \Delta P_g}$ or 'X') and a smaller uncertainty could possibly be obtained for the case of wet natural gas if only that particular data was used. (Of course wet natural gas metering was not Murdock's particular aim, that was to create a general equation for various fluid combinations across the spectrum of two-phase flow conditions). As will be discussed later not enough reliable natural gas / condensate data for wet gas flows through Differential Pressure Meters exists to form a natural gas / condensate wet gas flow equation using Murdock's method (or any other method). Also, it should be noted that Murdocks data does not reach the lower liquid loading required to cover the full range of the present research definition of "Wet Gas". Therefore the use of the Murdock Equation by the Oil and Gas Industry for the extremely low values of LGR is an extrapolation with no scientific basis.

Murdock's paper is unique in that the data used is presented in numerical form instead of just in plots like most other papers. This means other engineers can use the raw data and do not have to take it from graphs incurring errors.

The Murdock method is compared with the others methods and discussed later in this thesis.

2.5.1.1.1.3) The Chisholm Equation

Chisholm published a paper in 1967 [31] presenting a correlation for use in measuring two-phase flow through a sharp-edged orifice plate. A separated flow model is assumed to exist at the orifice plate. Its derivation (given in full in [58]) includes more detailed analysis of the flow phenomena than Murdock's derivation in as much as the shear force at the phase boundary is considered directly. However, similar to Murdocks derivation Chisholm assumes the flow to be incompressible (i.e. the pressure drop across the orifice plate is relatively small in comparison with the line pressure) and no significant thermodynamic effects are present (i.e. no mass transfer between the phases occurs).

The correlation is given in the form of the following two equations:

$$\frac{\dot{m}_{uncorrected}}{\dot{m}_g} = \sqrt{1 + CX + X^2}$$ (2.16)

and

$$\frac{\Delta P_{tp}}{\Delta P_g} = 1 + CX + X^2$$ (2.17)

where

$$X = \frac{\sqrt{\Delta P_l}}{\sqrt{\Delta P_g}} = \frac{(1-x)}{x}\sqrt{\frac{\rho_g}{\rho_l}}$$ (2.18)

'C' is a correcting factor for two-phase flow and is defined by the following equation:

$$C = \frac{1}{K}\sqrt{\frac{\rho_l}{\rho_g}} + K\sqrt{\frac{\rho_g}{\rho_l}}$$ (2.19)

where K represents the "slip ratio" between the phases, i.e. the ratio of their velocities, $K = \frac{U_g}{U_l}$, where U_g and U_l are the gas and liquid phase velocities respectively. In practice the slip value is unknown and 'C' is evaluated empirically.

Chisholm applied these equations to various sets of data obtained from different experimenters but only Murdock's data overlaps the "wet gas flow" range and therefore only this result is relevant here. It was found that when Murdock's data was used 'C' could be given the value 2.66 and all the data would lie within ± 1.5% of equation 2.16 or 2.17.

Hence

$$\frac{\dot{m}_{total}}{\dot{m}_{gas}} = \sqrt{1 + 2.66X + X^2}$$ (2.20)

and

$$\frac{\Delta P_{tp}}{\Delta P_{gas}} = 1 + 2.66X + X^2$$ (2.21)

45

Like Murdock's equations (2.13) and (2.14), these equations are the best fit to the available data which spans the range of two-phase flow, i.e. the wet gas region as defined in Section 2.2 but also a large amount of data outwith this range as well. The value of 'C' could therefore be improved upon for the case of wet gas flow if wet gas data only was used for the correlation. It is also worth while noting that Murdock used several different fluid combinations so this also reduces the accuracy of the equations for wet natural gas flow.

In 1977 Chisholm published a research note [32] in which the case of high quality flows (i.e. including wet gas flows) were discussed. For flows where the Lockhart-Martinelli parameter is less than unity, $X < 1$, (this includes the wet gas range) Chisholm proposes the use of the equation:

$$C = (\frac{\rho_l}{\rho_g})^{\frac{1}{4}} + (\frac{\rho_g}{\rho_l})^{\frac{1}{4}}$$ (2.22)

for use in equations (2.16) and (2.17). Therefore the resulting equation for the gas flowrate is:

$$m_g = \frac{K_g Y_g A_t \sqrt{2\rho_g \Delta P_{tp}}}{\sqrt{1 + \left(\left(\left(\frac{\rho_g}{\rho_l}\right)^{\frac{1}{4}} + \left(\frac{\rho_l}{\rho_g}\right)^{\frac{1}{4}}\right)\left(\frac{1-x}{x}\right)\sqrt{\frac{\rho_g}{\rho_l}}\right) + \left(\frac{1-x}{x}\right)^2\left(\frac{\rho_g}{\rho_l}\right)}}$$ (2.23)

In terms of m_{total} equation (2.23) becomes:

46

$$\dot{m}_{total} = \frac{1}{x} \left(\frac{K_g Y_g A_t \sqrt{2\rho_g \Delta P_{tp}}}{\sqrt{1 + \left(\left[\left(\frac{\rho_g}{\rho_l} \right)^{\frac{1}{4}} + \left(\frac{\rho_l}{\rho_g} \right)^{\frac{1}{4}} \right] \left(\frac{1-x}{x} \right) \sqrt{\frac{\rho_g}{\rho_l}} \right) + \left(\frac{1-x}{x} \right)^2 \left(\frac{\rho_g}{\rho_l} \right)}} \right) \tag{2.24}$$

This final form of the equation will be compared with other correlations and the results discussed later in this thesis.

2.5.1.1.1.4) The Smith and Leang Equation

The Smith and Leang equation [33] is using a different approach to that of the other four relevant wet gas Orifice Plate Meter correlations as it uses the concept of the "Blockage Factor". The single-phase orifice flow equation for gas:

$$\dot{m}_{gas} = K_g Y_g A_t \sqrt{2\rho_g \cdot \Delta P_g} \tag{2.1b}$$

can be modified to take account of the blockage by the liquid by introducing the blockage factor 'BF':

$$\dot{m}_{total} = \frac{K_g Y_g A_t (BF) \sqrt{2\rho_g \Delta P_{tp}}}{x} \tag{2.25}$$

The blockage factor changes the total area of the throat (which is available to a single-phase gas flow, A_t) to the effective area available to the gas $(A_t(BF))$. Smith and Leang state that the assumed primary influences on the blockage factor are:

a) The volume of liquid in the gas flow and the associated phenomena of wakes behind drops (i.e. the correlation does take some account of entrainment) and in between waves on liquid films.

b) Additional blockage caused by liquid break-up for lower quality flows and this is therefore of less importance to the measurement of wet gas flows (i.e. high quality flows).

Smith and Leang point out that the first influence (and the prime influence for wet gas metering) suggests that the relationship between the BF and quality (x) may be linear. However, it is also mentioned that the second influencing factor is significant for flows with changing flow patterns and as wet gas flows are reported to have more than one flow pattern this second effect can not be completely ignored. Its effects though, reduce rapidly as the quality increases.

From these reasons Smith and Leang postulated a linear relationship between the quality, x, and the blockage factor, BF, for high quality flow, with the higher the quality the smaller the blockage effect. However, the situation will become more complex as the quality reduces to below a critical value where a separate correlation may be required. However this does not become a real issue until qualities far below that of wet gas exist.

Smith and Leang chose to form a correlation for qualities above 10% (i.e. $x = 0.1$), evidence that they certainly did not consider the second mentioned influence of the blockage factor as significant for the extremely high qualities that wet gas is defined at.

The correlation is of the form:

$$BF = C_1 + C_2 x + \frac{C_2}{x^2} \qquad (2.26a)$$

The form of the Smith and Leang correlation was chosen by consideration of the flow phenomena. The first two terms represent the expected linear relationship between BF and x. The third term represents the increasing influence of the additional blockage caused by liquid blockage at lower qualities. The third terms exponent was simply an estimate.

Using orifice plate data from Murdock [30] (with some data in the wet gas range) and data from James [20] (with no data in the wet gas range) the following equation was fitted:

$$BF = 0.637 + 0.4211x - \frac{0.00183}{x^2} \qquad (2.26b)$$

The second term shows the linearity of the relationship between the BF and x at high quality flow conditions. It can be seen that for high quality flows the third term has little influence and only becomes significant at qualities far below the minimum limits of the wet gas definition.

Again, as with the previous correlations, it was not created with wet gas flow measurement specifically in mind. (All the data was for steam / water). Some of the experimental data used does overlap the wet gas region but other data used does not. This is the likely reason why at extremely high qualities (i.e. wet gas flows) equation (2.26b) gives Blockage Factors slightly in excess of unity which of course does not match the theory. The final equation formed by Smith and Leang for total mass flow of a two-phase flow is:

$$\dot{m}_{total} = \frac{K_g Y_g A_t \left(0.637 + 0.4211x - \dfrac{0.00183}{x^2} \right) \sqrt{2 \rho_g \Delta P_{tp}}}{x} \qquad (2.27)$$

It is clear that, like the rest of the two-phase flow metering correlations, there is a need for more wet gas data so that more accurate wet gas correlations can be produced without the significant errors introduced by the use of wide ranging data sets. This correlation is compared with others later in this thesis.

2.5.1.1.1.5) The Lin Equation

Prior to publishing the review "Two-Phase Flow Measurement with Orifices" [21], Lin presented a paper detailing his contribution to the subject and presenting a new correlation [34].

Lin assumes the phases flow separately. Like the other correlations, standard assumptions are made, i.e. the phases are considered incompressible, no thermodynamic effects are significant (so there is no mass transfer between phases), and the pressure drop of each phase through the orifice is the same as for the two-phase flow. In fact, Lin's analysis is very close to Murdock's analysis except he includes the effect of shear between the phases. The correlation Lin provides is:

$$\sqrt{\frac{\Delta P_{tp}}{\Delta P_l}} = \theta(1-x) + x\sqrt{\frac{\rho_l}{\rho_g}}$$

(2.28)

Where:

$$\sqrt{\Delta P_l} = \frac{\dot{m}_{total}}{K_l A\sqrt{2\rho_l}}$$

(2.29)

The function 'θ' is the correcting factor for shear effects. From theoretical considerations Lin shows θ is solely a function of the density ratio. It is clear that in effect, although he does not state as such, Lin has actually updated Murdock's equation to account for shear forces and has therefore advanced this equation to obtain a similar conclusion as Chisholm.

From experimental data Lin plotted θ vs. (ρ_g/ρ_l) and fitted the following equation:

$$\theta = 1.48625 - 9.26541(\rho_g / \rho_l) + 44.6954(\rho_g / \rho_l)^2 - 60.6150(\rho_g / \rho_l)^3$$
$$- 5.12966(\rho_g / \rho_l)^4 - 26.5743(\rho_g / \rho_l)^5$$

(2.30)

For a given density ratio (set by the line pressure) equation (2.30) gives the correction factor, θ, and the total mass flow, $\dot{m}_{total}$, can be therefore be calculated using the following equation:

$$m_{total} = \frac{K_l A_t \sqrt{2\rho_l \Delta P_{tp}}}{(1-x)\theta + x\sqrt{\dfrac{\rho_l}{\rho_g}}}$$
(2.31)

Like the other correlations previously discussed this correlation was not developed with wet gas flow specifically in mind. This is clear from the fact that equation (2.29) uses ΔP_l instead of ΔP_g which would be better for wet gas flow analysis. Even so, Lin's equation is deemed suitable for investigation as a possible wet gas flow measurement correlation as the experimental data range covers the defined range of wet gas flow. However, as in the other correlations much of the experimental data was at conditions far from wet gas conditions with fluids of quite different properties to wet natural gas (although Lin states that the density ratio is all that matters). Lin used R-113 (a refrigerant) for his experiments and included other researchers steam/water data. Unfortunately, not all the data used to find the θ function was from standard orifice meter tests. On a positive note, the data used included very high pressures (7.72 bar $\leq$ Pressure $\leq$ 188 bar), some wet gas quality flows, pipe diameters of 0.7" to 7.8", and orifice sizes of 0.4" to 5.6". Lin's correlation is compared with the other correlations and the results are discussed later in this thesis. Again the full derivation is given by this present author in [58].

2.5.1.1.1.6) A Note on the Work of V.C Ting, E.H. Jones and J.J.S Shen

As previously stated only Ting and Jones have published any significant work on wet gas flow through Orifice Plate Meters since Lin's review in 1986 [21]. In [35] and [36] it is stated that, from experiments with Orifice Plate Meters using air and water as the working fluids at relatively low line pressures, the meter under-reads the gas flow. This statement contradicts the conclusions of the other researchers discussed earlier.

It is generally accepted by many engineers that the presence of a small amount of liquid in a gas stream causes the differential pressure meter to over estimate the actual gas mass flowrate. This condition is often called "over-reading". The reasoning behind

this belief is as follows. As DP Meters use the pressure drop across the meter to predict the flowrate, when the higher velocity gas passes the slower velocity liquid it imparts energy to the liquid and the gas phase therefore losses more energy accelerating through the meter than it would do if it flowed alone. With the resulting larger pressure drop read by the meter, without correcting for this liquid effect, the meter will over estimate the gas mass flowrate (or "over-read").

The correlations discussed above predict that without any correction the meter will over-read. Ting and Jones are alone in stating that the liquid causes the meters to under-read. However, it must be noted that Ting is looking at the specific problem of wet gas flow and not general two-phase flow like the other work and therefore Ting's results should not be disregarded. No correlation was offered by Ting et al. and the papers simply state observations of wet gas experiments where air/water and wet natural gas were the flowing fluids. He concluded that more research needs to be done. Ting did not attempt to give any explanations of his data, but in the papers by McCrometer [7] and [8] it is suggested that the Orifice Plate meters under-reading in wet gas flow could be caused by the accumulation of liquid upstream of the plate. This clearly shows that a full understanding of the phenomena involved in wet gas flow through restrictions is not yet available.

2.5.1.1.2) The Nozzle Meter and Wet Gas Flow

It has been mentioned previously that the Nozzle Meter is not used by the Oil and Gas Industry and therefore no wet natural gas flow investigations have been undertaken for these meters. Only two published papers deal with two-phase flow through Nozzle Meters. These are "Metering of Wet Steam" by Chisholm and Leishman [39] and "The Flow of Air / Water through Nozzles" by Graham [40]. This second reference was unobtainable as it has been lost by the NEL.

In [39] Chisholm discusses the use of Sharp-Edged Orifices and Nozzles to meter general two-phase flows. The theory is the same as Chisholm's theory for Orifice Plate Meters (as described in Section 2.5.1.1.1.3)) but this time only Nozzle data was used and a value for the parameter C (defined by equation 2.19) was attained for

Nozzle Meters. However, Chisholm indicates that there is not enough data for the analysis to have any real accuracy. The data used was air and water at atmospheric conditions and Chisholm assumed this data matched wet steam at 0.365 MN/m^2, the pressure where the wet steam density ratio matched that of air / water at atmospheric conditions. From analysis a value of C = 14 was found for the nozzles, i.e. a considerably larger correction than needed for a Sharp-Edged Orifice Plate Meter. No mention of wet natural gas flow through nozzles was made and with no available data no investigation into the value of C can be conducted. Therefore, to develop a correlation for wet natural gas flows through Nozzle Meters a lot of testing would be required.

With the above exception, unlike the case for the Venturi Meter, no attempt has been made to use the Orifice Plate Meter two-phase correlations on Nozzle Meters to investigate their performance. As the Oil and Gas Industry engineers do not favour nozzles to meter flows, and it is extremely unlikely this situation will change, and no nozzles were available to the present author to test, Nozzle Meters will not be discussed further in this thesis. The present situation for Venturi Meters is significantly better than the Nozzle Meter situation.

2.5.1.1.3) The Venturi Meter and Wet Gas Flow

Significantly less work has been carried out in the field of Venturi Meter performance in two-phase flows than has been done for Orifice Plate Meters. However, much of the work that has been done stems directly from that done for Orifice Plate Meters. This work is split between papers dealing with useable correlations and mathematical models of the flow that are not directly applicable to current wet gas natural gas production flows as they require unknown parameters in order to operate (e.g. drop size, liquid film thickness etc.). These models are discussed in Section 2.5.2).

The papers on Venturi Meter performance with horizontal wet gas flows that have direct relevance to the Oil and Gas Industry are Refs.[1,3,4,5]. It is these papers that are discussed here.

All four relevant papers published on the flow of wet gas through Venturi Meters have come from Shell's Exploration & Production U.K. or Netherlands divisions with the latter working with the Dutch Gas Company NAM. The earliest two papers of the four are largely duplicates of each other [1,3] and they like, [4] do not offer any new correlations but investigate the possibility of extending the existing Orifice Plate Meter correlations to use with Venturi Meters. Only de Leeuw in [5] offers a correlation that is formed specifically for Venturis and offers an advance in the theoretical understanding of wet gas flow metering.

As previously stated [1] and [3] present the same research and are therefore effectively one paper. This paper discusses the results of a rare opportunity for test work on an actual off-shore wet gas production facility. The typical conditions were said to be between 80 and 100 bar and a liquid to gas ratio (LGR) of below 200 m^3/ $10^6 m^3$. They used the Orifice Plate Meter Correlations of Murdock and Chisholm and investigated their accuracy by using them with a Venturi Meter to calculate the gas flowrate of a controlled wet gas flow where the fluids were natural gas and water. Water was injected into the dry natural gas pipeline with a 100 mm ($\cong$ 4") diameter Venturi Meter through either a spray head at the pipe centre or through a wall tapping. The choice of injectors was aimed at investigating the influence the flow pattern has on the Venturi meter reading. (It should be noted here though that the authors simply assume that by injecting liquid into a dry gas line upstream of a meter by different methods you obtain different flow patterns at the meter inlet. This is not necessarily true. When liquid is injected into the gas the newly created two-phase flow will immediately enter into a flow pattern transition where it changes from the locally created flow pattern at the injector to the natural flow pattern for that set of line conditions. It is not yet known precisely how many pipe diameters downstream of the injector it takes for the flow pattern to become fully developed but during testing at NEL with different injection systems it was seen to be a relatively short distance. Hence, different injectors do not guarantee different flow patterns at the test location).

The effect on the meter reading of injecting the water was seen to be linear over the range tested (100-400 m^3/ $10^6 m^3$). However,.the gradient of the over reading to

the Liquid to Gas Ratio was seen to be slightly greater than those predicted by Murdock and Chisholm's correlations. As no difference with the method of injection was observed Washington concluded that "the liquid distributions in the line have no effect". This statement is therefore saying that the flow pattern has no effect on the meter readings. However, due to the results of the NEL tests conducted as part of this research showing the injectors to give the same flow pattern at the test section this author has reservations about this conclusion. At no point in the discussion of the results does Washington state that the flow pattern at the flow meter was actually known and therefore confirmed to be different for a given gas flowrate with different injectors injecting the same liquid flowrates. It is therefore possible that there was a long enough upstream length for the flow to have settled to its natural flow pattern for those pipeline conditions and hence the local flow pattern created by the particular injector system in use is irrelevant to the flow pattern downstream at the Venturi Meters inlet. The positioning of meters in off-shore platforms is seldom ideal (i.e. long straight upstream lengths are not common due to space and cost considerations), the flow patterns through the meters can be in transition due to the pipework directly upstream and knowing the effect of different flow patterns is therefore extremely important. Further evidence of the lack of knowledge of the flow pattern is seen from the authors statement "...if the standard deviation exceeded 0.1%, the run was rejected and repeated because the flow conditions were considered unstable". This statement suggests that the flow pattern could be in transition at the meter position for certain injector conditions (i.e. choice of mass flow rate and injector type). It is possible however that in the cases of small standard deviations the pattern has reached its equilibrium before the meter inlet and the Venturi Meter reads the pressure differential caused by that particular flow pattern. It would have been very useful to know which flow pattern exists for specific flow conditions as without this information the usefulness of the results is restricted. For example, the over reading was observed to grow linearly with the LGR up until 400 m^3/ 10^6m^3. If more than one pattern was known to exist within the test range then, due to the results linearity, it could be concluded that the flow pattern has no effect on the over reading. Without this flow pattern knowledge no such statement should be made.

A further concern with this work is that the authors do not state how the meter is mounted. From diagrams in [1] and [3] it appears that it is metering vertical upflow. If this is the case the flow pattern in the meter is very important as it is possible that the flow pattern will not exist in horizontal flow (e.g. "churn flow") and the results would therefore not be relevant to horizontal metering.

Nederveen and Washington [1] concluded that the effect of entrained liquid on the reading of a Venturi Meter in gas service can be predicted and no influence of flow pattern was found. Although the present author is cautious about the second statement the first statement seems to be true. Even without knowledge of the flow patterns the over-reading results were seen to be not random but linear and only slightly higher than the predictions of Murdock and Chisholm for Orifice Meters. As Lin [21] has shown that all the Orifice Plate correlations suitable for wet gas give very similar readings for several fluid combinations in the wet gas range it can be expected that these other correlations will likewise give only a slightly smaller gradient than the test results. However there is not enough information given by these authors to plot these predictions to confirm this. Furthermore, as the Murdock equation was formed from data up to 63 bar with Orifice Plates this study by Shell expands the useable range of the correlation to include Venturis with natural gas / water up to 100 bar.

In [1] Nederveen discusses a rare field test. The opportunity arose when two offshore satellite installations that produced to a main platform started to produce all the flow from that main platform when the main well was shut for three months. Due to one satellite platform having an undersized separator it had a liquid carry over. It was assumed that the dry gas flow from the other satellite well had no measurement error (even though such measurements still have an uncertainty of ± 1 % the quantity of this dry gas flow was relatively small compared to the wet gas flow). Hence the accuracy of the Orifice Plate Meter reading the flow with LGR of 15-20 $m^3/ 10^6\ m^3$ could be compared to the known flow leaving the main separator on the main platform. The results were an over-reading of approximately 3.5%. Nederveen says this agreed with the over-reading found by the Venturi tests in the same paper. It is not made clear however how this conclusion is reached. If ± 1% uncertainty is allowed for the dry gas measurement then the over-reading of 3.5 % means the effect

of the entrained liquid must be at least 2.5%. Given that the liquid content was known to be 15-20 m^3/ 10^6 m^3, according to the graph showing the Venturi test results, the over-reading due to this liquid content is in the region of +1%. As the raw test data is not offered, no deeper investigation is possible.

2.5.1.1.3.1) "Liquid Correction of Venturi Meter Readings in Wet Gas Flow" by R. de Leeuw [5].

This paper is of great significance to researchers dealing with measurement of wet gas flow as it is presently the latest research published on the development of a correlation for use with high pressure natural gas in a horizontally mounted Venturi Meter. The paper presents a new empirical correlation to predict the over-reading of a Venturi Meter measuring a wet natural gas flow. de Leeuw states that "The new correlation differs fundamentally from the well known Orifice Plate correlations of Murdock and Chisholm in that the observed dependence on the gas Froude Number is accounted for and the pressure dependence is verified from 15 bar to effectively dense phase conditions[4]".

In his introduction de Leeuw states that the results of the analysis of the Coevorden field data discussed by Washington [42] did not tell the whole story. de Leeuw claims that the fact that both the Murdock and Chisholm equations give good results at 90 bar, with up to 4% by volume liquid fraction, is a coincidence as extrapolation shows that for other line pressures Murdock's and Chisholm's methods do not agree (i.e. the existing correlations give varying predictions at high pressures). de Leeuw also states that the Venturi Meter has a higher over-reading than the Orifice Plate Meter. It is also pointed out that the experimental test range at Coevorden was relatively limited. That is, although natural gas at high pressure was used there was little variation in the pressure and the flow conditions were all located in a small part of the Shell Expro flow map, which indicated stratified wavy flow with no entrainment.

---

[4] "dense phase conditions" is a term used to describe the situation when the line pressure is causing the gas density to be equal to the liquid density in a two-phase flow.

Two points are of interest here. Firstly, for the first time a paper in the literature is clearly indicating that the particular flow pattern existing in the pipe is of direct importance to the over-reading by a Differential Pressure Meter and allowance can and should be made for the particular type of flow pattern. Secondly, it is of interest to know that the flow pattern in the Coevorden field test was "wavy stratified", as apart from indicating that Shell Expro must have a method for predicting the flow pattern in field pipelines, it also suggests a reason for the slightly larger over-reading occurring in these tests than the existing correlations predict. This has not been mentioned by Shell Expro's authors. Nederveen [1] & Washington [3] found that the Venturi Meter had a slightly greater over-reading than the Murdock and Chisholm correlations predicted but did not offer any reasons other than that the correlations were for Orifices under different conditions. It should be noted here that both Murdock and Chisholm assumed a separated (i.e. stratified) flow pattern, which of course is similar to stratified wavy flow. As stated earlier, it is widely believed that liquid content in a gas flow causes a Differential Pressure Meter to over-read due to the gas flow losing pressure having to drive the liquid along with it. It is possible that the extra pressure loss caused by the liquid presence will be slightly greater for wavy stratified flow than for stratified flow as an extra pressure loss is incurred by the local gas flow at the fluid interface as the gas expands and compresses as it flows over each wave. This would help to take account of the slightly higher over-reading found during the Coevorden field tests.

de Leeuw's new correlation was formed from data taken from the Coevorden field and from a comprehensive test series carried out at Trondheim in the SINTEF Multi-phase Flow Laboratory in Norway. This test apparatus allowed the effect of a wide range of pipeline conditions to be investigated. However one problem was that the fluids were not wet natural gas fluids but simulant fluids. (It is not unusual for experimental apparatus to use simulant fluids instead of natural gas due to the extremely hazardous nature of natural gas). The choice of fluids used at Trondheim was Nitrogen and Diesel Oil. No explanation for this choice was offered in the paper and nor were any properties of the Diesel Oil used. However, the present author agrees with this choice because a study of how to compare simulant fluids to wet

natural gas fluids has been carried out (see Appendix 1) and a Nitrogen / Hydrocarbon Liquid was seen to be the best that could be achieved. As the lighter the hydrocarbon liquid the more hazardous it is, diesel oil is probably the lightest hydrocarbon liquid allowable at Trondheim. It should also be noted that, like many other papers dealing with wet gas, de Leeuw did not attempt to define the term "wet gas" but from the test data range it can be seen that the correlation de Leeuw formed is suitable for the definition of wet gas given in Section 2 and also a wider range of Liquid to Gas Ratios (LGR).

According to the Shell Expro Flow Pattern Map presented in de Leeuw's paper, the Coevorden field had mostly stratified flow (although the text says "stratified wavy") and the Trondheim tests were varied between stratified and annular flow patterns. (See Figure 2.5).
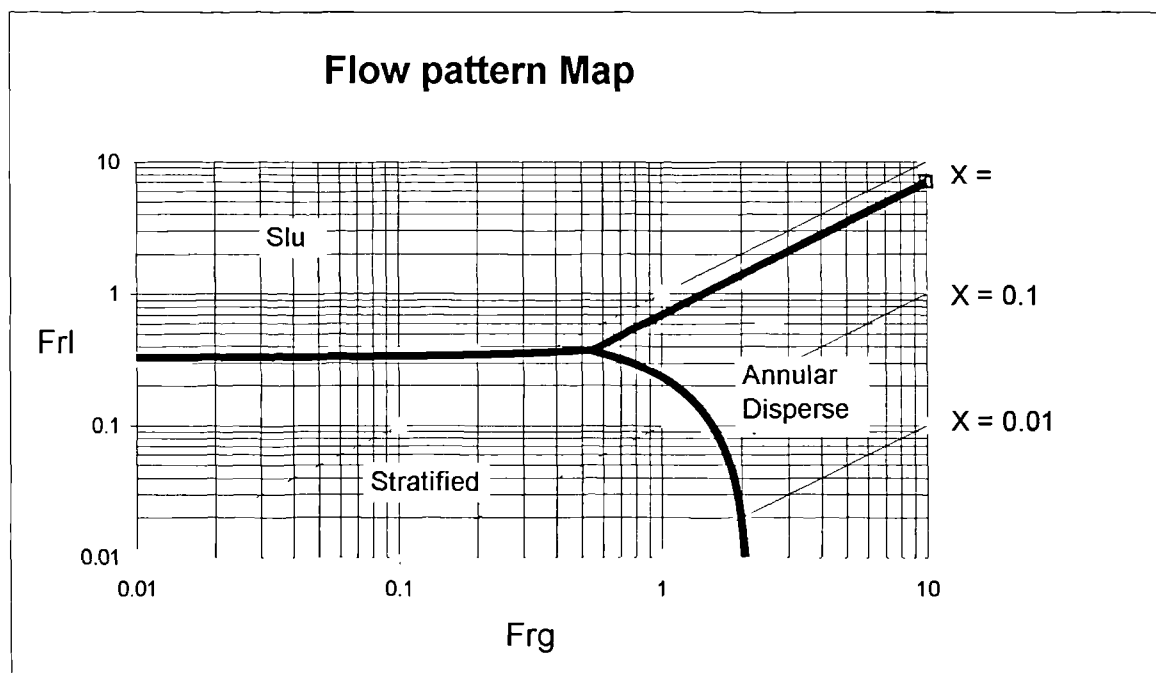
Figure 2.5 - Shell Two-Phase Flow Map

R. de Leeuw's analysis of the full data from both Coevorden and Trondheim led to some important advances in the understanding of wet gas flow through Venturi Meters.

Firstly, the data agreed with the theory that liquid content in a gas flow causes the Venturi meter to over-read. It was observed that as the line pressure increased for a set LGR the size of the over-reading reduced. (Note here that the line pressure and the gas density are directly linked).Thus, as the lowest line pressure tested (15 bar, which is therefore the minimum limit for the correlation) the greatest over-reading was obtained for a given value of the modified Lockhart / Martinelli parameter, 'X', i.e. the lower the line pressure the greater the gradient for Over-reading vs. 'X'. de Leeuw reports finding that as the line pressure was increased this gradient reduces to a constant as dense phase conditions are reached. (See Figure 2.6).

The next finding de Leeuw discussed was his discovery that for any set line pressure the over-reading depends on the gas velocity (or in other words, for a set pipe diameter, the over-reading depends on the gas Froude No.), i.e. de Leeuw is concluding that the gradient of over-reading vs 'X' is not only dependent on line pressure, but also on the gas velocity. That is, it is claimed that for a set pressure, varying the gas velocity for a given modified Lockhart Martinelli Parameter varies the over-reading. As an example de Leeuw offers a graph reproduced in Figure 2.7.

It is claimed that the lower the line pressure, the larger is the effect of varying the gas velocity on the over-reading. Therefore, what de Leeuw is saying is that the higher the line-pressure, the smaller the over-reading caused by a set amount of liquid (i.e. set 'X') at a set gas Froude No. and the smaller the effect of varying the gas velocity. It is this discovery, that the over-reading is dependant on the gas velocity, that allowed de Leeuw to form a new correlation. The paper points out that neither Murdock nor Chisholm took direct account of this in their theoretical development of the problem and their correlations are therefore of restricted use.
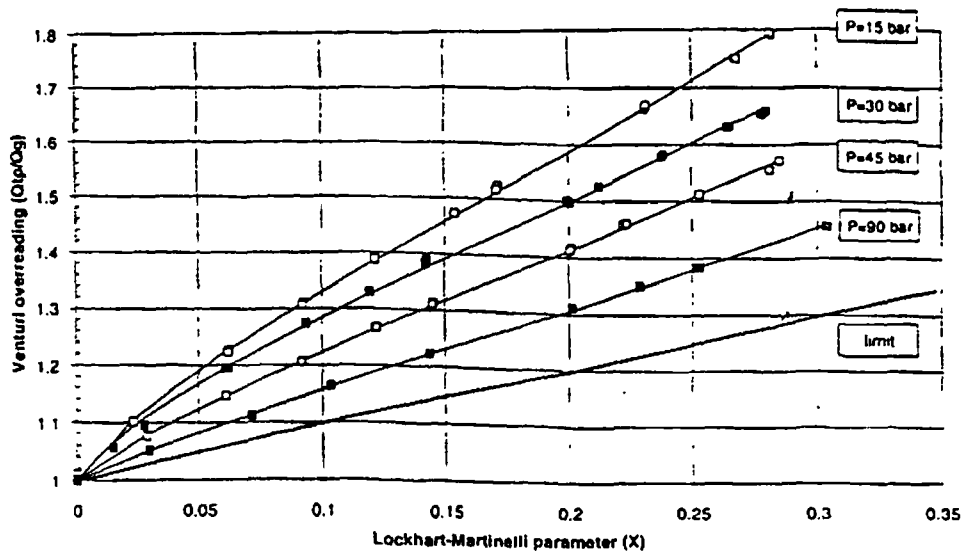
Figure 2.6 - de Leeuw's graph showing the Venturi over-reading against liquid fraction being dependant on the line pressure.
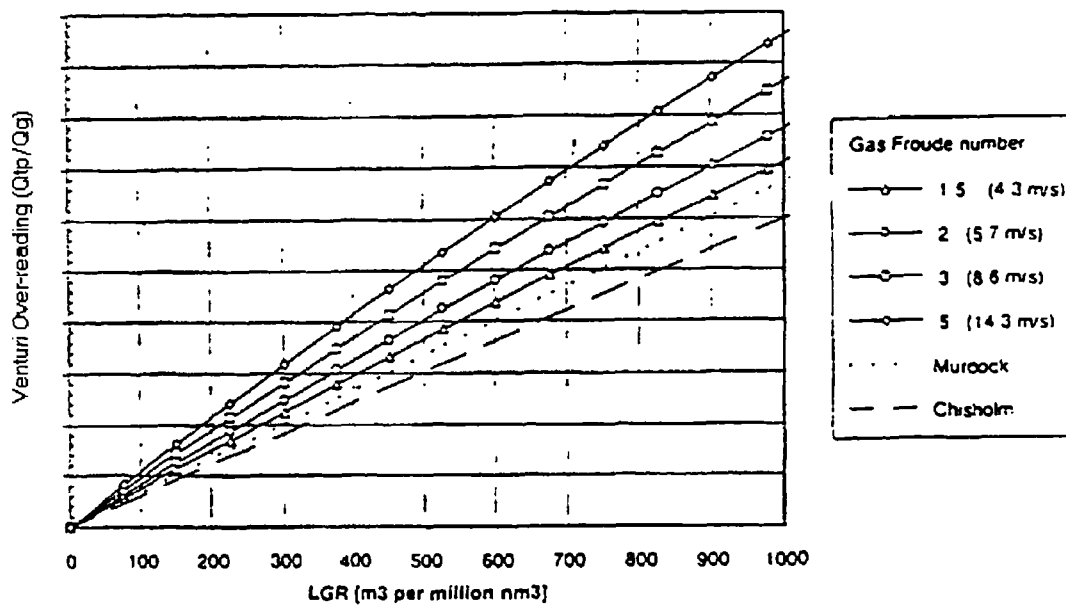
Figure 2.7. Typical test results showing the Venturi Meter over-reading at 45 bar and two different gas velocities.

The correlation de Leeuw presented is as follows:

$$\frac{Q_{tp}}{Q_g} = \sqrt{1 + CX + X^2}$$

(2.32)

where Qtp is the erroneous volumetric flowrate value that the meter will predict if no correction for the effect of liquid is made.

where

$$C = \left(\frac{\rho_l}{\rho_g}\right)^n + \left(\frac{\rho_g}{\rho_l}\right)^n$$

(2.33)

and

$$n = 0.606\left(1 - e^{-0.746 Fr_g}\right) \quad \text{for} \quad Fr_g \geq 1.5$$

(2.34)

$$n = 0.41 \quad \text{for} \quad 0.5 \leq Fr_g \leq 1.5$$

(2.35)

Figure 2.7 shows de Leeuw's correlation compared to the correlations of Murdock and Chisholm. The limits of the experimental data used and therefore this correlations limits are:

Line pressure must be 15 bar or above (this corresponds to gas density of 17 kg/m^3 or above), Gas Froude No. above 0.5 and Lockhart-Martinelli parameters 'X' of up to a value of 0.3.

It should be noted that de Leeuw calculates the value of 'X' using the following equation:

$$X = \sqrt{\frac{\Delta P_l}{\Delta P_g}} = \frac{Q_l}{Q_g}\sqrt{\frac{\rho_l}{\rho_g}}$$

(2.36)

This equation only holds true if an unmentioned assumption de Leeuw makes is correct. Equation (2.36) is simply the liquid and gas volume flow rate equations with the assumption that $K_l \cong K_g Y_g$. It is reasonable to assume that both the discharge coefficients will be close to unity for natural gas flows. For the case of Y_g the assumption only holds for cases where the pressure differential is small. This is the case for wet gas metering in field conditions but the necessity for a relatively small differential pressures is a limitation of the correlation never the less.

It is immediately noticeable to any engineer familiar with the Chisholm correlation that the form of these equations are identical. It is the fact that Chisholm's suggested exponent of 0.25 for wet gas flow in equation (2.22) has been replaced by a function of the gas Froude No. that separates the correlations. However, this small change seems to be a significant one as incorporating this function into the correlation allows for the apparently important effect of the gas velocity to be accounted for. The functions for 'n' (equations (2.34) and (2.35)) above was formed with Venturi meter data only and so, unlike Chisholm's equation, de Leeuw's correlation applies explicitly for Venturi meters only.

The reason that Chisholm's form was chosen by de Leeuw was because (unlike Murdock's correlation) Chisholm accounted for a varying line pressure through the inclusion of the gas density term in equation (2.24). Thus, all that needs to be done to incorporate the new finding of the meters over-readings dependence on the gas Froude No. into Chisholm's correlation is to include this relationship while determining the correct value of C (see equation (2.19)). From examining the data from Coevorden and Trondheim de Leeuw could plot the liquid / gas density ratio vs C, an exercise which clearly shows that for each set value of gas Froude No. a value of 'n' can be selected to be accurate for the whole range of line pressure. In finding the value of 'n' de Leeuw found that one expression was not enough to cover the range of data. This is the reason that two expressions are given to cover the data range of Fr_g (equations (2.34) and (2.35)). The fact that two expressions were needed is of great interest here. As it has been stated earlier, this is the first paper to indicate that the flow pattern has an important bearing on the meter over-reading. It is interesting to note that the border between the two expressions (i.e. $Fr_g = 1.5$) coincides with the

densimetric flow map boundary between stratified and annular flow patterns. This point did not go unnoticed by de Leeuw and he suggests that the reason for this change is due to the levels of liquid entrainment in the gas flow. The lower gas Froude No. data were obtained from the field test at Coevorden and the higher gas Froude No. data was therefore from Trondheim. All the Coevorden data points, which lie in the stratified region of the flow map, gave a value for 'n' approximately constant at 0.41. The lowest gas Froude Nos. obtained from Trondheim, which overlap the Coevorden data, agree with this constant value but as the data points get further into the annular dispersed flow region the value of n starts to increase, as can be seen from equation (2.34).

This author agrees with de Leeuw's suggestion that the amount of entrainment is the key to the value of 'n'. de Leeuw does not share his reasoning behind the statement but this author's reasoning is as follows. While the two-phase flow remains in a stratified flow pattern the pressure drop component occurring in the gas flow causing the over-reading (i.e. the excess pressure drop above that of single-phase flow) is due to the shear force at the fluid interface that drags the liquid along with the gas and the reduction in available throat area due to the liquid blockage. If entrainment exists in this wet gas flow and the area available for the gas therefore further decreases for the same quantity of liquid flow the effect is the same as a reduction in the throat diameter of a Venturi in dry gas flow. Although the Shell flow pattern map indicates that the flow patterns at Coevorden and Trondheim are either stratified or annular, like all flow pattern maps these are not rigid statements. At the borders between any two patterns there exists a "transition zone". Although the map indicates that the Coevorden data was stratified flow de Leeuw states that it is stratified wavy flow. Similarly, although the map indicates that the Trondheim data is annular, as the gas velocity (or gas Froude No.) increases the term annular mist will be more accurate (i.e. the higher the gas velocity the more entrainment in the flow increases). To understand why the value of 'n' is directly proportional to the entrainment level the following facts need to be considered. As the pattern changes from stratified wavy to annular with little entrainment it is reasonable to expect the over-reading to remain fairly constant (i.e. the value of 'n' should be expected to remain approximately

constant, as it does). Of course, the surface area of the interface will increase but to counter that the adverse effects of the previously existing waves will have disappeared. However, as the gas velocity continues to increase more liquid flows as droplets in the gas core. The size of these droplets is difficult and complex to estimate (in fact there is no proven method in existence) but it is clear that even with a considerable number of relatively large droplets suspended in the gas core the reduction of the annular films thickness and any change in the surface area of this interface will be small. With these droplets in the core being dragged along by the higher velocity gas stream the amount of pressure drop suffered by the gas must be greater than when there is no entrainment and the more entrainment present then the greater the extra pressure loss in the gas and therefore the greater the Venturi over-reading. For a correlation to account for this phenomenon in annular mist flow the correction will have to increase its over-reading prediction as the entrainment level increases. As the value 'C' in equation (2.33) is the correction for a given value of 'X', it must increase with entrainment levels. As the correlation must work for any chosen value of line pressure, and therefore density ratio, it must be the value of 'n' that increases in line with entrainment levels as indeed it does in de Leeuw's correlation.

de Leeuw claims that his correlation gives results within 2% of the data he collected. As with most other papers on two-phase metering no attempt was made to check the proposed correlation with separate external data not used in the formation of the correlation itself. The reason, although not stated, is almost certainly due to the complete lack of available relevant data for such a comparison.

2.5.1.1.3.2) A Modified Murdock Equation for Venturis in Wet Gas

It has always been clear to the Natural Gas Production Industry that the use of the original Orifice Plate Meter general two-phase flow Murdock Equation to correct wet gas flow Venturi readings cannot be as accurate as a correlation developed specifically with wet gas Venturi data. The continued use of the original Murdock Equation was due to the lack of wet gas Venturi data in order to update the Murdock constant (M). However recently, Phillips Petroleum collected data (which they did not

publish) from a Venturi installed in a wet natural gas flow at 45 bar at Della Well in the North Sea. (The flow rates were not released.) From this data they found that for the specific case of wet natural gas at 45 bar with Venturis the Murdock Constant is not 1.26 as stated for Orifices but 1.5. Therefore, the final correlation to be mentioned here is the unpublished Venturi correlation called the Venturi Murdock Equation. It is in fact Equation 2.14 with the constant M changed from 1.26 to 1.5 :

$$
\dot{m}_{total} = \frac{K_g Y_g A_t \sqrt{2\rho_g \Delta P_{tp}}}{x + 1.5(1-x)\left(\dfrac{K_g Y_g}{K_l}\right)\sqrt{\dfrac{\rho_g}{\rho_l}}}
\tag{2.37}
$$

2.5.1.1.4) The V-Cone and Wet Gas Flow

In May 1997 McCrometer Inc. released a paper describing work conducted by "The Southwest Research Institute" (or "SwRI") to examine the behaviour of V-Cone Meters in wet gas flows [7]. McCrometer Inc. are interested in the measurement of general wet gas flows and state steam and unprocessed natural gas flows as examples.

As has been discussed earlier there is a considerable body of work regarding the effects of liquid content in gas flows on Orifice Plate Meters but less for Nozzles and Venturi Meters. Naturally, as the V-Cone is a much more recently developed meter and is patented by McCrometer Inc. there has been no independent research into the V-Cone Meter wet gas flow performance. Therefore, [7], and the associated [8] are the only work available on the subject of V-Cone meter performance with wet gas flows.

The test matrix used consisted of testing three sizes of V-Cone Meter in a horizontal 4" pipe. The choice of fluids was nitrogen and water. No explanation for this choice was offered. However, although this choice can be seen to be a poorer model for simulating natural gas than a nitrogen / hydrocarbon combination (see Appendix 1) it must be remembered that this report was investigating general wet gas flows and was not therefore concentrating on the specific problem of high pressure unprocessed natural gas flows. This point is further emphasised by the fact that data

for only two line pressures were taken (2.0685 and 7.5845 bar), both being far below normal gas field operating pressures. The range of liquid content in the gas flow, given in terms of the "liquid mass fraction", (i.e. the ratio of liquid mass flow to the total mass flow) was 0% to 5%. This is therefore within the range of this researches definition of wet natural gas flow.

The test facility used for these V-Cone tests was similar to those used for the other wet gas flow testing of DP Meters previously mentioned. One point worth noting is that the liquid injection point, a simple pipe inserted into the gas pipe, was positioned 59 pipe diameters upstream of the test meter to allow the flows natural flow pattern to exist at the test piece. Naturally, as McCrometer were looking at the general case of wet gas flow metering attempting to recreate the typical flow patterns present at a meter in an actual natural gas field was not their aim. It is interesting to note however that the reported stable flow patterns attained by the facility were stratified-wavy and annular-mist, exactly the flow patterns Shell Expro claim to be present in the Coevorden natural gas field [5].

The results of these V-Cone Meter tests are presented in [7]. From them McCrometer formed several conclusions, which this author considers to be somewhat premature as much more testing is required to confirm them. These results do not adversely affect the possibility that the V-Cone Meter could be developed into as accurate a wet gas meter as any other DP meter, but to predict the behaviour of the V-Cone Meter in high pressure wet natural gas flows much more extensive testing using higher line pressures and flowrates, as well as more suitable simulant fluids or actual wet natural gas, needs to be undertaken.

The first conclusion stated is that ".... the V-Cone meter is capable of measuring the gas flow rate when small amounts of liquid are entrained in the gas stream". It is clear from the plots of the experimental results that the liquid presence does have an important bearing on the V-Cone's readings. The relationship between the flow quality, line pressure, gas flowrate and the geometry of the V-Cone meter is clearly a complex one. In general, for lower Liquid Mass Fractions (LMF< 3%) it is true to say that the liquid causes an over prediction of the gas flowrate. However from the experimental results it is not clear how a correlation could be formed as no trend can

be seen from the various graphs of meter error vs. LMF for different sized meters at the two line pressures used. For example, for the largest meter tested ($\beta = 0.45$), the higher the gas flowrate the larger the error for a given LMF, but for the smallest sized meter ($\beta = 0.67$) the situation was reversed. Also complicating the situation is the fact that at higher values of LMF some lines (i.e. flowrates) on these graphs which always start with a positive gradient, change to a negative gradient and the lowest flowrate line (LMF > 4%) actually gives an under-reading.

McCrometer do point out in their conclusions that even though a correlation predicting the V-Cone performance in wet gas flows is not yet obtainable the results obtained showed that even with this lack of ability to predicting the precise meter error for the cases of the two larger meters the maximum error up to 5% LMF is less than 1%. However, they concede that more tests need to be carried out in order to be certain that the error would be still less than 1% for flow conditions outside these test parameters (like wet natural gas flows).

Another valid point put forward in the report is that although no correlation for the V-Cone is offered, most wet gas flow correlations require knowledge of the flow quality, and that in many practical measuring situations it is not known. Therefore, McCrometer argue that the best that can be done is to select a meter that is known to have a maximum error of say 'x' % up to the maximum expected value of LMF for that particular flow. Then the uncertainty of the measurement would simply be 'x' %. To obtain the necessary information on which meter has the minimum error in particular flow conditions, many more experiments would need to be conducted. However, it is unlikely that the Oil and Gas Industry would be willing to accept such a solution as even a small error can lead to the 'loss' of large quantities of gas, and therefore money, over time, so their aim is to reduce the error to a minimum by finding the liquid content and then employing the most accurate correlation known. For the V-Cone Meter to be of any real use to the Oil and Gas Industry research on its performance in wet natural gas flows would have to be carried out to the extent that a reliable correlation could be developed.

It should also be noted here that [7] includes experiments aimed at finding any relationship between the meter accuracy and individually, the gas Reynolds No., the

differential pressure and the flow pattern. For all three cases the data obtained from the experiments did not indicate any clear relationship between the meter accuracy and any of these parameters. The present author suggests that these parameters effects on the V-Cone meter readings need further investigation across the full range of flow conditions before the following conclusion; "For the V-Cone meter, it appears that the operating pressure, liquid mass fraction, gas flowrate, and the beta ratio all affect the meter measurement accuracy. The Reynolds No., the two-phase flow pattern and the meter differential pressure did not correlate directly with the gas measurement error" in [7] can be confirmed.

The last point made in the report that requires discussion is the fact that the experimenters found the experiments on the V-Cone meters difficult to repeat (i.e. when three identical runs were made one after the other McCrometer reported a "considerable scatter" in the data). The experimental apparatus was apparently not the reason for this as a similar test was carried out with Orifice Plate meters and as expected the repeatability was good (quoted at $\pm 0.05\%$). All McCrometer Inc. then state is that: "The V-Cone meter runs showed more variation. The beta 0.67 meter appeared to have larger variation in the reading repeatability than the other two meters". It appears inconsistent that the repeatability of the Orifice Plate meter should be stated and yet the repeatability for the V-Cone meter, the central point of the discussion, is not given. Without any other explanation, this omission in the report leads impartial engineers to conclude that the data on the V-Cones repeatability was not good.

No explanation could be given for this poor repeatability but it is reported that water was found in the downstream pressure tapping during meter removal. It is therefore possible that one reason the data did not show any trends allowing a correlation to be formed was because of the different plots not being repeatable and therefore not suitable for comparison with to each other. Only when repeatability is good can real comparisons between different flow conditions be formed and trusted.

2.5.1.2) Wet Gas Ultrasonic Meter Research Directly Applicable to Industry

In 1991 the Ultraflow Wet Gas Development Project aimed at "producing a multi-path ultrasonic flow meter that could operate and indicate flow rate within 1% of reading in a wet gas environment of up to 0.1% free liquid". The meter was also required to "... resist corrosion and be able to automatically recover from liquid flooding". Two reports were made of the work carried out, however the consortiums conclusions [44] and [45] are protected by commercial confidentiality. A paper on this topic was released by the consortium in October 1996 at a presentation given at the National Engineering Laboratories seminar on "The Measurement of Wet Gas" [6]. The conditions of the tests, the results and the conclusions of the consortium are as follows.

The three year project began with the commercially available BG / Daniel dry gas multi-path ultrasonic flow meter (transient-time type) and aimed to create a meter for measuring "wet gas" (which was defined as < 0.1% of volume free liquids) that would be acceptable to the regulatory authorities. The consortium claim that the wet gas ultrasonic meter demonstrated an ability to operate at liquid volumes up to 0.2% for stratified flow and 0.7% for mist flow with a 1% additional uncertainty. In developing this wet gas meter from the dry gas design several changes needed to be introduced.

The first main problem that had to be overcome was to design the transducers to survive and operate successfully in the extreme conditions they encounter in unprocessed wet natural gas flows. The existing designs would not survive due to the wide temperature range and possible exposure to H_2S (i.e. sour gas). The final wet gas transducer design withstood exposure to 2% H_2S at 180 bar but the upper temperature limit was restricted to 110°C and not the desired value of 150°C. It was also stated that these transducers were susceptible to failure due to the epoxy bonding failing when exposed to sudden pressure drops. The conclusion of the consortium was that care must be taken when de-pressurising the meter. However, it is not made clear what effect real gas line pressure fluctuations will have on these sensitive transducers (e.g. the periodic pressure surges that have been known to be powerful enough to buckle orifice plates). It should be noted that the DP meter does not have these

problems. The temperature limit of the DP meter is simply that of the metallurgical temperature limit (although thermal expansion of the pipe diameter and meter throat needs to be accounted for to avoid any errors) and rapid large pressure fluctuations have little effect on the Nozzle and Venturi meters.

Deposits on the surface of the transducers also affect the signal reading. Deposits tested in both dry and wet gas conditions were iron oxide, salt and light oil at various thicknesses. It is reported that the dry deposits had little effect on the signals received for thicknesses up to 0.5mm. However for wet deposits (oil or water) thicknesses of 0.3mm resulted in significant attenuation of the signals. This fact therefore led to the transducers being made flush with the pipe wall instead of receding into the ports so a scouring action between the gas and the transducer surface is created and the likelihood of any liquid deposits accumulating is therefore reduced.

The other major design change required to convert the dry gas ultrasonic flow meter for use in wet gas arises from the need to eliminate the phenomenon called "bridging". This phenomenon is caused by liquid entering the transducer port and creating a "bridge" between the transducers face and the metal pipework. The result is the effective shorting out of the signal. The reason for this is as follows. All materials have a property called acoustic impedance and an ultrasonic wave takes the path of least resistance, which is the material with the highest value of acoustic impedance (this is analogous to the case of electricity taking the path of least resistance). As the acoustic impedance values of metals and liquids are an order of magnitude greater than those of gases when a liquid bridge is present between the transducer face and the pipework the ultrasonic wave jumps across the bridge and travels round the circumference of the pipework taking an unknown uncontrolled path instead of the desired path across the gas flow. For this reason the wet gas ultrasonic meters have transducers with larger wall to transducer clearance (therefore making the transducer diameter smaller and unfortunately the signal proportionately weaker) and drainage channels are introduced to the transducer ports.

It is this problem of the acoustic impedance "mismatch" (i.e. the low acoustic impedance of gases compared to metals) that causes even the dry gas meter to have the transducers in direct contact with the gas flow, instead of at a remote location (i.e.

fixed to the external surface of the pipe). So for the case of gas measurement it is not possible to have a non-intrusive / non-invasive transducer (although the effect of the ports in the pipe wall will be small). However, for unprocessed natural gas flows this is not usually of great importance as the advantage of non-intrusive / non-invasive transducers is the reduction of head loss, an aim of little concern to the Oil and Gas Industry.

These considerations on wet gas ultrasonic meter design were used in the design and construction of the two six inch trial meters. The consortium then had one meter tested at the National Engineering Laboratories Wet Gas Loop where the aim was to closely control the simulated conditions. Air was used for the gas phase and water or glycol for the liquid phase. No reasoning behind the choice of these fluids was offered. The liquid injection system could either inject directly into the pipe to attempt to create stratified flow or through nozzles to attempt to atomise the flow to get mist flow. The consortium wanted mist flow as they believed this to be the typical pattern emerging from a primary separator and stratified flow to give the submerged chord a stringent flooding test.

The second meter was tested at Shell Expro's Bacton Terminal on natural gas with condensate where the flow quantity was dependent on the process plant requirements but real two-phase flow conditions existed. This meter was left to run on whatever gas was being transferred to the processing plant and its accuracy was compared to a reference meter upstream. Condensate was then injected downstream of the reference meter at a known rate to compare the wet gas readings with the reference meter in the dry gas flow. The maximum liquid to total volumetric flow ratio created was 3.75%.

The Bacton facility, unlike the old National Engineering Laboratory facility had the ability to determine the flow pattern. The consortium reported that the two flow patterns obtained at Bacton gave different rates of error increase for increasing liquid injection rates. The stratified flow pattern had a considerably higher error for a given liquid to gas ratio (LGR) than the mist flow.

Suspicions that the old National Engineering Laboratory facility only created stratified flow arose from two separate points. Firstly, the data points plotted on the same meter error vs. LGR as the Bacton data all fall astride the stratified flow fitted

Combined NEL / Bacton Data
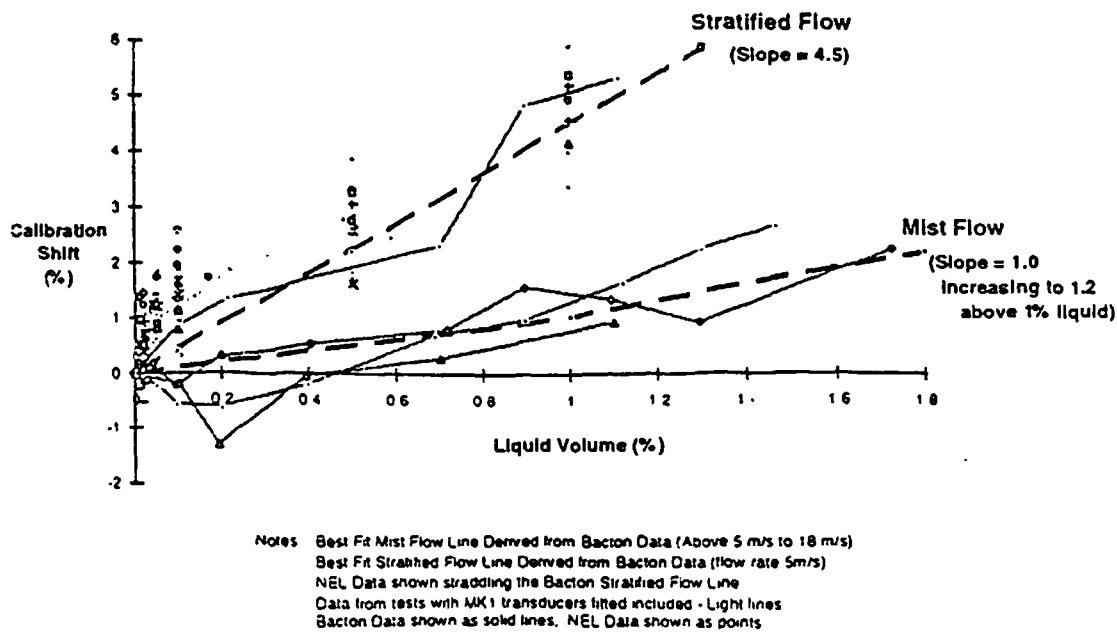
Figure 2.8 An Ultrasonic Meters performance in Wet Gas Flows. The Percentage Liquid by Volume is plotted against the Percentage Shift in Reading away from the correct Gas Flowrate (called the Calibration Shift here).

line created from the Bacton data which, as stated earlier, is clearly different to the mist flow data and associated fitted line. Therefore, the fact that both types of injection system used at the NEL gave such similar results (compared to Bactons stratified flow data) suggested that the NEL facility had stratified flow only. Secondly, the NEL data clearly showed that the rise of the LGR from 0%-1% gave a large error increase that did not occur at Bacton. (See Figure 2.8). The explanation offered for this coincides with this author's stated view that the fluid choice for simulating wet natural gas flows is extremely important and the fluid properties are one factor in dictating the flow pattern in particular conditions. The majority of papers on wet gas and general two-phase metering ignore this extremely important point. The consortium's explanation is as follows: as water has a considerably greater surface tension than condensate, and glycol has a considerably greater value of viscosity than condensate, both liquids will tend to coat the wall of the pipe to a much greater

73

degree than condensate and therefore a much thicker surface film will exist than for condensate. The report then points out that as even a small film of the order of 0.25mm thick makes a difference in the gas flow area of 0.65% for the six inch meter, a step increase in the meter reading of the order found could be expected. This is assuming that the consortium's report is referring to the increase in the gas flow velocity due to the relative flow area reduction, causing the meter to indicate a greater total gas flowrate (as the meter is set up to calculate for the total meter area). Hence, the meter has an over-reading for stratified flow as found by the National Engineering Laboratory tests and the stratified flow tests at Bacton. No mention of the effect that this film of liquid has on the transducers accuracy was given. However, it is clear from these considerations that water or glycol cannot simulate the behaviour of condensate.

Consequently, to examine the wet gas ultrasonic meter's accuracy in wet natural gas the consortium relied largely on the Bacton results. Over a period of one month the new wet gas meter configuration was tested in natural gas flow with no condensate injection, but with the inevitable periodic slugs. For the duration of the tests (which included a wide range of flow rates) the meter gave an accuracy better than 1% except for when rapid flow variations were occurring. The only problem in the performance mentioned by the consortium was meter flooding as discussed below.

The actual meter performance in wet natural gas was given as follows:
"In annular mist flow which occurred at 10 m/s, 15 m/s and 18 m/s flowrates it can be seen that the error was essentially directly proportional to the liquid content up to 1% liquid to total volumetric flow and the constant of proportionality only increasing slightly to 1.2 up to 2% liquid to total volumetric flow. Errors above 2% in mist flow become more erratic due to chord failures occurring and the meter resorting to substitutions on one or more chords. Even so the mean errors are still close to the liquid content".

For the case of stratified flow at Bacton the following was observed:
"In stratified flow the error curve tends to rise more rapidly than the liquid injection rate. In this flow regime which was encountered at 5 m/s the error rises rapidly with a mean constant of proportionality of 4 or 5". So, as stated earlier, when the condensate

flows in the stratified flow pattern the Bacton data is similar to the National Engineering Laboratory data.

An important question here is what percentage of wet natural gas flow metering situations in the real world have their particular flow patterns known with any certainty? If this information is not readily available how do the metering engineers know what the likely over-reading is? By the above account if the flow pattern is wrongly assumed a considerable error will occur. However, the long term survivability of these ultrasonic meters seems to have been proven.

The NEL tests on flooding the meter proved that the meter could drain and recover operations without any maintenance. For gas velocities greater than 2 m/s the meter was seen to recover within 3 to 4 minutes to within 1% of reading. Below this flowrate the recovery was much slower as the shear existing at the gas / liquid interface (the major draining mechanism) was much less. The other drainage mechanism is gravity as the meter in these tests was installed on a very shallow down slope. Furthermore, during the Bacton trial the meter was exposed to flooding when slugs passed through the pipeline. Again the meter resumed readings after draining with no manual intervention required. Visual inspection of the meter at the end of the trial showed that there were no mechanical problems caused by the flooding. However, there was one problem with the Bacton results. Although the meter did successfully drain with no intervention it was found that there was a significant change in the error when readings resumed. This has not been satisfactorily explained.

Along with flooding causing possible damage to the meter, another concern of the consortium was the liquid causing the chords to fail. (Chords are the available paths between each working pair of transducers that give information on the flows velocity field.) For mist flow where no chord was assumed to be submerged in liquid the meter operated successfully up to 0.7% LGR. Above this the chords started to fail. This is not a surprising result because as the LGR increases it is more likely that liquid will enter the transducer ports and cause bridging as stratified flow submerges the lower positioned chords. In stratified flow the failure of chords seemed to take place when the chord was submerged (almost certainly due to bridging). This conclusion comes from the consortiums comment that " ... the failure will be dependant on slippage and

therefore can occur at substantially lower levels [of LGR] at very low flow velocities", i.e. the lower the liquid film velocity the thicker the film is for a given liquid flowrate and the greater chance of a chord submergence.

The Consortium do not offer a correlation to correct the meter reading for the error caused by the liquids presence, however, like the case of the V-Cone meter, a maximum error for a maximum liquid content is declared.

The final conclusion of the consortium is that the meter design has been proven capable of operating and maintaining acceptable accuracy on natural gas / condensate applications beyond the original design aim of 0.1% LGR. In fact, for mist flows the uncertainty is found not to exceed an additional 1% up to 0.7% LGR and for stratified flows up to 0.2% LGR. The meter continued to function at reducing accuracy up to 4% LGR.

These findings allowed Daniel Industries Ltd. to offer a wet gas ultrasonic meter commercially and persuaded Philips Petroleum to install two Daniel 6" ultrasonic meters into an actual wet natural gas flow metering situation. In [59] Stobie discusses some results from these tests. In 1996 the above mentioned meter was giving a poor 6% uncertainty on the field trials. It was found that the new wet gas transducer design was not in fact practical for two reasons. Firstly, the reduced diameter of the transducer face meant a proportional reduction in signal power. Secondly, when examining the transducer face diameter and chord length ratio it was realised that the small wet gas transducers were spreading the signal much wider than the original dry gas design (i.e. the wet gas transducers had a half angle double that of the dry gas transducers). This meant some of the signal missed the opposite transducer further reducing the signal strength. Stobie then says these wet gas transducers were subsequently replaced with the original dry gas transducers in 1998 and claims the uncertainty caused by the liquid presence then dropped from 6% to 1%. Stobie makes no mention of any of the problems originally predicted to occur if these dry gas transducers were to be used in wet gas, actually occurring. However, he does not state how many chord failures happened per day before or after this alteration. It should also be noted that a new potential problem appeared when the upstream flow conditioner created hydrates that damaged a transducer. However, Stobie claims the

meter continued to work. He concludes by stating that the 1998 hourly data (460 points in total) has 91.2% of the readings within 1% uncertainty.

2.5.2) Academic Papers on Two-Phase Flow Metering Not Directly Applicable to Industry

There are a few papers that attempt to deal with two-phase flow through a Venturi Meter in a more in-depth manner than the previously mentioned papers. With the increase in sophistication of these models comes a reduction of their practical use as they inevitably require input parameters that are simply unknown to the field engineer. They are therefore not as yet applicable to industry but they are mentioned here as any discussion of Wet Gas Metering with Venturis would be incomplete with out discussing the most advanced mathematical modelling techniques attempted by researchers regardless of whether they are currently used in industry or if they are of academic interest only. These papers can be split between those of general mathematical modelling of two-phase flows through Venturis that have the aim of predicting the two-phase flow behaviour through the meter and those that discuss CFD work on the topic.

Most of the papers discussing mathematical models for two-phase flows through Venturis were created by Azzopardi et al. [15] to [19]. However, it should be noted that these models were not formed with wet natural gas metering in mind but rather Venturi Scrubber devices which are used to clean particles from gas flows. Nevertheless, the modelling attempts in these papers are still relevant to wet natural gas metering as Azzopardi models annular mist flow and attempts to predict this flows behaviour through the Venturi. In particular the possibility of predicting the liquid film flowrate, the film thickness and the pressure drop was investigated. Even though the industrial uses of Venturi Scrubbers means the fluids flowing, the pressures and the flowrates are all different to the wet natural gas metering case, Azzopardi still assumes annular mist flow as the inlet flow pattern and for the first time in the literature an attempt is made to mathematically predict the flow behaviour through the meter.

One of the biggest problems facing all engineers attempting to model two-phase flows through Venturi Meters is the lack of knowledge of the flow pattern at the meter inlet. That is, as the current methods of predicting the flow patterns for various flow conditions offer only a general prediction of the flow pattern type it is not possible to accurately calculate the desired information on liquid film thickness, wave size, liquid film to droplet ratio, entrainment and deposition of droplets etc. Without this information, any model of two-phase flow through a Venturi starts with these parameters being estimated and then further estimation of these parameters is required on the transient effect of the Venturi Meter. Azzopardi started this work in 1982 by investigating "Annular Two-Phase Flow in a Large Diameter Tube" [15]. The work was an attempt to predict the pressure drop and the entrained liquid flow rate in a constant area pipe. However, it should be noted that in this case Azzopardi considered upward vertical flow only which has quite different behaviour to horizontal flows. In 1983 this vertical upflow model was discussed in more detail in [16]. Here, Azzopardi discusses the methods of estimating parameters such as liquid entrainment rate and pressure drop. For the first time the effect of a constricting throat is discussed and a method of predicting the extra entrainment is offered that includes the effect of surface tension. Also here for the first time in Azzopardi's models, is a method of predicting the pressure drop component of the entrained drops although it is very similar method to the entrained model of El-Haggar and Crowe [66] briefly discussed below. The results of the comparisons made of model predictions and experiments are not of great interest here as the experiments are again for upward vertical flow. However what is of more interest are the modelling techniques used as it is possible they could be applied to horizontal flows. In 1985 Azzopardi and Govan presented a further advance in this work [17]. This time the experimental data was for vertical downwards flow so again the results of model prediction and experiment comparisons is not greatly relevant here but the further advance in the modelling is. In particular, Azzopardi and Govan now take more account of the waves on the film flow having a large effect on the entrainment mechanism and also of the extra entrainment that will occur at the converging section / throat edge of the Venturi. Problems of predicting drop size were also discussed. In 1988 Azzopardi et al.

published "An Improved Model for Annular Flow in a Venturi" [18] in which the previous 1-D models were further advanced to predict the pressure recovery in the diffuser as well as the traditional Venturi DP reading by taking into account the diffuser boundary layer. This model was compared to unpublished data so no further comment can be made here on the models performance with respect to horizontal flow. However, in 1989 Azzopardi presented an "Experimental Study of Annular Flow in a Venturi" [19] in which this model's comparison with the new data was discussed. This time the data was obtained from both horizontal and vertical experiments. (However, the pressure and flowrates were low and air and water were the fluids used so the experiments were still far removed from the reality of the wet natural gas production lines). In general Azzopardi et al. seemed satisfied that the model predicted the flow behaviour well. Of course that is not to say that it would work for the completely different conditions found in wet natural gas production lines. More research (and in particular more wet natural gas data) would be necessary before any conclusions on this matter could be formed. Unfortunately this model requires knowledge of the droplet size and as this is not obtainable from the NEL Wet Gas Loop no investigation into its performance was possible using data from the present research.

The other significant mathematical model for predicting two-phase flow through Venturis is the paper "Numerical Model for Disperse Two-Phase Steam/Water Flow in a Venturi" by S.M. El-Haggar and C.T. Crowe published in 1980 [66]. This model was created for steam / water flows and the flow pattern was considered to be totally dispersed (i.e. no annular film). The model is an attempt to predict the pressure drop across a Venturi with a known gas mass flowrate. Once this is achieved it should be possible to reverse the procedure in order to calculate the gas mass flowrate from the Differential Pressure. The model was formed by combining the gas and liquid mass flow equations with the quasi one-dimensional momentum equation. Like the Azzopardi models the major problem was the lack of knowledge of inlet conditions, in particular the droplet diameter. It should also be noted that this model was further complicated by including the thermodynamic effects on the fluids as the pressure and temperature changes in the Venturi. Such considerations led to the El-Haggar and

Crowe model being an iterative method. The final conclusion of El-Haggar and Crowe was that more research was required as their model was inadequate for general use since the drop size was seen to have a great influence on the pressure differential across the Venturi and this was not successfully predicted by their model. Although far from satisfactory, the Azzopardi models and the El-Haggar and Crowe model are the only annular / dispersed flow models in the literature.

Finally, before leaving the subject of academic papers on two-phase flow metering not directly applicable to industry a brief mention of the limited CFD work on this topic needs to be made. In 1998 an Elf EP project led by Couput was carried out by ONERA in France into the possibility of using CFD to predict wet gas flow through Venturi Meters [67]. After developing numerical code for wet gas flows based on existing solid particle / gas flow numerical code formed for combustion chamber analysis and running the model Couput et al. claimed that the results were "comparable with the empirical correlations published in the literature". However, similar to most other wet gas research they state "... this validation is incomplete because no detailed experimental work is available in the literature". By 2000 ONERA had a Wet Gas Test Facility commissioned that used air and water at up to 5 bar and gas and liquid flowrates of up to 650 m^3/hr and 250 l/h respectively. The pipe diameter was 100mm. Therefore, Couput et al. stated in [68] that after new experimental test data was compared to the CFD results it could be concluded that wet gas correlations have to be "sensitive to Froude Numbers, flow regimes and droplet size effects". They go on to say "... This indicates that there is no reliable correlation to correct Venturi measurements in wet gas flows with a good accuracy". This author agrees that the Froude Numbers, flow regimes and droplet size effects will be of importance but believes the second statement to be too sweeping and general. It is true that for all fluid combinations, flowrates, pressures, pipe and meter sizes etc. no one correlation will be effective but for the case of a known range of parameters falling within a correlations range there is no reason why that correlation would not be effective and give a good accuracy. Nevertheless, this author believes that further research and development of Wet Gas CFD work can only be good for the industry.

2.6) Comparison of the Differential Pressure Meter Correlations

Of the four Differential Pressure (DP) Meter types available to industry no comprehensive comparison of performance in wet natural gas flows have been carried out. The usefulness of the existing Differential Pressure Meter two-phase correlations with respect to their use with Venturis in wet gas flows is still not proven as not enough wet natural gas flow data exists that can be trusted to be accurate and independent of the correlations formation. Only the Orifice Plate has had any comparisons in correlations published and even these comparisons were investigations into their performance in general two-phase flows of various fluid combinations.

So far, there are three papers which compare the accuracy of the correlations for two-phase flows through an Orifice Plate Meter. These papers however are not independent of each other. Smith and Leang [33] were the first to make a comparison between different correlations. The method they chose was to compare the values of the "root mean square fractional deviation" of each correlation for particular sets of data. This "root mean square fractional deviation" is denoted by 'd' and is calculated by the following equation:

$$d = \sqrt{\frac{1}{n}\sum_{i=1}^{n}\left(\frac{\dot{m}_{g(predicted)i} - \dot{m}_{g(experimental)i}}{\dot{m}_{g(experimental)i}}\right)^2}$$

where the subscript "predicted" is the two-phase mass flow predicted by a particular correlation and the subscript "experimental" is the actual two-phase mass flow known to be flowing in the test facility and n is the total number of data points used in the analysis.

The method of comparing the correlations is to select suitable experimental data and then calculate 'd' for each correlation and compare results. This is a valid approach and the same method was subsequently used in papers by Smith and Murdock [37] and Lin [21]. The approach was also used in the present study (see Chapter 4).

However, although the concept of the comparison is sound it only remains so as long as the choice of data for the analysis is suitable. L. T. Smith and J.W. Murdock had much to say on the data choice of R. V. Smith and J. T. Leang. In a discussion published at the end of [33] they explain that the data used is not valid as some of it does not conform to Orifice Plate ASME Standards (e.g. non standard tap locations) and other data used was taken from throttling, not metering, devices. Hence, Smith and Murdock accept the method as valid but point out that the actual calculations are not, so that the conclusions of Smith and Leang may not be correct.

In [37], Smith and Murdock carry out a comparison between two-phase flow correlations and clearly state that the comparisons are for when ASME Sharp Edged Orifice Plates are in use. The considered correlations were those of Murdock, James, Marriott and Smith and Leang. As stated in Section 2.5.1.1.1), of these four correlations, only the Murdock and Smith and Leang correlations are of significance to wet gas flow. In this work the same method of comparison as used in [33] was used. Unlike [33] this paper attempts to deal not only with a one component flow (steam / water), but also with various two component flows.

In choosing the experimental data to use in the comparison these authors pointed out that for various reasons much of the available data is unsuitable. This is because some data came from non-standard Orifice Plates and/or some data is only presented in graphical form and the error introduced by reading off graphs was considered too great to allow an accurate comparison of correlations. There is therefore little valid data available for which to carry out the correlation comparisons. The final decision of Smith and Murdock was to use the same data as had been used to actually form the empirical equations used in the correlations. Therefore, for the one component flow (steam/water) Murdock's nine relevant data points and James's twenty-five relevant data points were chosen. For the two component flow Murdock's other eighty-one points were used to check his own correlation. Naturally therefore, only a limited amount of information can be taken from this comparison. With this selected database a suitable procedure would be to take each particular correlation and find its root mean square fractional deviation using the data that is in the database that was not used to create the correlations empirical equation. However, this was not what was

done, all the data points were used to find the values of each correlations root mean square fractional deviation for the single component and two component flows. It is obviously desirable in any such situation to have an abundance of relevant data for use in any comparisons but by including the data that was used to originally form the empirical equation of a correlation they are not just recalculating the trivial result of re-proving the correlations accuracy but worse, these data points will 'dilute' any possible larger errors that could be discovered by using the rest of the truly valid data. With this point in mind the present author is not sure why Smith and Murdock chose to include these data points other than that perhaps the amount of data left over for analysis was seen as too small a quantity.

The third paper that deals with comparison of the correlations is the paper by Lin [21]. Curiously, Lin does not mention any problems with the selection of valid data for either paper (even though a discussion at the end of [33] clearly casts doubt on the validity of its conclusions) and he extensively quotes both papers conclusions. However, Lin also discusses his own correlation and chooses a different graphical method to present the comparisons. Instead of reproducing the root mean square fractional deviation on a graph, a plot of the square root of the ratio of the two-phase pressure drop to the total flow being liquid pressure drop ($\sqrt{\Delta P_{tp}/\Delta P_{ol}}$) vs. the quality ($x$) was made. The data used appears to be the experimental data Lin used to form his empirical equation (refrigerant R-113 was the working fluid) therefore the fact that Lin's correlation is seen to perform well here is no more informative nor surprising than for Murdock's equation in [37]. What is interesting about this comparison however is how the other correlations, which were all formed using other fluid combinations, behave. Lin presents two graphs, each at a specific line pressure (although it is stated as specific density ratios) with the following correlations plotted: The homogeneous correlation, The Murdock correlation, The Chisholm correlation, The James correlation, The Smith and Leang correlation and The Lin correlation. These graphs are reproduced as Figures 2.9a and 2.9b.

Like the other two papers that compare two-phase correlations the scope of the comparison is the whole spectrum of quality and no specific mention of wet gas flow is made. The results of Lin's comparison are as follows. The lower line pressure

examined shows that the Murdock correlation has a relatively large over-reading compared to the majority of the correlations at low quality but at high quality (i.e. wet gas flow) all six correlations give very similar results. It should be noted that the Smith and Leang correlation while agreeing with all the other correlations at high quality, diverges from the others at lower qualities and is not plotted at lower qualities. This is not a completely surprising result when the reasoning behind this correlations formation is considered [33]. For the higher line pressure case the same results are seen, The Murdock correlation is still poor for low qualities but converges with the other results to give a similar over-reading in the wet gas region. For this higher line pressure the Smith and Leang correlation is not plotted and no reason is given.

Although the accuracy of Lin's method cannot be tested using the same data as that which was used to form it Lin does go on to test the correlation against some independent steam/water data from Orifice Plate measurements from Ragolin [38]. The raw data of Ragolin was unobtainable from the British Library so the details regarding its suitability are not available. However, from the graph presented by Lin [21] the correlation does seem to give good predictions, although for the specific case of wet gas flow there is not enough detail on the plot to make any firm conclusions.

It can therefore be said that for the two line pressures examined by Lin all six correlations gave similar results for the wet gas flow region and these seem to give reasonable agreement with the given data points plotted. However, although the good predictions by all the correlations for the R-113 data is promising (as it shows the correlations working for other two-phase fluid combinations than those they were formed with) this is in no way conclusive evidence that these correlations will therefore extend to working satisfactory for Venturi metering of wet natural gas flows. It should also be noted that the experimental data used by Lin was for a pipe diameter of 1.25 inches which is considerably smaller than pipes transporting unprocessed natural gas from a well to a platform. It can however be concluded that
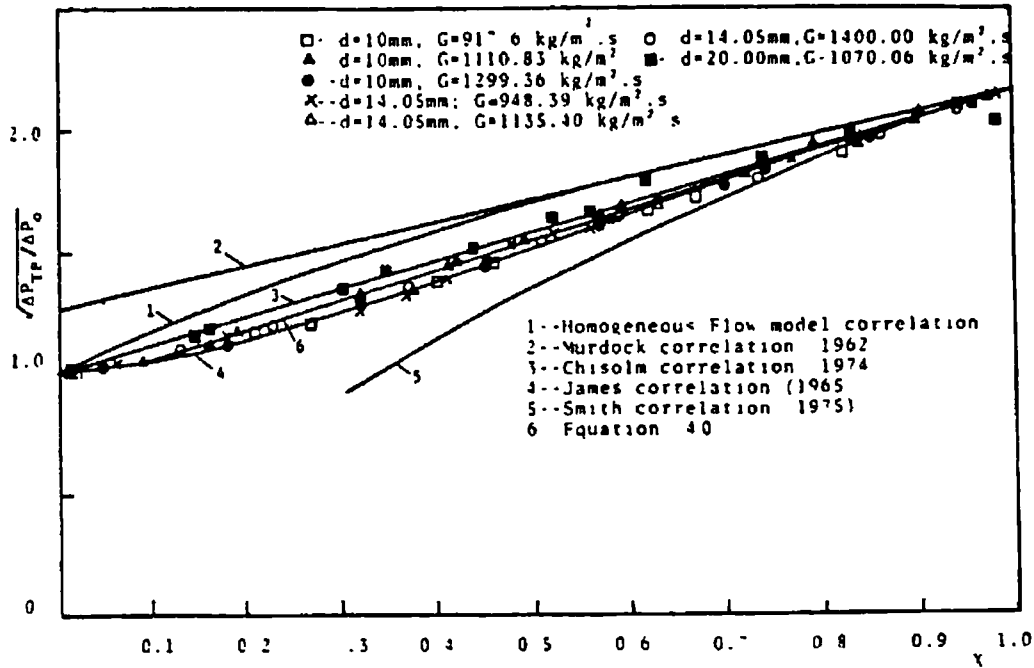
Figure (2.9a) Lin's Orifice Plate Meter Comparison for Low Pressure $\left(\rho_g/\rho_l\right)$=0.215
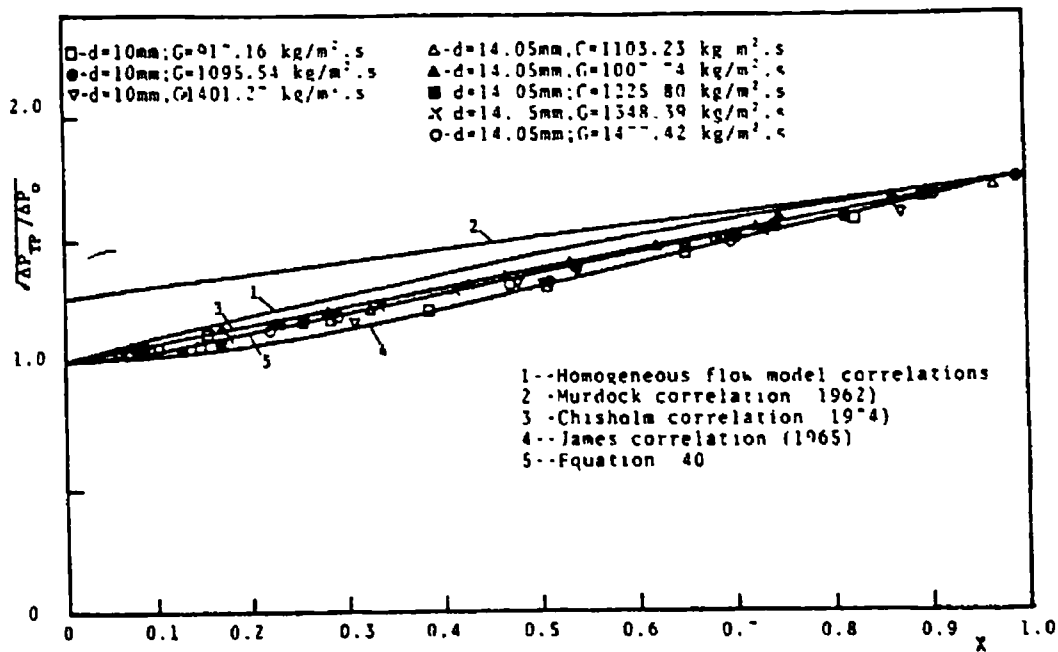
Figure (2.9b) Lin's Orifice Plate Meter Comparison for High Pressure $\left(\rho_g/\rho_l\right)$=0.328

to compare these two-phase correlations for wet natural gas flow properly, detailed reliable data of wet gas flow through orifice plates that correspond to the correct standards is required.

For this reason the present author attempted to gather together all the existing available data for wet natural gas flows through differential pressure meters. It quickly became clear that very little relevant data existed. It proved extremely difficult to add to the Murdock Natural Gas/ Condensate data given in [30]. A request for data was sent to all the major Oil and Gas Companies. Only Philips Petroleum (U.K.) and Chevron Petroleum (U.S.) replied but not enough data was available between them for a correlation comparison to be made.

The new wet gas loop at the National Engineering Laboratory is designed to simulate the flow of natural gas as closely as possible so data from the wet gas tests should be suitable for checking these correlations. It must be noted however that these correlations were formed for Orifice Meters only (except Smith and Leang) and only a Venturi Meter was tested for this project in the NEL Wet Gas Loop so it was only possible to check and compare the accuracy of the correlations with respect to Venturis. As Venturis are now replacing Orifices as the main DP Meter used in unprocessed wet natural gas flows this fact does not retract from the usefulness of the comparison .

2.7) The Simultaneous Metering of Gas & Liquid Mass Flowrates

It was stated in the opening section of this review that the vast majority of the published correlations offered to date give an empirical equation that will calculate either the total mass flow or the flow quality for either Orifice or Venturi Meters as long as the other of these parameters is known. As this is a problem for flows where neither the total mass flowrate nor the flow quality are known (such as flows from natural gas wells) there is a recognised requirement for the development of a meter capable of measuring both these parameters at once, i.e. a meter that could be simply plugged into a line of unknown flowrate and quality and provide accurate readings without the need for any other additional devices such as tracer dilution systems etc.

(see Section 2.4.3.5). In a literature search for such meter development only six papers were found that made any comment on this particular aspect.

Two papers [47, 70] were summarised in Lin's 1986 paper "Two-Phase Flow Measurement with Orifices" [21]. Due to the fact that these proposed systems are designed to find the two parameters, total flowrate and quality, Lin has called them two-parametric measurement systems. The next paper to declare the possibility of developing a meter capable of measuring these two parameters simultaneously was the Ultraflow Wet Gas Development Project "The Development and Testing of an Ultrasonic Flow Meter for Wet Gas Applications" [6]. In 1997 and 2000 ISA Controls and published two papers [61,65] discussing joint work in this field and a patent has been registered [62,63].

Finally, in the paper "Liquid Correction of Venturi Meter Readings in Wet Gas Flow", by de Leeuw [5] the author mentions a possible way to develop a "two-parametric" meter. These papers are discussed in turn below:

2.7.1) Method of using Two Orifices in Series

In the paper "Two-Phase Flow Measurement with Orifice-Couple in Horizontal Pipe Line (1st report)" by Sekoguchi [70] two segmental orifices are used in series to conduct air-water two-parametric two-phase measurements. Unfortunately, the paper is in Japanese and has not been translated. However, the paper is summarised by Lin [21] and the following information is taken from that summary.

Sekoguchi mounted four separate sets of two segmental orifice plates in series (i.e. of geometries shown in Figure 2.10) to conduct air-water two-parametric two-phase flow measurements in a test pipe (see Figure 2.10). From examination, the data obtained using configuration 'C' was chosen as Sekoguchi considered this configuration to give the best results. The reasons for this are not explained by Lin.
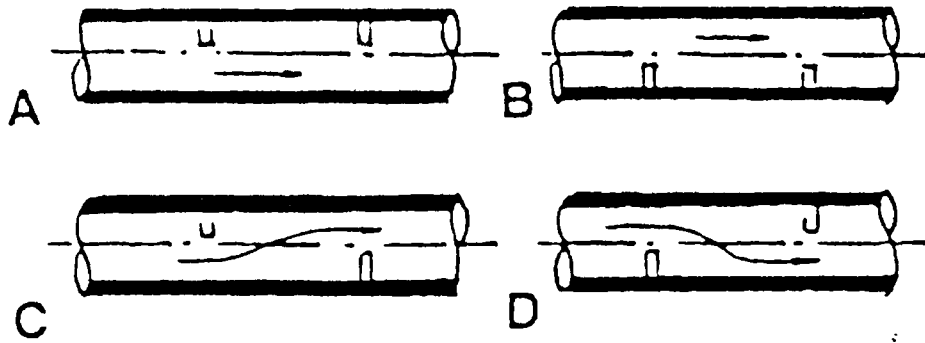
Figure 2.10 The four sets of Segmental Orifice Plates in Series Tested by Sekoguchi.

The test results (i.e. the two differential pressure readings from the two orifice plate meters) were plotted in the form of a nomogram with the differential pressure ratio as the ordinate and the sum of the pressure differential as the abscissa. Lines of constant superficial gas and liquid velocities are presented on the graph, see Figure 2.11.
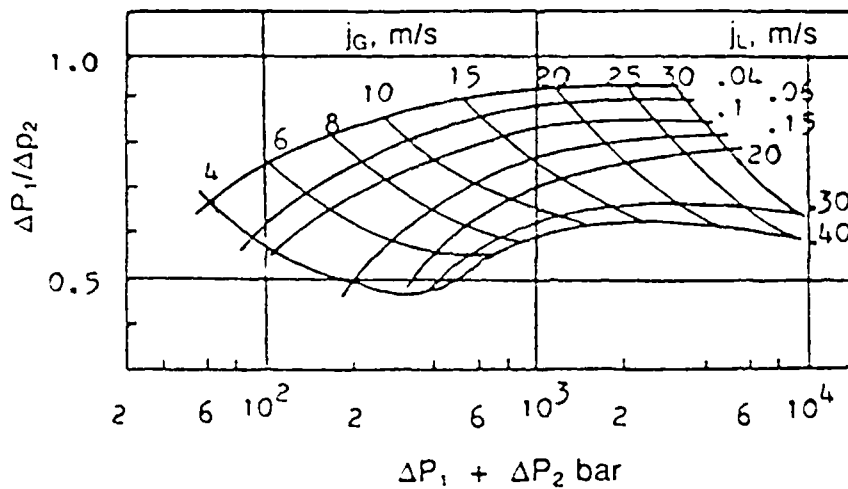
Figure 2.11: A Sekoguchi Nomogram.

This form of presentation is set up to give the required information to the metering engineers with the minimal of effort on their part. The nomograms present the information in an extremely useful way for a metering engineer. Once the two differential pressures are read off the meters the nomogram gives the superficial velocities of both liquid and gas directly. To find the volumetric flowrates, all that is required is the multiplication of these values by the pipe area. Furthermore to find the mass flowrate all that needs to be done is multiply the volumetric flowrate by the respective densities.

However, the theory behind this method and the reason why Sekoguchi decided to develop this method in such a way is not given in Lin's summary. The accuracy of the method is extremely poor, the error is quoted as $\pm 30\%$. There is no mention of the effects of line conditions such as line pressure and flow patterns or of different fluid properties. In fact in Lin's summary the range of conditions including the LGR and line pressures tested are not mentioned. No analytical correlation was offered. To have a system capable of metering a wide range of line pressures would mean having many nomograms formed from experiments as the line pressure dictates the size of the pressure drop across an orifice. Clearly then, this method currently falls a long way short of the requirements of the Oil and Gas Industry.

2.7.2) <u>Method of using a Volumetric Flow Rate Meter and an Orifice in Series</u>

In [47] and [48] Lin reports that a volumetric flow rate meter and an oval gear meter respectively were placed in series with an Orifice meter to conduct two-parametric two-phase flow measurements. Air and water were the test fluids and a wide range of Liquid to Gas Ratios was covered. By combining the information from both meters it was possible to develop equations that gave the volumetric flow rate of each phase to a R.M.S. of less than $\pm 7\%$. However, for the particular case of well natural gas, flow meters such as oval gear meters are not sturdy enough to withstand the extreme conditions. Damage to the moving parts is likely to be caused by periodic pressure pulses, slugs and debris from the well that must pass through the meters. Thus, while this method may well work for industrial applications that have less

extreme conditions (or at least shows promise of being capable of being developed into a successful measurement method) it is not well suited to measure natural gas flows.

2.7.3) Liquid Flowrate Measurement by the Wet Gas Ultrasonic Flow Meter

In [6] it is mentioned that there is hope in the Oil and Gas Industry that the recently developed wet gas ultrasonic meter that is now commercially available from Daniel Industries could be developed to measure the liquid flow rate in a wet gas flow along with the gas flow rate. When analysing the tests conducted at the NEL and Bacton Terminal to investigate the performance of this wet gas ultrasonic flow meter it was observed by the experimenters that certain parameters measured by the ultrasonic meter signal processor showed trends of change which may be related to the flows liquid content. In particular it was noticed that the three measured parameters "speed of sound" (usually denoted by "c"), "standard deviation" (usually denoted by "std DLLT") and "gain" were particularly affected by liquid content.

The "speed of sound" is another term for "acoustic velocity" and is simply the velocity at which an ultrasonic wave travels through a stationary medium. As the acoustic velocity is considerably different for gases and liquids the amount of liquid the wave has to pass through compared to the amount of gas during its journey between transducers obviously effects the time of travel and the ultrasonic meter manufacturers hope that this time difference between wet and dry gas flows can be related to the liquid content (by volume).

The "standard deviation" is the difference in the times measured for the ultrasonic wave to travel from the downstream transducer to the upstream transducer and vice-versa. Slip usually exists between the phases and the phase velocities are therefore different along with the acoustic velocities being different. The meter manufacturers hope that the standard deviation holds the information needed to derive the liquid flow rate along with the gas flow rate either outright or in conjunction with other parameters.

The "gain setting" is the value of the "boost" given to the received signals to increase the signal to the best processing size. As the manufacturers consider it likely that increased liquid content will reduce the signal received due to scatter (i.e. the path of the wave is altered by diffraction as it passes between mediums, or phases, so less of a signal will reach the desired transducer) a direct relationship between the liquid content and the amount of gain needed to boost the signals may well exist.

The start of the data analysis is the examination of the three variables acoustic velocity, standard deviation and gain setting in dry gas. Their relationship with gas velocity is represented in Figure 2.12
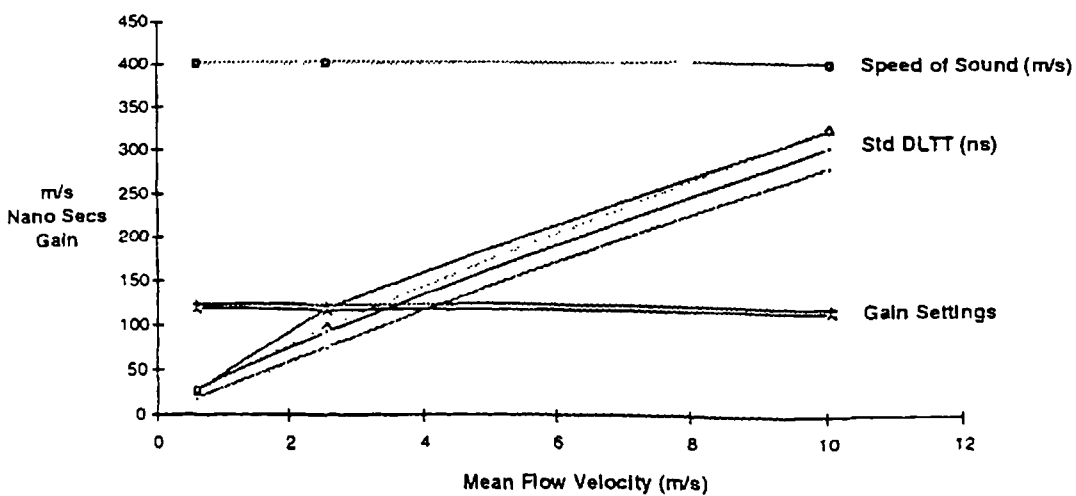
Figure 2.12 Ultrasonic Meter Parameter relationships

As would be expected the acoustic velocity and the gain setting remain constant. (The acoustic velocity is dependent on the fluid properties and the temperature while the gain setting is dependent on the amount of signal attenuation caused by the medium. As the dry gases mean flow velocity does not effect these parameters they remain constant as shown in Fig.2.12). However, as the standard deviation is the difference in times for ultrasonic waves to travel upstream and downstream along a chord, as the gas velocity increases this time difference will of course increase with it as seen in the Figure 2.12. These dry gas relationships are the reference conditions for examining the effect of wet gas flows on these parameters.

The parameters examined were plotted against liquid volume fraction for 70 bar and a gas velocity of 10 m/s (i.e. mist flow only) in [6] and data plots are reproduced in Figures 2.14, 2.15 and 2.16. The four path USM had chords as shown in Figure 2.13.
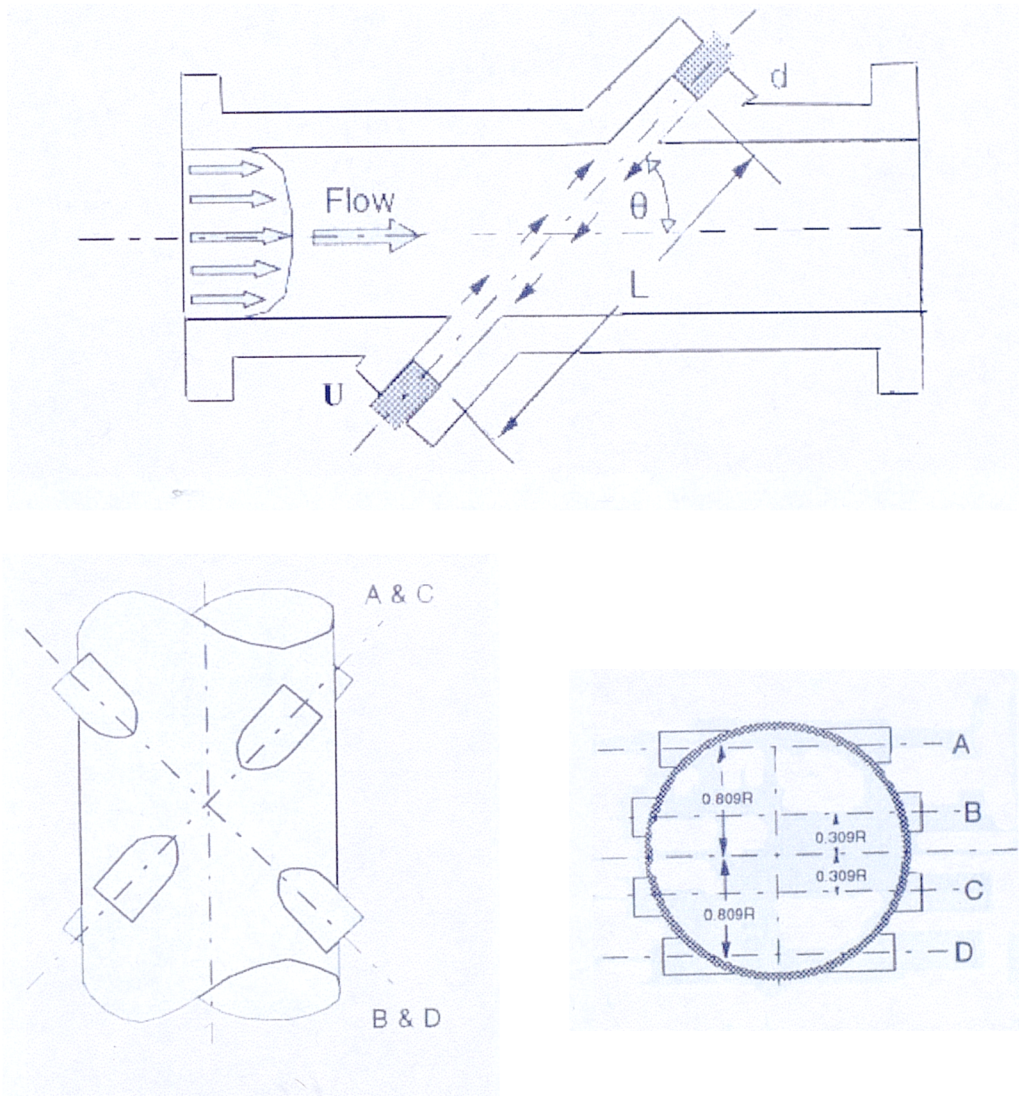
Figure 2.13 Schematic Diagrams of an Ultrasonic Meter.
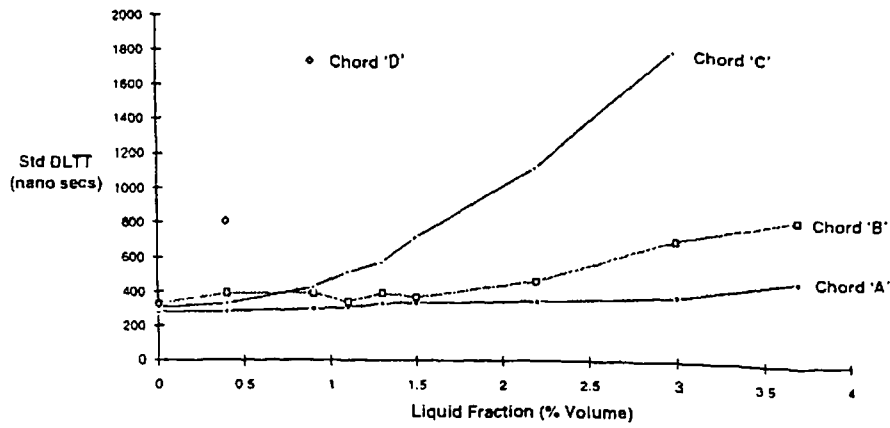
Figure 2.14 Liquid Fraction vs.Std DLTT for 70 Bar & Superficial Gas Velocity of 10 m/s.
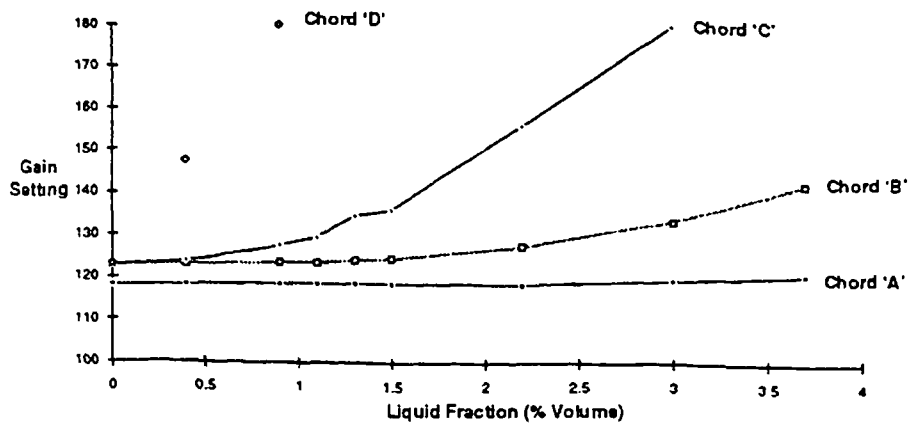
Figure 2.15 Liquid Fraction vs. Gain for 70 Bar & Superficial Gas Vel. of 10 m/s.
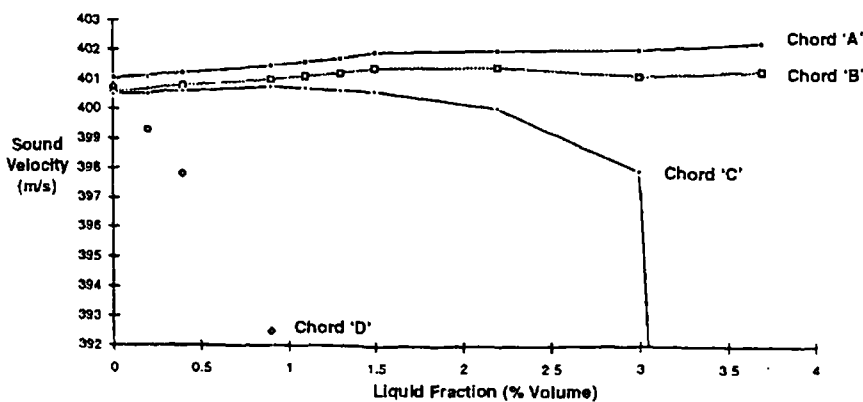
Figure 2.16 Liquid Fraction vs. "C" for 70 Bar & Superficial Gas Velocity of 10 m/s.

It is clearly evident from Figures 2.14 to 2.16 that the presence of liquid has a considerable effect on the individual chords. In general it can be seen that chord 'D' is by far the most sensitive. As this chord is the lowest chord in the pipe (see Fig.2.13) it must be assumed that although mist flow is said to exist the gravitation effect concentrates more liquid in the vicinity of chord 'D'. It is also evident that the order of sensitivity for all three parameters examined reduces the higher the chord is set in the meter. The standard deviation and gain setting are clearly both sensitive with respect to liquid content. The acoustic velocity did show the trends expected of it up until chord failure but this parameter was considerably less sensitive than the others. The Ultraflow Consortium's conclusion was that "... from looking at the ultrasonic signal behaviour with liquid entrainment in the gas it looks feasible that the meter can be made to measure liquid content as well as tolerating and operating successfully in wet gas. To achieve reasonable accuracy in this measurement it is likely that many experiments on test rigs and probably field tests will be required to fully understand the relevant parameters behaviour for various line conditions. It may well be necessary to analyse the separate parameter readings together as one parameter may not give enough information. It should also be noted that in real wet natural gas flows the flow pattern is not always mist flow (the only pattern considered so far) but other flow patterns as well. For a meter which can be relied upon to read the liquid flowrate accurately, regardless of the flow pattern, the amount of testing to achieve confidence in the meter reading will indeed be high. However, this proposed method of using the ultrasonic meter signal data to find the liquid flowrate as well as the gas flowrate in the flow pattern, the amount of testing to achieve confidence in the meter reading will indeed be high. However, this proposed method of using the ultrasonic meter signal data to find the liquid flowrate as well as the gas flowrate in a wet gas flow is as promising as any other proposed idea for the much sought after meter which would be capable of effectively measuring the flow quality and gas flowrate simultaneously.

2.7.4) The Proposed Method of using a Venturi Meter with an Extra Downstream Tapping.

In [5], de Leeuw mentions that as the pressure loss through a Venturi meter (i.e. upstream to downstream static tapping) is greater when liquid is entrained in the gas flow compared to dry gas, the actual pressure loss should depend on the liquid content. The author stated that the experimental results obtained at the SINTEF Multi-Phase Laboratory in Norway using a Venturi with an extra tapping downstream of the Venturi diffuser confirm this. Furthermore, similar to de Leeuw's conclusions on the Venturi meter over-reading being dependent on the gas Froude No. (see Section 2.5.1.1.3.1)) or [5] he goes on to conclude that this overall pressure differential through the venturi is also dependent on the gas Froude No. The paper points out that this relationship could lead to the development of "a simple two-phase flow meter". What is meant by this is a meter that is capable of measuring the total mass flow and quality of the flow at the same time. de Leeuw did not research the topic much further and the only additional comment was that it had been noted that the relationship between the overall pressure differential and the LGR (or Lockhart-Martinelli parameter 'X') is more sensitive at lower values than at higher values of the wet gas range. However, de Leeuw then says... "To date, however, no acceptable correlation formula has yet been found which would relate the pressure loss ratio to the actual liquid content and the over-reading". The present author suggests that this proposed method merits further investigation as along with the wet gas ultrasonic meter it seems to offer a real chance of developing into a commercially acceptable "two-parametric" meter if enough research and development is conducted.

2.7.5) The BG Technology and ISA Controls Ltd. Joint Meter Development

In 1997 British Gas Research and Technology published research into the development of a meter capable of metering both the gas and liquid phase flowrates simultaneously for a wet gas flow [61]. The concept used was as follows. One DP Meter in a wet gas flow can correct the error induced by the liquid presence by use of

a Murdock type equation only if the liquid flowrate is known. However, by placing a different geometry DP device in series with the first meter two different Murdock constants (M) are obtained which means that there are two equations and two unknowns (i.e. the gas and liquid flowrates). In other words the liquid flowrate need not be initially known.

In [61] the researchers chose to use a mixing plate upstream of a Venturi Meter to get the first differential pressure reading (as the Murdock method can be applied to any DP device). The mixing plate was a plate with many small holes designed to attempt to homogenise the two-phase flow before its entry into the Venturi Meter. This arrangement was tested at the Low Thornley test facility. The tests were at 30 barg in a 4 inch line with a Venturi with a beta ratio of 0.5. Flowrates were up to 1.9 kg/s for gas and 4 kg/s for liquid so clearly a wider test matrix than was required for wet gas testing was created. No explanation was given to why a mixer plate was seen as preferable to two DP Meters. The appropriate values of the "Murdock constant" for the Mixer Plate and the Venturi were 2.0 and 2.7 respectively. However they did state that these values are different from Murdock's value of 1.26 "most likely due to the non-standard geometry's of both the homogenising unit and the Venturi". The fact that the flow was vertically downwards is also bound to have been a major factor. It was concluded that the method gave the gas mass fraction to +/-4% for gas mass fractions above 0.6. However, the errors on the liquid flowrate were said to be considerably greater, so this method was proposed for gas flowrate predictions only.

After the 1997 research BG Technology filed for a UK Patent [62] and an International Patent [63] for this technology. In 1999 BG Technology published a paper [64] in which the work in [61] was again discussed but this time the analysis included testing done on a horizontally mounted wet gas meter. These tests were conducted at 25 bar g with liquid flowrates up to 1.58 kg/s and Gas Volume Fractions of 0.3 to 1.0. This work led the authors to make the new claim that the method gave the gas mass fraction to +/-4% and the liquid flows to within +/- 6%. By now ISA Controls became involved and the technology was developed in commercial confidence between these companies. A series of horizontal wet gas flow tests were conducted on the NEL Wet Gas Loop in late 1999 / early 2000 and this research was

discussed by ISA Controls Ltd in [65]. This paper describes the development of this meter from the original design at Low Thornley to a new combination of DP devices which are kept commercially secret. The NEL Wet Gas Loop test matrix was 20 to 60 bar, gas flow rates of 200 to 800 m^3/hr and GVF's ranging from 90% to 100%. An accuracy of 2.5% for gas flowrates and "generally better than" 10% for liquid flowrates is claimed.

That completes an in-depth review of the state of the art of wet natural gas metering. It is clear that currently industry has no preferred method of metering wet gas and all available methods are considerably less accurate than is desired by industry. With the demand for wet gas metering growing rapidly there is a need for more research into the topic, for both cases of a known liquid flowrate and an unknown liquid flowrate combined with an unknown gas flowrate requiring to be metered.

From the literature review, discussions with operators and ISA Controls Ltd. (a main supplier of Venturi Meters to the oil and gas industry and sponsors to this project) the following research objectives were identified.

3.1) A Correlation Comparison

It had been clear from the outset of the project that there was no one Venturi Meter wet gas correlation universally accepted by the industry and in fact there were only two found to be in existence, the previously mentioned de Leeuw correlation and the unpublished modified Venturi Murdock correlation used by Phillips Petroleum on Della Well, a well in the North Sea that produces wet gas. (Other correlations may exist which are used by operators in-house but only Phillips Petroleum have openly discussed their unpublished correlation.) Furthermore, due to the lack of any Venturi correlations whatsoever before 1997, operators had been using older existing Orifice Plate Meter general two-phase correlations (usually the original Murdock equation) to attempt to correct the error caused by the liquid presence in the flow through the Venturis. It was not known how accurate these techniques were. It was therefore decided that, as the existing Orifice Plate Meter general two-phase correlation had sometimes been used to correct Venturi Meters with wet gas flows, and as the two existing wet gas Venturi correlations had not been tested with independent data, the first aim of this research should be the comparison of all existing Orifice Plate and Venturi Meter correlations that could be thought of as being suitable for wet gas metering. The literature had many general two-phase flow Orifice Plate Meter correlations but as was stated in the literature review most were not considered by the present author as being suitable for use with wet natural gas flows for various reasons. It should be noted of course that the choice of which Orifice Plate Meter correlations to include and which to disregard in a correlation comparison was done by means of engineering judgement and the merits of other correlations omitted could therefore perhaps be successfully argued. In general an Orifice Plate Meter correlation

was chosen as valid if the data that created it (i.e. pressures, phase flowrates, pipe diameters, gas volume fraction, etc.) came anywhere near data typical of the natural gas production lines. Hence, the first research conducted was the use of the new independent data to compare the performance of the seven correlations, the Homogenous, Murdock, Chisholm, Lin, Smith and Leang, Modified (or "Venturi") Murdock and de Leeuw correlations.

3.2) The Verification of de Leeuw's Conclusions

Once this comparison was complete and the relative performance of the correlations found it was considered logical to then examine the data to discover trends. In particular, as Chisholm and Lin both stated that any two-phase correlation for Orifice Plate Meters needs to take account of pressure the new NEL wet gas Venturi data would be examined for any dependence on pressure. This it must be said had been done before for Venturis in 1997 by de Leeuw. However, de Leeuw had gone on to say that the Venturi reading also showed a dependence on gas flowrate (although he expressed this as a dependence on the gas densiometric Froude No.) and this had never been verified by the use of another set of independent wet gas Venturi data. It was therefore an objective to get independent proof of this statement.

3.3) The Requirement for New Correlations: Updating Murdock's Equation

With the industries increasing use of Venturi Meters in wet gas applications there is increased interest in improving the existing Venturi correlations. As with all heavy industry the tried and tested methods tend to be preferred and change is slow in occurring. With this in mind it must be noted that most natural gas metering engineers have heard of the Murdock Equation while few have heard of Chisholm's Equation and still fewer have heard of de Leeuw's Equation (which it will be remembered is developed from Chisholm's Equation to include the effect of the gas flowrate). Hence, there is a general acceptance that by calibrating a Venturi Meter to a particular flow a new "Murdock constant" can be found and that the modified Murdock Equation can

then be used for that particular application. This of course does not take into account the findings of de Leeuw that pressure and gas flowrate need to be accounted for while correcting the error in the Venturi Meters gas flowrate prediction. It was therefore decided that, assuming these factors were indeed seen to be of importance, it would be suitable to determine the value of the "Murdock constant" (which now should be more aptly called the "Murdock Gradient") as a function of pressure. This would "update" the Phillips Petroleum "Modified" or "Venturi" Murdock Equation for Venturi Meters in the way that Lin's Equation updated the original Murdock Equation for general two-phase flow through Orifice Plate Meters. That is, it lets the correlation account for pressure. Then it would be of further use to find the "Murdock Gradient" as a function of pressure and gas flowrate. This would effectively bring the Venturi Murdock Equation up to date with de Leeuw's correlation and it would be in a form more readily understood and accepted by field engineers.

3.4) Attempting to Meter the Gas and Liquid Flowrates Simultaneously.

The final investigation this author saw as necessary was the attempt at metering the gas and liquid mass flowrate simultaneously. There were only three methods sited in the literature review and two of them, the Sekoguchi method and the ISA/BG Technology method, required two meters in series which was not possible in this project due to financial constraints. However, de Leeuw showed that the combined information of the standard Venturi Meter differential pressure reading (i.e. upstream to throat) and the overall differential pressure reading (i.e. upstream to downstream) could contain information on the gas *and* liquid flowrates. This could be investigated as the ISA Controls Ltd. Venturi had been supplied with downstream tappings. Just how the gas and liquid flowrates were to be found from these readings was not suggested by de Leeuw. He had finalised his discussion by saying "...To date, however, no acceptable correlation formula has been found which would relate the pressure loss ratio to actual liquid content and the over-reading". (The "Venturi pressure loss ratio" is simply defined by de Leeuw as the ratio between the overall static pressure drop across the meter divided by the upstream to throat differential

pressure.) The de Leeuw graph showing the pressure loss ratio vs. The Modified Lockhart Martinelli parameter relationship for different gas velocities at one pressure is reproduced in Figure 3.1.
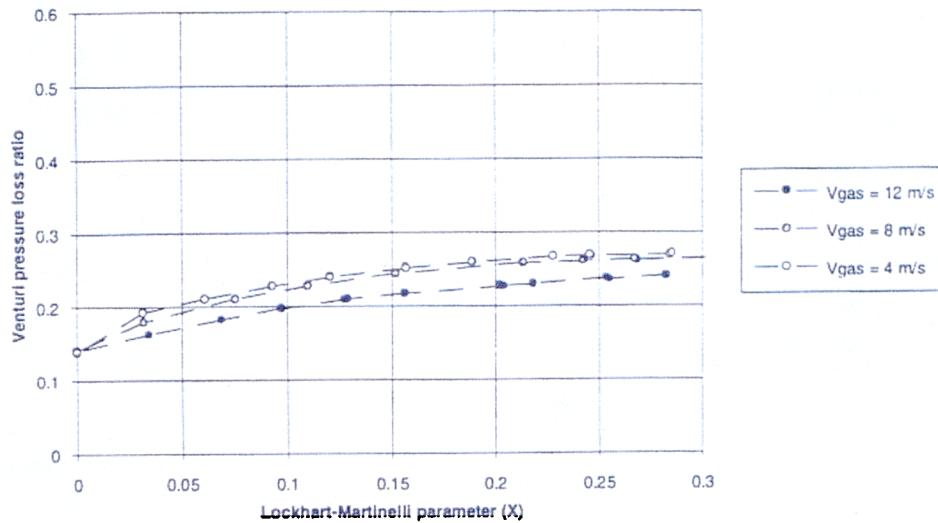
Figure 3.1. de Leeuw's graph showing the Pressure Loss Ratio to modified Lockhart Martinelli Parameter for different gas flowrates at one set pressure.

The proposed method to be researched was as follows. For each chosen line pressure a three dimensional surface would be found for The Pressure Loss Ratio vs. The Modified Lockhart Martinelli Parameter vs. Superficial Gas Flowrate. It was noted that the required data to create these three dimensional graphs were the same as the data taken for the correlation comparisons with the sole addition of the extra downstream tapping data. Therefore, by recording this data along with that required for the correlation comparison this research could be conducted with no extra testing required.

Once these three dimensional graphs existed the following iteration could then be performed on any future wet gas Venturi Meter readings. It is given here as a series of steps:

1) Read off the line pressure upstream of the Venturi Meter. (Call this P_1).
2) Knowing P_1 select the appropriate 3-D surface of the Pressure Loss Ratio vs. X

vs. gas flowrate $\dot{Q}_g$.

3) Read off the Pressure Loss Ratio from the Venturi.

4) Make a first ESTIMATE of the value of the modified Lockhart Martinelli Parameter, X.

5) For this chosen value of the Modified Lockhart Martinelli parameter, X, go to the previously chosen 3-D surface (chosen in step 2) and from information from step 3 and step 4 obtain the associated gas volume flowrate, $\dot{Q}_g$.

6) Note now that the de Leeuw wet gas Venturi Meter correlation is like the new proposed Modified Venturi Murdock Equation to be created by this research project. They are both of the form:

$$\dot{Q}_g = \frac{\dot{Q}_{tp}}{correction\ factor}$$

where

$$correction\ factor = f\left(P, X, \dot{Q}_g\right)$$

Therefore, with the pressure (P) measured upstream of the Venturi, and the value of X estimated we get an associated estimated value of the actual gas volumetric

flowrate ($\dot{Q}_g$) from step 5. Therefore, either of these correlations give an

estimated value for the meter uncorrected reading $\dot{Q}_{tp}$.

7) The actual uncorrected meter reading would be known as it is simply the meter output before any correction for the liquid presence is added. Therefore, if the estimated value for X was correct in step 4 then the associated estimated value of the uncorrected reading should equal the actual reading from the meter. If not, return to step 4 and iterate.

8) On convergence of the iteration in step 7 the value of X and therefore $\dot{Q}_g$ is known. As X is calculated by the equation:

$$X = \frac{K_g Y_g}{K_l} \frac{\dot{Q}_l}{\dot{Q}_g} \sqrt{\frac{\rho_l}{\rho_g}}$$

where the product $K_g Y_g$ is solely a function of $\dot{Q}_g$ (for a given pressure). K_l (the superficial liquid flow coefficient) is always considered to be known. It is defined as the product of the discharge coefficient, the Velocity of Approach and the Expansibility factor. The Velocity of Approach and the Expansibility factor are simply functions of the meters Beta Ratio for a given fluid, line pressure and differential pressure. Hence the discharge coefficient is the only unknown. However, for single-phase flows of Reynolds Numbers less than one million the ISO standards assume a Venturi Meter has a discharge coefficient of 0.995. For single phase flows of Reynolds Numbers in excess of one million there are no standards and the meter is calibrated to give a relationship between the flow coefficient and either the Reynolds Number or the gas mass flowrate, hence the statement that $K_g Y_g$ is solely a function of $\dot{Q}_g$. The term $\sqrt{\rho_l / \rho_g}$ is known from the fluid properties and upstream line pressure reading. Having determined all other components of the equation then the liquid volumetric flowrate ($\dot{Q}_l$) can be obtained.

These research proposals were the main areas identified for research during the early part of this work. Thus, it was apparent from early in the project that to successfully carry out the proposed research it was necessary to obtain reliable new wet gas Venturi data. In early 1998 the NEL started to develop the New Wet Gas Loop and the author joined the design team to assist with the development process.

Chapter 4

<u>The NEL Wet Gas Loop: The Design and Commissioning of the System</u>

4.1) <u>The General Design of the NEL Wet Gas Loop</u>

The general design of the NEL Wet Gas Loop is discussed here. A schematic diagram of the system is given in Figure 4.1a and a simplified line diagram is given in Figure 4.1b. This section discusses the design of the system and the role the author had in the design team (with the exception of the work done on liquid injector choice which is discussed later in Section 4.3).

At the start of the author's involvement in the design process the gas flow system was largely completed. It was known that it was financially and legally impossible to create a system that simulated real conditions perfectly. The financial problem was two-fold. Firstly, to get the correct pressure range the pipework would cost considerably more then the existing 62 bar rated (6", schedule 40) pipework and secondly, to get the correct flowrates of actual wet gas production lines a blower costing several million pounds would be required. Due to the budget available to the NEL and the predicted cost of running such a blower it was viewed as not commercially viable to build such a system. The legal problem was health and safety regulations would not allow the use of light hydrocarbons in industrial sites with a close proximity to populated areas (such as the NEL). It was therefore not possible to use natural gas and condensate and it was thus necessary to select suitable simulant fluids. The chosen combination was nitrogen and a kerosene substitute. This was chosen using engineering judgement by the design team prior to the author becoming involved. On joining the design team the author investigated the choice of simulant fluids with the aim of validating the choice made. This investigation is discussed in Appendix 1.

The gas blower (item 8 in Figure 4.1) purchased by NEL was the most powerful available within the limits of the projects budget. It was a 200kW Howden centrifugal blower. It was estimated to be capable of supplying 1600 m^3 / hr in dry air for the proposed gas pipework for pressures up to 60 bar. It was specially designed to cope

with traces of kerosene in the nitrogen should the new separator fail to be 100 % efficient.

The Wet Gas Separator (item 1 in Figure 4.1) with a volume of approximately 11.2m^3 was rated to 77 bar. It was located upstream of the blower separated from it by a single ball valve (item 4) at the separator outlet (item 2) and then two T-junctions. The first T-junction, directly downstream of the ball valve, had one line going to the second T-junction while the other line led to another ball valve (item 5) and then the main test line downstream of the test piece (item 17). The purpose of this second line was to allow the system to operate as a dry gas facility when required. This second T-junction had two butterfly valves, one in the upstream line before the junction (item 6) and one in the blower by-pass line (item 7). That is, the pipeline split with one pipe (with no valve) leading to the blower inlet and the other pipe (with the valve) by-passing the blower and the gas cooling system (item 9).

The original gas cooling system was retained due to financial constraints. It was a Bi-Water High Pressure Air Cooler positioned directly downstream of the blower. It was rated to 80 kW. As the blower was rated to 200 kW this initially caused some concern as the nitrogen may have heated faster than it could be cooled. However it was subsequently found that only at the higher gas and liquid flowrates was the blower using most of its power and even then, during the one minute of testing necessary for each test conducted, the gas temperature did not rise enough for any change in flow conditions to be considered significant.

The gas flow leaving the cooling system passed to the next T-Junction (i.e. the blower by-pass rejoining the main pipework) and then the pressurising / de-pressurising system (item 10) before turning up through two 90^0 bends taking it from the basement (the position of all components so far mentioned) into the main gas hall. A straight length of pipework 10 diameters long downstream from the pipe bend led the dry gas flow to a Spearman Flow Conditioner (item 11) and then to the dry gas reference meter (item 12) situated a further 10 diameters downstream. This gas reference meter was an Instromet turbine meter rated to a maximum of 1000 m^3/hr. The reason for this reduced maximum gas flowrate will be given shortly. The gas reference meter was calibrated at NMI for flowrates of 50 to 1000 m^3/hr and the
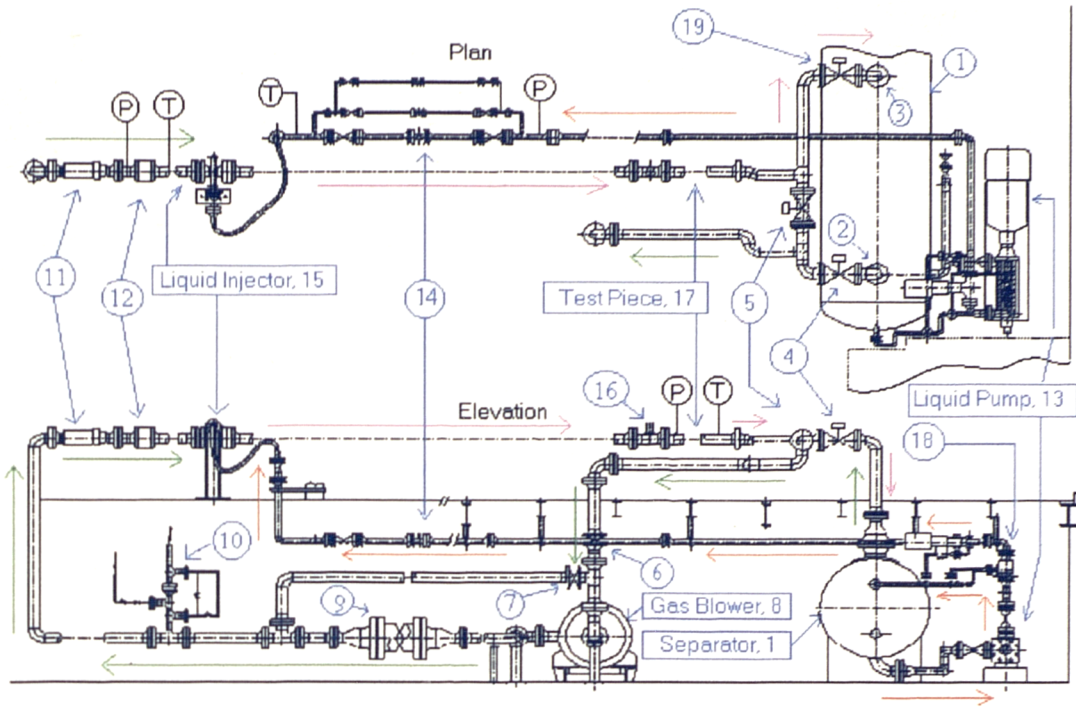
Figure 4.1a Schematic Diagram of the NEL Wet Gas Loop.
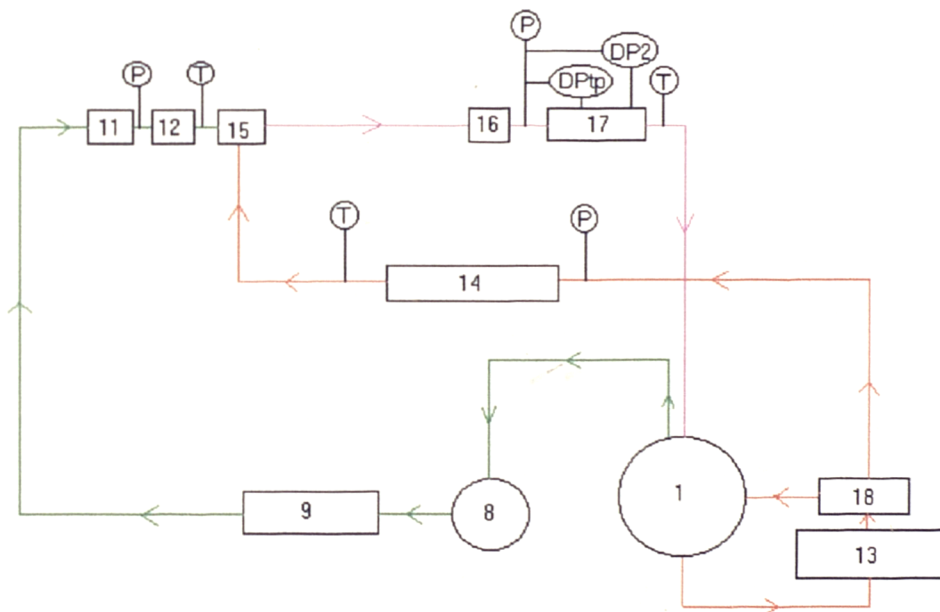
Figure 4.1b Simple Line Diagram of the NEL Wet Gas Loop.

Where:

Single Phase Gas Flow

Single Phase Liquid Flow

Wet Gas Flow

Legend for Figures 4.1a and 4.1b:

Item 1	Separator
Item 2	Gas Flow Outlet from Separator
Item 3	Gas Flow Inlet to Separator
Item 4	Ball Valve
Item 5	Ball Valve
Item 6	Butterfly Valve
Item 7	Butterfly Valve
Item 8	Gas Blower
Item 9	High Pressure Heat Exchanger
Item 10	Gas Pressurisation / Venting System
Item 11	Flow Conditioner
Item 12	Gas Reference Turbine Meter
Item 13	Liquid Pump
Item 14	Bank of Liquid Reference Turbine Meter
Item 15	Liquid Injector System
Item 16	Camera Installation
Item 17	Test Piece (i.e. Venturi Meter)
Item 18	Automatic Re-Circulation Valve
Item 19	Ball Valve

pressure was read by a Yokogawa Pressure Transducer (0-70 Bar). A further 10 diameters downstream from the meter there was a Platinum Resistance PT100 standard temperature probe and 5 diameter further down was a weir plate followed at a further 5 diameters by the liquid injector position (item 15). With a liquid injector installed just 20 diameters downstream of the reference turbine meter a weir plate must be installed to avoid liquid flow back into the meter during low Gas Volume Fraction testing or during start up and shut down procedures. From the injection point there was a distance of 50D to the test piece (item 17) which allowed the two-phases

to mix before entering to the test piece. The non-intrusive "Sea Spy" high pressure camera supplied by Tritech Ltd was installed 10 diameters upstream of the test piece (item 16). Downstream of the test piece the two-phase flow continues for 20 diameters before reaching a T-Junction. One pipe leads to the T-Junction mentioned early which forms the dry gas set up (i.e. the closing off of the separator) and the other leads to a double out of plane bend with a ball valve between the bends (item 19) which takes the two-phase flow vertically down to the wet gas separator inlet (item 3) located in the basement.

The reason that the dry gas turbine meter was only rated to 1000 m^3/hr instead of the originally expected 1600 m^3/hr was that, with the addition of the weir plate and the intrusive injector system and their significant effect on the overall resistance of the system and of course the effect of the liquid in the flow the Howden dry gas flow estimate of 1600 m^3/hr was estimated to be reduced to 1000 m^3/hr.

With this design work completed the task of designing the liquid system was undertaken. The first task was to decide upon the desired liquid injection range for the system. From the definition of wet gas and the estimated range of gas flowrates over the available pressure range, the associated liquid flowrate range was calculated. Calculations were then made to enable selection of a suitable liquid pump. The one problem encountered during this calculation was the pressure drop across the injector system. There was a requirement to test more than one injector design (due to reasons explained in section 4.3) and it was therefore required to estimate the pressure drop across different proposed injector systems. The two injection methods chosen to be compared were a straight pipe open at the end and a straight pipe with a spray nozzle attached, both injecting in the downstream direction. Their respective pressure drops were reasonably predicted using conventional calculation methods. The liquid pump was correctly sized as it operated satisfactorily over the necessary range of flows. (However, it should be noted that at the higher gas flowrates when the pump delivered the associated high liquid flowrate for the lower Gas Volume Fractions the increased resistance in the flow prevented the blower providing a flowrate of 1000 m^3/hr. This problem will be discussed in greater depth in Section 4.4.)

The pump calculations led to the choice of an eleven stage Ingersoll-Dresser pump which could supply up to 60 m³/hr of kerosene. Naturally, no pump could economically and safely give the full range of liquid flowrates required as they are designed for use in industry at optimum efficiency, i.e. at one inlet pressure and flowrate. As this test apparatus required a relatively wide range of liquid flowrates it was necessary to take into account the susceptibility of the pump to damage at lower liquid flowrates. Therefore, the pump was sized for the maximum required flowrate and an Automatic Re-circulation Valve supplied by Schroedahl Ltd. (item 18) was set up downstream of the pump exit to split the minimum practical flowrate from the pump into two flows, one that leads the required injection flowrate to the injector and one that leads the excess back into the separator.

The full liquid injection system is shown in Figure 4.1a and is as follows. The kerosene substitute is drawn from the base of the separator by the pump (item 13). It then flows through the liquid input / extraction and into the pump. At the pump exit the liquid flow rises vertically to the Automatic Re-circulation Valve which splits the flow according to the choice of the valve setting. This choice is dictated by the reading from the bank of liquid reference flow meters (item 14) described next. The correctly set Automatic Re-circulation Valve allows the desired split between the two liquid flows. That is, the desired liquid flowrate travels through the reference meter in use and on through the injector into the gas flow while the rest of the liquid flow is diverted back into the separator. It was necessary to use a bank of liquid reference flow meters as the liquid flow range required for the full wet gas test matrix (listed in Section 4.4) crossed the range of three different meters. Therefore, the 1/2", 1" and 3" turbine meters (supplied by Emo Ltd.) were capable of metering 0.15 to 1.5 m³/hr, 1.5 to 15 m³/hr and 5 to 150 m³/hr respectively and all three were calibrated by the NEL. Each had a PT100 Temperature Probe positioned upstream to allow a density calculation. They were assembled in parallel to each other with ball valves before and after each individual meter. On deciding on the required liquid flowrate prior to each test the appropriate meter is selected, its valves opened and the others shut. With the correct Automatic Re-circulation Valve setting, the desired flowrate is then metered

and taken to the injection point by a high pressure rated flexible hose. A final ball valve is positioned directly upstream of the injector.

4.2) The ISA Controls Ltd. Venturi Meter

The experimental investigation into wet gas metering was performed using an ISA Controls Ltd. standard specification North Sea Venturi Meter as used by operators both on and off-shore. ISA Controls Ltd. kindly supplied a purpose built test meter for this work because of their interest in the research proposal.

The specification of the ISA Controls Ltd. Venturi Meter is as follows:

The Venturi was delivered with an upstream section of 2630mm of schedule 120 pipework. This has an inside bore of 139.7mm and therefore this upstream section is 18.8 diameters in length. Schedule 120 is used in actual natural gas production lines because of the extreme pressures. A radial step reduction of 7.19mm existed between the NEL schedule 40 pipework (inside bore 154.08mm) and the ISA pipework. The overall length of the ISA supplied upstream pipework, Venturi Meter and downstream pipe work was 4061mm. The Venturi Meter was 1000mm and the downstream length was 418mm. The rest of the 4061mm was made up by the standard 6" clamp set connecting the upstream and downstream pipe lengths to the Venturi Meter.

The Venturi was made to ISO 5167 standards. It had a Beta Ratio of 0.55 meaning that, as the inlet diameter was 139.71mm, the throat was 76.84mm in diameter. There were two non-standard aspects of this meter. The first was the lack of the traditional four tappings set round the circumference of the Venturi. Such tappings are used in single-phase flow to get a more accurate pressure reading by averaging the four pressure readings from the equally spaced tappings round the circumference of the Venturi. This is not done with wet gas flows due to the inevitable flooding of the lower tapping. Wet gas Venturis have a single pressure tapping located at the top of the pipe. The second non-conformity with the standards

was the two additional downstream tappings. As was discussed in Section 2.4 there is a benefit in reading the downstream static pressures for the case of wet gas flows. The first downstream tapping was positioned at the diverging section / downstream pipe interface and the second was positioned one diameter (i.e.139.7 mm) further downstream. All tappings were 6mm in diameter. Figures 4.2 and 4.3 give details of the meter and the installation arrangement.
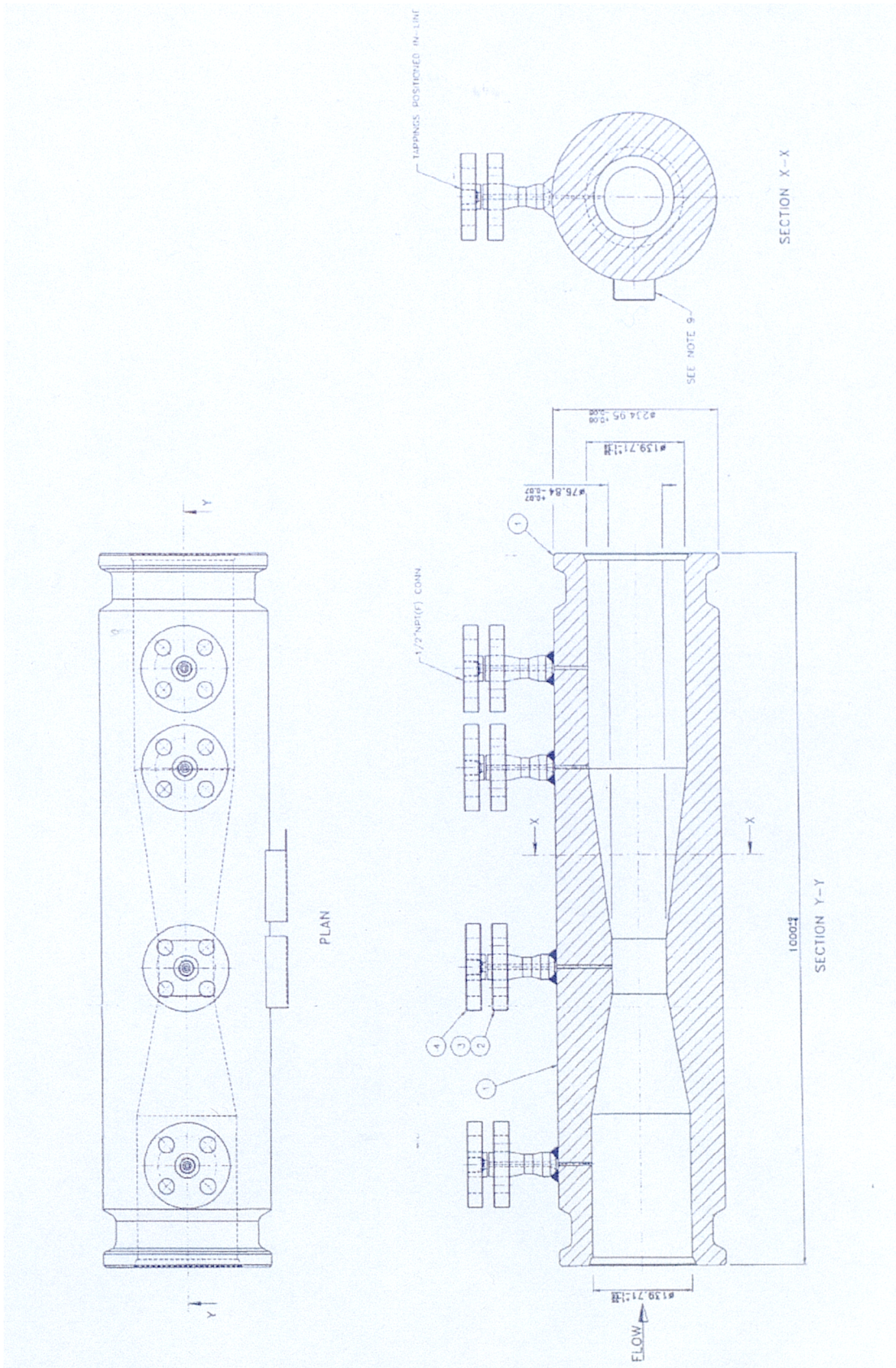
Figure 4.2 Schematic Diagram of ISA Controls Ltd. Wet Gas Venturi
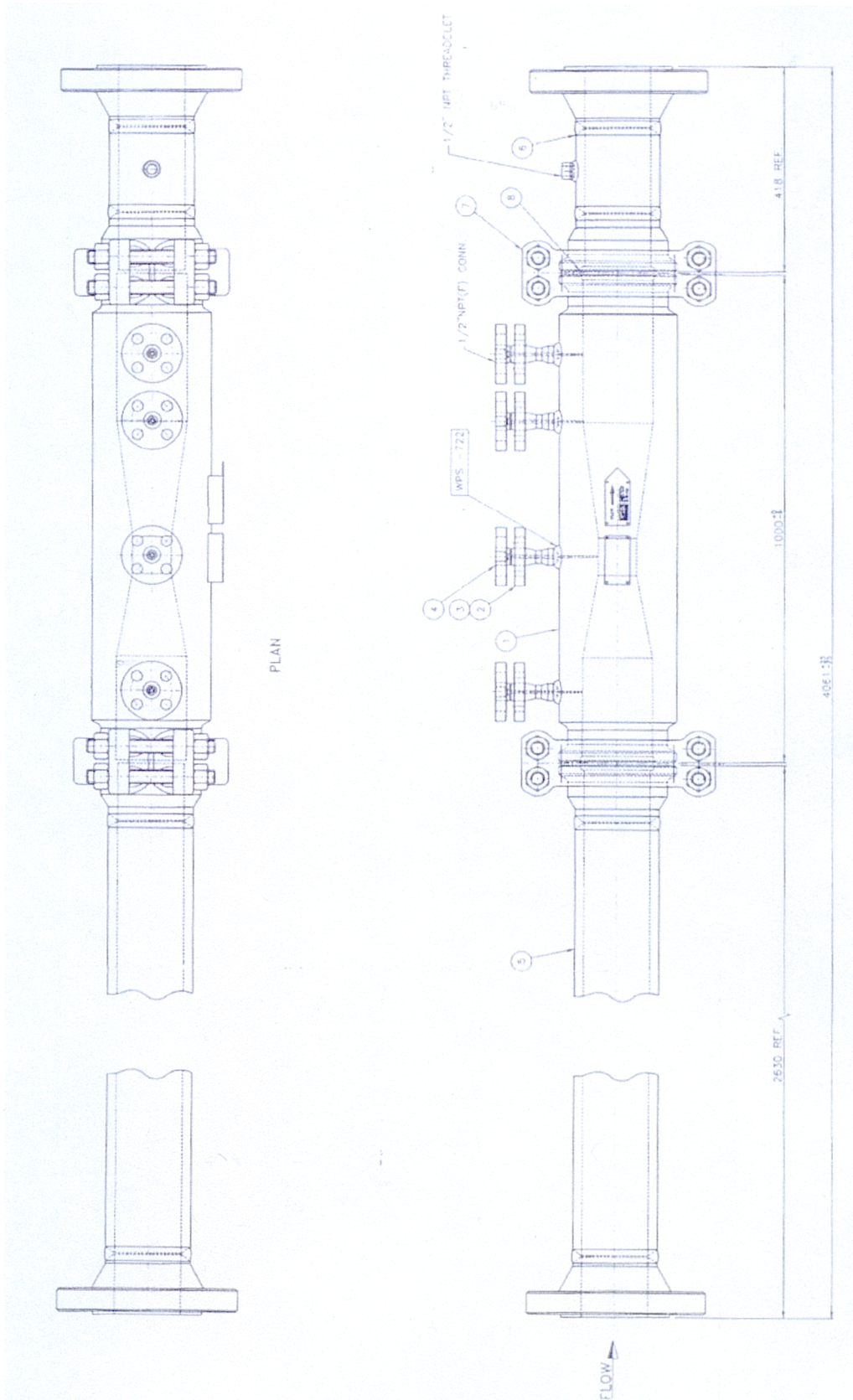
Figure 4.3 Schematic Diagram of the Upstream Pipework and Wet Gas Venturi
Meter supplied by ISA Controls Ltd.

4.3) The Choice of Liquid Injector and the Commissioning of the NEL Wet Gas Loop

4.3.1) Predicting the Fully Developed Flow Patterns of Actual Wet Natural Gas Flows and of the Simulant Fluid Flows

It was stated earlier in this chapter that the choice of liquid injector had not been decided upon when this author joined the design team. The responsibility of choosing a suitable injection method led to a close analysis of the problems involved. The main problem was ensuring that the flow pattern was indeed the same as would be found in actual wet natural gas production lines.

It is generally accepted that the particular flow pattern that exists at the inlet to a wet gas meter dictates the way the meter behaves. That is, in the case of Differential Pressure (DP) Meters, different flow patterns for given phase flowrates gives rise to different pressure drops across the meter. For example, losses caused by a stratified flow pattern (i.e. the loss due to the shear at the phase interface) will not necessary be equal to the losses incurred if the same phase flowrates flow as annular dispersed flow (i.e. the loss due to the drag on droplets and the shear at the annular liquid ring / gas core interface). Therefore, in order to consider meter performance in actual wet natural gas flows it is vital to re-create the correct flow pattern in the test apparatus. Thus, if the flow patterns that exist in actual wet natural gas flows have to be created they must be initially known. As stated previously, industry tends to assume annular dispersed flow. However in order to perform a scientific investigation it is necessary to prove that this is the case using existing flow pattern prediction methods.

Two-Phase flow pattern prediction is still a difficult subject. There are several published flow pattern maps, generally created for particular industries. That is, as the flow pattern is partially dependent on fluid properties and as most flow pattern maps are purely empirical they are only relevant to similar types of fluids. This limits the choice of relevant flow pattern maps available for the present study. For the Oil and Gas Industry, Shell Expro have a flow pattern map which is becoming generally accepted as the best available. This map is shown in Figure 2.5 of the literature review. The most academically accepted prediction method is the Taitel and Dukler

semi-empirical method. It was these two methods that were used here to predict the actual wet natural gas flow patterns and those in the NEL Wet Gas Loop. Note that both methods are used to predict the flow pattern of a fully developed flow. That is, they assume the flow pattern has had sufficient length of pipe since the last obstruction for the flow pattern to be fully developed and not be in transition. Often in real production lines, metering is the last consideration of the producer and to avoid the expense of extra pipework meter skids are installed in any available position regardless of whether it is ideal for metering or not. The result of this is that meters can be directly downstream of systems such as valves and pipe bends. Hence, often in reality flow patterns are still in transition when they reach the inlet to the meter. However, as each of these conditions is unique the best a researcher can do is to test at the equilibrium (i.e. the fully developed flow pattern) condition.

Thus, it was first necessary to prove that a "typical" wet natural gas flow in real production metering conditions did indeed have an annular dispersed flow pattern and so would the NEL Wet Gas Loop. It was then necessary to prove that the NEL test facility did indeed have a fully developed flow pattern at the meter inlet. This second investigation was required due to the fact that it takes the two-phase flow an unknown length of pipe downstream of the liquid injection point for the flow pattern to become fully developed. Therefore, as there is a limited length of 50 diameters between the liquid injection point and the meter inlet in the NEL Wet Gas Loop, proof of a fully developed flow pattern was required before the meter data can be considered valid.

The flow patterns for natural gas / condensate flows were predicted for the NEL flowrates in six inch pipes and then predictions for the NEL Wet Gas Loop Nitrogen / Eversol D80 (the chosen Kerosene substitute) were made. It was known that the NEL Wet Gas Loop flowrate capability was at the low end of real production flows but it was known that if this prediction was for annular dispersed flow then the higher real flowrates would most certainly be also.

In reality each well has a unique composition of natural gases and condensates so a "typical" composition was suggested by the Physical Properties Department at NEL and for the typical conditions of the production lines the Physical Properties Data

System (PPDS) estimated the fluid properties. The "typical" composition chosen is given in Table 4.1.

METHANE	0.603	mol.	PENTANE	0.005	mol.
ETHANE	0.14	mol.	HEXANE	0.002	mol.
PROPANE	0.1	mol.	NITROGEN	0.02	mol.
BUTANE	0.05	mol.	CARBON DIOXIDE	0.08	mol.

Table 4.1 Typical make up of a North Sea Natural Gas Flow.

The Physical Property Data System (PPDS) was used by the "Fluids & Process Technologies Division" of the NEL to calculate the fluid properties at various pressures and temperatures. As this wet natural gas flows in the actual well pipelines it is this pipeline pressure and temperature that must be considered. The pressure and temperature can vary depending on the meter position. A range of pressures is considered. For this analysis the temperature was held at 293K. If metering takes place at the "Christmas tree" (i.e. the series of sub-sea valves positioned at the flows exit from the well) the temperature can be higher but by the time the platform is reached the sea can have cooled the flow to the seawater temperature. Analysis at 293K is therefore considered to be a reasonable average temperature. The properties of such a gas flowing at a volumetric flowrate of 1000 m^3/hr (the maximum flowrate of the NEL Wet Gas Loop) and a 'β' range of $0.95 \leq \beta \leq 0.99$ were calculated by PPDS and the results are shown in Table 4.2.

Fluid Properties	Gas Density (kg/m^3)	Gas Viscosity (centipoise)	Liquid Density (kg/m^3)	Liquid Viscosity (centipoise)	Surface Tension (N/m)
Pressure					
70 Bar	98.6368	1.41E-05	437.821	5.71E-05	0.00464
60 Bar	80.6667	1.32E-05	457.909	6.45E-05	0.005301
50 Bar	64.8669	1.25E-05	477.38	7.36E-05	0.006076
40 Bar	50.6112	1.20E-05	497.449	8.53E-05	0.00703
30 Bar	37.4182	1.15E-05	520.8	0.00010197	0.008308

Table 4.2 PPDS Predicted Natural Gas and Condensate Properties.

The Physical Property Data System (PPDS) was then used by the "Fluids & Process Technologies Division" of the NEL on the request of this author to calculate the fluid properties of the Nitrogen / Eversol D80 at the same various pressures and temperatures. The results are shown in Table 4.3.

Fluid Properties	Gas Density (kg/m^3)	Gas Viscosity (centipoise)	Liquid Density (kg/m^3)	Liquid Viscosity (centipoise)	Surface Tension (N/m)
Pressure					
70 Bar	82.056	1.90E-05	841.339	0.00152857	0.027912
60 Bar	70.5771	1.88E-05	840.492	0.00152857	0.027912
50 Bar	59.0392	1.86E-05	839.638	0.00152857	0.027912
40 Bar	47.4621	1.83E-05	838.777	0.00152857	0.027912
30 Bar	35.8659	1.82E-05	837.909	0.00152857	0.027912

Table 4.3 PPDS Predicted Nitrogen and Eversol D80 Properties.

These properties were used with the Shell Expro Flow Pattern Map and the Taitel and Dukler prediction method. Both prediction methods agreed well with each other. The only difference found was that for both flows the Shell Expro Map predicted that the transition to annular dispersed flow from stratified flow occurs at a slightly higher gas flowrate for a given liquid flowrate than the Taitel and Dukler method predicted. However, these gas flowrates are below the minimum of this projects interest. The gas velocity range associated with the gas volumetric flowrate of 400 m^3/hr to 1000 m^3/hr was approximately 6 m/s to 15 m/s. Figures 4.4 and 4.5 show the results of the investigation for natural gas / condensate in actual pipelines and the Nitrogen / Eversol D80 in the NEL Wet Gas Loop at 60 bar. The red box in Figure 4.5 show the approximate range of the NEL wet gas tests. Clearly annular dispersed flow (designated by AD on the map) is predicted for both flows in the required gas volumetric flowrate range. The full comparison for 20, 40 and 60 bar from the Shell Expro Flow Pattern Map and sample calculations of the Taitel and Dukler prediction method are given in [58].

It can be seen from the Figures 4.4 and 4.5 that at 60 bar, across the flowrate range being tested, the simulant flows of Nitrogen / Eversol D80 tend to hold the stratified flow pattern slightly longer than the natural gas / condensate. That is, it can be seen that for a given liquid flowrate the Eversol D80 remains stratified for a slightly higher value of Nitrogen flowrate than would the condensate with natural gas. However, with no lighter hydrocarbon being legally allowed at the NEL site and no surfactant being found to radically reduce the Eversol D80 surface tension value (see Appendix 1) there was no way of improving the situation. Nevertheless, at the desired flowrates both fluid combinations were predicted by both prediction methods to be annular dispersed flows with the exception of the Nitrogen / Eversol D80 at 400 m^3/hr and low liquid loading (and even here the flow is in the transition zone). Hence this analysis successfully proved that if the NEL Wet Gas Loop achieved a fully developed flow pattern at the test piece inlet the flow pattern of actual production flows would be reasonably well matched. The term "reasonably well" is used to indicate that of course the match is not perfect. With the natural gas / condensate flow giving annular dispersed flow for slightly lower gas flowrates than the Nitrogen / Eversol D80
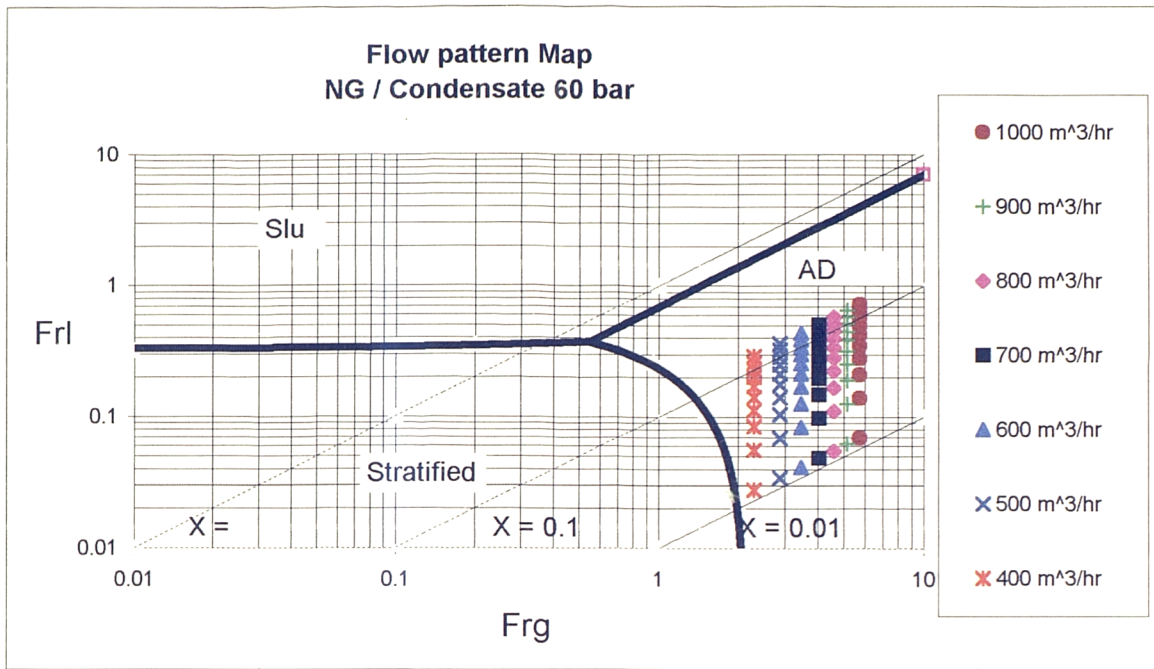
Figure 4.4 Flow Pattern Map, Natural Gas / Condensate Flow at 60 Bar.
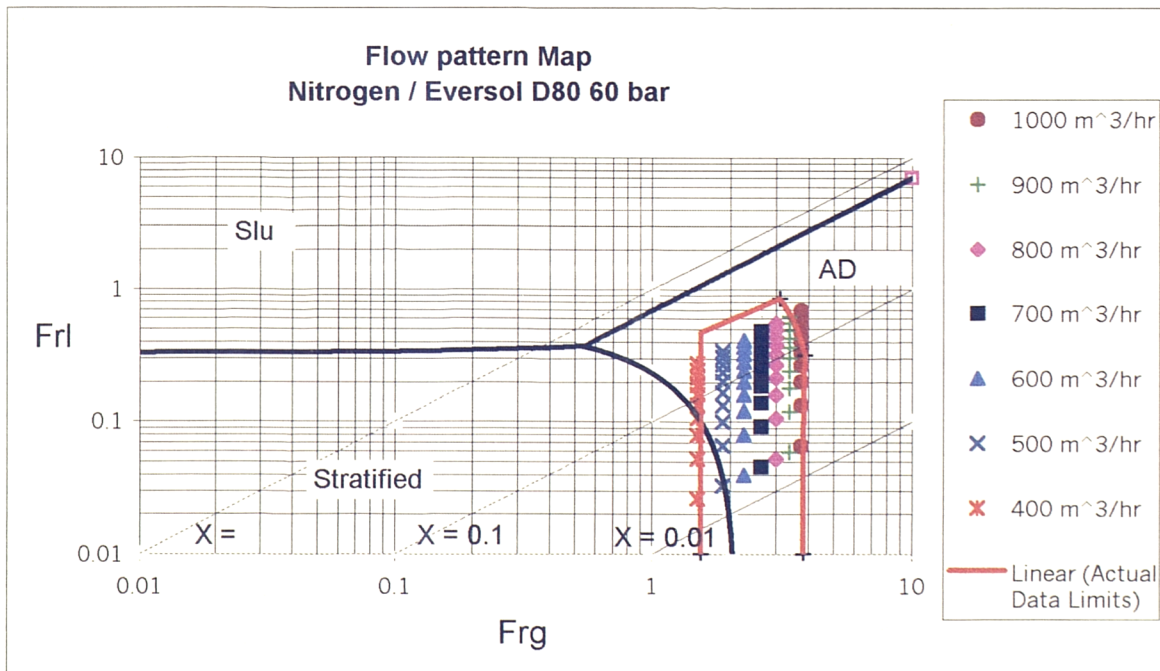
Figure 4.5 Flow Pattern Map, Nitrogen / Eversol D80 Flow at 60 Bar.

flow it is clear that for a given gas and liquid flowrate it will have a slightly more developed annular dispersed flow pattern. That is, the annular film and droplet size will be slightly smaller for the same values of pressures and flowrates and this would affect the test meters readings. However, it is hoped that this effect is small and the NEL Wet Gas Loop is still capable of closely matching the desired flow pattern, if not matching it exactly.

Finally, it must be remembered that no two natural gas / condensate flows are the same and therefore the comparison here is not precise. Different natural gas production flows would all give slightly different fluid properties and therefore flow pattern predictions. Therefore, it must be noted that the use of any one particular actual natural gas / condensate fluid combination in the NEL test rig would not necessarily give a better match for each individual production flow being considered. With these factors taken into account there was confidence that a suitable test apparatus had been created for testing wet gas meters as long as a fully developed flow pattern was achieved at the test piece inlet.

4.3.2) The Method Chosen to Investigate if the Flow Pattern at the Test Piece was Fully Developed

On a search through the available literature no references regarding injector choice to ensure a desired flow pattern was found. All descriptions of two-phase flow test apparatus simply state the injection location relative to the test section. Typically, no mention of the injector was made at all. As the whole exercise of re-designing the NEL Wet Gas Loop was based on the premise that the wrong flow pattern had previously existed some means had to be found to ascertain weather annular dispersed flow was being achieved or not. This was not an easy task. There was a camera installed upstream of the test piece but in reality it was of limited help. The camera in the pipework looked vertically down into the pipe. However, when a stratified flow changes to an annular dispersed flow it will go through a phase of being largely wavy stratified flow with some liquid entrainment into the gas. This relatively small percentage of liquid in droplet form could be enough to obscure the cameras view.

Hence the camera was only useful for showing if the flow pattern was completely stratified with no droplets present or that there was a liquid presence with droplets entrained from a liquid film of unknown geometry. Thus, the camera was clearly not capable of indicating the type of flow pattern. Also it could not indicate if the flow pattern was still in transition as the flow passed the camera location.

No simple method giving proof of annular dispersed flow could be found. The method decided upon for this study was as follows. The Venturi Meter installed in the line is the only component offering any information on the flow conditions, other than the camera, and therefore meter readings must somehow be used. It was decided to carry out the chosen test matrix twice using a different injector each time. That is, first an open pipe was used to inject the liquid downstream (therefore attempting to create a stratified flow with some entrainment at the local area of the injector). Then an atomising nozzle was attached onto this open pipe injector (therefore attempting to create a fully dispersed flow at the local area of the injector). It was assumed that for each set flow condition the balance of the relevant forces would cause each local injector created flow pattern to immediately undergo transition to the natural fully developed flow pattern as it moves down the pipe towards the test piece. As the DP Meter reading is suspected to depend on the type of flow pattern then it was assumed that if the two injectors gave the same results (i.e. meter readings) for every pair of points tested then the flow patterns must be fully developed by the inlet to the meter and therefore the injector type is irrelevant. If the two test matrices were different then it would indicate that the flow patterns were also different and the flows were still in transition at the meter inlet. It was shown previously using the available prediction methods that in the NEL Wet Gas Loop the fully developed flow pattern should be annular-dispersed flow (Section 4.3.1). Thus, it could be concluded with reasonable confidence that if the two test matrix results are the same then it is indeed fully developed annular-dispersed flow that exists at the meter inlet. An added bonus to finding similarity between both test matrices was that if both injectors gave the same results then both sets of data would be seen to be giving valid information on the performance of a Venturi in a wet gas flow with a fully developed flow pattern and therefore both sets of results could be used together to give a larger data set.

4.3.3) The Dry Gas Calibration of the ISA Controls Venturi Meter

As the NEL Wet Gas Loop was designed to be capable of testing meters in dry and wet gas the NEL were keen to start the general commissioning of the system with a dry gas test. This suited this research program as there was a requirement to test the ISA Controls Venturi Meter in dry gas before testing in wet gas. As stated in the literature review, all wet gas DP Meter correlations to date assume that the dry gas reading of the meter is correct and the 'corrections' given by the correlations are due to the liquid presence in the gas flow only.

It is stated in ISO 5167 that Venturi Meters made to the given standard which operate below a Reynolds Number of 10^6 should use a flow coefficient, C, of 0.995. However, there are no standards for higher Reynolds Numbers. As actual natural gas flows usually have high Reynolds Numbers the operators either still use 0.995 or calibrate the meter at as high a Reynolds Number as possible. In this project the meter was calibrated.

The NEL Wet Gas Loop was pressurised to 20 bar with nitrogen. With the liquid system shut down the gas system was run at approximately 400, 600, 800 and 1000 m^3/hr. For each of these flowrates Yokogawa Differential Pressure Transducers (0-1 bar) took twenty spot pressure readings over a period of two minutes. (A spot measurement was the average of 1000 readings taken in one second.) The average of these twenty readings were obtained and logged. The same was then done at 60 bar. (All three differential pressure transducers were installed for this dry gas calibration run.) Then a graph of The Flow Coefficient (K_g) vs. The gas mass flowrate was produced for each pressure and a linear line fitted to the data. The data is reproduced in Appendix 2. The graphs are given here as Figures 4.6 and 4.7.
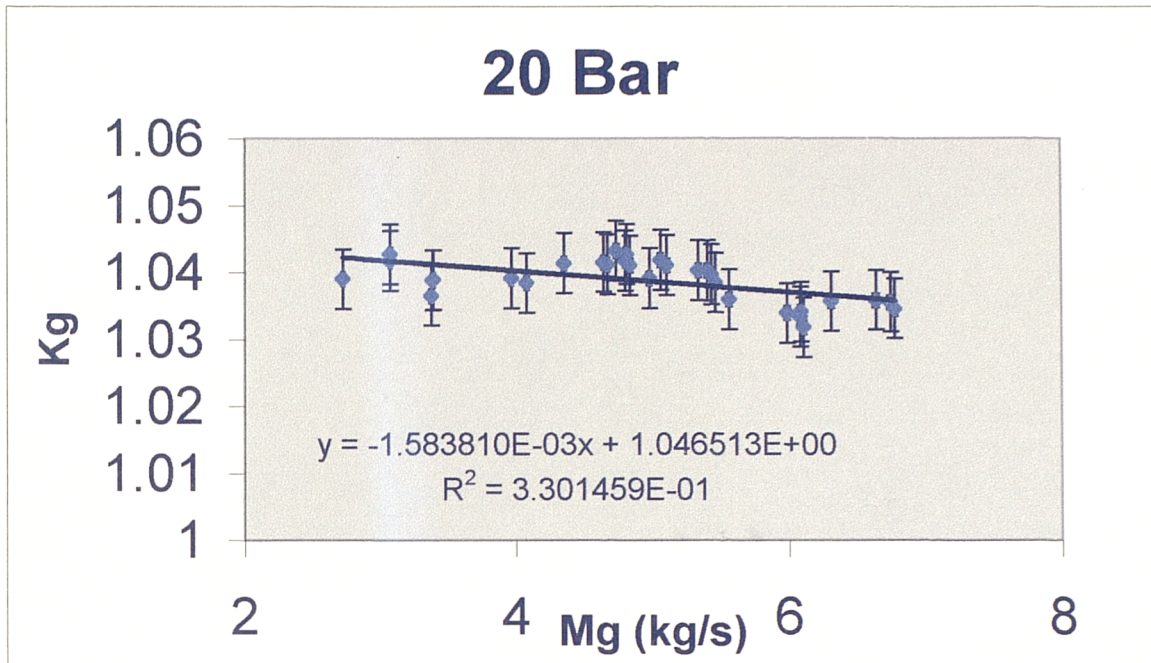
Figure 4.6 The Dry Gas Calibration Graph at 20 Bar.
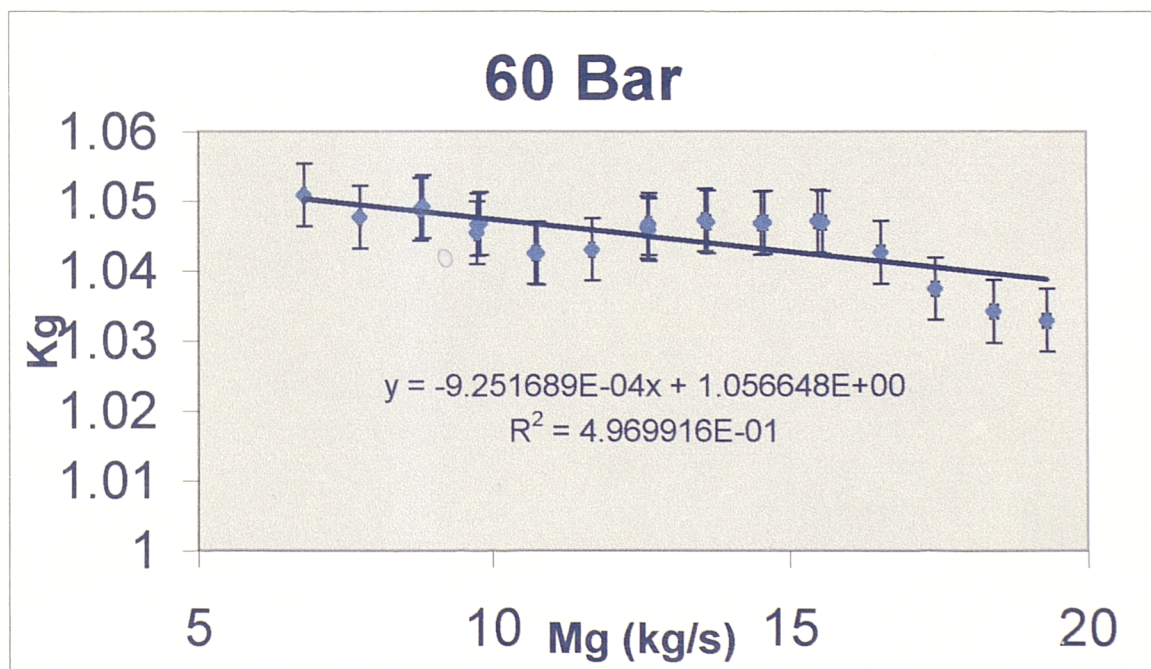
Figures 4.7 The Dry Gas Calibration Graph at 60 Bar.

123

4.3.4) The Chosen Test Matrix

As it was the intention of this study to keep the research industrially relevant the test matrices were formed to cover the definition of wet gas flows as described in (Section 2.2). That is, the Shell Expro definition of a Gas Volume Fraction of 95% was aimed at being the largest liquid content. Shell Expro claim that this value roughly corresponds with a flow of equal liquid and gas mass flowrates for many two-phase production wells. Now, as the modified Lockhart-Martinelli parameter is defined as:

$$X = \sqrt{\frac{\Delta P_l}{\Delta P_g}} \approx \frac{\dot{m}_l}{\dot{m}_g} \sqrt{\frac{\rho_g}{\rho_l}}$$

A reasonable maximum for the test matrices would be:

$$X_{max} \approx \sqrt{\frac{\rho_g}{\rho_l}}$$

For the cases of 20, 40 and 60 bar with nitrogen and Eversol D80 this corresponds to X_{max} values of approximately 0.175, 0.243 and 0.296 respectively. Hence, for chosen gas flowrates (Q_g) of 400, 600, 800 and 1000 m³/hr the corresponding maximum desired liquid flowrates (Q_l) are as shown in the Table 4.4.

	20 Bar	40 Bar	60 Bar
Qg max (m³/hr)	Ql max (m³/hr)	Ql max (m³/hr)	Ql max (m³/hr)
400	12.27	23.64	34.96
600	18.40	35.46	52.44
800	24.54	47.28	69.93
1000	30.67	59.10	87.41

Table 4.4. The Desired Maximum Liquid Flowrates at each set Gas Flowrate.

However, with the power input limitation at the higher gas flowrates it was not possible to match this desired range. Table 4.5 indicates the actual maximum liquid flowrates run during testing for each gas flowrate.

	20 Bar	40 Bar	60 Bar
Qg max (m³/hr)	Ql max (m³/hr)	Ql max (m³/hr)	Ql max (m³/hr)
400	10.96	22.22	36.44
600	16.39	32.15	48.40
800	16.36	41.13	65.11
1000	3.04	13.51	24.25

Table 4.5. The Actual Maximum Liquid Flowrates at each set Gas Flowrate.

Actual flowrates for the pressures tested against the ideal test matrix are given below in Figures 4.8, 4.9 & 4.10.
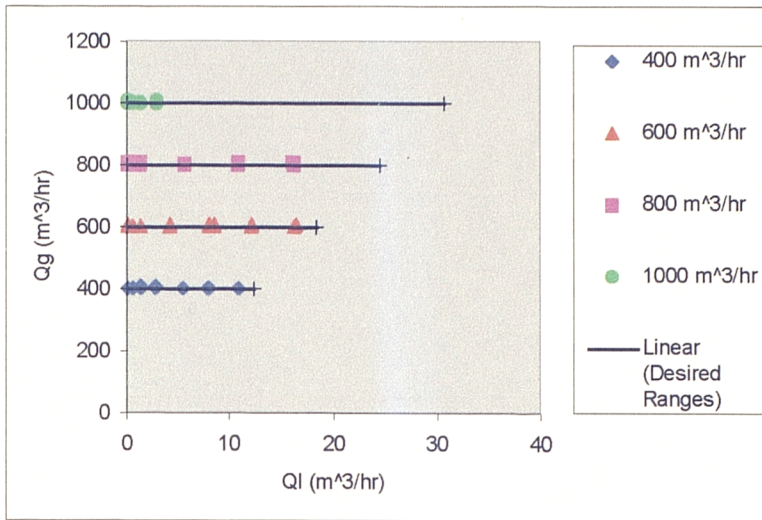
Figure 4.8. Plot of the 20 Bar Test Actual to Desired Flowrates.
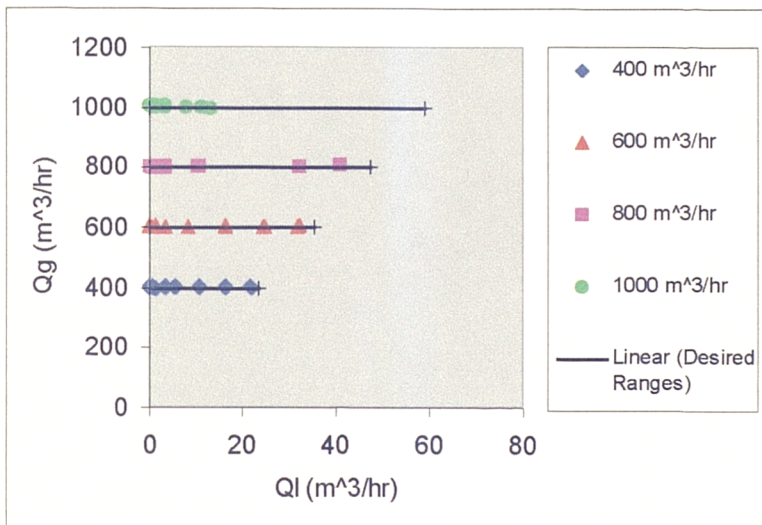
Figure 4.9 . Plot of the 40 Bar Test Actual to Desired Flowrates.
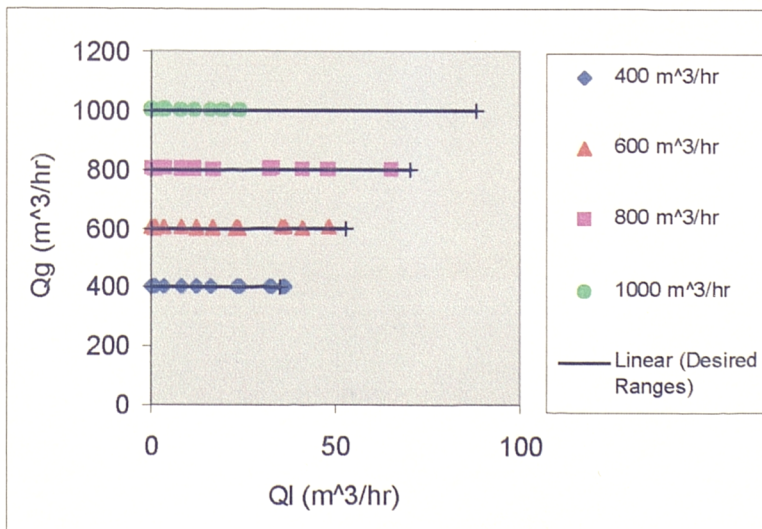
Figure 4.10. Plot of the 60 Bar Test Actual to Desired Flowrates.

The black lines in Figures 4.6, 4.7 and 4.8 indicate the desired liquid flowrate range for the each chosen gas flowrate being tested. The colour points indicate the actual test data as shown in Appendix 3. It can be seen that generally the full range was obtained for the 400 m³/hr and 600 m³/hr gas flowrates and most of the 800 m³/hr gas flowrate. However, for all three pressures the blower could not maintain 1000 m³/hr as the liquid flowrate increased towards the maximum desired quantity. It should also be noted that as the liquid flow reference meters had a minimum flow that could be accurately metered then of course the liquid flowrate could not be less than the meter minimum.

Although it was found to be impossible to obtain data from across the whole of the desired test range with the available blower it is still clear that data over much of the desired range was obtained. It should further be noted (as stated in the literature review) that most wet gas flows of industrial interest are at the upper end of the Gas Volume Fraction meaning the 243 data points recorded are of great value to industry. As researchers in the natural gas production industry traditionally indicates the liquid quantity in a gas flow by using the Modified Lockhart-Martinelli Parameter, the range of the test matrix, is given in these terms in Table 4.6:

Pressure	20 Bar	40 Bar	60 Bar
Qg (m³/hr)	X range	X range	X range
400	0.0032 to 0.1559	0.0012 to 0.2299	0.0011 to 0.3086
600	0.0021 to 0.1536	0.0008 to 0.2192	0.0007 to 0.2716
800	0.0015 to 0.1174	0.0006 to 0.2102	0.0006 to 0.2756
1000	0.0012 to 0.0175	0.0005 to 0.0562	0.0004 to 0.0816

Table 4.6. Table of Actual Lockhart-Martinelli Parameter Ranges at Each Set Pressure and Gas Flowrate.

The full data set obtained from these test matrices is given in Appendix 3.

4.3.5) The Test Procedure

The procedure for running the tests was as follows. The whole system was pressurised, from banks of high pressure nitrogen tanks, to the desired pressure. Then, with the liquid system shut off by the appropriate valves, the blower was switched on and set to stabilise at the first required gas flowrate. For each pressure the lowest gas flowrate was always used first, i.e. 400 m³/hr. Once the flowrate reading was stable and the temperature and pressures were steady the liquid injector system had the appropriate flow meter opened and the other two meters securely closed off. The ball valve at the injector point remained closed at this stage. The liquid pump was then run up to speed with the entire liquid flow being byby-passed into the separator. The ball valve at the injector system was then opened and the Automatic Re-circulation Valve was activated sending a percentage of the liquid flow to the injector. It was found during testing that fine tuning of the liquid flowrate by use of the ball valve at the injector was considerably easier than using the Automatic Re-circulation Valve. With the liquid being injected the gas flowrate, previously constant for the dry gas, invariably fell off to a new lower value as the resistance on the blower increased. It was found that changing the liquid flowrate while the blower was set to a constant power had a considerably greater effect on the gas flowrate than if the opposite were done. Hence, after the initial gas flowrate was set in dry gas and the liquid subsequently injected at the desired flowrate, causing the gas flowrate to drop, usually all that was required was a boost in blower power. Only at the highest gas and liquid flowrates did the liquid flowrate shift enough by this blower power boost to demand a further alteration of the pump speed.

Once the system was seen to be in equilibrium, i.e. the gas and liquid flowrate readings were steady and the pressure and temperature stable, the readings of the Venturi Meter were taken. One data point consisted of the liquid and gas reference turbine meter frequencies and the averaging of 20 spot readings (i.e. each 100 readings in one second) of pressures and temperatures taken at intervals of 10 seconds. These readings were collected by the systems data logger and processed by the computer which saved the data to disc (i.e. the raw data listed in Appendix 3).

4.3.6) The Liquid Injector System Comparison

With data obtained from two tests involving both injectors used across a similar test matrix it was possible to verify that the type of injector had no effect on the meter reading. The method chosen to do this was as follows. For each pressure both sets of data were plotted on a "Murdock" type graph, i.e. $\sqrt{\Delta P_{tp}/\Delta P_g}$ vs. $\sqrt{\Delta P_l/\Delta P_g}$ where ΔP_{tp} is the upstream to throat pressure differential of the wet gas flow and ΔP_g and ΔP_l are the calculated pressure differentials that would be read if the gas and liquid flowed alone respectively. As ΔP_g and ΔP_l are derived from the single phase reference meters and the two tests followed the same test matrix as closely as possible only ΔP_{tp} should have a significant difference if using a different type of injector effects the meter performance. Therefore, if the comparison between the two data sets shows each injectors data for set pressures and gas flowrates to be of no significant difference then it could be concluded that the choice of injector is irrelevant as both injectors give the same results for set conditions. This is in fact what was found. Figures 4.9, 4.10 & 4.11 show that there is very good agreement between the results of the two injectors. In these graphs Injector A was the open pipe and Injector B was the nozzle. Due to these tests the NEL now uses the open pipe injector as the nozzle was seen to offer no advantage while giving the disadvantage of a larger pressure drop in the liquid system.

With both injectors giving the same results for the same flow conditions it was assumed that both flows had reached the equilibrium flow state (i.e. fully developed two-phase flow) before the Venturi meter inlet. Both the Shell Expro and Taitel and Dukler flow pattern prediction methods predicted annular dispersed flow across the NEL test matrix if a fully developed flow pattern was reached. Therefore, a further assumption was then made that annular dispersed flow was the probable flow pattern in existence for both injector tests. In all tests the camera showed a mist.

With the two different injector tests giving very similar results, both data sets are suitable for use in the analysis of the Venturi Meters performance, both in the comparison of the performance of the existing general DP Meter two-phase flow

correlations with respect to Venturi Meters and in developing new improved correlations. It is this comparison which is discussed next in Chapter 4.
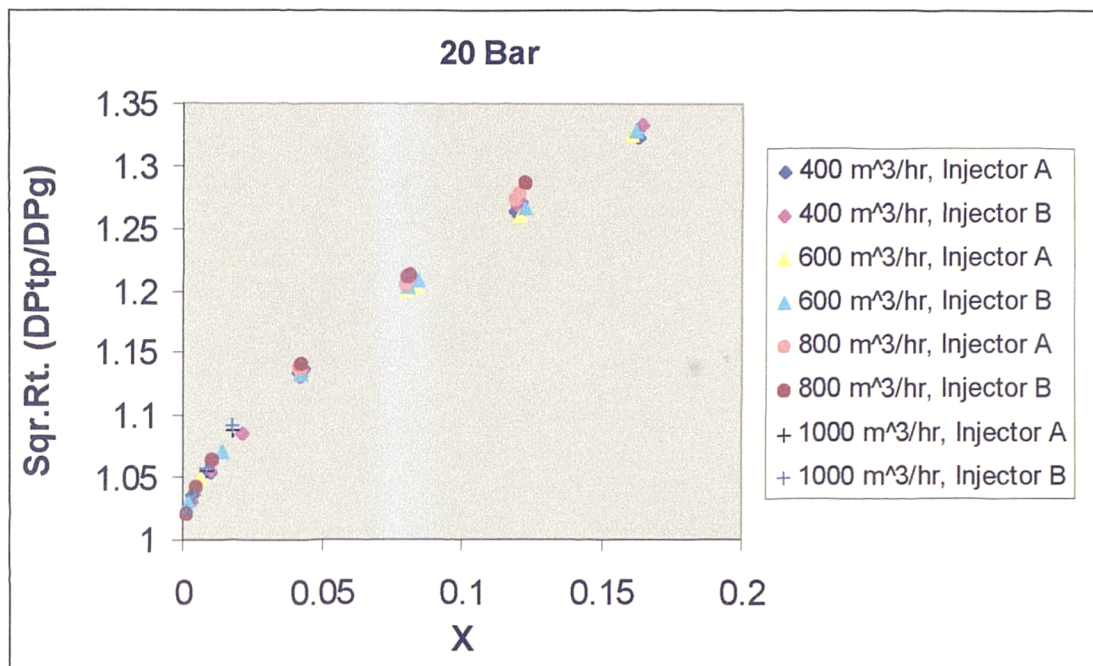
Figure 4.11. The 20 Bar Injector Comparison
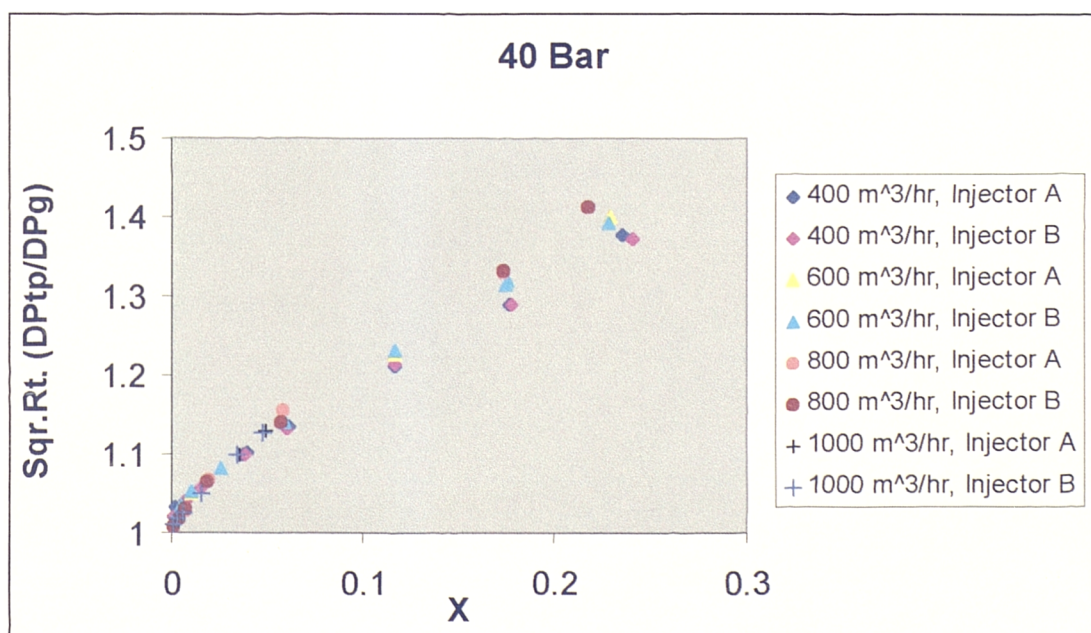
Figure 4.12. The 40 Bar Injector Comparison
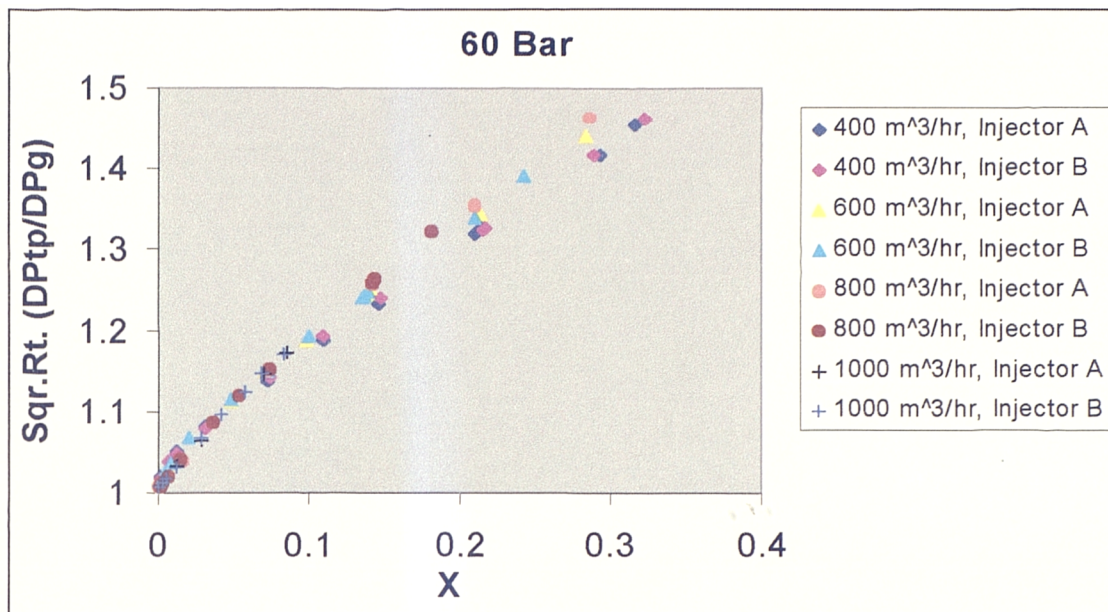
Figure 4.13. The 60 Bar Injector Comparison

4.3.7) The Uncertainty in the NEL Wet Gas Loop Data

As with all experimental data there is a degree of uncertainty associated with the values read from the NEL Wet Gas Loop. However, as this system is UKAS[1] accredited the uncertainty of the primary measurements are well known and stated in the NEL quality document "Procedure for Uncertainty Budgets for the Gas Flow Laboratory" [50].

It is stated [50] that the pressure readings have an uncertainty of 0.1%, the temperature readings have an uncertainty of 0.05%, the gas mass flow reference turbine reading has an uncertainty of 0.322% and the liquid mass flow reference turbine reading has an uncertainty of 0.2%. It is known from ISA Controls Ltd. that the Venturi Meter has an inside bore uncertainty of 0.9% and a throat diameter uncertainty of 0.1%. All the Yokogawa Differential Pressure Transducers are held in calibration by the NEL to within 0.1%. The liquid flow coefficient, K_l, (i.e. the product of the liquid compressibility factor and the discharge coefficient) is stated to have an uncertainty of 1% for flows with a Reynolds Number less than one million [9]. (All superficial liquid flows in this research are within this boundary.)

131

In order to carry out the required research it was necessary to use these primary measurements to calculate the values of more complex parameters. These parameters and their associated calculated uncertainties are as follows.

1) The gas density. The uncertainty was 0.113572 % for all three pressures tested.

2) The liquid density. The uncertainty was 0.05 % for all three pressures tested.

3) The dry gas flow coefficient, K_g, (i.e. the product of the gas compressibility factor and the gas discharge coefficient). The uncertainty was found to be 0.802452 % for 20 Bar, 0.923704% for 60 Bar and therefore with no 40 Bar dry gas testing carried out in this research an estimation of 0.863078 % for 40 Bar was made.

4) The ratio of the square roots of the actual two-phase differential pressure between the upstream and throat pressure tappings and the differential pressure that would be read if the gas phase flowed alone. The uncertainty was found to be 0.904069% for 20 Bar, 0.956912 % for 40 Bar and 1.010445% for 60 Bar.

5) The Modified Lockhart Martinelli Parameter. That is, the ratio of the square roots of the differential pressure between the upstream and throat pressure tappings for when the liquid phase flows alone and the gas phase flows alone. The uncertainty was found to be 1.237006 % for 20 Bar, 1.245914% for 40 Bar and 1.255001% for 60 Bar.

6) The Gas Densiometric Froude Number. That is, the square root of the Inertial to Gravity Forces on a liquid drop in a gas flow. The uncertainty was found to be 2.296913 % for 20 Bar, 2.271593% for 40 Bar and 2.271843% for 60 Bar.

7) The dry gas flow coefficient, K_g^*, (i.e. the flow coefficient which is defined as the product of the gas compressibility factor, the discharge coefficient and the velocity of approach for when the flow expansion between the throat and the downstream pressure tapping is used to meter the flow). The uncertainty was found to be 1.068254 % for 20 Bar, 0.8485228 % for 60 Bar and therefore with no 40 Bar dry gas testing carried out in this research an estimation of 0.9583883 % for 40 Bar was made.

---

[1] United Kingdom Accreditation Service.

8) The ratio of the square roots of the actual two-phase differential pressure between the throat pressure tapping and the downstream pressure tapping and the differential pressure that would be read if the gas phase flowed alone. The uncertainty was found to be 0.937704% for 20 Bar, 1.031696% for 40 Bar and 1.124958% for 60 Bar.

The calculations of these uncertainties are given in Appendix 7.

Chapter 5

5.1) Comparison of the Performance of Existing Correlations for DP Meters in General Two-Phase Flows with Respect to Wet Gas Flows Through Venturi Meters.

The method of comparing the seven correlations performances was chosen to be by comparison of the root mean square fractional deviation (d), as was done in [33] and [37]. That is:

$$d = \sqrt{\frac{1}{n} \sum_{i=1}^{n} \left(\frac{\dot{m}_{g(predicted)_i} - \dot{m}_{g(experimental)_i}}{\dot{m}_{g(experimental)_i}} \right)^2}$$

A secondary method of comparison was to plot the data on the type of graphs used by Lin in [21], i.e. a plot of the ratio Predicted to Actual Gas Mass Flowrates against The Flow Quality. The 243 data points in the test matrix were used to calculate the root mean square fractional deviation (d) and plot these graphs. These root mean square fractional deviation calculations are given in Appendix 4.

For the case of the root mean fractional deviation, results were calculated for all the data together and then for the individual pressures. The results are shown in Table 5.1. For the case of the graphical comparisons, plots for 20 bar, 40 bar and 60 bar cases are shown in Figures 5.1, 5.2 and 5.3 respectively.

All Pressures	d		40 Bar	d
de Leeuw	0.0211		de Leeuw	0.0193
Homogenous	0.0237		Homogenous	0.0220
Lin	0.0462		Murd, M=1.5	0.0410
Murd, M=1.5	0.0482		Lin	0.0448
Murd, M=1.26	0.0650		Murd, M=1.26	0.0589
Chisholm	0.0710		Chisholm	0.0658
Smith & Leang	0.1260		Smith & Leang	0.1199
20 Bar	d		60 Bar	d
de Leeuw	0.0279		de Leeuw	0.0140
Homogenous	0.0285		Homogenous	0.0202
Lin	0.0449		Murd, M=1.5	0.0287
Murd, M=1.5	0.0677		Lin	0.0479
Chisholm	0.0793		Murd, M=1.26	0.0504
Murd, M=1.26	0.0823		Chisholm	0.0675
Smith & Leang	0.1159		Smith & Leang	0.1401

Table 5.1. The Results of the Root Mean Square Fractional Deviation for All Pressures Together and for each Individual Pressure.

It should be noted that as Table 5.1 presents the seven correlation performances in terms of the root mean square fractional deviation between the gas mass flow predictions and the "actual" gas mass flow metered by the gas reference turbine it is not possible to differentiate between correlations that have root mean square percentage deviations less than the uncertainty of the reference meter (i.e. 0.322%).

The de Leeuw correlation appears to have the best overall performance across the test range although the Homogenous Model performs similarly well at conditions other than 60 Bar. Only at 60 Bar is it clear that the de Leeuw correlation is more accurate than the Homogenous model as the difference in the root mean square percentage deviation is only then greater than the uncertainty in the gas turbine reference meter.

The good performance of the de Leeuw correlation is perhaps not surprising considering it was created from data that was obtained from a Venturi Meter that had similar flow conditions to the NEL tests (i.e. a pressure range of 15 to 90 bar, gas flowrates up to 1000 m^3/hr, a Modified Lockhart Martinelli Parameter range of 0 to 0.3 and similar simulant fluids). This comparison therefore confirms the de Leeuw correlation as the best currently available to engineers required to meter wet gas flows with Venturi Meters. Of course, like the new correlations developed in this thesis (see Chapter 6), it is still limited to a maximum gas flowrate of 1000 m^3/hr which is a major problem to the natural gas production industry as many of their flows have flowrates well in excess of this value. However, with no test facilities in existence capable of creating higher flowrates the only course of action open to the operators is to extrapolate the most accurate correlation for these lower flowrates. Hence, of the correlations tested here, as de Leeuw's correlation has a similar performance to the Homogenous Model at 20 Bar and 40 Bar and has the best performance at 60 Bar it is the best choice for industry when faced with the problem of metering wet gas flows with Venturi Meters.

A far more surprising result was the good performance of the Homogenous Model. With no modelling of the likely flow pattern this author expected it to have one of the poorest performances of the correlations tested. However, this simple model for a pseudo-single phase flow was clearly as good as the de Leeuw correlation at 20 Bar and 40 Bar and was only marginally less accurate at 60 Bar.

The author expected the Venturi Murdock correlation to perform better than it did. As it was the second of the two Venturi Meter specific correlations available for testing it was expected that its performance would be reasonably good. However, this correlation is seen to be inferior to both the de Leeuw and the Homogenous

correlations at all pressures. In fact, at 20 Bar the Lin correlation performs better while at 40 Bar the difference in performance between these correlations is barely enough to distinguish over the gas turbine reference meter uncertainty. It should be noted that the performance of the Venturi Murdock correlation improves with increasing pressure. However, it will be seen in Chapter 6, where the Murdock Gradients for the new NEL data are calculated for each of the three test pressures, that this is just a coincidence as these gradients drop from 2.3775 at 20 bar to 1.6173 at 60 bar. Hence the correlation performance seems to improve simply because the correlations set gradient of 1.5 happens to be being approached as the pressure increases. Clearly then, this correlation does not fit this researches data well at all (compared to the Homogenous Model and the de Leeuw correlation) and even at the 40 bar test case which is close to the pressure the correlation was created for the performance is relatively poor.

Of the Orifice Plate Meter correlations, the Lin correlation had the best overall performance. The well known Murdock correlation did not perform well compared to the Lin correlation at 20 Bar and 40 Bar. Only at 60 Bar did the Lin and Murdock Orifice Plate correlations have similar performances. It therefore appears that the Murdock's mathematical model does not include all the important parameters and / or the data set used is unsuitable for extending the correlations use to Venturi meters. The Lin correlation was based on a very similar model to Murdock's correlation except that it took account of a pressure effect. Due to the difference in the performance between the Lin and Murdock correlations it appears that taking account of the pressure is important.

Chisholm's correlation gave a poor result. Like the Murdock correlation it appears that this general two-phase flow Orifice Plate Meter correlation does not fit wet gas Venturi Meter data at all well. The poorest of the seven correlations by far was the Smith & Leang correlation. It appears that the form of the Blockage Factor equation was perhaps not the best to model wet gas flows through a Venturi Meter.

Finally, it should also be noted that both the Smith & Leang and Lin correlations do not predict the no error situation at the dry gas condition of 100% quality (see Figs 5.1, 5.2 & 5.3) as is required by theory if a condition of no error for dry gas is

assumed. Note that the other correlations all converge on the no error point of the predicted to actual gas flowrate ratio value of unity at 100% quality. The reason for the Smith & Leang and Lin correlations non-compliance with the required result at x = 1 is almost certainly due to the data sets used. Both correlations have been fitted to the available data sets that did not have any extremely high quality data and hence the extrapolation done in this comparison has produced this error.
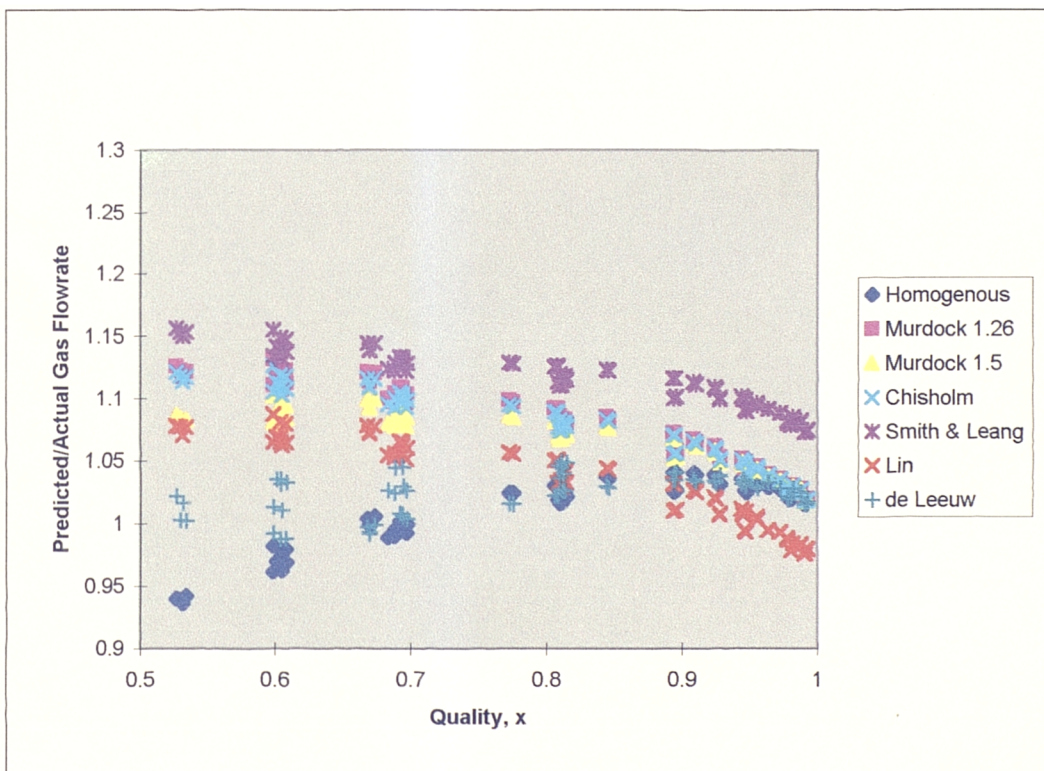
Figure 5.1. The 20 Bar Correlation Comparison.
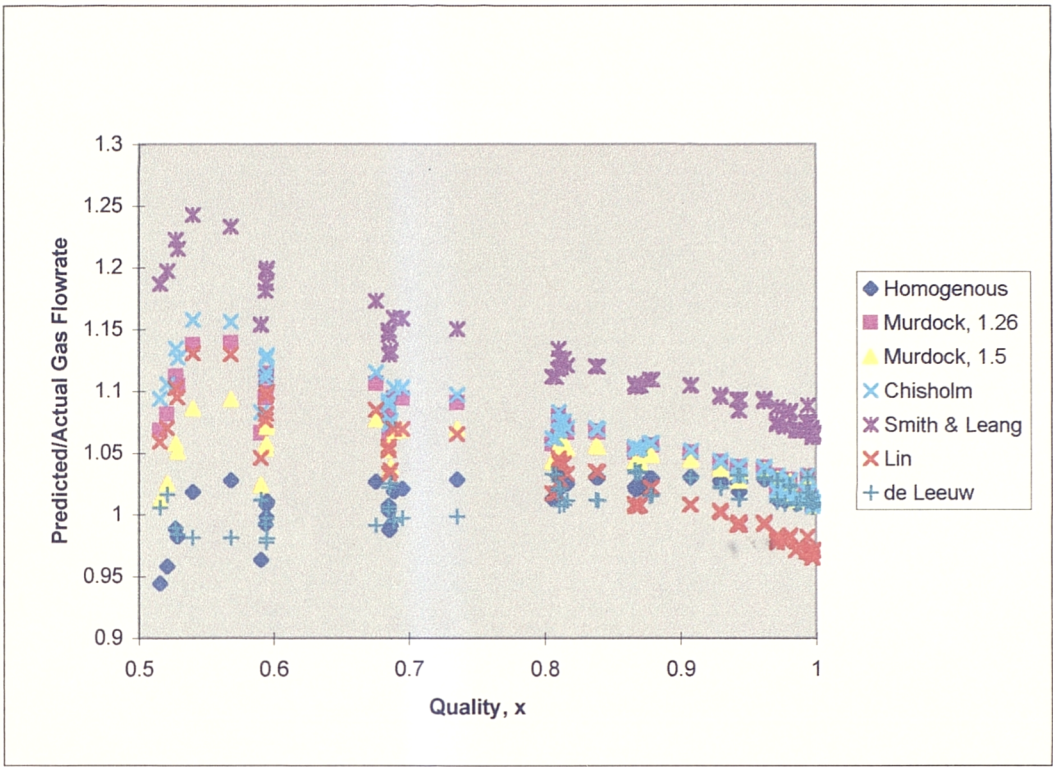
Figure 5.2. The 40 Bar Correlation Comparison.
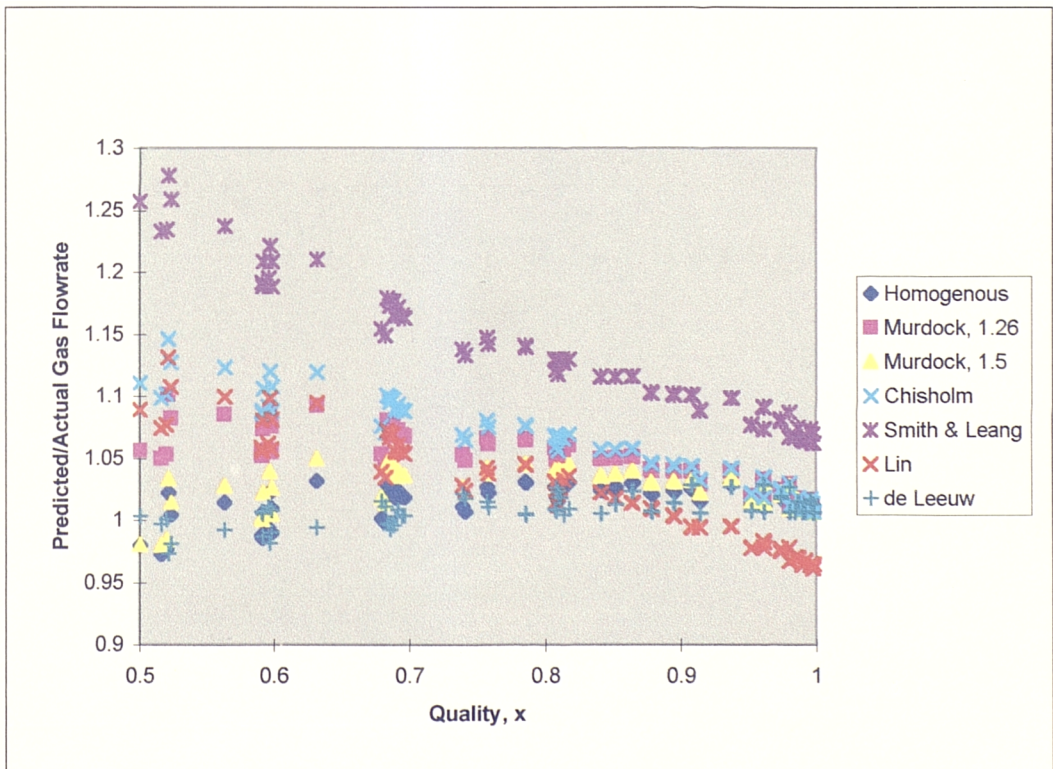
Figure 5.3. The 60 Bar Correlation Comparison

5.2) <u>Summary and Discussion of the Comparison Results</u>

It is clear that for wet natural gas metering with Venturi Meters the Homogenous Model and the de Leeuw correlation are similar in performance to each other and better than the other correlations. Only at 60 Bar is the de Leeuw correlation clearly better than the Homogenous Model as only at this pressure was there a large enough difference between the correlation performances for the uncertainty in the gas turbine reference meter not to be significant.

The good performance of the Homogenous Model was initially a surprising result. However, with the wet gas flows considered to have a large amount of entrainment it was realised that perhaps a pseudo-single phase assumption was not unreasonable. Furthermore, as the pressure increased the performance of the Homogenous Model improved. It has been postulated that the reason for this result is that with greater pressure there is a reduction in the difference between the gas and liquid densities and this should lead to a reduction in the magnitude of the slip (i.e. the velocity difference between the phases). With the Homogenous Model assuming a pseudo-single phase flow it automatically stands that the Homogenous Model assumes no slip exists between the phases. Hence, with increasing pressure reducing the magnitude of the slip it is considered likely that the higher the pressure the better the Homogenous Model performance. (Nevertheless, at 60 Bar the Homogenous Models performance was still clearly inferior to de Leeuw's correlation.)

The relatively poor performance of the Venturi Murdock correlation is probably due to the data set used in its creation being for a quite different set of conditions, e.g. different gas and liquid flowrates, a different beta ratio, etc. As stated in the Literature Review Phillips Petroleum did not divulge any information other than the tests were done at 45 Bar.

The fact that the Murdock correlation is the best known general two-phase flow DP Meter correlation makes its poor performance a disappointing result. It is very likely that field engineers have used this correlation in the past due to the lack of any alternative when attempting to correct the liquid induced error in a wet gas flow being metered by a Venturi Meter. Unless there is a major effect caused by the greater gas

flowrates in actual production flows then a significant error in the metering would have occurred.

It was noted that although the Murdock correlation performed poorly, the Lin correlation performed slightly better at 20 Bar and 40 Bar. (At 60 Bar the correlations have a similar performance.) Now, as the Lin model and the Murdock model which create the correlation forms are very similar with the exception that Lin accounts for an effect due to pressure it looks like an update of the well known Murdock correlation to account for pressure could be useful. Lastly, as de Leeuw stated that the Densiometric Gas Froude No. had an effect as well as pressure (or in other words the pressure and gas flowrate effect the wet gas Venturi Meter error) it is necessary to check for these relationships in the data as when and if they are found an equation relating Murdocks gradient (M) to the pressure and gas flowrate could be created. This would allow field engineers a quick and easy substitution of this new equation into the original Murdock correlation (a correlation many are already familiar with) giving a new correlation for wet gas metering. In Chapter 6, relationships between the Venturi meter wet gas error and the pressure and gas flowrates are examined and new correlations are offered.

Chapter 6

New Correlations

During the early stages of this research the author looked into the possibility of creating an improved mathematical model for predicting the two-phase flow phenomena as it flows through a Venturi Meter. However, from an examination of the literature that deals with mathematical modelling of general two-phase flows in simple straight pipes it became clear that due to the scale of such a task it was impractical for this research which was sponsored on the condition the research would yield results of practical use to industry. Therefore this project had to resort to the use of best fit equations to obtain new correlations. However, it should be noted that the existing correlations discussed in Chapter 2 have little physical basis. Furthermore, only two of the seven correlations discussed in Chapter 2 were based on Venturi Meter data and even then the Modified Venturi Murdock correlation only used data for a single pressure. Also de Leeuw used data from a 4" line with Venturi Meter of beta ratio 0.401. Therefore, as these new correlations are formed using a large number of wet gas Venturi Meter (6", 0.55 beta ratio) data they can be regarded as valuable additions to the wet gas metering literature.

The statement that the existing correlations have little physical basis is based on the following facts. The Homogenous Equation is not based on any physical model other than the assumption that the phases mix so completely that a pseudo-single phase flow is created. This method was shown to work reasonably well in Chapter 5 but it was less accurate than de Leeuw's correlation which used data from two different flow patterns. The Murdock, Chisholm, Lin and Murdock Venturi correlations are all modelled on the assumption that the flow pattern is stratified flow only with no liquid entrainment in the gas flow. This is clearly not the case in most wet natural gas industrial applications and therefore fitting actual two-phase flow data from industrial applications to these models makes little more physical sense than using any other form of equation. The Smith and Leang correlation was based very loosely on modelling the expected flow pattern when choosing the form of the

correction factor but the performance was so poor there is no justification for the use of this correlation form with the data obtained during this research.

Finally, the most recent wet gas Venturi Meter correlation proposed by de Leeuw which at first glance appears to model the flow pattern to a greater degree than the other correlations actually does little more. The equation is of Chisholm's form with the only difference being that a constant given by Chisholm has been replaced by an empirical equation found using Shell Expros wet gas test data.

These facts indicate that using this researcher's 6 inch diameter (0.55 beta ratio) meter data to form a new empirical wet gas Venturi meter correlation offers a valid advance in the field of wet gas metering. First however, before attempting to fit an equation to the data, an examination of the data for physical trends was carried out.

6.1) Venturi Meter Performance Trends Obtained from the NEL Wet Gas Loop Data

The two trends that were expected to appear were mentioned previously in Chapters 2 and 4, namely the meters over-reading dependence on pressure and on the gas mass flowrate (or in other words, gas on the Densiometric Froude No.). These relationships were investigated by plotting the appropriate data sets on a Murdock type graph (i.e. plot of $\sqrt{\Delta P_{tp}/\Delta P_g}$ vs. X) and comparing the results. That is, for the case of the over-readings anticipated dependence on pressure, the three test pressures of 20, 40 and 60 bar had all their data points (for all gas flowrates) plotted and then compared with each other. For the case of the over-readings expected dependence on the gas mass flowrate, three Murdock type graphs were used (one for each test pressure) and the data for each of the four gas volumetric flowrates (400, 600, 800 and 1000 m^3/hr) plotted on each of these three graphs.

6.1.1) The Relationship between the Liquid Induced Meter Error and the Pressure.

In the literature review it was shown that the Murdock Equation does not take account of any influence of pressure on the meter error induced by the liquid presence. Since Murdock published his correlation both Chisholm and Lin have stated

that pressure has an effect on Orifice Plate Meter readings in two-phase flows. For the case of Venturi Meters de Leeuw assumed that pressure would have an effect on the meter error.

The wet gas data obtained from the NEL Wet Gas Loop showed that there is indeed a relationship between the pressure and the meter error. To show this the three data sets (one for each pressure tested with all flowrates at each pressure included) where plotted in a Murdock type graph, see Figure 6.1.
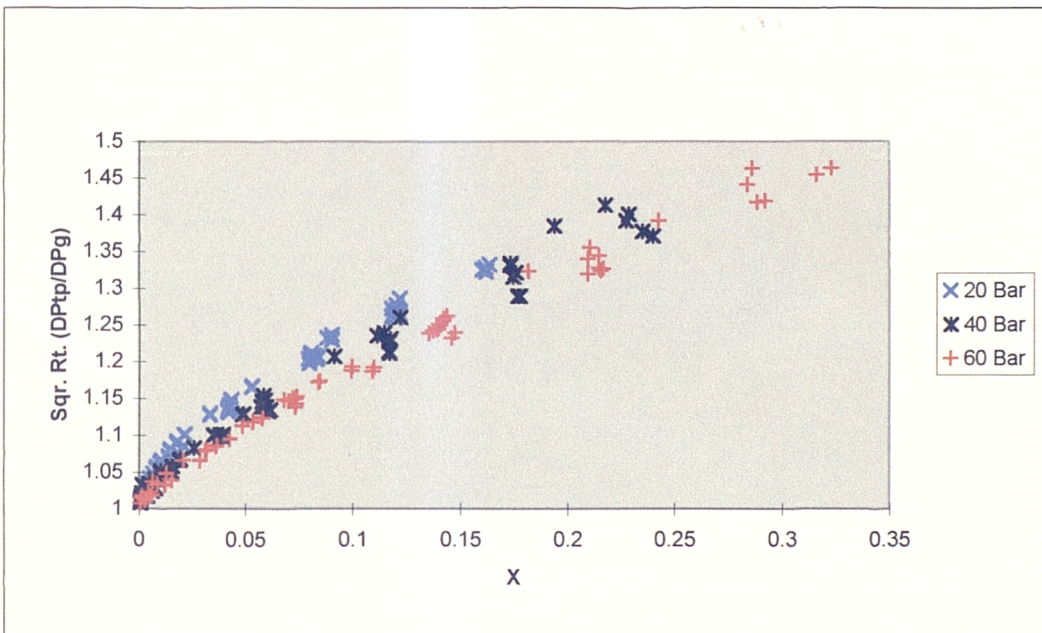
Figure 6.1. All Data Plotted on a Murdock Type Graph.

Clearly the pressure is an important parameter in estimating the meter error. This makes physical sense as the pressure partially dictates the type of flow pattern and as it is now accepted that the flow pattern directly influences a DP Meter reading it is reasonable that a new correlation would require to take the pressure effects into account. A trend that is clear from Figure 6.1 is that with increasing pressure the gradient of the curve reduces. This fact is used to create a new correlation that is developed later in this Chapter (Section 6.3).

6.1.2) The Relationship between the Liquid Induced Meter Error and the Gas Flowrate.

de Leeuw stated that it was not only pressure that dictated the error of a Venturi Meter in wet gas but also the gas Densiometric Froude No. As this parameter is solely dependant on pressure and gas flowrate for given fluid properties and meter geometry it was decided to discuss this phenomenon in terms of the more basic parameter, the gas flowrate, rather than the gas Densiometric Froude No.

Again, just as with pressure, it was found that the gas velocity did indeed influence the Venturi Meter over-reading. The Murdock type graph is again used to show this. Individual graphs are shown in Figures 6.2, 6.3 and 6.4 for each of the set pressures. It can be seen that for each pressure the increasing gas flowrate gives a steeper curve, more pronounced at the higher pressures and with the higher values of X. Again, this makes physical sense. For a set pressure and set fluid properties when considering one value of the Modified Lockhart Martinelli Parameter, as the gas volumetric flowrate increases then so must the liquid volumetric flowrate. However, for the higher gas flowrates a greater proportion of the liquid will be entrained in the gas. As it is likely that the energy losses due to the drag on the droplets will increase more than the energy losses will reduce due to a reduced shear on the stratified or film liquid flow, an increasing gradient for an increasing gas flowrate on the Murdock graphs shown in Figures 6.2 to 6.4 is expected.
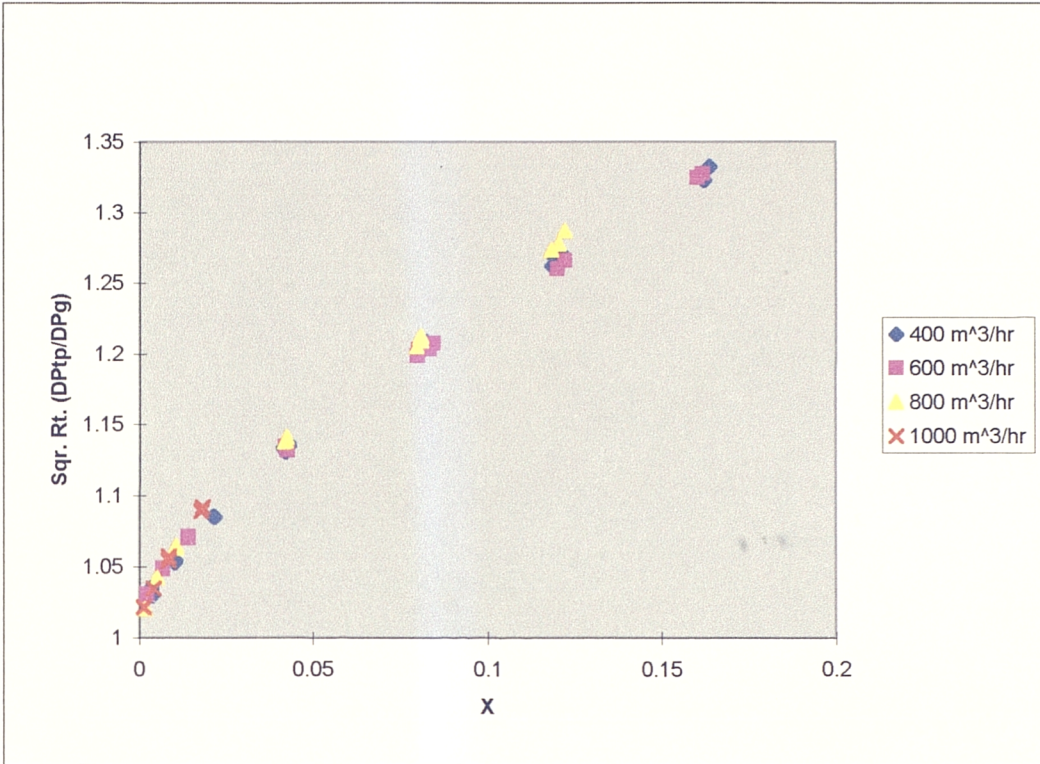
Figure 6.2. The 20 Bar Data Plotted on a Murdock Type Graph.
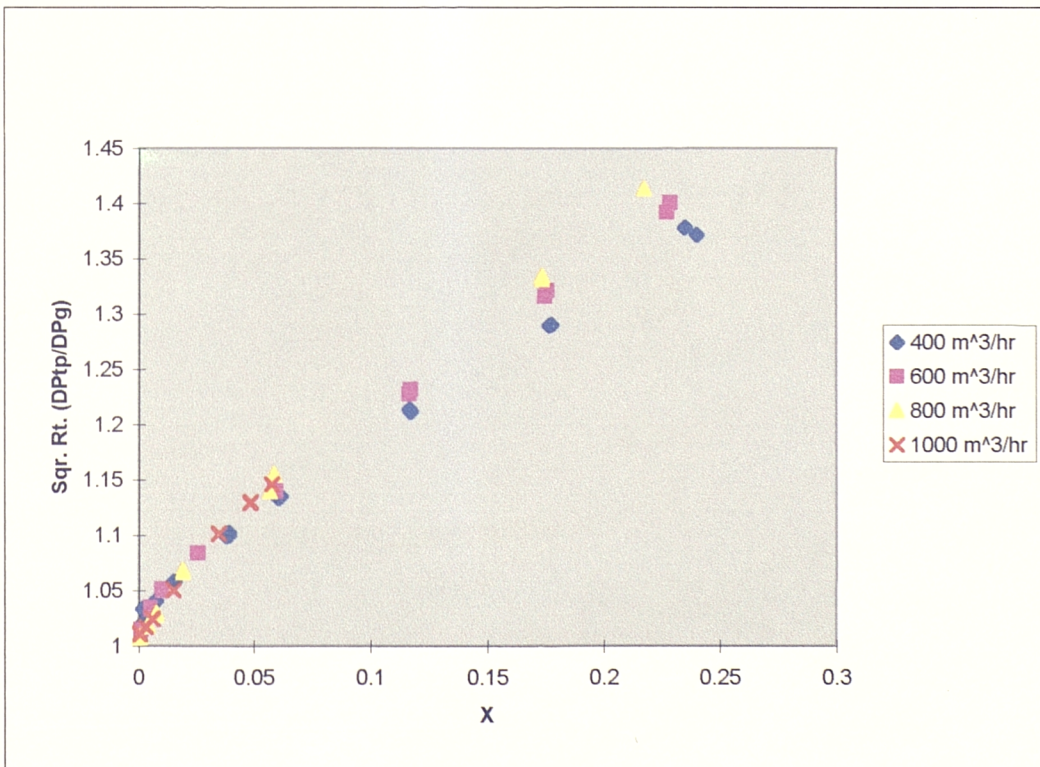
Figure 6.3. The 40 Bar Data Plotted on a Murdock Type Graph.
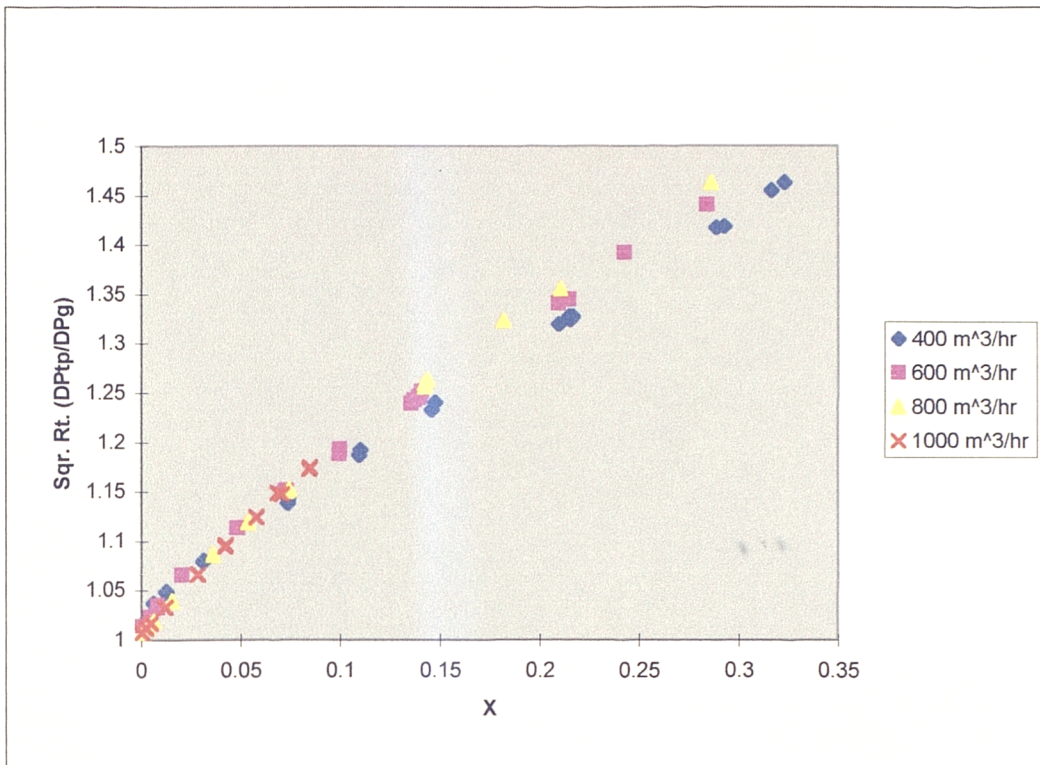
Figure 6.4. The 60 Bar Data Plotted on a Murdock Type Graph.

A final comment on the trends found in the new NEL wet Gas Data is required at this point. It should be noted that the data gives a definite curve rather than a straight line when plotted on a Murdock graph. It is therefore clear that a best fit straight line is not as effective as fitting a polynomial expression to the data. However, the increase in complexity when trying to obtain polynomials for different pressures and gas flowrates is considerable for what maybe a small reduction in uncertainty. As industry likes simplicity in field situations and field engineers are well aquainted with the Murdock correlation, it was decided to continue with the plan to update the Murdock equation by finding the best linear fit Murdock gradient for each pressure and gas flowrate. However, it was decided that once this was done a search for a better correlation should be undertaken.

6.2) Updating the Murdock Gradient

The Murdock Venturi Equation was formed when Phillips Petroleum obtained reliable data for Venturi Meter performance in a wet natural gas flow. This data was simply used to find a new Murdock gradient that suited Venturi Meters better than the original value that was for Orifice Plate Meters only. However, Phillips Petroleum did not divulge the gas and liquid phase flowrates but did state the data was for one particular pressure of 45 bar. Of course, for the original Murdock Equation the gradient was obtained from a test matrix that included data of several different fluid types, pressures, flowrates, pipe diameter etc. Hence, the Murdock Venturi Equation was certainly better than the original Murdock Equation for the specific needs of Phillips Petroleum at that particular well (where they used a Venturi Meter of unknown beta ratio) but a question mark existed on whether it was better across the full range of wet natural gas flow conditions. This question was answered fairly conclusively when the results of the correlation comparison in Chapter 4 showed this correlation to have a significantly poorer performance than de Leeuw's correlation. The first work done in forming new correlations was to repeat Murdocks method using the available new data to get a new average gradient for the ISA Controls Venturi Meter tested at the NEL. The resulting plot and best fit line are shown in Figure 6.5.
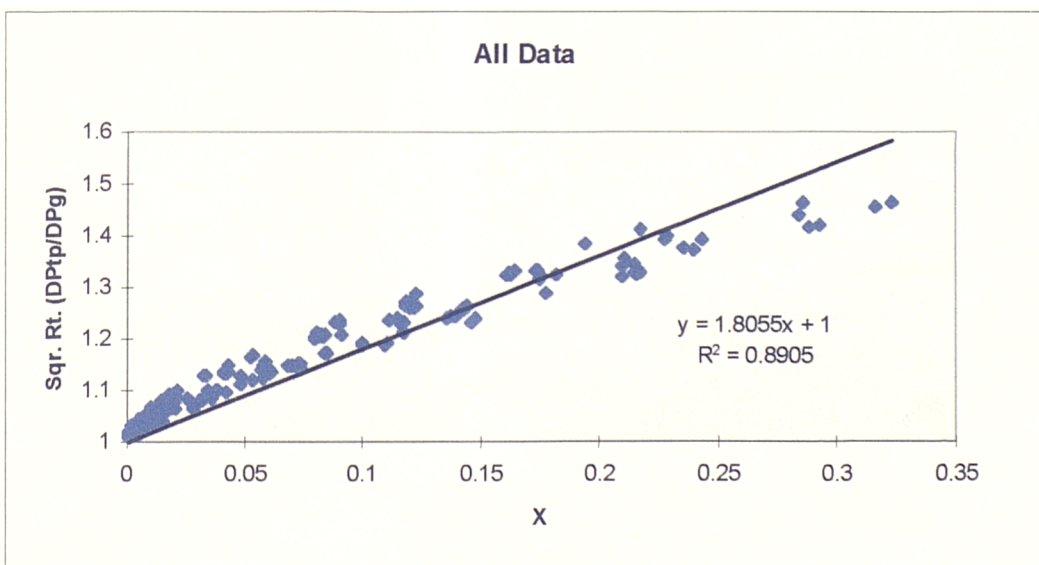
Figure 6.5. An updated Murdock Graph showing a best linear fit through all the data.

The new gradient is M=1.8055. The new correlation is therefore:

$$m_{gas} = \frac{K_g A_t \sqrt{2\rho_g \Delta P_{tp}}}{1 + 1.8055X}$$

(6.1)

The range of applicability of this new equation is:

$$20 \text{ Bar} \leq \text{Pressure} \leq 60 \text{ Bar}$$

$$400 \text{ m}^3/\text{hr} \leq \text{ Gas Volumetric Flowrate} \leq 1000 \text{ m}^3/\text{hr}$$

The range of the Lockhart Martinelli Parameter, X, is more difficult to state. All the sets of pressure and gas flowrates have individual maximum and minimum values of X. Ideally of course, for each pressure, X was to range from zero up to the equal gas and liquid mass flowrate condition, which translates to an X value given by the square root of the gas to liquid density ratio. However, due to the minimum liquid injection rate being set by the capability of the liquids reference meters each pressure and gas flowrate had a non-zero minimum liquid flowrate (and hence Lockhart Martinelli Parameter). Rather than producing a complex function to get the precise minimum X value for each pressure and gas flowrate combination the largest minimum X value is given here as the minimum value for which the correlation is valid. (There was however not a great difference between the minimum values and they are an order of magnitude less than the maximum X values.) The minimum value for the correlation range is:

$$X_{min} = 0.001312$$

The maximum X value is considerably more difficult to define. It was discussed in Chapter 3 that the liquid pump did not have the capability to reach the desired maximum liquid flowrate for the 1000 m^3/hr case. Hence, from 400 to 800 m^3/hr the desired maximum Lockhart Martinelli Parameter was achieved but for 1000 m^3/hr the actual maximum fell far short of that which was desired. Therefore, to find the maximum limits of the correlation it is necessary to produce a function that gives the

maximum Lockhart Martinelli Parameter in terms of pressure and gas flowrate. The values of each maximum value for set pressures and gas flowrates were plotted against these pressures and gas flowrates and an equation for the surface was fitted by the TableCurve 3D software. This maximum Lockhart Martinelli Parameter is given by equation 6.2. The surface fit is shown in Figure 6.6.

$$X_{max} = \frac{a + bP + CP^2 + d\,\dot{Q}_g + e\,\dot{Q}_g + f\,\dot{Q}_g^{\,2}}{1 + gP + hP^2 + i\,\dot{Q}_g + j\,\dot{Q}_g^{\,2}} \qquad (6.2)$$

where P is pressure (in bar g) and Qg is volumetric flowrate (in m³/hr).
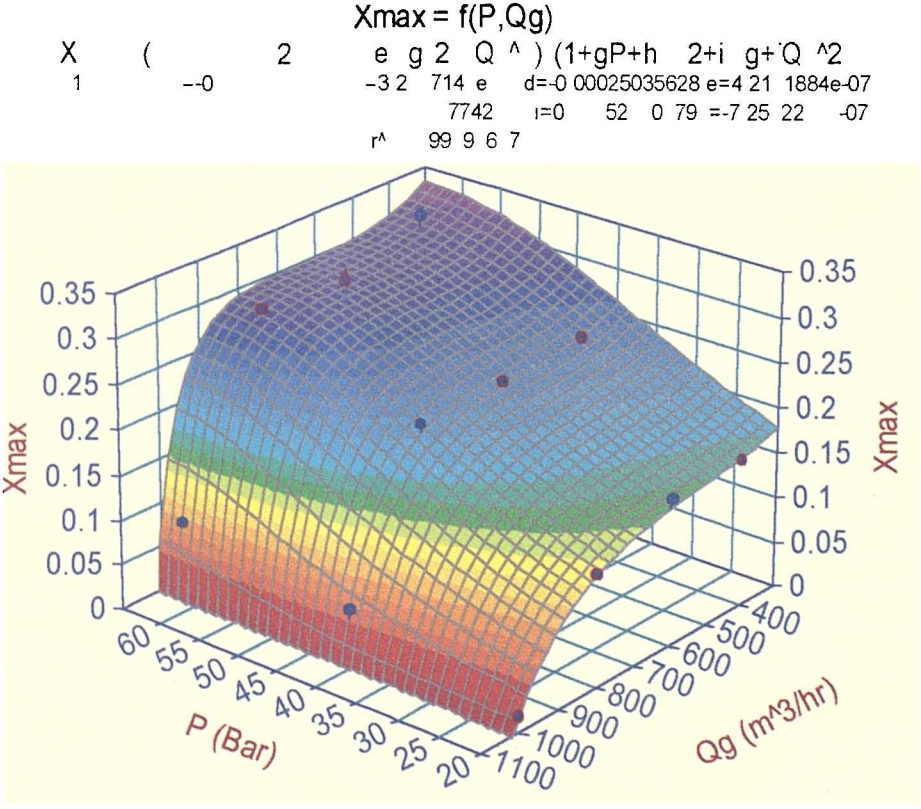
Figures 6.6. Surface Showing the Maximum Modified Lockhart Martinelli Parameter vs. Pressure (gauge) vs. Gas Flowrate.

150

The constants required for equation 6.2 shown in Figure 6.6 are reproduced in Table 6.1 for clarity.

a	0.17838019		f	-3.3612255e-10
b	-3.1985224e-4		g	-2.2550318e-2
c	3.2457147e-6		h	1.7742744e-4
d	-2.5035628e-4		i	5.2110779e-4
e	4.219188e-7		j	-7.2532252e-7

Table 6.1. The constants of Equation 6.2.

Using the newly determined value of the Murdock gradient gave a root mean fractional deviation of 0.0383 for all the data together which was certainly better than the performance of the existing Murdock (M = 1.26) and Venturi Murdock (M=1.5) correlations (which had root mean fractional deviations of 0.0650 and 0.0482 respectively). However this is still inferior to the de Leeuw and Homogenous correlations (which had root mean fractional deviations of 0.02108 and 0.02372 respectively). For the individual pressures the root mean square fractional deviations are given in Table 6.2. The calculations are presented in Appendix 5.

Pressure	All	20 Bar	40 Bar	60 Bar
d (+/-)	0.0383	0.0505	0.0267	0.0340

Table 6.2. Root Mean Fractional Deviations of Equation 6.1.

It is clear that this correlation does not perform particularly well for all cases. Even though this new correlation was created using the same data as was used to check the root mean fraction deviations, two of the existing correlations have a better performance overall. Furthermore, at 20 bar the Lin correlation is better and at 60 bar the Venturi Murdock is better.

6.3) Updating the Murdock Gradient to Allow for Pressure Effects

It was stated in the literature review that the Murdock Equation did not take account of any pressure or gas flowrate effects. As the Murdock Venturi Equation is exactly the same model with different data being used to find the Murdock gradient (i.e. the correlation constant) then it also does not take account of any pressure or gas flowrate effects. It was also stated in the literature review that since Murdock published his equation several other investigators have stated that the pressure must be included in any correlation. Therefore, the next new correlation formed during this research was the updating of the Murdock Venturi Equation to take account of pressure. As no mathematical model was available to aid the formation of a new correlation it was considered suitable to attempt to refine the Murdock equation by finding the relationship between the Murdock gradient and the pressure as suggested in the last section.

The method used was as follows. For each pressure the data was plotted separately. That is, for the 20, 40 and 60 bar tests Murdock style plots were used to obtain the best linear line fits. At this point it should be noted that these pressures were the chosen ideal values for the tests but of course in reality the pressures obtained varied slightly during the test series so the averaged pressures for each of the three data sets were 20.325 bar, 40.324 bar and 60.526 bar. The resulting graphs are shown in Figures 6.7, 6.8 and 6.9.
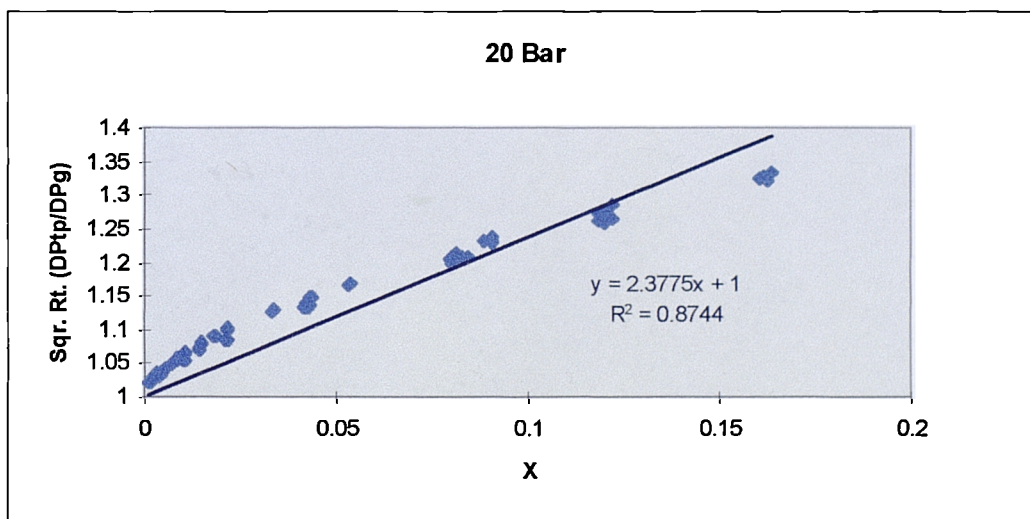
Figure 6.7. The best linear fit for the 20 Bar data plot.
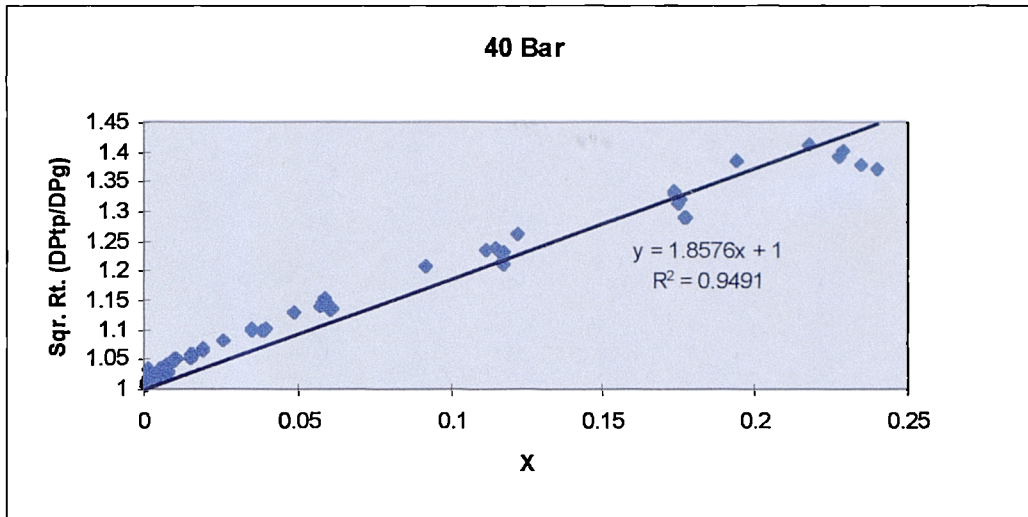
Figure 6.8. The best linear fit for the 40 Bar data plot.
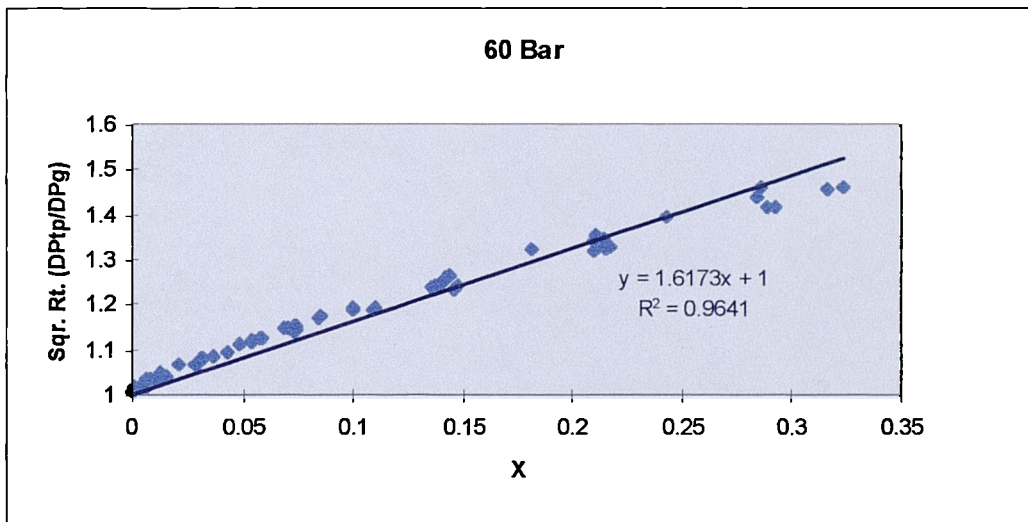
Figure 6.9. The best linear fit for the 60 Bar data plot.

A gradient for each test pressure was then obtained. Ideally of course, this process should be carried out for many pressures in order that the relationship between the gradient (M) and the pressure could be found with greater accuracy. Table 6.3 lists the results obtained.

Pressure (Bar g)	Murdock Gradient "M"
20.325	2.3775
40.324	1.8576
60.526	1.6173

Table 6.3. Murdock Gradients found at Each Line Pressure Tested.

The contents of Table 6.3 were then used to plot Murdock gradient M, vs. pressure, P and a best fit line was found by use of the software "TableCurve 2D". This was preferred to using a simple polynomial fit as an appropriately chosen equation found by TableCurve 2D was seen as being both more accurate and less likely to diverge out with the limits of the data range. The graph and line fit are presented in Figure 6.10.
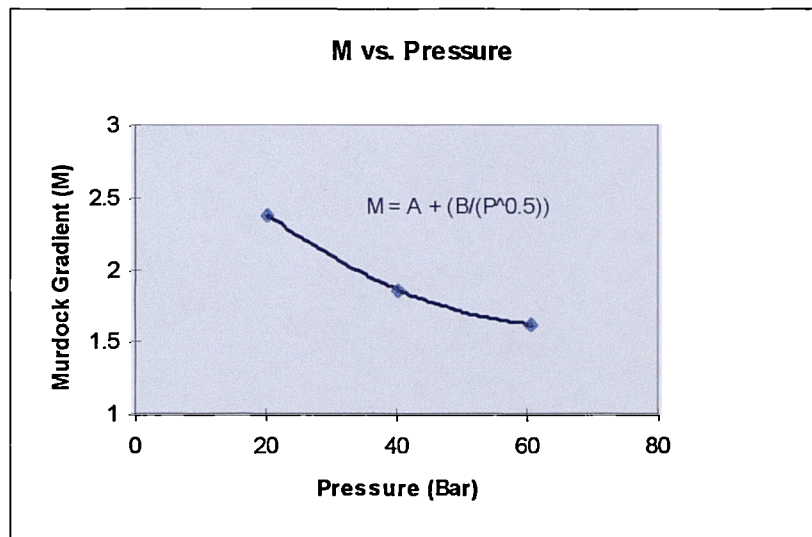
Figure 6.10. The Relationship between the Murdock Gradient and Gauge Pressure.

The equation found by TableCurve 2D is:

$$M = 0.57308671 + \frac{8.1389047}{\sqrt{P}}$$
(6.3)

Where P is the line pressure in bar g.

The new correlation is therefore:

$$\dot{m}_{gas} = \frac{K_g A_t \sqrt{2\rho_g \Delta P_{tp}}}{1 + MX}$$
(6.4)

where M is found from equation 6.3. The range of applicability of this correlation is the same as for the previous correlation (equation 6.1).

On using this equation with the NEL Wet Gas Loop data the root mean standard fractional deviation (d +/-) for each test pressure was found and these results are reproduced in Table 6.4.

Pressure	All	20 Bar	40 Bar	60 Bar
d (+/-)	0.0281	0.0324	0.0266	0.0250

Table 6.4. Root Mean Fractional Deviations when using Equation 6.3 with Equation 6.4.

This was therefore an improvement on the previously created correlation given in Section 6.2 and shows that there is a pressure effect that needs to be accounted for. However, although this result shows a distinct improvement over equation 6.1 it is still seen to be inferior to the Homogenous and de Leeuw correlations. On the positive side this method clearly shows that by taking account of the pressure effect across the test range a marked improvement in the prediction was achieved.

The investigation into the trends in the NEL Wet Gas data (see Section 6.1) showed that the pressure and gas flowrate directly effect the Murdock gradient. de Leeuw's correlation takes account of both pressure and gas flowrate effects and appears subsequently to have the best performance of the published correlations. It was therefore decided that the Murdock gradient should be further refined by expressing it as a function of the pressure and gas flowrate.

6.4) Updating the Murdock Gradient to Allow for Pressure and Gas Flowrate Effects

In order to update the prediction of the Murdock gradient to include the effects of both pressure and gas flowrate it was necessary to find the value of this gradient (M) for each case of set pressure and gas flowrates. Hence, as the test matrix had been carried out to set the gas flowrate from 400, 600, 800 to 1000 m^3/hr for each pressure of 20, 40 and 60 bar in turn, and of course in actual test conditions these ideal values

varied slightly, the actual average pressure and gas flowrate values for each desired data set were found to be as shown in Table 6.5.

Average Gauge Pressure (Bar)	Average Gas Flowrate (m^3/hr)
20.177	401.09
20.247	602.24
20.363	801.99
40.024	400.49
40.218	601.28
40.280	800.98
60.143	400.72
60.411	600.77
60.727	801.17

Table 6.5. The Average Set Pressures and Gas Flowrates across which the Liquid Flowrate Range was Injected.

Note that the 1000 m^3/hr test data has not been included since, as stated earlier, the NEL Wet Gas Loop could not maintain 1000 m^3/hr when the liquid injection rate was increased to give mid to upper values of the modified Lockhart Martinelli Parameter (X). This meant that when the 1000 m^3/hr data is plotted on the Murdock type graph for all three pressures there is not enough spread in the values of X to give a reliable gradient. Therefore, the range for this correlation will be restricted to a maximum gas flowrate of 800 m^3/hr.

With these separate data sets Murdock type graphs were plotted and the corresponding gradients were obtained. The nine Murdock style graphs, with the associated linear line fit, are presented in Figures 6.11 to 6.19.
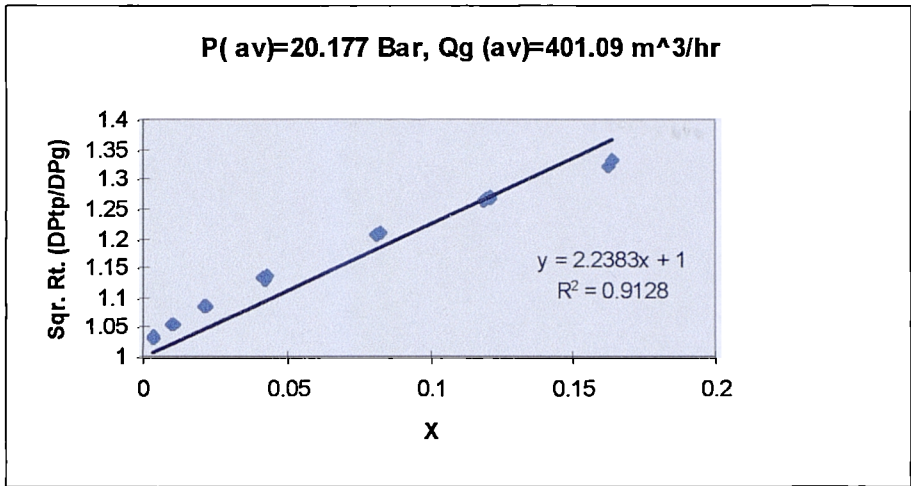
Figure 6.11. The best linear fit for the 20 Bar, 400 m³/hr data plot.
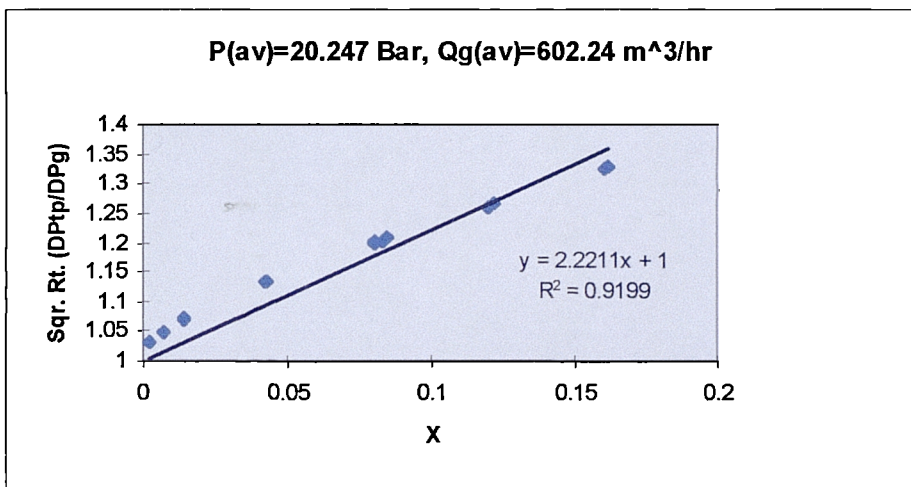
Figure 6.12. The best linear fit for the 20 Bar, 600 m³/hr data plot.
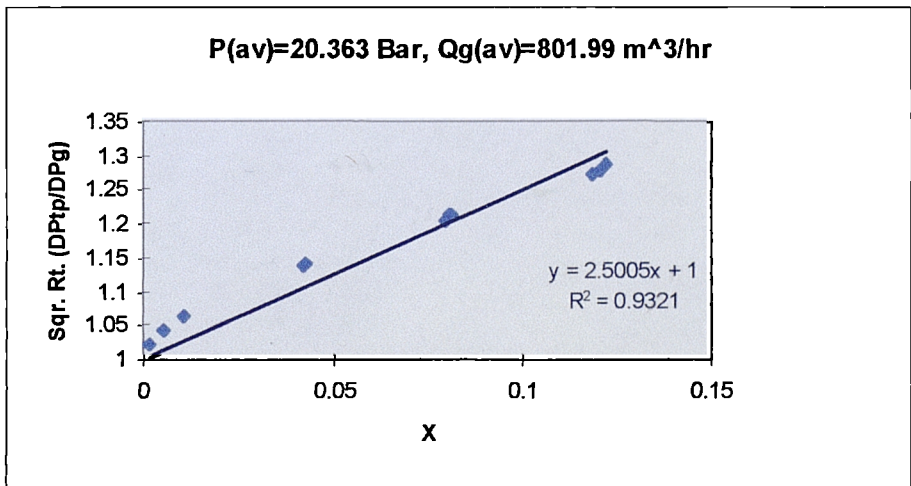
Figure 6.13. The best linear fit for the 20 Bar, 800 m³/hr data plot.

157
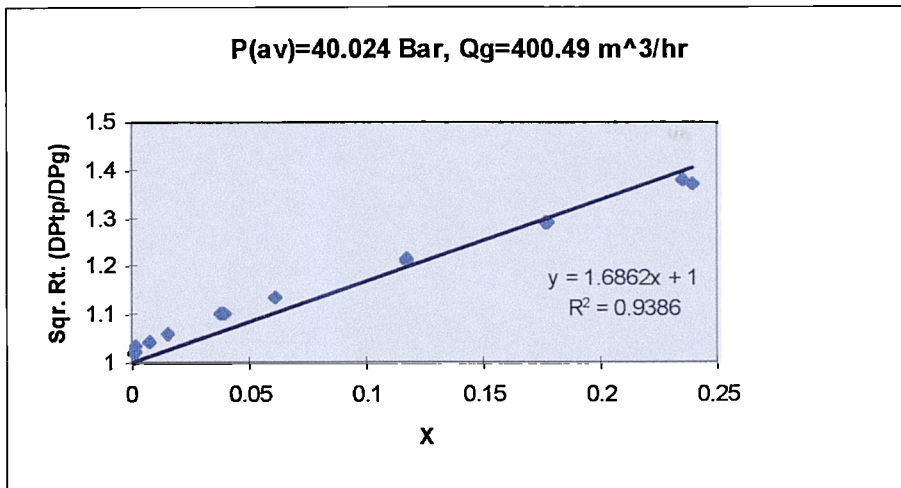
Figure 6.14. The best linear fit for the 40 Bar, 400 m³/hr data plot.
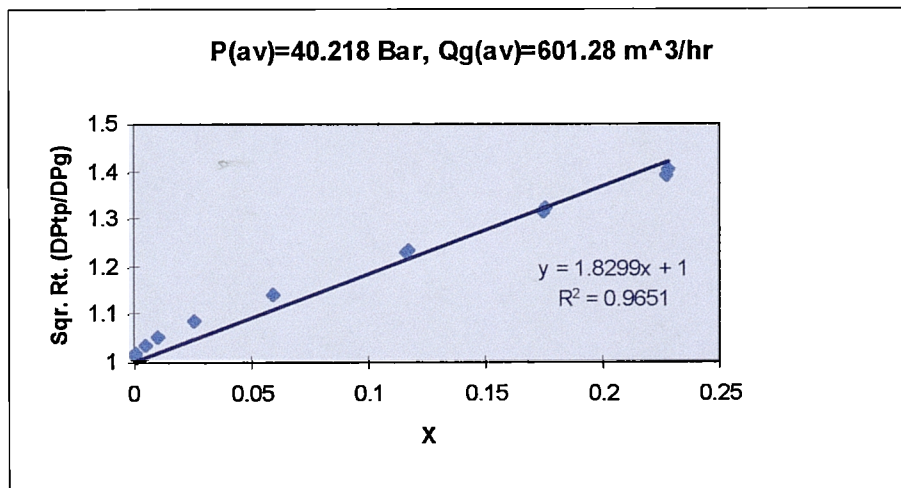
Figure 6.15. The best linear fit for the 40 Bar, 600 m³/hr data plot.
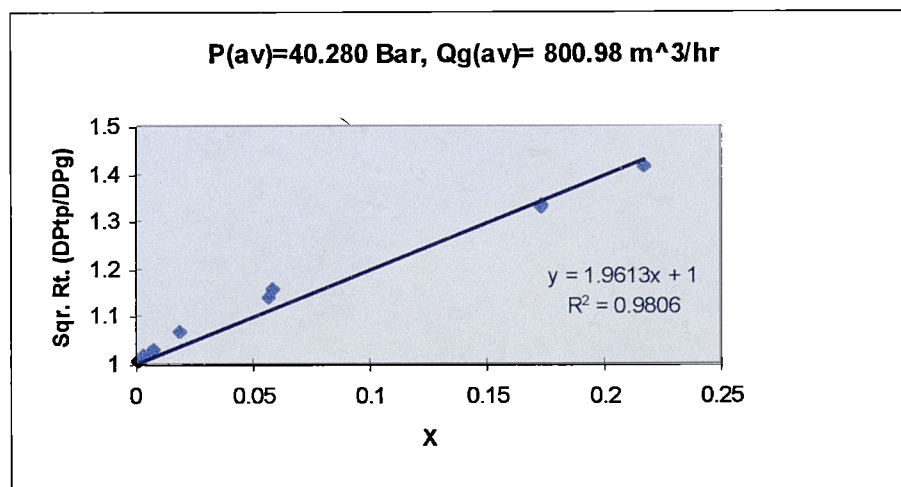
Figure 6.16. The best linear fit for the 40 Bar, 800 m³/hr data plot.
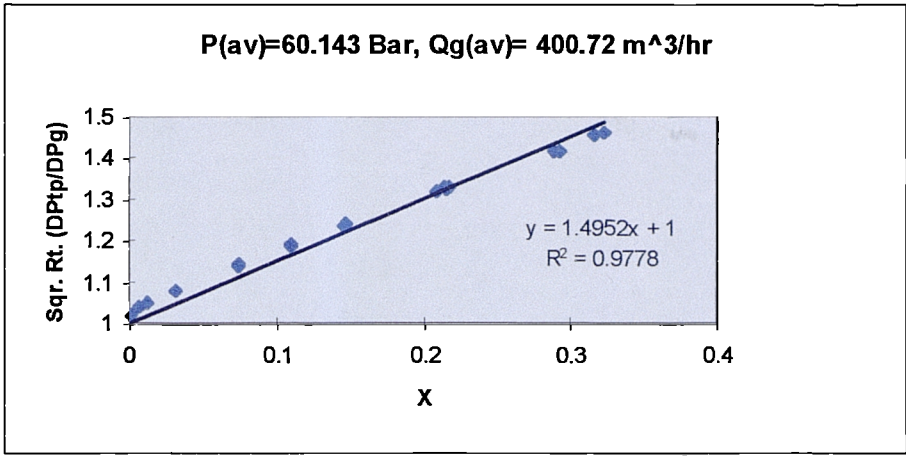
Figure 6.17. The best linear fit for the 60 Bar, 400 m^3/hr data plot.
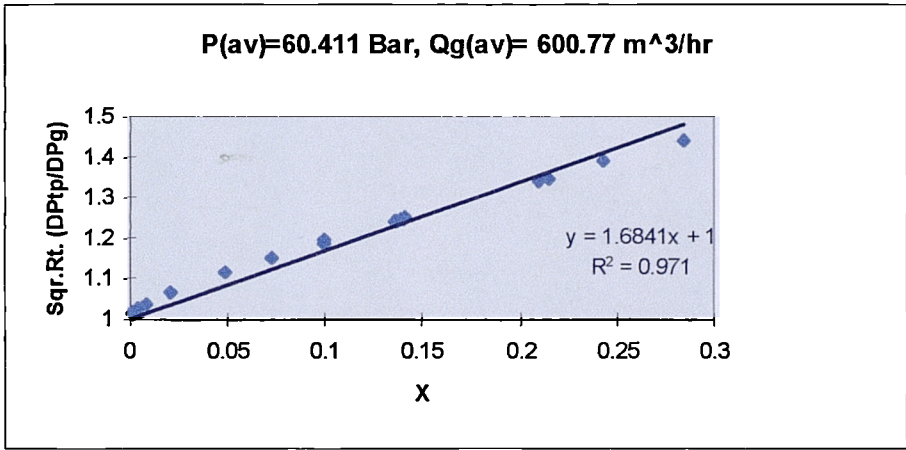
Figure 6.18. The best linear fit for the 60 Bar, 600 m^3/hr data plot.
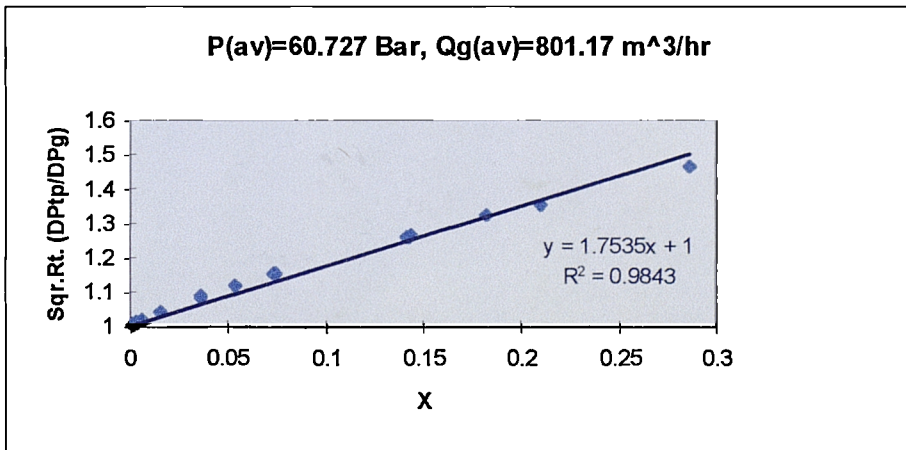
Figure 6.19. The best linear fit for the 60 Bar, 800 m^3/hr data plot.

Table 6.6 lists the gradients.

Data Set	Average Pressure (Bar g)	Average Gas Flowrate (m^3/hr)	Gradient, "M"
1	20.177	401.09	2.2383
2	20.247	602.24	2.2211
3	20.363	801.99	2.5005
4	40.024	400.49	1.6862
5	40.218	601.28	1.8299
6	40.280	800.98	1.9613
7	60.143	400.72	1.4952
8	60.410	600.77	1.6841
9	60.727	801.17	1.7535

Table 6.6. The Gradients Obtained from the Nine Set Pressure and Gas Flowrate Sets.

Using the software package TableCurve 3D a surface fit was created that gave an equation for the Murdock gradient in terms of the pressure and gas flowrate. The plot of this surface is given in Figure 6.20. The equation selected from the choice offered by this software was the best "simple" fit. That is the closest equation to the data that used just one term for each of the two variables. Many more complex equations were offered but the author was concerned with the possibility of "over-fitting" the data and it was noticed that these more complex equations did not greatly improve the fit. The resulting equation is:

$$M = 1.128356 + \left(\frac{20.48415}{P}\right) + \left((1.8010599E - 8)Q_g^{2.5}\right) \tag{6.5}$$

where P is upstream line pressure in bar g and Q_g is the gas flowrate in m^3/hr.
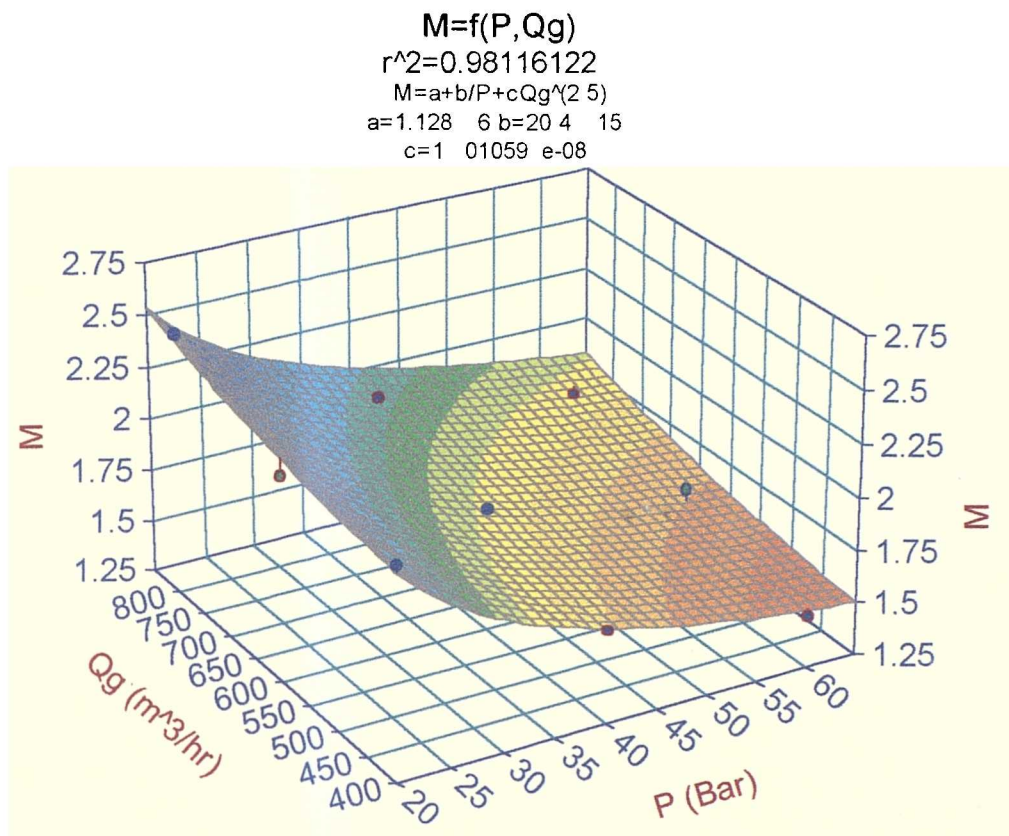
Figure 6.20. The Surface Fit for the Gradients to the set Pressure and Gas Flowrates.

Therefore, the refined correlation is again equation (6.4) with M given by equation (6.5). The range of this correlation is as before with the exception that the upper limit of the gas flowrate is restricted to the 800 m³/hr case.

The standard root mean fractional deviation, d (+/-), of this method was found to be 0.0229 for all the pressures case. Clearly, this calculation does not include the 1000 m³/hr data. The calculation is given in Appendix 5. Table 6.7 shows the correlation performance for the individual pressures.

Pressure(Barg)	All	20 Bar	40 Bar	60 Bar
d (+/-)	0.0229	0.0282	0.0214	0.0181

Table 6.7. Root Mean Fractional Deviations when using Equation 6.5 with Equation 6.4.

Clearly this correlation is the best of those created so far in this Chapter. It has therefore been shown that both the pressure and the gas volumetric flowrate influence the error induced in a Venturi Meter, as claimed by de Leeuw, and that taking account of the pressure and gas flowrate effects has greatly improved the Murdock type correlation.

It was found that an increasing pressure for a set gas volumetric flowrate caused a reduction in the meter error while for a set pressure and an increasing gas flowrate the meter error increased. It should be noted that the pressure is seen to have a greater influence than the volumetric gas flowrate on the value of the Murdock equation. From equation 6.5 it can be seen that raising the pressure from 20 to 60 bar reduces the Murdock gradient by 0.6828 and raising the gas flowrate from 400 to 800 m³/hr increases the Murdock gradient by 0.2684.

It will be noted however, that this latest correlation still does not predict the gas flowrate as well as the de Leeuw correlation. At first it may seem surprising that a correlation created from the same data set used to test it does not perform better than an existing correlation created from another data set. However, this situation is the result of the fact that this researcher was attempting to update the Murdock correlation rather than form a new correlation as this project has industrial practicalities in mind. However, it is clear that fitting a straight line to the new NEL Wet Gas data when plotted on a Murdock type graph is not the most accurate way to fit the data to a correlation. In fact the linear line fits are fairly crude attempts to fit data which can be seen to actually have a slight curve when plotted on a Murdock type graph.

Now that it has been shown that the Murdock model is not going to give a correlation which is as accurate as possible using the new NEL data it was necessary to create a new correlation.

6.5) <u>The Creation of a New Wet Gas Venturi Correlation</u>

It was decided that the new correlation should still be the relationship between the values of $\sqrt{\Delta P_{tp}/\Delta P_g}$ and X as in the Murdock correlation as this is the form best

known in the field of Natural Gas Production. However, it was necessary to create a correlation capable of taking account of the effects of pressure and gas flowrate. The method chosen was to plot the data for each pressure set on a three dimensional plot with co-ordinate axes $\sqrt{\Delta P_{tp}/\Delta P_g}$, X and Fr_g using the software TableCurve 3D. This was therefore the Murdock type plot extended into three dimensions by the inclusion of a third axis, the gas Densiometric Froude Number, Fr_g. (The gas Densiometric Froude Number was chosen instead of the gas flowrate directly as it allowed the correlation constants to remain dimensionless. It is also dependent on the pipe diameter which means the correlation will not be limited to a single pipe size.) The software gave a list of the best surface equation fits to each of the three pressures tested for the form:

$$\sqrt{\Delta P_{tp} / \Delta P_g} = f\left(X, Fr_g\right)$$

Naturally, for the three separate pressure cases the software picked many highly complex equations that fitted an individual data sets very well but fitted the other two data sets relatively poorly. Furthermore, it was clear when examining these complex equations that they were inevitably an "over fit" anyway and therefore not the slightest bit reliable for predicting the meter behaviour at new points between the existing data points. Therefore, to avoid an over fit and find an equation that suited all three surfaces well only relatively simple surface equations were considered. The best overall performance was obtained with the equation form shown in equation 6.6.

$$\sqrt{\frac{\Delta P_{tp}}{\Delta P_g}} = \frac{1 + AX + BFr_g}{1 + CX + DFr_g} \qquad (6.6)$$

The three plots produced by using TableCurve 3D are presented in Figures 6.21, 6.22 and 6.23.

20 Bar

Sqr Rt.(DPtp/DP)=(1+AX+BFrg)/(1+CX+DFrg)

a–8 5392202 b⁻0 025702191 c=5.0252674 d=0 014280677

r^2=0 99455107
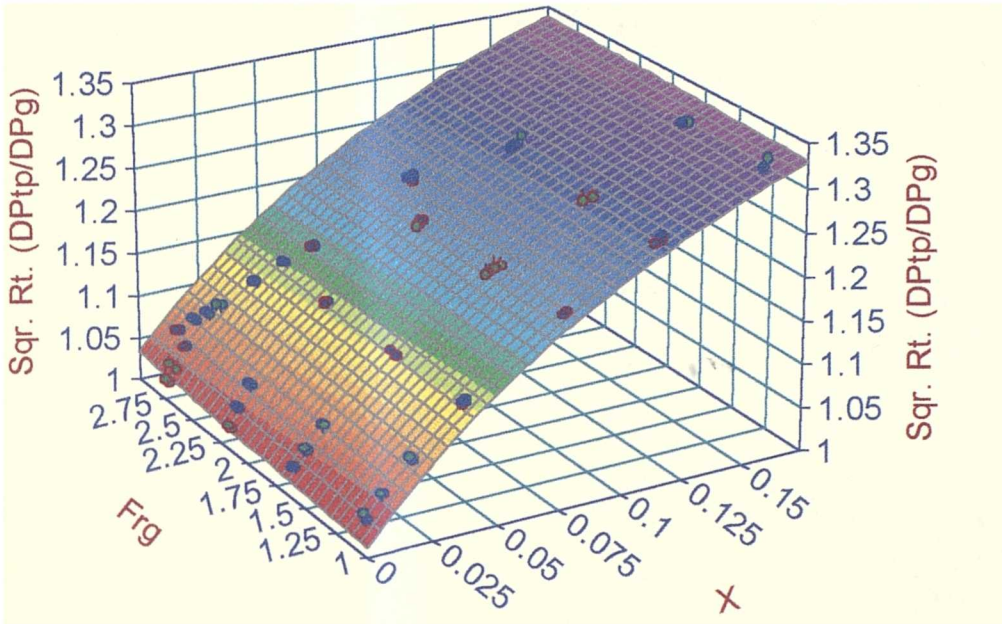
Figure 6.21. The 20 Bar Plot of $\sqrt{\Delta P_{tp}/\Delta P_g}$, X and Fr$_g$.

40 Bar

Sq .Rt (D D)=(1+AX+BFrg) (1+CX+dFrg)

23 8 ⁻1 0 4 62 =-0 5727433

r^2= 16 5
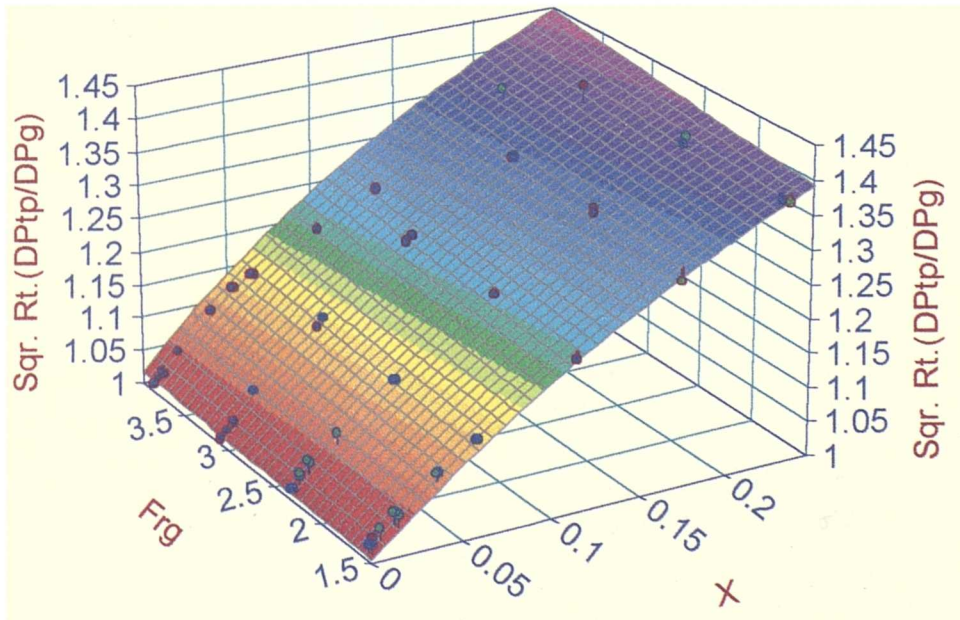
Figure 6.22. The 40 Bar Plot of $\sqrt{\Delta P_{tp}/\Delta P_g}$, X and Fr$_g$.

164

60 Bar
Sqr Rt. (DPt /DPg)=(1+AX+BFrg /(1+CX+DFrg)
a=2.8570 74 b= 0 03 665951 c=1 0672221 d=-0 036900386
r^2-0 99576105
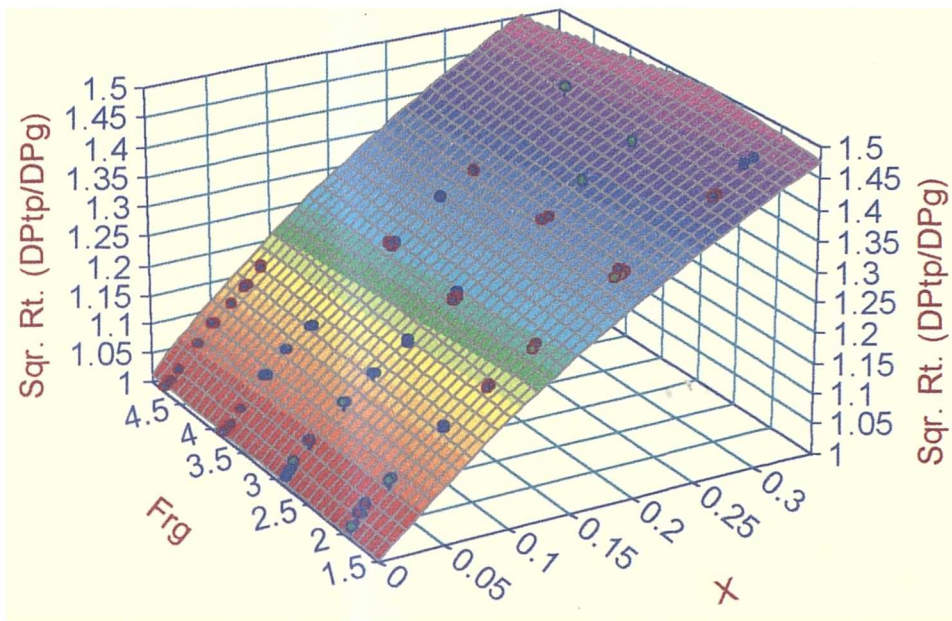
Figure 6.23. The 60 Bar Plot of $\sqrt{\Delta P_{tp}/\Delta P_g}$, X and $\mathrm{Fr_g}$

Table 6.8 lists the values of these constants to the gauge pressure.

Pressure (Bar g)	A	B	C	D
20.325	8.5392202	0.025702191	5.0252674	0.014280677
40.324	3.7872298	-0.053812388	1.7044162	-0.057274331
60.526	2.8570674	-0.034665951	1.0672221	-0.036900386

Table 6.8. Equation 6.6 constants at each pressure.

Therefore for each pressure set there was therefore a different set of values for the constants A, B, C and D. It was then necessary to find the relationship between these constants and the pressure. Here again was the problem of a small amount of data being used in a curve fit. Excel was used to fit a polynomial to each of the desired curves (i.e. each of the "constants" A, B, C and D vs. pressure). Ideally, of course more points would have led to a better fit of the A, B, C and D values to the pressure and the use of only three points is likely to lead to some errors. However with data

for only three pressures available nothing can be done about this. These equations are given as equations 6.7 to 6.10.

$$A = ((4.777285\text{E-}3)P^2) - (0.5242366P) + 17.11304 \tag{6.7}$$

$$B = ((1.233263\text{E-}4)P^2) - (0.0113753P) + 0.203878 \tag{6.8}$$

$$C = ((3.354571\text{E-}3)P^2) - (0.3673168P) + 11.02978 \tag{6.9}$$

$$D = ((1.149112\text{E-}4)P^2) - (0.0104724P) + 0.177765 \tag{6.10}$$

Note that the pressure is in bar g.

As X is a function of the pressure and gas and liquid flowrates equation (6.6) expands to the form:

$$\frac{K_g A_t \sqrt{2\rho_g \Delta P_{tp}}}{\dot{m}_{gas}} = \frac{1 + A\left(\dfrac{\dot{m}_{liquid}}{\dot{m}_{gas}} \dfrac{K_g}{K_l} \sqrt{\dfrac{\rho_g}{\rho_l}}\right) + B\left(\dfrac{\dot{m}_g}{\rho_g A \sqrt{gD}} \sqrt{\dfrac{\rho_g}{\rho_l - \rho_g}}\right)}{1 + C\left(\dfrac{\dot{m}_{liquid}}{\dot{m}_{gas}} \dfrac{K_g}{K_l} \sqrt{\dfrac{\rho_g}{\rho_l}}\right) + D\left(\dfrac{\dot{m}_g}{\rho_g A \sqrt{gD}} \sqrt{\dfrac{\rho_g}{\rho_l - \rho_g}}\right)} \tag{6.11}$$

where the units are mass flows are in kg/s, densities in kg/m^3, the throat area in m^3 and differential pressure in N/m^2.

Therefore, as g is the gravitational constant and $\dot{m}_{liquid}$ is assumed known, A, D and A_t are known from the geometry of the meter, K_g and K_l are known from the single phase meter performances, ρ_g, ρ_l and A, B, C and D are all known from the upstream pressure reading (P), which is read by the meter along with the ΔP_{tp} reading, the equation is solvable by a computational iteration for $\dot{m}_{gas}$. Like all correlations however care must be taken to ensure that the limits of the experimental data is not exceeded during use. Therefore, if this prediction method is used and the resulting value of the volumetric gas flowrate results in the value of the modified Lockhart Martinelli parameter being greater than the maximum allowed by equation

(6.2) then the result is doubtful. If the predicted modified Lockhart Martinelli parameter is less than the minimum permitted value (i.e. X = 0.001312) then again the prediction is doubtful.

The root mean fractional deviation for this method using the data that formed the correlation was found to be 0.0084 so it is the best fit to the NEL / ISA data of these four new correlations produced in this report. Table 6.9 below shows the methods performance below for the individual pressure sets. These calculations are shown in Appendix 5.

Pressure (Barg)	All	20	40	60
d (+/-)	0.0084	0.0063	0.0100	0.0086

Table 6.9. Root Mean Fractional Deviations when using Equation 6.11.

The results obtained during this study suffer from the same problem as encountered by previous researchers into two-phase flow metering, i.e., the lack of independent data means that this correlation cannot be compared objectively with other existing correlations. Such an objective comparison of this correlation with other existing correlations needs must wait until further independent data becomes available.

Tables 6.10 and 6.11 summaries the root mean fractional deviation calculations in this study so far.

	All Pressures	20 Bar g	40 Bar g	60 Bar g
Equation 6.1	0.0383	0.0505	0.0267	0.0340
Equation 6.3	0.0281	0.0324	0.0266	0.0250
Equation 6.5	0.0229	0.0282	0.0214	0.0181
Equation 6.11	0.0084	0.0063	0.0100	0.0086

Table 6.10. Root Mean Fractional Deviations for the New Correlations.

Note that Table 6.10 shows that only at 40 Bar is the difference between equations 6.1, 6.3 and 6.5 to small to indicate an improvement in performance as the difference is not greater than the data sets gas mass flow uncertainty of 0.322%.

	All Pressures	20 Bar g	40 Bar g	60 Bar g
No Correlation	0.1777	0.1642	0.1656	0.1998
Homogenous	0.0237	0.0285	0.0220	0.0202
Murdock(1.26)	0.0650	0.0823	0.0589	0.0504
Chisholm	0.0710	0.0793	0.0658	0.0675
Smith & Leang	0.1260	0.1159	0.1199	0.1401
Lin	0.0462	0.0449	0.0448	0.0479
Murdock(1.5)	0.0482	0.0677	0.0410	0.0287
de Leeuw	0.0211	0.0279	0.0193	0.0140

Table 6.11. Root Mean Fractional Deviations for the previously existing correlations.

To supplement the root mean fractional deviation calculations given in Tables 6.10 and 6.11 the maximum percentage over and under-readings found in the data set for each correlation are give in Table 6.13. Note that in this table a negative sign indicates the percentage under-reading (i.e. the percentage difference of the actual gas flowrate to the under predicted flowrate). In the cases where the "under reading" is denoted as positive there was actually no under-reading (i.e. at no data point did the correlation under predict the actual gas flowrate) and the value given therefore indicates the closest the correlation got to the desired result. To compare the correlation performances with the uncorrected meter performance Table 6.12 shows the maximum errors that exist if the meter has no correction applied to it (i.e. the errors that exist with the maximum liquid injection rates).

Pressure	All	20 Bar g	40 Bar g	60 Bar g
Maximum Error (%)	+45.833	+30.074	+40.590	+45.833

Table 6.12. The Wet Gas Meter Error at the Maximum Liquid Injector Rates.

	Homogenous	Murdock (M=1.26)	Murdock (M=1.5)	Chisholm	Smith & Leang	Lin	de Leeuw	Equ. 6.1 (M=1.8055)	Equ. 6.3 (M-f(P))	Equ. 6.5 M-f(P,Qg)	Equ. 6.11
All Pressures											
Max Under Reading %	-6.362	+0.605	-2.148	+0.613	+6.173	-3.928	-2.724	-11.960	-7.494	-4.290	-1.745
Max Over Reading %	+4.120	+13.887	+10.263	+15.729	+27.795	+13.130	+7.296	+4.933	+4.223	+2.289	
20 Bar											
Max Under Reading %	-6.362	+1.793	+1.753	+1.779	+7.319	-2.406	-1.248	+1.700	-6.213	-4.290	-1.235
Max Over Reading %	+4.120	+13.163	+10.263	+12.609	+15.648	+8.803	+4.926	+7.296	+4.933	+4.223	+1.109
40 Bar											
Max Under Reading %	-5.607	+0.652	+0.636	+0.655	+6.223	-3.537	-2.252	-6.169	-7.494	-3.502	-1.745
Max Over Reading %	+3.577	+13.887	+9.323	+15.729	+24.242	+13.008	+3.525	+4.819	+4.448	+3.643	+2.289
60 Bar											
Max Under Reading %	-2.755	+0.605	-2.148	+0.613	+6.173	-3.928	-2.724	-11.960	-5.897	-3.822	-1.085
Max Over Reading %	+3.186	+10.091	+4.981	+14.580	+27.795	+13.130	+2.878	+2.810	+3.683	+3.269	+2.102

Table 6.13. The Maximum and Minimum Percentage Error of Each Correlation Assuming No Error in the Gas Mass Flow Reference Turbine Meter.

It should be noted that Table 6.13 assumes that the correct value of the liquid flowrate is known at all times. Without this knowledge the uncertainty will increase in proportion to the uncertainty of the liquid mass flowrate measurement. Assuming the liquid mass flowrate uncertainty is +/- 10% (as quoted by Shell Expro [43]) then the new correlation (equation 6.11) has appropriately poorer values of root mean fractional deviation. Equation 6.11 had the Root Mean Fractional Deviation calculated when the liquid mass flows shifted to 90% and 110% of the reference meters read values. The resulting poorest performance is shown in Table 6.14.

Pressure	All	20 Barg	40 Barg	60 Barg
d (+/-)	0.0152	0.0118	0.0153	0.0178

Table 6.14. The Root Mean Fractional Deviation for Equation 6.11 when Liquid Flowrate Uncertainty is +/- 10%.

A method of metering the gas and liquid flowrates simultaneously must therefore improve upon the results in Table 6.14 to better the uncertainty achieved by the use of Equation 6.11 and the Tracer Dilution Method. However, as the Tracer Dilution method is a spot measurement and therefore cannot detect periodic changes in the liquid flowrate, industry has repeatedly stated that a continuous two phase metering method even somewhat less accurate than a DP Meter correlation / Tracer Dilution combination would be a useful advance in technology.

Chapter 7

The Simultaneous Measurement of the Liquid and Gas Flowrates

It is generally known in the Natural Gas Production Industry that one of the greatest problems in wet natural gas metering is the difficulty in finding the liquid flowrate. All the correlations discussed in Chapters 4 and 6 require that the liquid flowrate be known. As stated in the literature review, in practice methods such as the Tracer Dilution method are used and these only guarantee that the uncertainty in the liquid flowrate will be no more than +/-10%. In addition to this unsatisfactory situation is the fact that the results obtained using the Tracer Dilution method are spot measurements and hence engineers do not know if liquid flowrates have changed until the next time the method is used. Hence, a metering system that gives simultaneous metering of both phases is greatly desired by the industry.

The existing research into this topic was discussed in the literature review. In the literature review (section 1.7.4) the final statements of de Leeuw on the matter of simultaneous phase metering were discussed.

What de Leeuw stated was that a Venturi Meter that read the traditional upstream to throat differential pressure and an additional pressure differential, upstream to downstream of the diffuser, could, in theory, predict both the gas and liquid flowrates simultaneously. That is, de Leeuw believed that these two pressure differentials give enough information to determine the gas and liquid flowrates.

What is clear is that it is not possible to predict both flowrates from only the traditional pressure differential reading because at any line pressure the one differential pressure reading can occur for different combinations of the liquid to gas ratio. That is, as it can generally be stated that the greater the liquid flowrate the greater the over-reading for a set gas flowrate, then any given value of differential pressure could be for any flow from a small gas flowrate / large liquid flowrate to a large gas flowrate / small liquid flowrate to a dry gas flow. Figure 7.1 shows this point graphically. The dashed line indicates the pressure drop in the pipe if the meter was not installed. The black points indicate a measured differential pressure. The path is arbitrarily drawn between the meter inlet (denoted as x=0) and the throat (denoted

171

as x=1) as it is unknown. Note that two of the infinite number of possible gas and liquid flowrate combinations which give one differential pressure reading are shown here in terms of their superficial gas flows differential pressures.

Two-Phase Differential Pressure Readings
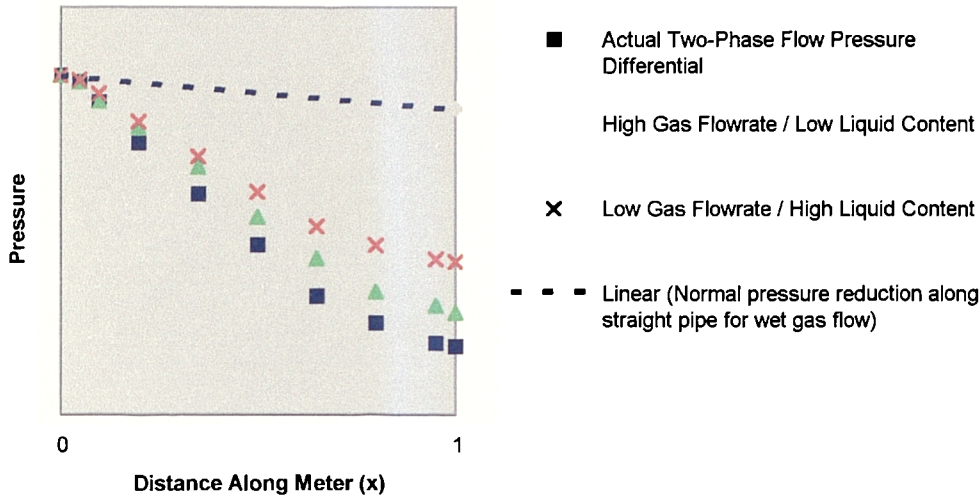
Figure 7.1. Possible Liquid to Gas Ratios for a particular Wet Gas Pressure Differential.

Clearly, the lower gas flowrate (denoted by the red points) will have a larger liquid flowrate than the higher gas flowrate (denoted by the green points) to raise the differential pressure to the actual measured differential pressure of this example. Therefore, if the liquid content is not already known the one traditional reading of differential pressure for a given pressure cannot alone indicate the gas and liquid flowrate. In fact it cannot even indicate the gas flowrate through the use of the wet gas correlations until the liquid flowrate is known. However, it was thought that with knowledge of the downstream pressure reading this situation can be improved upon.

It is known that not all of the energy transferred from the gas to the liquid phase during the flow in the converging section and throat is transferred back to the gas in the diffuser. Hence, it is considered possible that if two different wet gas flows give the same inlet to throat differential pressure reading the flow with the higher liquid content (and therefore smaller gas flowrate) should have a greater upstream to downstream differential pressure reading than the flow with the smaller liquid content

(and therefore larger gas flowrate). For example, see Figure 7.2. (Note that the Venturi downstream tapping is positioned at x=2 and here the green and red points indicate assumed actual pressures in the Venturi rather than assumed pressures of the superficial gas flows).

Total Head Loss & Liquid Content
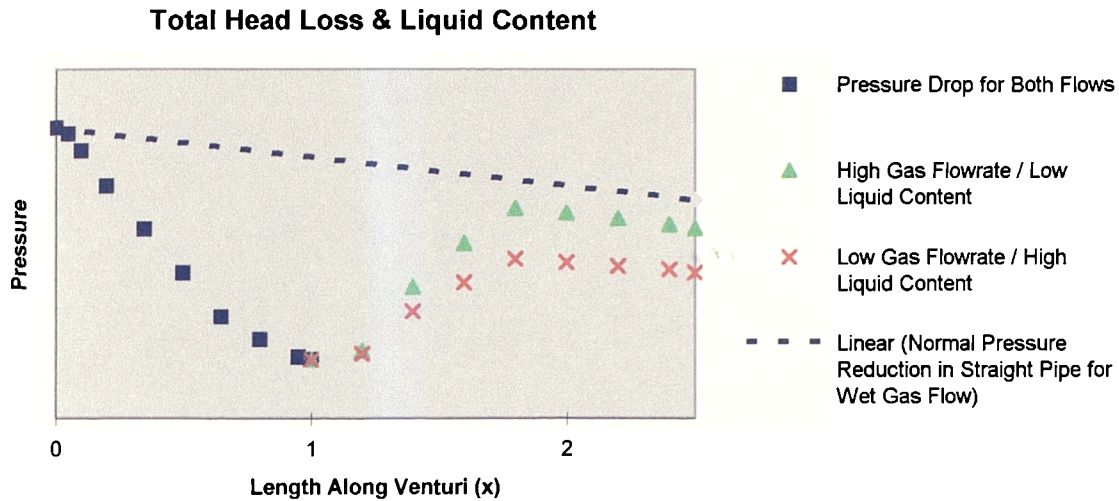
Figure 7.2. . Possible Liquid to Gas Ratios Pressure Recovery for a particular Wet Gas Pressure Differential.

However, it should be noted that even though the smaller gas / higher liquid content flow will have this phenomenon acting to increase its total head loss through the meter (and therefore the upstream to downstream differential pressure reading) there is a countering phenomenon. That is, lower gas flowrates will have smaller losses than higher gas flowrates. In single phase flows the higher the flowrate the greater the total head loss due to larger friction forces. As wet gas has a high void fraction there may still be opportunity for this dry gas effect to have some influence. It was therefore possible that this phenomenon would counter the first phenomenon to some unknown extent. That is, even though the greater the gas to liquid ratio of the flow means the smaller the pressure loss component due to the presence of the liquids there will be a larger pressure loss component due to the higher frictional effects. However the relationship between the upstream to downstream differential pressure reading and the inlet to throat differential pressure reading for flows with the same inlet to throat differential pressure reading but different liquid and gas flowrates is as yet unknown. However, de Leeuw believed that these two readings could be sufficient to calculate

the flowrates of both phases. In this chapter idea is considered and a method is proposed for developing the idea into a metering method for the simultaneous metering of both the phases.

7.1) Investigating the Proposed Development of de Leeuw's Method

From Chapter 3 (section 4) it can be seen that de Leeuw produced a graph of The Pressure Loss Ratio (DP2/DPtp) (i.e. the ratio between the upstream to downstream differential pressure divided by the upstream to throat differential pressure) vs. The Modified Lockhart Martinelli Parameter (X) for one pressure with the different gas flowrates plotted separately (see Figure 3.1). From this he concluded "... the results show that the pressure loss ratio depends on the actual liquid content" and "...the pressure loss ratio also depends on the actual gas velocity, or gas Froude number". The first research aim was therefore to test de Leeuw's claims by making use of the new NEL wet gas data obtained during this study. Therefore, for each of the three pressures tested the NEL data were plotted on the same type of graphs as de Leeuw for the different gas flowrates. These graphs are presented in Figure 7.3, 7.4 and 7.5. The data set required for constructing these plots is given in Appendix 3.

The result obtained from plotting the de Leeuw type graphs was the discovery that the relationship between the parameters was somewhat more complex than was implied by de Leeuw.
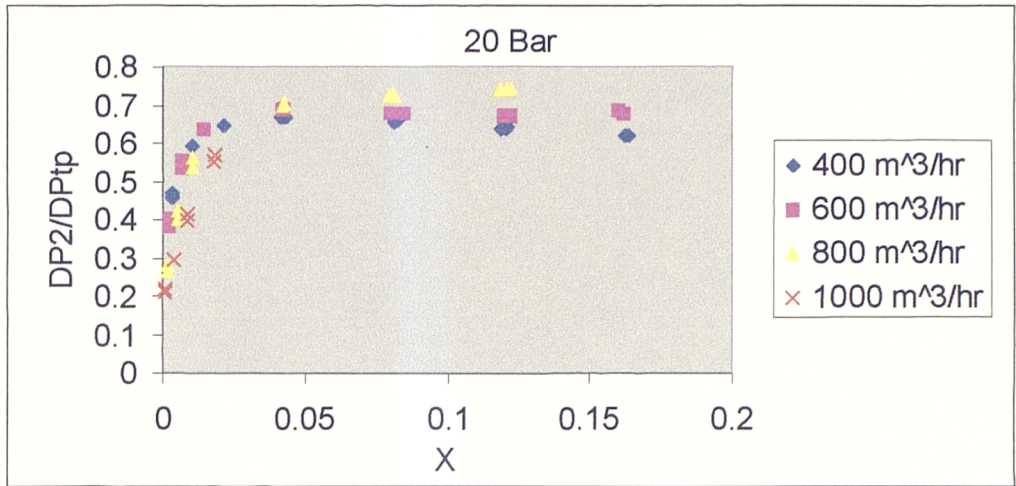
Figure 7.3. 20 Bar de Leeuw type plot.
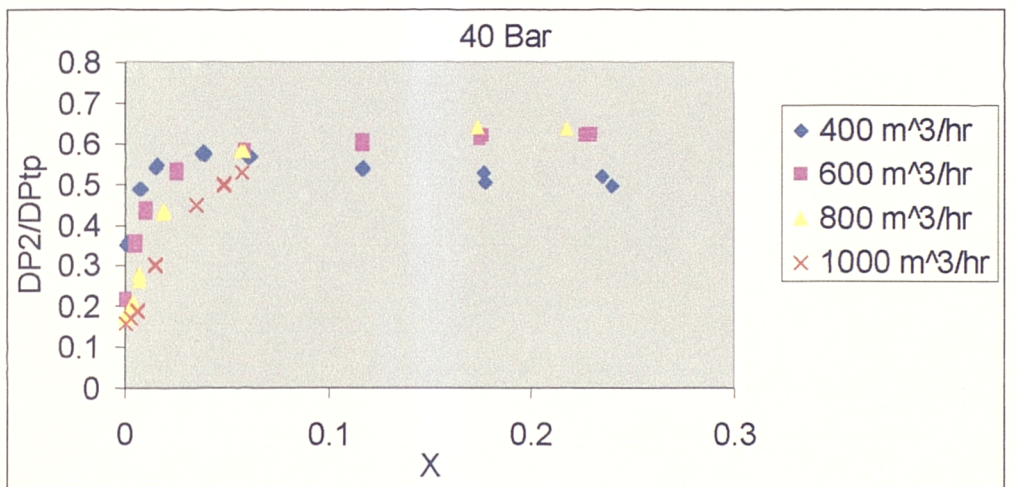
Figure 7.4. 40 Bar de Leeuw type plot.
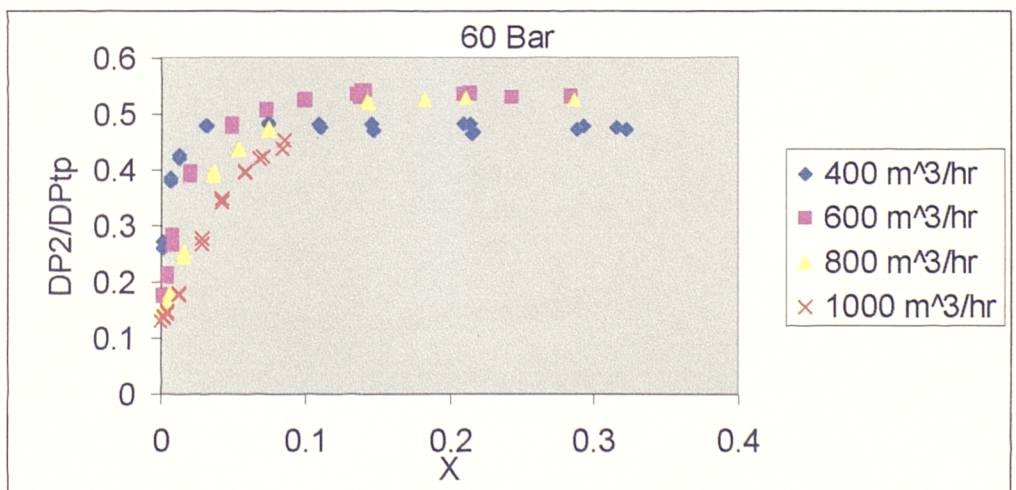
Figure 7.5. 60 Bar de Leeuw type plot.

175

A significant finding, obtained for the smaller values of the Modified Lockhart-Martinelli Parameter (X), was that the gradient was larger than the de Leeuw graph indicates in this region. However, for each pressure it does appear that there is some relationship between the value DP2/DPtp and the Modified Lockhart-Martinelli Parameters (X) and gas flowrate (Q_g). It is clearly more pronounced for the lower values of X but this is not too great a problem as most practical wet gas metering situations are in this region.

It was therefore decided that an attempt be made to obtain a method for predicting the gas and liquid flowrates simultaneously as described in Chapter 3 (section 4).

The method relies upon the creation of surface equations for relating the parameter DP2/DPtp to X and Q_g. That is, for each pressure a three dimensional plot of DP2/DPtp vs. X vs. Q_g was made and TableCurve 3D was then to be used to find a single appropriate surface equation of the type DP2/DPtp = f(X, Q_g) that fitted the data well (with each pressure having its own values of equation constants). It was then noted that if the equation could be of the form that gave the expression for X in terms of DP2/DPtp and Q_g then the amount of iteration the method would require would be substantially reduced as the equation could then be directly substituted into an existing wet gas Venturi Meter correlation. This would then permit a straightforward iteration to give the gas flowrate and hence a value for X which would lead directly to the liquid flowrate.

Once such an equation was identified as suitable for each pressure the constants could be plotted against pressure to give their relationship with pressure across the test range. Once this was done the method would be complete.

Thus, by knowing the line pressure the equation constants could be found and by reading DPtp and DP2 from the meter an equation giving X in terms of Q_g would be obtained. By directly substituting this equation into equation 6.6 (Chapter 6) a result could be obtained by a simple iteration.

On attempting to create these surfaces it quickly became apparent that there was a serious problem. The data for each pressure when plotted on the 3D graphs did not fit well with any of the numerous possible equations fitted by the software. Furthermore, when applying each equation form that was best for an individual pressure on the other two pressures the results were considerably worse fits. It was therefore clear that it was not going to be possible to create an equation of the desired form that would have an acceptable accuracy.

It was possible to find a considerably more complicated equation for DP2/DPtp vs. X vs. $\dot{Q}_g$ that would fit the data better than equations that allowed rearranging to the form $X = f(DP2/DPtp, \dot{Q}_g)$. However when these more complex equations were used there was still a relatively poor fit over some of the domain. It was found that on some data points the iteration would not offer a valid solution.

However, since the writing of the original research another idea had developed into how to use the data. Because of time constraints a choice had to be made into which concept to develop. It was decided that, on balance, the newer idea was the more worthy to pursue. This idea is described in the following section.

7.2) The Development of a New Method for Metering Liquid and Gas Flowrates Simultaneously

7.2.1) Using a Venturi Meter with a Downstream Pressure Tapping to Meter a Single Phase Flow

It was stated at the start of this chapter that the Sekoguchi and ISA Controls / BG Technology methods were not able to be developed by this research as they required two meters in series. However it should be noted that, although only one meter was installed, during data collection for this research an extra measurement not usually taken by Venturi Meters was taken, i.e. the upstream to downstream differential pressure. Hence the throat to downstream tapping pressure differential can be obtained. Of course for a single phase flow, reading the upstream pressure and the

pressure differential upstream to throat of a Venturi leads to a mass flow prediction as long as the fluid properties are known. The same principles can of course also be applied to the case of an expansion in the flow area. That is, the same principles apply for metering with a DP Meter whether the pressure differential is produced by a constriction or expansion in the flow area.

In this project the ISA Controls Venturi meter used gives two opportunities to meter the flow as there are two pressure differentials available, one for the constriction between upstream and the throat and one for the expansion between the throat and downstream. Hence, in a sense, there is the equivalent of two meters installed and it was considered well worth while examining if these two separate metering systems could be combined to meter the gas and liquid flowrates simultaneously.

Naturally, this "second" meter needed to be calibrated in dry gas just as all non-standard Venturi Meters are. Luckily during the dry gas tests carried out during the initial testing of this meter the downstream pressure readings were included in the data collection. This data can be seen in Appendix 2. Here the value Kg* denotes the flow coefficient for the "second" meter (see Figures 7.6 and 7.7). Therefore, for dry gas the "second" meter equation is:

$$\dot{m}_g = K_g^* A_t \sqrt{2\rho_g \Delta P_g^*}$$
(7.1)

where $\Delta P_g^* = \Delta P_t - \Delta P_2$ (i.e. the pressure difference upstream to throat minus the upstream to downstream pressure difference). The gas density, ρ_g, is estimated from the upstream pressure, P_1. The value of Kg* is always predicted to be greater than unity. This is due to the fact that the flow area increases in the direction of flow and the area used in the equation is the Venturi throat area.

The performance of this "second" meter in dry gas is not as good as the traditional "first meter" method (the root mean fractional deviations (d +/-) are 0.00078 and 0.00330 for the traditional and second meters respectively). However, this dry gas "second" meter is still extremely accurate compared to current wet gas metering

methods and this gave confidence that this "second" meter could be developed as a second wet gas meter and could therefore be used along with the traditional "first" meter to simultaneously meter both phases of a wet gas flow.

20 Bar

$y = -2.6509E\text{-}03x + 1.1158E\text{+}00$
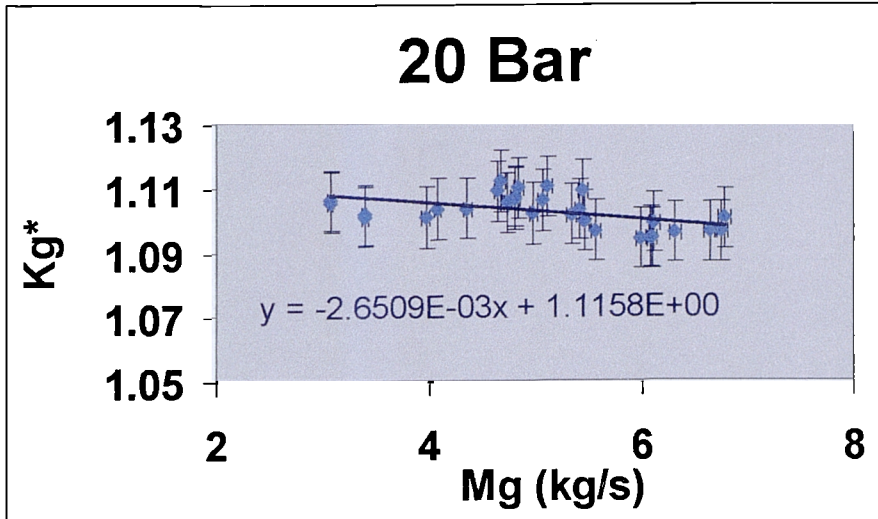
Figure 7.6. The 20 Bar Kg^* linear line fit.

60 Bar

$y = -9.1000E\text{-}04x + 1.1179E\text{+}00$
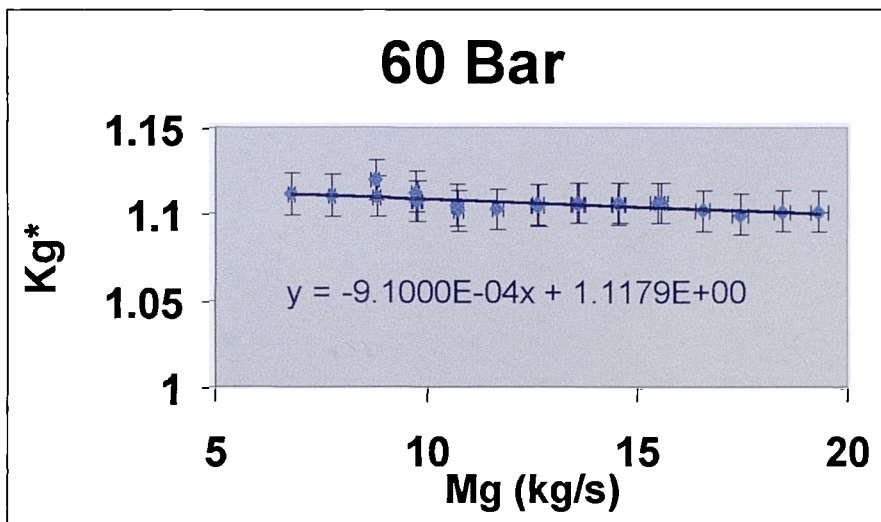
Figure 7.7. The 60 Bar Kg^* linear line fit.

7.2.2) Using a Venturi Meter Downstream Tapping to Meter a Wet Gas Flow when the Liquid Flowrate is Known

In order to prove that the combination of the traditional Venturi Meter differential pressure reading and the upstream to downstream differential pressure reading can be used to predict both phase flowrates simultaneously it is first necessary to show that the throat to downstream differential pressure knowledge can be used as a wet gas meter in its own right. That is, it will now be shown that if the liquid flowrate is initially known then knowledge of the throat to downstream pressure differential can be used to predict the gas mass flowrate in a similar way as the traditional Venturi differential pressure reading can be used.

In order to treat the diffuser as a second meter the same method was used to create a wet gas correlation as was used as for the final correlation construction presented in Chapter 6. That is, for each of the three pressures a plot of $\sqrt{\Delta P^{*}_{tp}/\Delta P^{*}_{g}}$ vs. X vs. Fr_{g} was obtained. Here X and Frg are as before. ΔP_{tp}^{*} is defined as the pressure differential between the Venturi downstream tapping and the throat tapping in the wet gas flow and ΔP_{g}^{*} is the pressure differential between the downstream tapping and the throat tapping that would exist if for that particular wet gas flow the gas alone flowed through the meter. All the required data to plot these points is available in Appendices 2 & 3. (An equation for Kg* is also required (see Appendix 2)). Note that after some consideration it was decided that X should be used as in the original correlation development instead of a parameter denoted by X^{*} as would be used if an exact replica of the original correlation development in Chapter 6 was carried out. The parameter X^{*} would be defined as:

$$X^{*} = \sqrt{\Delta P_{l}^{*}/\Delta P_{g}^{*}} \tag{7.2}$$

where ΔP_{l}^{*} and ΔP_{g}^{*} are the superficial liquid and gas pressure differentials for between the downstream and throat pressure tappings. The reasoning behind this was

as follows. The reason for creating this second liquid flowrate dependent wet gas correlation is solely to use it in conjunction with the previously developed correlation (Chapter 6) and hence it is beneficial to keep the correlations parameters similar in order to facilitate combination of the correlations.

The values of $\sqrt{\Delta P^*_{tp}/\Delta P^*_g}$ vs. X vs. Fr_g for each pressure tested were plotted using the TableCurve 3D software and then surface equations were fitted to these plots. It was found that it was not possible to get a surface equation that fitted the data as well as was found to be the case during the development of equation 6.6. Furthermore, it was not possible to get the surface equation of $\sqrt{\Delta P^*_{tp}/\Delta P^*_g} = f\left(X, Fr_g\right)$ into a form where it would be possible to separate out X in order to express it in terms of only gas flowrate. This would of course have been advantageous as this would then have allowed a direct substitution into equation 6.6 and enable a simple iteration to obtain the gas flowrate. The form of the equation for the surface that fitted all three pressures was unfortunately considerably more complicated than equation 6.6. The form is:

$$\sqrt{\frac{\Delta P^*_{tp}}{\Delta P^*_g}} = a + b \ln X + c \ln Fr_g + d(\ln X)^2 + e\left(\ln Fr_g\right)^2 + f \ln X \ln Fr_g + g(\ln X)^3$$
$$+ h\left(\ln Fr_g\right)^3 + i \ln X\left(\ln Fr_g\right)^2 + j(\ln X)^2 \ln Fr_g$$

(7.3)

where the constants a to j are functions of pressure (in bar g) and these are given in Table 7.1.

Constant	20 Bar g	40 Bar g	60 Bar g
a	1.7997391	1.9902269	2.0005307
b	0.74355904	0.69299046	0.6165648
c	-0.34477141	-0.96165947	-0.95718874
d	0.15215836	0.12327537	0.10732058
e	-0.51365813	0.26784086	0.39231471
f	-0.23341981	-0.33274401	-0.2641242
g	0.0090986738	0.0070473691	0.0064444087
h	0.15813909	0.027636102	-0.015711681
i	-0.084860661	0.058777198	0.066086891
j	-0.030173975	-0.02096224	-0.011228205

Table 7.1. The Constants of Equation 7.3 for each Pressure.

20 Bar

$z=a+b\ln x+c\ln y+d(\ln x)^2+e(\ln y)^2+f\ln x\ln y+g(\ln x)^3+h(\ln y)^3+i\ln x(\ln y)^2+j(\ln x)^2\ln y$

a=1.7997391 b=0.74355904 c=-0.34477141 d=0.15215836 e=-0.51365813
f=-0.23341981 g=0.0090986738 h=0.15813909 i=-0.084860661 j=-0.030173975
r^2=0.98166848
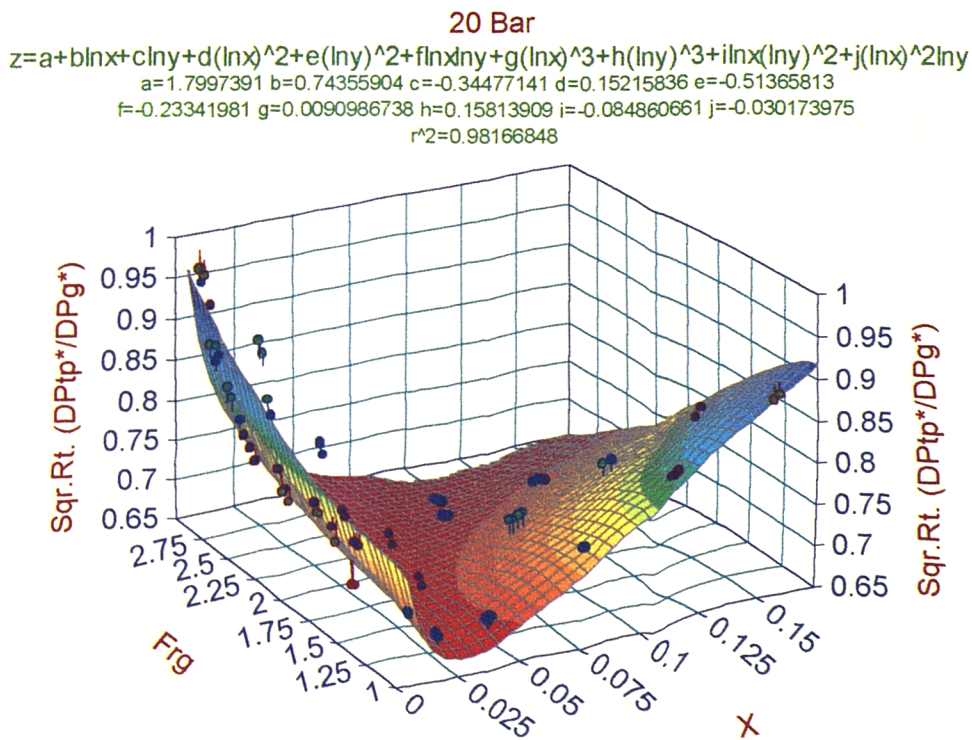
Figure 7.8. The 20 Bar plot.

40 Bar

$z=a+b\ln x+c\ln y+d(\ln x)^2+e(\ln y)^2+f\ln x\ln y+g(\ln x)^3+h(\ln y)^3+i\ln x(\ln y)^2+j(\ln x)^2\ln y$

a=1.9902269 b=0.69299046 c=-0.96165947 d=0.12327537 e=0.26784086
f=-0.33274401 g=0.0070473691 h=0.027636102 i=0.058777198 j=-0.02096224
r^2=0.97877708
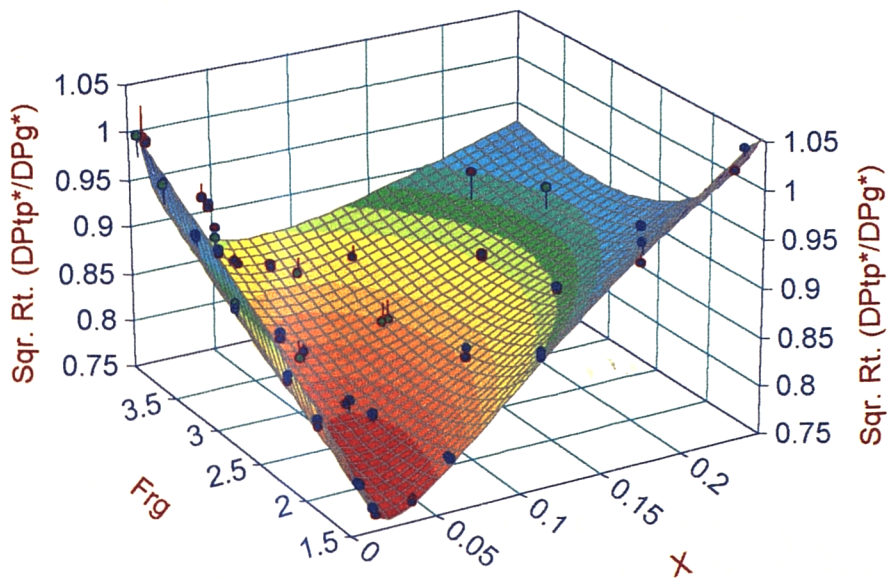
Figure 7.9. The 40 Bar plot.

60 Bar

$z=a+b\ln x+c\ln y+d(\ln x)^2+e(\ln y)^2+f\ln x\ln y+g(\ln x)^3+h(\ln y)^3+i\ln x(\ln y)^2+j(\ln x)^2\ln y$

a=2.0005307 b=0.6165648 c=-0.95718874 d=0.10732058 e=0.39231471
f=-0.2641242 g=0.0064444087 h=-0.015711681 i=0.066086891 j=-0.011228205
r^2=0.94385399
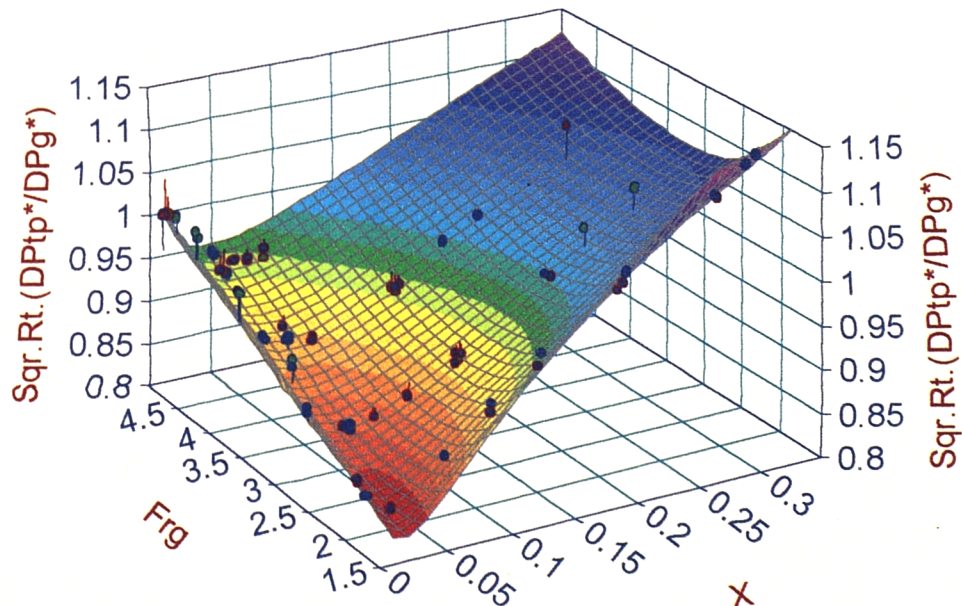
Figure 7.10. The 60 Bar plot.

The ten values (a to j) required for equation 7.3 are found from the following equations:

$$A = (-2.252299E-4)P^2 + (2.303818E-2)P + (1.429067) \qquad (7.3\ a)$$

$$B = (-3.232136E-5)P^2 - (5.891471E-4)P + (0.7682705) \qquad (7.3\ b)$$

$$C = (7.766985E-4)P^2 - (7.744631E-2)P + (0.8934754) \qquad (7.3\ c)$$

$$D = (1.616025E-5)P^2 - (2.413765E-3)P + (0.1939695) \qquad (7.3\ d)$$

$$E = (-8.212814E-4)P^2 + (8.835183E-2)P - (1.952182) \qquad (7.3\ e)$$

$$F = (2.0993E-4)P^2 - (1.756201E-2)P + (3.384842E-2) \qquad (7.3\ f)$$

$$G = (1.81043E-6)P^2 - (2.11191E-4)P + (1.259832E-2) \qquad (7.3\ g)$$

$$H = (1.08944E-4)P^2 - (1.306179E-2)P + (0.3757973) \qquad (7.3\ h)$$

$$I = (-1.704102E-4)P^2 + (1.740651E-2)P - (0.3648267) \qquad (7.3\ i)$$

$$J = (6.528738E-7)P^2 + (4.214143E-4)P - (3.886341E-2) \qquad (7.3\ j)$$

A wet gas correlation for the "second"meter has now been obtained. The way it is implemented is given below:

1) Read off the pressure (P) from the upstream tapping on the Venturi.

2) Use this pressure reading to calculate the phase densities and then the values of A to J from equations above.

3) Read off the upstream to throat differential pressure from the Venturi $\left(\Delta P_{tp}\right)$ and the upstream to downstream differential pressure $\left(\Delta P_2\right)$.

4) Calculate the value of $\Delta P_{tp}^{\ *}$ (i.e. $\Delta P_{tp} - \Delta P_2$).

5) Assuming knowledge of the liquid flowrate solve equation 7.3 for the gas mass flow $\left(\dot{m}_{gas}\right)$ by iteration.

6) Calculate the corresponding value of the gas volumetric flowrate $\left(\dot{Q}_{gas}\right)$.

Note that as the data used to form this correlation is the same as for the final correlation given in Chapter 6 the same limits apply.

This completes the work involved in the formation of a wet gas correlation using the throat to downstream pressure differential information. The performance of this new correlation is shown in terms of the standard root mean square fractional deviation (d +/-) in Table 7.2.

Pressure (Barg)	All Pressures	20 Bar	40 Bar	60 Bar
d (+/-)	0.0182	0.0205	0.0173	0.0167

Table 7.2. The Root Mean Fractional Deviation of Equation 7.3.

The printouts of these calculations are given in Appendix 6. These results clearly show this method to be inferior to the final correlation developed in Chapter 6. However, it is also still clearly better at predicting the gas flowrate (of the NEL data at least) than the previously existing correlations compared in Chapter 4 (with the exception of the de Leeuw correlation at 60 bar).

The maximum and minimum percentage errors of equation 7.3 are show in Table 7.3.

Pressure	All Pressures	20 Bar g	40 Bar g	60 Bar g
Maximum Mg Under (%)	-5.26	-5.26	-3.91	-4.41
Maximum Mg Over (%)	+4.13	+1.82	+0.89	+4.13

Table 7.3. The Maximum % Differences between the Actual and Predicted Gas Mass Flowrates for Equation 7.3 across the Data Set.

Note that the results in Table 7.3 are not significantly better than the de Leeuw or Homogenous correlations (see Table 6.13.). This shows that even though the root mean fractional deviation of equation 8.3 is significantly better than the correlations compared in Chapter 4 equation 8.3 does not fit all the data range as well as would be liked.

7.2.2) Combining the Two Correlations to Simultaneously Meter the Liquid and Gas Flowrates.

7.2.2.1) The Problem of Substituting One Correlation Into the Other.

With the two correlations now in existence that use the different readings obtained from the same meter the question is now whether it is possible to combine these two equations to obtain a solution to their two common unknown values (i.e. the liquid and gas flowrates).

With this "second" meter correlation not having a form whereby the value of the Modified Lockhart Martinelli Parameter can be easily separated out, such that it could be expressed in terms of pressure and gas mass flow and substituted directly into equation 6.6 another method of finding the solutions was required. It was noted that the first correlation (equation 6.6) could have the Modified Lockhart Martinelli Parameter separated from the other parameters and it would therefore be possible to substitute this expression into equation 7.3. However this procedure led to the iteration procedure for equation 6.6 on many data points failing to converge. It was therefore decided that a graphical solution using equations 6.6 and 7.3 was the best way to proceed. This method is now explained.

7.2.2.2) A Graphical Solution for Combining the Two Wet Gas Correlations to Simultaneously Meter the Liquid and Gas Flowrates.

Wet gas correlations have now been created that estimate the gas mass flowrate if the liquid mass flowrate is known and is used as an input parameter. The two equations that are used here to find the gas and liquid flowrates simultaneously are equations 6.6 & 7.3 which are listed below for convenience.

$$\sqrt{\frac{\Delta P_{tp}}{\Delta P_g}} = \frac{1 + AX + BFr_g}{1 + CX + DFr_g} \tag{6.6}$$

$$\sqrt{\frac{\Delta P_{tp}^{*}}{\Delta P_{g}^{*}}} = a + b\ln X + c\ln Fr_{g} + d(\ln X)^{2} + e\left(\ln Fr_{g}\right)^{2} + f\ln X\ln Fr_{g} + g(\ln X)^{3}$$

$$+ h\left(\ln Fr_{g}\right)^{3} + i\ln X\left(\ln Fr_{g}\right)^{2} + j(\ln X)^{2}\ln Fr_{g} \tag{7.3}$$

It should be noted that both equations have the same two unknowns, the gas volumetric flowrate the Modified Lockhart Martinelli Parameter. It therefore stands to reason that if the value of the gas mass flowrate was calculated using each of the above equations for a chosen value of X, then two values of the gas mass flowrate would be obtained. Thus, by calculating values of the gas mass flowrates for the possible range of X values and then plotting the results from each equation on a single Gas Mass Flowrate vs. Modified Lockhart Martinelli Parameter graph, the gas flowrate which satisfies both equations can be obtained.

To illustrate the procedure a mid range point in the test matrix was chosen. A point at 40 Bar and 800 m³/hr with a mid-ranged value of X was selected (point 116 in Appendix 3).

Step 1) The line gauge pressure was recorded as 40.387 Bar. The upstream to throat differential pressure was recorded as 57136.29 N/m² and the throat to downstream differential pressure was recorded as 32788.13 N/m².

Step 2) The values of A to D in equation 6.6 are given by equations 6.7 to 6.10.

A	B	C	D
3.73297	-0.05438	1.66663	-0.05775

Step3) The gas density was found to be 47.146 kg/m³ and the liquid density was found to be 801.57 kg/m³.

Step 4) Equation 6.2 gives the maximum value of the Lockhart Martinelli Parameter if the pressure and gas flowrate are known. As the gas flowrate is as yet unknown this

equation cannot be used here. However as only a rough estimate of the maximum value of the Modified Lockhart Martinelli Parameter is required equation 7.4 can be used.

$$X_{maximum} = (0.0038*P) + 0.0781$$

The maximum value of X at 40.387 Bar was therefore found to be 0.23157.

Step 5) This author chose to calculate one hundred and one values of X. (This number comes from dividing the Modified Lockhart Martinelli Parameter range by 100 (an arbitrary choice) and adding the increments to the minimum Modified Lockhart Martinelli Parameter value of 0.001312 until the maximum value is reached.) For each X value the associated values of the gas mass flowrate are calculated by equation 6.6. The graph obtained is shown in Figure 7.9.
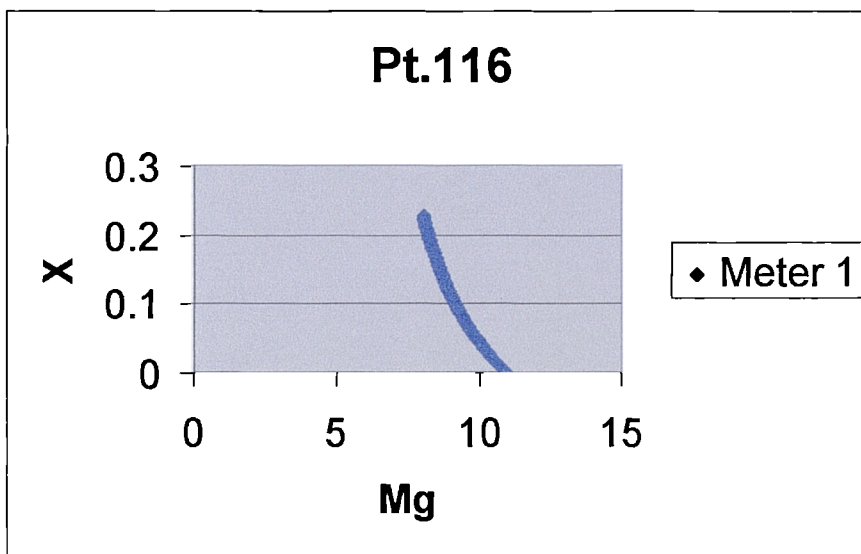
Figure 7.11. The "First" Meter Predictions.

Step 6) The values for a to j in equation 7.3 were obtained from equations 7.3a to 7.3j and listed below.

a	b	c	d	e
1.429067	0.768271	0.893475	0.19397	-1.95218
f	g	h	i	j
0.033848	0.012598	0.375797	-0.36483	-0.03886

Step 7) Using the X value range as in step 5 the associated m_g were obtained equation 7.3.

Step 8) The results of Step 7 are plotted on the graph from Step 5. The combined plot is shown in Figure 7.10.
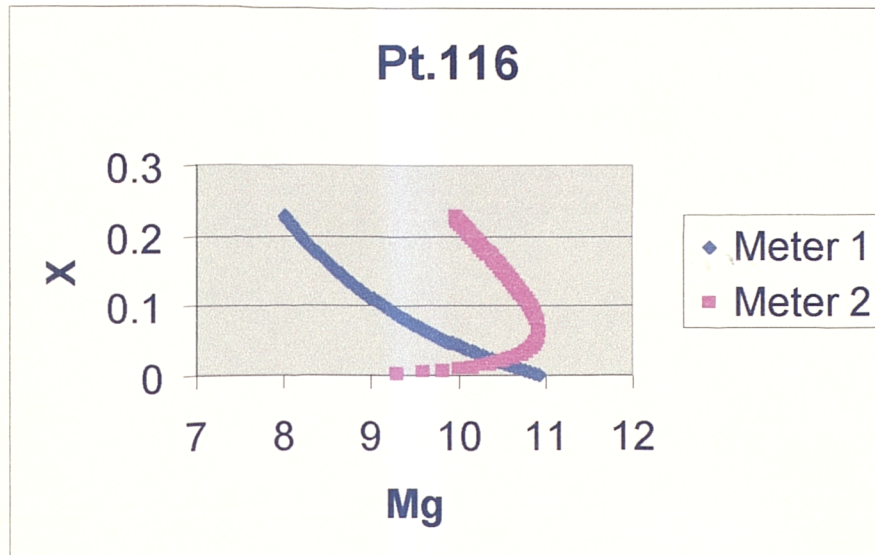
Figure 7.12. The Combined Meter Predictions.

Step 9) From examination of the intersection of the two lines (using Excel) it was seen that the estimated Gas Mass Flowrate was 10.449 kg/s. The actual Gas Mass Flowrate was recorded by the gas flow reference meter as 10.472 kg/s. This is a difference of -0.216%. The estimated value of the Modified Lockhart Martinelli Parameter is 0.0186 whilst the actual value was recorded as being 0.019366. This is therefore an error of –3.955% and this error is then passed on to the liquid flowrate prediction. The predicted value of the liquid flowrate of was 0.774 kg/s compared with the actual value of 0.801 kg/s, a percentage difference of –3.37%.

Appendix 6 lists the results of the individual 230 data points. (Note that not all the 243 points in the data set are listed as 13 points did not have the downstream pressure recorded.)

The result for the estimation of the gas flowrate in the above example is very good. The prediction of the liquid flowrate is not so good as the gas prediction but it

is still good compared to the uncertainty given by the tracer dilution method. Unfortunately however, not all the results calculated using this method were as accurate. All but three gas flowrate estimations where within 6% of the actual gas flowrate. The remaining three were considerably less accurate but the reason for this is known and will be discussed later. The liquid flowrate prediction could be extremely poor at the low liquid flowrates. Here even a small error in the liquid quantity would lead to a significant percentage error. It should be remembered however that this research was not aimed at metering the liquid mass flowrate as accurately as the gas flowrate. Therefore, a method giving an accurate estimation of the gas flowrate for an unknown liquid flowrate is of great value in these situations where it is the natural gas flowrate that is of prime importance.

As stated not all the points gave as good a gas flowrate prediction as the example shown above. Four problems arose from this method. These are dealt with in turn next.

1) The first problem was that due to the shape of the $\dot{m}_g$ vs. X graph obtained from the "second" meter calculation it was possible to get two solutions. That is, the lines could intersect twice across the range of X. It therefore appears that for a given line pressure, upstream to throat pressure differential and throat to downstream pressure differential there can be two combinations of $\dot{m}_g$ and X which cause the Venturi Meter to give these same readings. Data point 60 is shown as an example in Figure 7.13.
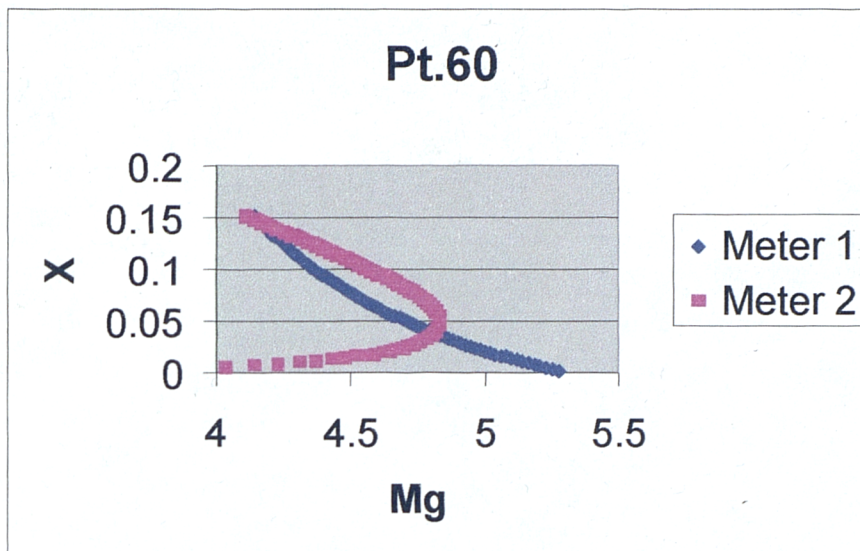
Figure 7.13. Data Point 60.

The actual gas mass flowrate is 4.095 kg/s, the Modified Lockhart Martinelli Parameter is 0.1618 and the actual liquid flowrate is 3.629 kg/s. However, two results are indicated in Figure 7.11. One result has the gas mass flowrate as 4.182 kg/s, the Modified Lockhart Martinelli Parameter as 0.144 and the liquid flowrate as 3.298 kg/s. The second result has the gas mass flowrate as 4.816 kg/s, the Modified Lockhart Martinelli Parameter as 0.039 and the liquid flowrate as 1.03 kg/s. The metering engineer would therefore have two possible solutions and from this method alone no way of deciding which result was the correct one. However, it was always seen to be the case that when two solutions existed there was always a considerable difference in the two sets of results. (Note that for point 60 the first result had more than three times the liquid flowrate of the second result.) That is, the two values of X are always such that the associated predictions of the liquid mass flowrates are very different. Therefore the operators should be able to easily judge which result is the correct one from other indications in the production flow. Examples are the magnitude of the liquid quantity finally being separated from the combined flow pipeline and the pressure drop in the pipework compared to what it would be if the quantity of produced gas flowed alone in the line. In Appendix 6 points with two solutions are marked by an asterisk on the right hand side of the column.

2) A second problem is that sometimes the two curves have very similar steep gradients and therefore the uncertainties from the chosen correlations not fitting the data perfectly are carried through to the two produced $\dot{m}_g$ vs. X curves. That is, with any inaccuracy causing a slight shift in a curve then due to the similar gradients this can cause a considerable change in the X prediction. However, as stated earlier, this research is primarily interested in the gas mass flowrate prediction and the estimation of the liquid mass flowrate is of secondary importance. Due to the steep gradients a slight shift in a curve can cause a significant difference to the X value predicted but much less of an affect is seen on the gas mass flowrate prediction. Therefore, this is not seen as a great problem here.

A more obvious indication of the liquid flowrate estimation dependence on the accuracy of these gradients is the eleven points where no intersection occurs. Figure 7.14 shows the example of point 66. Clearly in Figure 7.14 the two lines do not intersect. It is also clear that any slight inaccuracy in either lines formation causing these lines to shift away from one other would cause this situation. However, for all eleven points (denoted by a double asterisk on the right hand side of Appendix 6) there was an obvious closest distance as the two lines always came extremely close to intersecting. For these points the average values of the closest points were taken as the result. This invariably led to a prediction close to the actual gas flowrate. For point 66 the actual gas mass flowrate is 5.443 kg/s, the Modified Lockhart Martinelli Parameter is 0.1221 and the actual liquid flowrate is 3.645 kg/s. The predicted gas mass flowrate is 5.482 kg/s, the Modified Lockhart Martinelli Parameter is 0.1024 and the actual liquid flowrate is 3.079 kg/s.
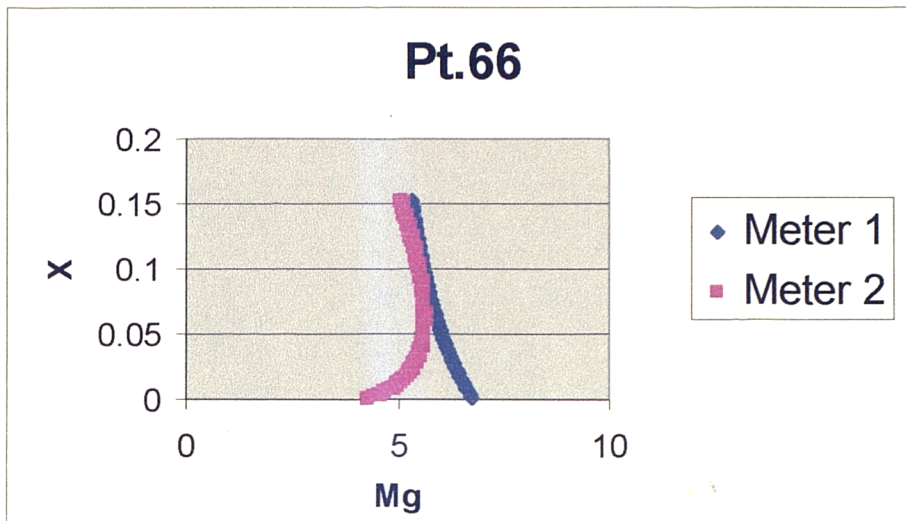
Figure 7.14. Data Point 66.

3) Another minor problem was found to exist occasionally at the highest values of X. With the gas mass flowrate predictions being more accurate than the X predictions for these high actual values of X, if the method slightly over predicted the value of X then of course the range had to be extended by a few percent to allow a solution. This only occurred four times and in Appendix 6 these points are marked on the right of the column with the letter E. At no time did extending the range of X by a few percent cause the iteration to diverge and acceptably accurate estimations of the gas mass flowrate were obtained each time.

4) The major problem encountered was that three particular points gave much poorer gas mass flowrate estimations. Whereas all other points had an accuracy better than +/- 6%, points 198, 200 and 240 deviated from the actual gas flowrates by +13.689%, +9.874% and +10.467% respectively. The reason for this is likely to be the relatively poor fit of equation 7.3 at 60 bar (see Figure 7.10). Whereas the 20 and 40 bar data fitted equation 7.3 well (with r^2 values of 0.9817 and 0.9788 respectively) the 60 bar data fitted equation 7.3 less well (with a r^2 value of 0.9439). In fact, in Figure 7.10 point 198 (with a Fr_g value of 2.91 and a X value of 0.284), point 200 (with a Fr_g value of 3.88 and a X value of 0.286) and point 240 (with a Fr_g value of 2.91 and a X value of 0.242) can be clearly seen to have a considerably poorer fit than the neighbouring data points.

193

The root mean fractional deviation of this method is given in Table 7.4.

Pressures	All Pressures	20 Bar g	40 Bar g	60 Bar g
d (+/-)	0.0254	0.0197	0.0199	0.0330

Table 7.4. The Root Mean Fractional Deviation of the Method for Measuring the Gas Phase Without Knowledge of the Liquid Phase.

The root mean fractional deviation of this method excluding the three 60 bar points 198 , 200 and 240 is given (so as to show the methods ability if a closer fitting equation were to be applied to the data) in Table 7.5.

Pressures	All Pressures	20 Bar g	40 Bar g	60 Bar g
d (+/-)	0.0220	0.0197	0.0199	0.0254

Table 7.5. The Root Mean Fractional Deviation of the Method for Measuring the Gas Phase Without Knowledge of the Liquid Phase with the Three Poorly Fitted Points at 60 Bar Removed.

The maximum % differences between the actual and predicted gas flowrates across the 230 points are presented in Table 7.6.

Pressure	All Pressures	20 Bar g	40 Bar g	60 Bar g
Maximum Mg Under (%)	-5.452	-4.601	-4.993	-5.452
Maximum Mg Over (%)	+13.689	+3.403	+4.373	+13.689

Table 7.6. The Maximum % Differences between the Actual and Predicted Gas Mass Flowrates for the Simultaneous Gas and Liquid Flowrate Prediction Method across the Data Set.

Again, a separate table is presented for when the three poorly fitted 60 bar points (points 198 , 200 and 240) are removed from the data set (so as to show the methods ability if a closer fitting equation were to be applied to the data). This is presented as Table 7.7.

Pressure	All Pressures	20 Bar g	40 Bar g	60 Bar g
Maximum Mg Under (%)	-5.452	-4.601	-4.993	-5.452
Maximum Mg Over (%)	+5.158	+3.403	+4.373	+5.158

Table 7.7. The Maximum % Differences between the Actual and Predicted Gas Mass Flowrates for the Simultaneous Gas and Liquid Flowrate Prediction Method across the Data Set for the Case of the Three Poorly Fitted 60 Bar Points Removed.

These results are of course not as good as for the new correlation offered in Chapter 6 (i.e. equation 6.6) where the liquid mass flowrate is assumed to be known. However, they are still good compared to the results obtained from the previously existing correlation comparisons discussed in Chapter 5 and these are for methods that assume the liquid mass flowrate is known. Furthermore if the Tracer Dilution Method was required in order to apply equation 6.6 (meaning the liquid flowrate was only known to an accuracy of +/- 10%) the performance of equation reduces accordingly. Tables 7.8 and 7.9 show this reduced performance.

Pressures	All Pressures	20 Bar g	40 Bar g	60 Bar g
d (+/-)	0.0152	0.0118	0.0153	0.0178

Table 7.8. The Increased Values of the Root Mean Fractional Deviation of Equation 6.6 when the Tracer Dilution Method is Required.

Pressure	All Pressures	20 Bar g	40 Bar g	60 Bar g
Maximum Mg Under (%)	-1.196	-1.196	-0.813	-0.678
Maximum Mg Over (%)	+4.865	+2.671	+4.280	+4.865

Table 7.9. The Maximum % Differences between the Actual and Predicted Gas Mass Flowrates for Equation 6.6 when the Tracer Dilution Method is Required.

It can be seen by comparison of Tables 7.4 and 7.8 that the use of the Tracer Dilution Method in conjunction with equation 6.6 is the best method for metering the liquid and gas mass flowrates simultaneously. However, compared to the correlations considered in Chapter 5 it is clear that the simultaneous measurement method presented in this Chapter has a good performance. If the de Leeuw or Homogenous

correlations (i.e. the best performing correlations that existed previous to this study) were applied with the Tracer Dilution Method then a similar accuracy would be expected as would be found with this studies simultaneous liquid and gas mass flowrate metering method. The exception to this is the 60 bar data where the poorer fit of equation 7.3 results in the poorer performance of the equation. Nevertheless the methods resulting performance at 60 Bar is still reasonable compared to the de Leeuw and Homogenous correlations. Furthermore, even though over all the equation 6.6 and Tracer Dilution Method combination has the best performance it should be remembered that a metering method that can meter the gas and liquid flowrates simultaneously holds a significant advantage over spot measurement techniques. Therefore this study has proved a method for metering wet natural gas flows that is a significant advance in the metering technology of the Oil and Gas Industry.

Chapter 8

Conclusions

Over the three years since the start of this research the prediction by the NEL that the subject of wet natural gas metering would become increasingly important to the natural gas production industry has come true. Although manufacturers of all types of gas flow metering equipment promote their meters as being capable of use the reality is that the oil and gas industry is increasingly looking to the Venturi Meter and the Ultrasonic Meter as their meter of choice for wet gas applications. Thus the research undertaken in this study of Venturi Meter performance in wet gas flows is of direct industrial relevance.

On reviewing the existing correlations used with a DP Meter metering wet gas it was found that there were only seven correlations and that five of these had been developed for Orifice Plate Meters only and covered a greater range of two-phase flow flow conditions than just wet gas flow. However, as the two Venturi Meter wet gas correlations were very recent, and industry had been using the five older two-phase Orifice Plate Meter correlations for many years, all the correlations were included in the correlation comparison made possible by the data obtained from the new NEL Wet Gas Loop during this study.

The best performing correlation was the most recent wet gas Venturi Meter correlation of de Leeuw closely followed by the Homogenous Model. Only at 60 Bar was the de Leeuw correlation seen to perform better than the Homogenous Model. The other wet gas Venturi Meter correlation developed by Phillips Petroleum was found not to perform well based on the NEL data. Finally, it was noted that the Murdock correlation, which is the best known of the general two-phase Orifice Plate Meter correlations and which has been used by industry for wet gas Venturi Meter situations, performed poorly.

It has often been stated that the line pressure is an important parameter in the prediction of the error that a DP Meter has due to the presence of liquid in the flow. de Leeuw went further and stated that, as well as the line pressure, the gas flowrate itself is important in determining the Differential Pressure Meter error. This last point

had never been verified by independent research. The current investigation into trends apparent from the NEL data has shown indeed that both the line pressure and the gas flowrate are important parameters in determining the meter error. It was found however, that the pressure effect was greater than the gas flowrate effect.

Four new correlations have been developed during this study. Three of these are updates of the original Murdock Equation. The first of the new correlations was derived simply by using the new Wet Gas data to determine a new constant applicable to Venturi Meters. This was identical to the method used by Phillips Petroleum when they created a Modified Murdock correlation using their field data. However, it was found that the NEL test data gave a considerably different constant value than that quoted by Phillips Petroleum. The second new correlation was created by considering the Murdock gradient to be a function of only the line pressure. This resulted in an improvement in accuracy but the performance was still considerably poorer than the de Leeuw correlation. The third Murdock type correlation which was developed was obtained by considering the Murdock gradient to be a function of the line pressure and the gas mass flowrate. This resulted in a further improvement in performance over the other new correlations but it still did not match that of the de Leeuw correlation.

The foregoing work made it clear that a completely new form of correlation was required. Recognising that a mathematical model capable of accurately predicting wet gas Venturi Meter performance is beyond the capabilities of current researchers, this new form had to be obtained using a surface fitting software package. The new correlation obtained using the new data (equation 6.6) was found, not unnaturally, to perform extremely well when used on the data that created it. (It should be noted that for the new correlation, just as for the original ones, it is a requirement that the liquid flowrate known before they can be applied to determine the gas flowrate.) However this study suffers the same problem faced by all research into two-phase flow metering, i.e., the lack of available independent data with which to test the new correlation. Only when new reliable data becomes available will the true effectiveness of the new correlation be determined.

However, the present study has found that it is possible to use the information obtained from a downstream pressure tapping information in conjunction with the

traditional Venturi Meter readings to predict the gas and liquid flowrates simultaneously, i.e. with no prior knowledge of the liquid flowrate. The method developed during this study to achieve this goal is promoted as being suitable for use when the flow parameters lie within the NEL Wet Gas data range. It is of course not advisable to extrapolate the method to situations where the flow conditions lie out with the range over which the basic correlations used in the method apply. However, this research shows that the simultaneous metering of gas and liquid flowrates is possible. The proposed method predicts the gas flowrates with reasonable accuracy but there was found to be a considerable error in the liquid flowrate, particularly at low liquid flowrates.

This research was conducted using one six-inch Venturi meter with a beta ratio of 0.55. However, in industry there is a requirement for different sized meters with different beta ratios. The effect of the pipe diameter on DP Meter readings in wet gas flows is as yet undetermined, as is the effect of the beta ratio and different fluid properties. Therefore, for any given meter to be useable as a reliable wet gas meter it should be fully tested across the relevant range. Only when such data is made available will it perhaps be possible to obtain a correlation which may be regarded as being of general applicability. However, the lack of reliable data for flows at production pressures and flowrates is a situation that is not likely to change quickly as the power required to drive a wet gas flow test rig at such conditions makes such testing extremely expensive.

REFERENCES

1) Nederveen.N, Washington G.V. and Batstra F.H., "Wet Gas Flow Measurement", SPE 19077, 1989.

2) Stobie. G, "Wet Gas Flow Measurement in the Real World", One Day Seminar "Practical Developments in Gas Flow Metering" at National Engineering Laboratory, East Kilbride, Scotland. Paper 6, April 1998.

3) Washington. G, "Measuring the Flow of Wet Gas". North Sea Workshop, 1989.

4) A. W. Jamieson A.W. and Dickinson P.F, "High Accuracy Wet Gas Metering" North Sea Workshop 1993.

5) de Leeuw. R, "Liquid Correction of Venturi Meter Readings in Wet Gas Flow", North Sea Workshop 1997.

6) Wilson M. "The Development and Testing of an Ultrasonic Flow Meter for Wet Gas Applications". One Day "Seminar on the Measurement of Wet Gas" National Engineering Laboratory, East Kilbride, Scotland. October 1996.

7) Svedeman. S. "V-Cone Meter Measurement Accuracy for Wet Gas Flow" McCrometer Inc.. Internal Report 04-8369-002. May 1997.

8) Ifft S.A. "Wet Gas Testing with the V-Cone Flowmeter" North Sea Workshop, Paper 22, 1997.

9) ISO Standard 5167-1.

10) ASME, "Measurement of Fluid Flow in Pipes using Orifices, Nozzle, and Venturi". ASME MFC-3M-1989. (Reaffirmed 1995).

11) ASME text book, "Fluid Meters - Their Theory & Application". 5th edition. Published 1959.

12) Ting V.C., "Effects of Non-Standard Operating Conditions on the Accuracy of Orifice Meters", SPE Production, Vol. 8, No.1, pp58-62, 1993.

13) Ting V.C & Jones E.H., "Wet Gas Metering Performance" Procedures of the International Conference on Offshore Mechanics and Artic Engineering, ASME Vol. 5. Pages 297-303, 1996.

14) Shaw .R, "The Influence of Hole Dimensions on Static Pressure Measurements" Journal of Fluid Mechanics, Vol. 7, 1960.

15) Azzopardi B.J., Taylor. S and Gibbons D.B. "Annular Two-Phase Flow in a Large Diameter Tube", Engineering Sciences Division, AERE Harwell, (AERE R10570), June 1982.

16) Azzopardi B.J., "Annular Two-Phase Flow in Constricted Tubes", Engineering Sciences Division, AERE Harwell, (AERE -R 10930), June 1983.

17) Azzopardi B.J. and Govan A.H., "Annular Two-Phase Flow in Venturis", Thermal Hydraulics Division , AERE Harwell, June 1985

18) Azzopardi B.J., Govan A.H. and Bott T.R.,"An Improved Model for Annular Flow in a Venturi", Thermal Hydraulics Division , AERE Harwell (AERE-R13060). May 1988.

19) a) AzzopardI B.J., Memory S.B. and Smith. P., "Experimental Study of Annular Flow in a Venturi", 4th Int. Conference on Multi-Phase Flow, Nice, France, Paper E2. 19-21 June 1989, And the associated:

19) b) Azzopardi B.J., Memory S.B. and Smith. P., "Data from an Experimental Study of Annular Flow in a Venturi", Thermal Hydraulics Division , AERE Harwell (AERE-R 13352), Dec. 1989.

20) James. R., "Metering of Steam-Water Two-Phase Flow by Sharp-Edged Orifices" Process Instrumentation for Mechanical Engineers , Vol.180,pp549-566, 1965

20) Lin. Z.H., "Two-Phase Flow measurement with Orifices", Encyclopedia of Fluid Mechanics, Chapter 29, 1986.

22)* Hoopes J.W., "Flow of Steam-Water Mixture in a Heated Annulus and through Orifices" AIchE J., Vol. 3, No.2,pp268-275, 1957.

23)*Bizon.E, "Two-Phase Flow Measurements with Sharp-Edged Orifices and Venturies", AECL-2273,1965.

24)*Marriott P.W., "Two-Phase Steam-Water through Sharp-Edged Orifices", NEDO 10210, 1970.

25) Collins D.B. and Gacesa. M., "Measurement of Steam Quality in Two-Phase Upflow with Venturimeters and Orifice Plates", Journal of Basic Engineering, March 1971.

26)* P.P. Kremlevskii P.P. and I.A. Dyudina I.A., "Measurements of Moist Vapour Discharge by Means of Gauging Diaphragms", Measurement Techniques, Vol.15, No.5, pp 741-744,1972.

27) Davies A.D. and Daniels T.C., "Single and Two-Phase Flow of Dichlorodifluoromethane,(R-12), Through Sharp Edged Orifices" ASHRAE Transaction, Vol. 79,pt 1, pp109-123, 1973.

28)* Lorenzi A. and Muzzio A., "Two-Phase Flow Rate Measurement with Sharp Edged Orifices", Journal of Termotecnics, No. 3, 1977.

29) Matter L., Nicholson M. and Aziz K., "Orifice Metering of Two-Phase Flow" Journal of Petroleum Technology, pp955-961, August 1979.

30) Murdock. J.W., "Two-Phase Flow Measurements with Orifices", Journal of Basic Engineering, Vol.84, pp 419-433, December 1962.

31) Chisholm D., "Flow of Incompressible Two-Phase Mixtures through Sharp-Edged Orifices", Journal of Mechanical Engineering Science, Vol. 9, No.1, 1967.

32) Chisholm D., "Research Note: Two-Phase Flow Through Sharp-Edged Orifices", Journal of Mechanical Engineering Science, Vol. 19, No. 3, 1977.

33) Smith R.V. and Leang J.T., "Evaluation of Correlations for Two-Phase Flowmeters Three Current - One New", Journal of Engineering for Power, pp 589-594, October 1975.

34) Lin Z.H., "Two-Phase Flow Measurements with Sharp-Edged Orifices" International Journal of Multi-Phase Flow, Vol. 8, No. 6, pp 683-693, 1982.

35) Ting V.C., " Effect of Orifice Meter Orientation on Wet Gas Flow Measuring Accuracy", SPE 26158, 1993.

36) Shen J.S. and Ting. V.C., "Diagnosis and Improvement of Wellhead Gas Metering: A Case Study", SPE 35610, 1996.

37) Smith L.T., Murdock J.W. and Applebaum R.S.,"An Evaluation of Existing Two-Phase Flow Correlations for use with ASME Sharp Edge Metering Orifices", Journal of Engineering for Power, pp 343-347, July 1977.

38)* Ragolin. N.V, "Measurements of Steam-Water Flow", Teploenergetika, Vol. 2, No. 5, pages 51-55 (1958).

39) Chisholm D. and Leishman J.M., "Metering of Wet Steam", Journal of Chemical & Process Engineering, pp103-106, July 1969.

40) Graham E.J., "The Flow of Air/Water Mixtures Through Nozzles" National Engineering Laboratory Report No. 308, East Kilbride, Glasgow, Scotland, 1967. (Since lost by the NEL).

41) de Leeuw R., "Wet Gas Flow Measurement by Means of a Venturi Meter and a Tracer Technique", North Sea Workshop, Peebles, Scotland, October 1994.

42) Washington G., "Measuring the Flow of Wet Gas" North Sea Workshop, Haugesund, Norway, Oct.1991.

43) Shaw .R, "The Influence of Hole Dimensions on Static Pressure Measurements" Journal of Fluid Mechanics, Vol. 7, 1960.

44) NEL Report, "A Report from the NEL for the Testing of the Daniel Industries Ultrasonic Flowmeter in Wet Gas Conditions for the Ultrasonic Flow Consortium", March 1995. (Restricted-Commercial).

45) NEL Report, "Annex to the Report on the Testing of the Daniel Industries Ultrasonic Flowmeters in Wet Gas Conditions for the Ultraflow Consortium", Dec. 1995. (Restricted-Commercial).

46) Zhihang C., Zaisan Z., and Menghao W., "The Research and Development of Gas-Liquid and Vapour - Liquid Two-Phase flow measurement", Journal of Shanghai Institute of Mechanical Engineering. Vol. 1. 1979.

47)* Medvejev V.F., "Gas and Liquid Flow Rate Measurement in Gas-Liquid Mixture", Journal of Instrumentation and Control System, No. 10, pp 18-20, 1972.

48) Chen Z.H., Chen Z.A.Y, and Xu Y.L. et al., "Two-Parametric Flow Measurement in Gas-Liquid Two-Phase Flow" Proceedings of the 7th Int. Heat Transfer Conference, Sept. 1982.

49) Harris D.M. and Shires G.L., "Two-Phase Pressure Drop in a Venturi" UKAEA, Winfrith, Dorset. 1982.

50) NEL Management System , "Procedure for Uncertainty Budgets for the Gas Flow Laboratory", QWI/FL/1190, Dec. 2000.

51) Azzopardi B.J., "Use of a Quasi-One- Dimensional Model for optimising a Venturi meter in Gas-Solid Applications", Environmental & Mining Engineering, July 1998.

52) Ting V.C. and Corpon G.P.,"Effect of Liquid Entrainment on the Accuracy of Orifice Meters for Gas Flow Measurements" International Gas Research Conference, 1995.

53) Nangea A.G., Reid L.S., Huntington R.L. and Joyce M.P., "The Effect of Entrained Liquid on the Measurement of Gas by an Orifice Meter". University of Oklahoma Report. June 1965.

54) Jobson D.A, "On the Flow of a Compressible Fluid through Orifices", Proc. Instn Mech. Engrs., Vol. 169, (No. 37), pp 767. 1955.

55) Chisholm D., "Research Note: Void Fraction during Two-Phase Flow", Journal of Mechanical Engineering Science, Vol. 15, No. 3, 1973.

56) Taitel. Y and Duckler A.E., "A Model for Predicting Flow Regime Transitions in Horizontal and Near Horizontal gas-Liquid Flow", AIChE Journal (Vol. 22, No.1), Jan. 1976.

57) Hall A., "Measurement & Simulation of Liquid Content of High Pressure Wet Gas Flows", NEL Report No. 176/2000, 2000.

58) Steven R., "Report to ISA Controls Ltd. On Wet Gas Metering with Use of a Horizontally Installed Venturi Meter", May 2000

59) Stobie G., "Metering in the Real World, Part2", Practical Developments in Gas Flow Metering Workshop, Aberdeen, 2000.

60) Vedapuri C. and Gopal M., "Design of a Clamp-On Ultrasonic Liquid Flowrate Monitor for Wet Gas Pipelines" Second North American Conference on Multiphase Technology, Banff, Canada, 21-23 June 2000.

61) Roberts P.A., "Low Cost Wet Gas Flow Measurement", IChemE, 1997.

62) UK Patent Application (GB 2 336 681 A), Title: "Measuring a Gas Mass Fraction", Application No. 9820074.4, Date Filled: 16/09/1998.

63) International Patent No. WO 99/56091, Title: "Measuring a Gas Mass Fraction", International Publication Date: 4/09/1999.

64) Lund J.S., Tait A.R. Clark S.,"A Wet Gas Meter for Gas / Condensate Flow Measurement", Ninth International Conference on Multiphase, pp303-315, 1999.

65) Daniel P., "A Venturi Based Wet Gas Meter with On-Line Gas Mass Fraction Estimation", North Sea Workshop 2000, (Paper 6.3).

66) El-Haggar S.M. and Crowe C.T., "Numerical Model for Disperse Two-Phase Steam/Water Flow in a Venturi", Journal of Basic Mechanics in Two-Phase Flow and Heat Transfer, 1980.

67) Couput J.P. et al., "Numerical Investigation of Wet Gas in a Venturi Meter", Flomeko 1998.

68) Couput J.P., "Wet Gas Metering in the Upstream Area: Needs, Applications and Developments", North Sea Flow Measurement Workshop 2000, Paper 6.1.

69) Wallis, G.B., "One-Dimensional Two-Phase Flow" McGraw-Hill Book Co., New York, 1969.

Note: * indicates that the paper was unobtainable by the British Library and all knowledge derives from information given from other references. These references are as given in the reference lists of the above available documents.

Appendices

Appendix One

Method for Comparing Test Fluid Properties to Actual Wet Natural Gas Flows

The first question that requires to be addressed is what dimensionless groups are important when comparing simulant fluids to model actual two-phase natural gas flows in pipes? It was assumed that the pressure drop (ΔP) is a function of the following parameters:

$$\Delta P = f(\rho_g, \rho_l, \bar{U}_g, \bar{U}_l, D, l, e, \mu_g, \mu_l, \sigma_l, g)$$

i.e. the total number of parameters is twelve (n=12) where:

ΔP = pressure drop along the pipe.

ρ_g = gas density

ρ_l = liquid density

$\bar{U}_g$ = gas velocity

$\bar{U}_l$ = liquid velocity

D = pipe diameter

l = unit length of pipe

e = surface roughness of pipe wall

μ_g = gas viscosity

μ_l = liquid viscosity

σ_l = liquid surface tension

g = gravity

The above properties can expressed in terms of the three fundamental (primary) dimensions of length (l), mass (m) and time (t), (i.e. 'r'=3):

ΔP	$\rho_g \& \rho_l$	$\bar{U}_g \& \bar{U}_l$	D, l, e	$\mu_g \& \mu_l$	σ_l	g
$\dfrac{m}{lt^2}$	$\dfrac{m}{l^3}$	$\dfrac{l}{t}$	l	$\dfrac{m}{lt}$	$\dfrac{m}{t^2}$	$\dfrac{l}{t^2}$

Choosing the three parameters (i.e. m=3) $\rho_g, \bar{U_g}, D$ then nine dimensionless groups (i.e. n-m=12-3=9) are formed.

It is therefore required to determine the form of the following groups:

$$\Pi_1 = f(\Pi_2, \Pi_3, \Pi_4, \Pi_5, \Pi_6, \Pi_7, \Pi_8, \Pi_9)$$

Therefore:

1) $\Pi_1 = \rho_g{}^a U_g{}^b \ D^c \Delta P = \left(\dfrac{m}{l^3}\right)^a \left(\dfrac{l}{t}\right)^b l^c \left(\dfrac{m}{lt^2}\right) = m^0 l^0 t^o$

m: a+1=0

l: -3a+b+c-1=0

t: -b-2=0   Therefore a= -1, b= -2, c= 0

So, $\Pi_1 = \rho_g{}^{-1} U_g{}^{-2} \ D^0 \Delta P$ i.e. $\Pi_1 = \dfrac{\Delta P}{\rho_g \bar{U_g}^2}$

By repeating this the following is obtained.

$$\dfrac{\Delta P}{\rho_g \bar{U_g}^2} = f\left(\dfrac{\rho_l}{\rho_g}, \dfrac{U_l}{\bar{U_g}}, \dfrac{L}{D}, \dfrac{e}{D}, \dfrac{\mu_g}{\rho_g U_g D}, \dfrac{\mu_l}{\rho_g U_g D}, \dfrac{\sigma_l}{\rho_g U^2{}_g D}, \dfrac{gD}{U^2{}_g} \right) \ \text{------ (1)}$$

Analysis of the Dimensionless Groups

$\Pi_1 - \dfrac{\Delta P}{\rho_g \bar{U_g}^2}$ can be rewritten as $\Pi_1 = \dfrac{\Delta P}{\frac{1}{2}\rho_g \bar{U_g}^2}$ where the added constant simply

requires accounting for in the function on the right hand side of equation (1). If it is assumed that ΔP is the same for both phases (i.e. $\Delta P = \Delta P_g = \Delta P_l$) then Π_1 is in fact

defined as the "Euler Number" (Eu) or the "pressure coefficient" (C_p) of the gas phase.

$$\text{i.e. } \Pi_1 = Eu = C_p = \frac{\Delta P}{\rho_g \, U_g{}^2}$$

$\Pi_2 = \dfrac{\rho_l}{\rho_g}$ is the ratio of the phase densities. The liquid density (ρ_l) is set by the choice of liquid and is generally regarded as constant even for high pressures. Therefore the experimenter can alter the value of Π_2 by changing only the gas density (which can be done by varying the line pressure).

$\Pi_3 = \dfrac{U_l}{U_g}$ is the ratio of the phase velocities. Note that the reciprocal of this term is commonly defined as the slip 's'. Therefore $\Pi_3 = f(\dfrac{U_g}{U_l}) = g(s)$. Where f and g are particular functions. Π_2 and Π_3 are used later to make sense of the other dimensionless groups and are incorporated into these later groups.

The next two dimensionless groups are $\Pi_4 = \dfrac{L}{D}$ and $\Pi_5 = \dfrac{e}{D}$ which are dependent on the pipe geometry only and are therefore irrelevant to the choice of simulant fluids.

The next dimensionless group is Π_6. As the Reynolds Number for a single phase is defined as $Re = \dfrac{\rho U D}{\mu}$ it is clear that we therefore have the reciprocal of the gas

Reynolds Number: $\Pi_6 = \dfrac{\mu_g}{\rho_g U_g D} = \dfrac{1}{Re_g}$, i.e. $\Pi_6 = f(Re_g)$.

The other dimensionless group with a simple definition is Π_9. The definition of the single phase Froude Number (Fr) is: $Fr^2 = \dfrac{U^2{}_g}{gD}$.

Therefore we have:

$$\Pi_9 = \frac{gD}{U^2_g} = \frac{1}{Fr_g^2} \text{ , i.e. } \Pi_9 = f(Fr).$$

The last two groups to be considered (Π_7 & Π_8) are slightly more complicated to analyse. This is due to the mixing of the gas and liquid phase parameters that of course does not occur with single phase dimensional analysis. We have

$\Pi_7 = \dfrac{\mu_l}{\rho_g U_g D}$ and $\Pi_8 = \dfrac{\sigma_l}{\rho_g U^2_g D}$. The important point to note here, while

attempting to find the information held in these two dimensionless groups, is that in

undertaking the dimensional analysis the choice of the three parameters $\rho_g, \bar{U}_g, D$ is

arbitrary as long as the three fundamental dimensions (l, m, t) are represented at least

once each. Therefore it is equally valid to select $\rho_l, \bar{U}_l, D$ as the parameters. If that

had been done then the dimensionless groups would have been similar but with the

difference that we would have got $\Pi_7 = \dfrac{\mu_l}{\rho_l U_l D}$, which of course could be written

as Π_7 f (Re$_l$) and the present value of $\Pi_6 = \dfrac{\mu_g}{\rho_g U_g D} = \dfrac{1}{Re_g}$ would have come out as

Π_6 $\dfrac{\mu_g}{\rho_l U_l D}$. A similar situation exists for the cases of not only Π_8 but Π_9 as well.

Π_8 would turn out as $\Pi_8 - \dfrac{\sigma_l}{\rho_l U^2_l D}$ and $\Pi_9 = \dfrac{1}{Fr_l^2} = \dfrac{gD}{U^2_l}$. Note that

Π_8 $\dfrac{\sigma_l}{\rho_l U^2_l D}$ is by definition the reciprocal of the "Weber Number" (We). Therefore

we have: $\Pi_8 - \dfrac{\sigma_l}{\rho_l U^2_l D}$ $\dfrac{1}{We}$, i.e. $\Pi_8 = f(We)$.

Hence Π_{10} $\dfrac{\mu_l}{\rho_l U_l D}$ $\dfrac{1}{Re_l}$ and $\Pi_{11} = \dfrac{gD}{U^2_l} = \dfrac{1}{Fr_g^2}$.

It should also be noted that the original dimensionless groups, i.e.

$$\frac{\Delta P}{\rho_g U_g^{\ 2}} = f(\ \frac{\rho_l}{\rho_g},\frac{U_l}{U_g},\frac{L}{D},\frac{e}{D},\frac{\mu_g}{\rho_g U_g D},\frac{\mu_l}{\rho_g U_g D},\frac{\sigma_l}{\rho_g U_g^{\ 2} D},\frac{gD}{U_g^{\ 2}}\ )$$

do indirectly indicate the existence of the other graphs (i.e. $\Pi_{10} = \dfrac{\mu_l}{\rho_l U_l D}$

and $\Pi_{11} = \dfrac{gD}{U_l^{\ 2}}$). That is:

$$f(\ \frac{\rho_l}{\rho_g},\frac{U_l}{U_g},\frac{\mu_l}{\rho_g U_g D}\ )= g(\ \frac{\mu_l}{\rho_g U_g D}\ )= g\left(\frac{1}{Re_l}\right)=\Pi_{10}$$

and $\qquad h(\dfrac{U_l}{U_g},\dfrac{gD}{U_g^{\ 2}})\ \ j(\dfrac{gD}{U_l^{\ 2}})=\ j\left(\dfrac{1}{Fr_l^{\ 2}}\right)=\Pi_{11}$

where f,g,h and j are particular individual functions.

Therefore, from the above analysis the following result is obtained:

$$Eu = C_p = f\left(Re_g,Re_l,We_l,Fr_g,Fr_l\right) \ \ \text{--------------- (2)}$$

which is the result that most engineers would predict as the likely outcome of such an analysis. That is, as the Euler Number is the ratio of the pressure forces to the inertial forces, the Reynolds Number is the ratio of inertial forces to viscous forces , the Weber Number is the ratio of the inertial forces to surface tension of liquid in contact with a particular gas and the Froude Number is the ratio of the inertial forces to gravity / buoyancy forces, equation (2) states that the two-phase flow conditions are dictated by the inertial, pressure, viscous, buoyancy and surface tension forces. However as these dimensionless groups are currently separated in equation (2), as if each phase flows completely separately, it is therefore clear that the result of the

analysis is simply telling us the important forces in the flow and not how to go about comparing the relative magnitudes of these forces in two-phase flows of various fluid combinations. Hence the way the relationships between these relevant forces are calculated is not given by the conventional single-phase dimensional analysis. However, finding an accurate way of predicting these force relationships is known to be important for a successful choice of a simulant fluid.

What form of Dimensional Groups is suitable for Comparing Test Fluids to Wet Natural Gas?

Expressions to estimate the following ratios in wet gas flow are required.

$$\text{Re} = \frac{Inertial\ Forces}{Viscous\ Forces}\ , \quad Fr = \sqrt{\frac{Inertial\ Forces}{Gravity\ Forces}}\ , \quad We = \frac{Inertial\ Forces}{Surface\ Tension\ Forces}$$

A major problem in trying to apply these definitions to two-phase flow is the fact that the current two-phase flow mathematical models are not very reliable. The relevant forces depend strongly on the flow pattern that exists and for predicting this there are only a few semi-empirical flow charts. It is therefore clear that a precise relationship between these forces for a range of two-phase flows is a difficult task.

A suitable starting point for choosing the two-phase dimensionless group expressions is given in [5]. Here Shell Expro define the "Gas Densometric Froude Number" and the "Liquid Densometric Froude Number" (i.e. the two-phase Froude Numbers) , Fr_g & Fr_l respectively, as the following:

$$Fr_g = \frac{U_{sg}}{\sqrt{gD}}\sqrt{\frac{\rho_g}{\rho_l - \rho_g}} \quad \& \quad Fr_l = \frac{U_{sl}}{\sqrt{gD}}\sqrt{\frac{\rho_l}{\rho_l - \rho_g}}$$

Here the terms U_{sg} & U_{sl} are the superficial velocities of the gas and liquid respectively. The definition of superficial velocities is the velocity obtained by dividing the volume flowrate of a single phase by the total pipe area, i.e.:

$$U_{sg} = \frac{Q_g}{A} \qquad \text{and} \qquad U_{sl} = \frac{Q_l}{A}$$

This definition appeasrs to come from the following considerations:

$$Fr = \sqrt{\frac{Inertial\ Forces}{Gravity\ Forces}}$$

For the case of a liquid drop in a gas stream the buoyancy force (F_b) is the difference between the weight of the drop and the buoyancy of the drop due to the "misplaced" gas. Therefore:

$$F_b = (\rho_l - \rho_g)gV$$

where V Volume of the liquid drop and the other symbols are as before. The inertia of a fluid is $\rho U^2 D^2$ and Shell Expro chose to use the superficial velocities to calculate the inertia of the individual phases so the gas Froude Number becomes:

$$Fr_g = \sqrt{\frac{\rho_g U_g^2 D^2}{(\rho_l - \rho_g)gV}}$$

Now as D is the pipe diameter and V is the drop volume the units cancel to a single length and for convenience in the final expression it is simpler to use the superficial velocities, as these are more often known than the actual velocities. Shell Expro therefore chose to give the "Densometric Froude Numbers" by the following expressions:

$$Fr_g = \frac{U_{sg}}{\sqrt{gD}} \sqrt{\frac{\rho_g}{\rho_l - \rho_g}} \qquad \text{and} \qquad Fr_l = \frac{U_{sl}}{\sqrt{gD}} \sqrt{\frac{\rho_l}{\rho_l - \rho_g}}$$

Shell Expro have used these expressions to form a flow pattern map (see Figure 1.5), and a wet gas correlation and hence their expressions seem a good choice to use here. As these are to be used, then for consistency the expressions for the inertial forces used in calculating the Reynolds Number and Weber Number must be:

$$\text{gas inertial force} = \rho_g U_{sg}^2 D^2 \quad \text{and} \quad \text{liquid inertial force} = \rho_l U_{sl}^2 D^2$$

Therefore, by using the superficial velocities to calculate the single phase viscous forces the following is obtained:

$$\text{gas viscous force} = \mu_g U_{sg} D \qquad \text{and} \quad \text{liquid viscous force} = \mu_l U_{sl} D$$

Hence single phase Reynolds Numbers are:

$$\text{Re}_g = \frac{\rho_g U_{sg}^2 D^2}{\mu_g U_{sg} D} = \frac{\rho_g U_{sg} D}{\mu_g} \qquad \text{and} \qquad \text{Re}_l = \frac{\rho_l U_{sl}^2 D^2}{\mu_l U_{sl} D} = \frac{\rho_l U_{sl} D}{\mu_l}$$

However, these definitions of the Reynolds Numbers are simply the Reynolds Numbers that would exist if the fluids flowed alone through the pipe (i.e. the "superficial Reynolds Numbers"). It is "wet gas flow" being investigated in this project and as the gas flowrate is greater than the liquid flowrate there may be some merit in comparing Re_g values but less for comparison of Re_l.

A major factor in the creation of shear forces is the scale of the "slip" (s), defined as the ratio of the phase velocities. It is commonly accepted that the gas phase travels faster than the liquid phase (and drags the liquid along). This is the case for both separated / annular flow and mist flow although the slip would be likely to be less for mist flow than separated or annular flow. Since in wet gas flow the liquid quantity is

small in comparison to the gas quantity the viscous forces caused by internal friction in the gas phase alone will be relevant to comparing the various simulant fluids to the natural gas. The viscous forces in the liquid phase will be small in comparison to the gas phase and are therefore less relevant. However it cannot be assumed that they are irrelevant as the liquid viscosity influences the flow pattern and hence comparing Re_l for the various condensate simulant fluids is also necessary.

It is definite that the viscous forces caused by the slip between the phases must be included in some dimensionless form as this mechanism is suspected of being important in dictating the type of flow pattern in the pipe. The most suitable expression was considered to be a modification to a particular Reynolds Number used by investigators of gas / solid flows. This is a dimensionless expression for the relative inertial force due to the greater velocity of the gas to the liquid compared to the gas viscous forces due to the "slip".

As the viscous force on the gas *relative to the liquid* = $\mu_g \left(U_g - U_l \right) D$ and the inertial force of the gas *relative to the liquid* = $\rho_g \left(U_g - U_l \right)^2 D^2$, then,

$$Re_g = \frac{relative\ inertia\ forces}{relative\ viscous\ forces} = \frac{\rho_g \left(U_g - U_l \right)^2 D^2}{\mu_g \left(U_g - U_l \right) D} = \frac{\rho_g \left(U_g - U_l \right) D}{\mu_g}$$

The final required expression needed to compare various simulant fluids is an expression that relates the two-phase flows liquid surface tension to the inertial force, i.e. a two-phase Weber Number.

As before, liquid inertial force $\rho_l U_d^2 D^2$ and the Surface Tension is defined as σD

Therefore the Weber Number is: $We = \dfrac{inertial\ forces}{surface\ tension} = \dfrac{\rho_l U_d^2 D}{\sigma}$. However it is the relative velocity between the two phases that is of importance here hence the expression for the Weber Number will be:

$$We = \frac{\rho_l \left(U_g - U_l \right)^2 D}{\sigma}$$

The dimensionless ratios considered suitable to investigate the similarity of proposed simulant fluid pairs are the following six:

a) $\quad Re_g = \dfrac{\rho_g U_{sg} D}{\mu_g}$

b) $\quad Re_l = \dfrac{\rho_l U_{sl} D}{\mu_l}$

c) $\quad Re = \dfrac{\rho_g \left(U_g - U_l \right) D}{\mu_g}$

d) $\quad Fr_g = \dfrac{U_{sg}}{\sqrt{gD}} \sqrt{\dfrac{\rho_g}{\rho_l - \rho_g}}$

e) $\quad Fr_l = \dfrac{U_{sl}}{\sqrt{gD}} \sqrt{\dfrac{\rho_l}{\rho_l - \rho_g}}$

f) $\quad We = \dfrac{\rho_l \left(U_g - U_l \right)^2 D}{\sigma}$

The *dimensionless group is actually* the ratio of the superficial liquid inertia and the *buoyancy force* of a vapour bubble in a liquid flow. It is of limited use for the case of "wet gas flow" but is included as its calculation is required in order to use the Shell two-phase Froude Number map.

A major problem in the above is that the values of the actual velocities of the phases, U_g and U_l are not known. The Taitel & Duckler model does make predictions for the superficial flow velocities for stratified flow but not for other flow patterns (i.e. annular dispersed flow, the relevant flow pattern for wet gas flows). There is no published method that gives a way of accurately predicting actual average phase velocities for various flow patterns in two-phase flow. Therefore, to attempt to determine the correct "blower" setting (i.e. the correct simulant gas flowrate) to match the dimensionless groups (c) and (f) a method of predicting the actual average phase velocities would be required. However, the following considerations of the required superficial gas velocities to match dimensionless groups (a) and (d) show that the available blower cannot give the necessary superficial gas flow velocities and, as actual gas velocities are always higher, any attempt at creating a

method for predicting the required actual average velocities would therefore in practice still not result in the matching of dimensionless groups (c) and (f).

Method of Comparison

In order to have dimensional similarity between actual and simulant flows it is necessary to match six dimensionless groups. Each group is presented as a velocity ratio of the relevant phases simulant velocity (subscript 'sim') to the actual natural gas (subscript 'ng') velocity. As will be seen this means that the left hand side of the equation containing the velocity ratio is the parameter that is controllable by the investigator as the correct values of simulant phase velocities required to match any dimensionless group. This of course is assuming that the line pressure is fixed and hence so is the gas density. (It also assumes the required gas flow velocity is obtainable). Therefore:

a)   Ideally $\left(\text{Re}_g\right)_{ng} = \left(\text{Re}_g\right)_{sim}$

i.e. $\left(\dfrac{\rho_g U_{sg} D}{\mu_g}\right)_{ng} = \left(\dfrac{\rho_g U_{sg} D}{\mu_g}\right)_{sim}$

but in reality $\left(\text{Re}_g\right)_{ng} \neq \left(\text{Re}_g\right)_{sim}$

i.e. rearranging we get $\dfrac{\left(U_{sg}\right)_{sim}}{\left(U_{sg}\right)_{ng}} = \dfrac{\left(\rho_g\right)_{ng}}{\left(\rho_g\right)_{sim}} \dfrac{\left(\mu_g\right)_{sim}}{\left(\mu_g\right)_{ng}} = \alpha(say)$

So α (i.e. the velocity ratio of the simulant flow velocity to the actual flow velocity) is the factor the actual natural gas flow velocity has to be multiplied by to create similarity between this particular dimensionless group.

Likewise the other five dimensionless groups give the following relationships:

b)
$$\frac{(U_{sl})_{sim}}{(U_{sl})_{ng}} = \frac{(\rho_l)_{ng}}{(\rho_l)_{sim}} \frac{(\mu_l)_{sim}}{(\mu_l)_{ng}} = \beta(say)$$

c)
$$\frac{(U_g - U_l)_{sim}}{(U_g - U_l)_{ng}} = \frac{(\rho_g)_{ng}}{(\rho_g)_{sim}} \frac{(\mu_g)_{sim}}{(\mu_g)_{ng}} = \lambda(say)$$

d)
$$\frac{(U_{sg})_{sim}}{(U_{sg})_{ng}} = \sqrt{\left(\frac{\rho_g}{\rho_l - \rho_g}\right)_{ng} \bigg/ \left(\frac{\rho_g}{\rho_l - \rho_g}\right)_{sim}} = \gamma(say)$$

e)
$$\frac{(U_{sl})_{sim}}{(U_{sl})_{ng}} = \sqrt{\left(\frac{\rho_l}{\rho_l - \rho_g}\right)_{ng} \bigg/ \left(\frac{\rho_l}{\rho_l - \rho_g}\right)_{sim}} = \varepsilon(say)$$

f)
$$\frac{(U_g - U_l)_{sim}}{(U_g - U_l)_{ng}} = \sqrt{\frac{(\sigma_l)_{sim}(\rho_l)_{ng}}{(\sigma_l)_{ng}(\rho_l)_{sim}}} = \xi(say)$$

The best choice of a simulant fluid pair is therefore the best combination of these six parameters $\alpha, \beta, \lambda, \gamma, \varepsilon$ and ξ. It is clear that for a perfect match of simulant fluids to natural gas /condensate the conditions of $\alpha, \beta, \lambda, \gamma, \varepsilon$ and ξ all equal to unity needs to be obtained. However, as it is clear this will not be possible in reality, engineering judgement on the which dimensionless groups are best matched is required.

Once the simulant fluids have been chosen any one dimensionless group could be matched by selecting the correct flow velocity for each phase to allow the appropriate value of $\alpha, \beta, \lambda, \gamma, \varepsilon$ or ξ to be matched. (That is assuming the test apparatus can achieve the desired flow velocities). The problem will then be which dimensionless group to set equal and which can be ignored.

The Fluids chosen for the Comparison

The first fluid combination properties required for the comparison are of course those of wet natural gas. A "typical" composition was given in Chapter 3 and the properties of this fluid at different pressures was also given along with the properties of the simulant fluids. The present analysis also includes a water / air combination to compare against the chosen simulant fluids. The relevant values of $\alpha, \beta, \lambda, \gamma, \varepsilon$ and ξ are given in the following table.

Ratios	Alpha & Lambda	Beta	Gamma	Epsilon	Zeta
Pressure					
70 Bar	1.617212122	8.92892502	1.629136	1.07858228	7.976643
60 Bar	1.623521165	8.26145877	1.5180918	1.05393064	7.303607
50 Bar	1.628767108	7.54998407	1.4343222	1.03685814	6.642921
40 Bar	1.637059681	6.79011852	1.3679645	1.02456266	5.98363
30 Bar	1.654392244	5.94799699	1.3106051	1.01535634	5.301612

Table A1. The Comparison of the Natural Gas and Condensate to Air and Water.

Ratios	Alpha & Lambda	Beta	Gamma	Epsilon	Zeta
Pressure					
70 Bar	1.619494561	13.9376428	1.6403947	1.07931153	3.130557
60 Bar	1.624192414	12.9069545	1.5273072	1.05446937	2.868902
50 Bar	1.627980619	11.805748	1.4419042	1.03724449	2.611668
40 Bar	1.634985903	10.6269669	1.3741988	1.02482744	2.35455
30 Bar	1.651196393	9.31732602	1.3156922	1.01552534	2.088045

Table A2. The Comparison of the Natural Gas and Condensate to Nitrogen and Eversol D80.

It is clear that for both simulant fluid combinations that beta (β) is by far the furthest from unity for both cases. Fortunately this value is estimated to be the least significant to accurate modelling of the flow and will therefore be ignored. For alpha (α) and lambda (λ), gamma (γ) and epsilon (ε) both fluid combinations give very similar results. However it is the value of zeta (ξ) that shows the greatest difference. Neither combination has a good value of zeta but the nitrogen and Eversol D80 is considerably better than air and water. This result was expected as the surface tension of natural gas condensate is extremely low compared to other liquids.

As the surface tension is assumed to have a considerable influence on the flow pattern a reduction of the value of zeta is desired. As no lighter hydrocarbon liquid can be used due to safety reasons the only way of reducing the surface tension of eversol D80 is to use some additive to the liquid.

On the advice of the NEL Physical Properties Department tests on the effects of the particular additives Separol, Aquanox and Magnatreat at 5, 50 & 500 ppm concentrations at atmospheric conditions on the surface tension of the Eversol D80 substitute was carried out. It was found that none of these additives reduced the surface tension more than a few percent and as it was the case that the additive would degrade over time this avenue of research was abandoned.

In a search of the available literature on tests carried out on meters used in wet natural gas no mention is ever made about the reason why particular fluids were used. Often air water or nitrogen/oil is used and hence the present author is confident that even though the liquid surface tension is higher than would ideally be required the choice of substitute kerosene (i.e. Eversol D80) and nitrogen as the simulant fluids is still better than any tests previously carried out.

The ISA Controls Ltd. Venturi Meter was tested with dry gas flows at 20 Bar and then at 60 Bar before the wet gas tests commenced. Tables A2.1 and A2.2 present the resulting data.

Point No	Barametric Pressure	Absolute Pressure	Gas Density	Gas Volume Flowrate	Gas Mass Flowrate	Gas Reynolds No.	Test Point Temp.	ΔP_1	ΔP_2
	N m³	N m²	kg/m³	m³/hr	kg/s		K	N m²	N m²
1	98568	2091601	24 371	602 648	4 076	2093024	290.467	14702.0	1679.2
2	98614	2085787	24 332	686.941	4 639	2384111	290.136	18957.7	2226.4
3	98641	2084260	24 321	711 306	4 801	2467919	290.069	20306.0	2322.0
4	98659	2084211	24 318	712 424	4 807	2470993	290.086	20321.1	2268.3
5	98679	2081864	24 277	645 845	4 351	2235363	290 247	16716.1	1825.9
6	98684	2082253	24 279	588 201	3 962	2035647	290.270	13924 0	1517.5
7	98695	2082733	24 281	503 135	3 389	1741051	290 311	10191.3	1118 6
8	98698	2082681	24 282	456 047	3 072	1578109	290.301	8326.9	932.3
9	98697	2081894	24 277	456 374	3 074	1579342	290 246	8322 8	928.6
10	98701	2080535	24 267	503 135	3 387	1740525	290 186	10185 3	1129.4
11	98706	2076490	24 242	739 583	4 976	2558918	289.928	21994.4	2432 1
12	98699	2075912	24 248	751 787	5 060	2602784	289 784	22613 0	2542 1
13	98697	2074696	24 234	803 114	5 402	2779158	289 785	25875 0	2862 3
14	98693	2073895	24 201	905 370	6 083	3127331	290.044	33292.3	3606.7
15	98685	2074830	24 165	1004 85	6 743	3461631	290 585	40792 6	4392.4
16	98685	2081825	24 215	905 277	6 086	3121661	290 938	33260 8	3548 9
17	97607	2056022	24 007	710 561	4 734	2435392	289 871	19945.0	2174 7
18	97661	2053865	23 977	801 857	5 337	2744891	289 922	25518 6	2759 5
19	97700	2054544	23 967	835 992	5 561	2859016	290 132	27956 5	2999 6
20	97743	2056613	23 973	820 485	5 460	2805108	290 336	26804 6	2888 9
21	97797	2056148	23 943	900 994	5 989	3074663	290 624	32579 0	3471.3
22	97840	2057582	23 925	949 922	6 309	3236095	291 023	36068 1	3853 5
23	97882	2059684	23 904	1000 19	6 638	3399926	291 555	39945 5	4268 9
24	97822	2092455	24 463	687 546	4 670	2403668	289 551	19125 1	2354.3
25	97827	2091324	24 454	712 191	4 836	2489200	289 494	20516 4	2460 0
26	97831	2090201	24 439	752 439	5 106	2628147	289 514	22884 1	2759 5
27	97831	2089670	24 423	801 065	5 433	2795498	289 625	25991 4	3148 9
28	97834	2087860	24 386	902 018	6 109	3141860	289 810	33419 3	3953 1
29	97832	2087820	24 346	1001 45	6 772	3479436	290 249	40925 8	4738 0

Table A2.1. The 20 Bar Dry Gas Test Results.

Point No.	Barametric Pressure	Absolute Pressure	Gas Density	Gas Volume Flowrate	Gas Mass Flowrate	Gas Reynolds No.	Test Point Temp.	ΔP_1	ΔP_2
	N/m^2	N/m^2	kg/m^3	m^3/hr	kg/s		K	N/m^2	N/m^2
1	97910	5985728	70.002	349.771	6.798	3341398	290.451	13897.0	1472.6
2	97920	5980145	69.949	398.927	7.746	3808138	290.399	18169.5	1999.4
3	97910	5977576	69.915	452.131	8.773	4313510	290.407	23269.8	2854.0
4	97915	5977156	69.887	501.597	9.729	4782787	290.472	28815.2	3381.8
5	97930	5978394	69.855	552.453	10.711	5263393	290.621	35131.0	3856.9
6	97970	5982859	69.825	602.415	11.674	5733117	290.897	41714.7	4409.4
7	98010	5990066	69.795	651.996	12.630	6196687	291.283	48503.0	5042.9
8	99900	5998434	69.822	651.716	12.629	6192246	291.541	48481.0	5021.8
9	96000	5997904	69.778	651.344	12.615	6183252	291.674	48445.5	5014.5
10	98040	6005661	69.765	701.243	13.579	6650339	292.019	56024.6	5803.9
11	98063	6017332	69.725	750.529	14.526	7103693	292.621	64206.5	6682.2
12	98081	6033639	69.683	800.133	15.478	7554348	293.428	72898.9	7624.2
13	97581	5989186	70.240	452.038	8.815	4339816	289.729	23367.1	2489.8
14	97589	5983990	70.201	499.778	9.739	4795983	289.634	28677.5	3066.0
15	97591	5982598	70.194	502.063	9.782	4817495	289.600	28926.2	3087.6
16	97590	5984806	70.155	551.986	10.748	5290745	289.811	35226.6	3691.4
17	97598	5994941	70.073	649.759	12.637	6210620	290.480	48436.2	5043.3
18	97650	6012341	70.026	700.731	13.619	6679193	291.353	56179.5	5852.0
19	97596	6028326	69 980	750.390	14.576	7134515	292.154	64400.1	6717.2
20	97593	6047636	69 930	801.810	15.565	7600695	293.114	73492.9	7706.4
21	97606	6073571	69 873	852.570	16.538	8050902	294.383	83722.7	8764.1
22	97616	6092515	69 820	900.202	17.450	8475946	295.327	94220.9	10344.0
23	97624	6128982	69 763	951.598	18.435	8917234	297.029	105893	12511.3
24	97631	6157810	69.704	997.912	19.317	9312444	298.433	116647	14035.1

Table A2. The 60 Bar Dry Gas Test Results.

Appendix Three

The ISA Controls Ltd. Venturi Meter was tested in wet gas flows at 20 Bar using an open pipe injector and then a Nozzle Injector.

Table A3.1 presents the open pipe injector 20 Bar test data.

Point No.	Liquid Density	Liquid Mass Flowrate	Liquid Volume Flowrate	Liquid Volume Fraction	Gas Volume Flowrate	Gas Mass Flowrate	Gas Reynolds Number	Test Point Temperature	Test Point Pressure	Test Point Gas Density	ΔP_{tp}	ΔP_2
	kg/m³	kg/s	m³/hr		m³/hr	kg/s		K	N/m²	kg/m³	N/m²	N/m²
1	802.607	0.051	0.229	0.0568	402.611	2.764	1.42E+06	290.96	2.03E+01	24.707	7082.6	32416
2	802.544	0.051	0.227	0.0563	402.471	2.763	1.42E+06	290.92	2.03E+01	24.704	7082.5	32360
3	802.43	0.050	0.225	0.0374	602.694	4.135	2.12E+06	291.24	2.03E+01	24.704	15788.9	60078
4	802.393	0.050	0.225	0.0373	601.995	4.130	2.12E+06	291.25	2.03E+01	24.702	15772.0	60250
5	802.368	0.050	0.223	0.0279	801.437	5.495	2.81E+06	291.80	2.03E+01	24.688	27486.3	72266
6	802.345	0.050	0.225	0.0280	801.298	5.493	2.81E+06	292.12	2.03E+01	24.683	27485.2	72476
7	802.31	0.050	0.223	0.0222	1003.31	6.878	3.50E+06	293.32	2.04E+01	24.671	43363.9	90161
8	802.305	0.050	0.222	0.0221	1004.89	6.888	3.51E+06	294.44	2.04E+01	24.667	43459.5	90374
9	799.498	0.641	2.887	0.7181	399.207	2.753	1.40E+06	294.44	2.04E+01	24.550	8444.9	56434
10	801.084	1.217	5.469	1.3492	399.906	2.765	1.40E+06	295.17	2.05E+01	24.550	9559.5	62841
11	802.051	1.778	7.980	1.9540	400.419	2.769	1.40E+06	295.19	2.05E+01	24.564	10504.5	67079
12	802.434	2.442	10.956	2.6590	401.072	2.775	1.41E+06	295.29	2.05E+01	24.576	11580.6	71916
13	802.827	3.654	16.387	2.6366	605.118	4.198	2.13E+06	295.20	2.06E+01	24.713	26626.1	182048
14	802.733	2.728	12.234	1.9825	604.838	4.186	2.12E+06	295.05	2.06E+01	24.689	23990.9	161212
15	802.519	1.894	8.494	1.3845	605.024	4.181	2.12E+06	294.95	2.05E+01	24.666	21876.1	147972
16	801.6	0.958	4.301	0.7059	604.978	4.171	2.12E+06	294.41	2.05E+01	24.650	19390.0	132744
17	802.181	1.269	5.694	0.7032	803.999	5.560	2.82E+06	294.71	2.06E+01	24.754	34689.6	242700
18	802.275	1.282	5.754	0.7110	803.487	5.553	2.82E+06	294.89	2.06E+01	24.753	34659.1	242864
19	802.988	2.417	10.836	1.3296	804.092	5.572	2.82E+06	295.30	2.07E+01	24.804	39017.0	282016
20	803.204	3.583	16.060	1.9634	801.903	5.567	2.82E+06	295.49	2.07E+01	24.856	43403.3	320985
21	803.166	3.645	16.338	1.9965	801.996	5.566	2.82E+06	295.63	2.07E+01	24.859	43678.1	322958
22	802.875	3.060	13.719	1.5118	893.777	6.211	3.14E+06	295.94	2.08E+01	24.899	50409.7	375991
23	802.557	1.551	6.957	0.7289	947.501	6.565	3.32E+06	295.94	2.08E+01	24.859	49281.6	344989
24	802.368	1.553	6.968	0.7310	946.245	6.557	3.32E+06	296.15	2.08E+01	24.855	49232.3	345232
25	800.47	0.625	2.812	0.6960	401.305	2.759	1.41E+06	293.58	2.03E+01	24.509	8459.6	56539
26	802.279	1.812	8.132	1.9885	400.839	2.767	1.40E+06	294.81	2.04E+01	24.507	10559.6	67353
27	802.456	1.811	8.125	1.3284	603.487	4.167	2.12E+06	294.27	2.04E+01	24.604	21572.8	145937
28	802.94	2.446	10.969	1.3508	801.065	5.550	2.82E+06	294.61	2.06E+01	24.746	38969.2	282472
29	803.132	3.052	13.680	1.5097	892.459	6.192	3.14E+06	295.32	2.07E+01	24.842	50255.0	375537

Table A3.1. The Open Pipe Injector 20 Bar Wet Gas Test Data.

Point No.	Liquid Density	Liquid Mass Flowrate	Liquid Volume Flowrate	Liquid Volume Fraction	Gas Volume Flowrate	Gas Mass Flowrate	Gas Reynolds Number	Test Point Temperature	Test Point Pressure	Test Point Gas Density	ΔP_{1p}	ΔP_2
	kg/m³	kg/s	m³/hr		m³/hr	kg/s		K	N/m²	kg/m³	N/m²	N/m²
30	802.788	1.861	8.346	0.8885	931.022	6.440	3.26E+06	295.68	2.07E+01	24.809	489429	351324
31	802.393	1.212	5.438	0.5604	964.864	6.662	3.37E+06	295.81	2.07E+01	24.786	491597	328966
32	801.815	0.676	3.035	0.3016	1003.4	6.910	3.50E+06	295.78	2.07E+01	24.741	495274	273725
33	800.355	0.402	1.809	0.1728	1044.68	7.177	3.63E+06	295.97	2.06E+01	24.683	510439	214096
34	799.352	0.565	2.545	0.2493	1018.2	7.011	3.54E+06	296.36	2.07E+01	24.709	500911	248623
35	799.908	0.800	3.603	0.3628	989.255	6.828	3.45E+06	296.61	2.07E+01	24.746	492656	294893
36	802.906	0.321	1.438	0.3555	403.031	2.768	1.42E+06	292.08	2.03E+01	24.659	78158	50406
37	802.877	0.319	1.430	0.2371	601.949	4.136	2.11E+06	292.05	2.03E+01	24.696	170548	108493
38	802.801	0.318	1.425	0.1765	805.722	5.537	2.83E+06	292.76	2.04E+01	24.719	302456	161638
39	802.731	0.317	1.421	0.1416	1001.96	6.887	3.51E+06	293.64	2.05E+01	24.718	462043	183471
40	802.486	0.155	0.694	0.0681	1019.09	6.985	3.55E+06	294.76	2.05E+01	24.666	456670	118987
41	802.091	0.154	0.690	0.0860	801.344	5.499	2.79E+06	294.33	2.05E+01	24.701	287032	115341
42	801.731	0.153	0.689	0.1146	600.318	4.125	2.10E+06	293.67	2.05E+01	24.726	162515	86819
43	801.392	0.153	0.687	0.1710	400.792	2.758	1.41E+06	293.15	2.05E+01	24.740	72892	43050

Table A3.2 presents the nozzle injector 20 Bar test data.

Point No.	Liquid Density (kg/m³)	Liquid Mass Flowrate (kg/s)	Liquid Volume Flowrate (m³/hr)	Liquid Volume Fraction	Gas Volume Flowrate (m³/hr)	Gas Mass Flowrate (kg/s)	Gas Reynolds Number	Test Point Temperature (K)	Test Point Pressure (N/m²)	Test Point Gas Density (kg/m³)	ΔP_{tp} (N/m²)	ΔP_2 (N/m²)
44	804.18	0.053	0.236	0.0589	401.025	2.689	1.38E+06	290.35	1.97E+01	24.154	6794.4	3178.3
45	804.107	0.052	0.234	0.0390	600.364	4.026	2.07E+06	290.31	1.97E+01	24.162	15319.5	6100.9
46	804.037	0.052	0.233	0.0290	801.624	5.372	2.75E+06	290.71	1.97E+01	24.145	26871.7	7601.3
47	803.97	0.052	0.233	0.0232	1001.59	6.708	3.43E+06	291.64	1.98E+01	24.128	42221.9	9124.8
48	803.44	0.154	0.689	0.0688	1000.05	6.714	3.42E+06	293.02	1.99E+01	24.173	43243.9	12616.9
49	802.953	0.153	0.689	0.0860	798.224	5.364	2.73E+06	292.97	2.00E+01	24.199	27888.9	11754.6
50	802.472	0.153	0.687	0.1141	599.852	4.035	2.06E+06	292.59	1.99E+01	24.216	15887.2	8777.3
51	802.004	0.152	0.683	0.1705	399.999	2.694	1.38E+06	292.31	1.99E+01	24.227	7126.1	4212.4
52	800.948	0.319	1.434	0.3580	399.113	2.698	1.38E+06	292.64	2.00E+01	24.229	7534.3	4867.6
53	800.564	0.315	1.418	0.2353	601.203	4.065	2.07E+06	292.34	2.00E+01	24.276	16701.4	10615.4
54	800.187	0.316	1.420	0.1770	800.739	5.417	2.76E+06	292.90	2.00E+01	24.308	29454.3	16522.6
55	799.896	0.316	1.424	0.1421	1001.03	6.771	3.44E+06	293.78	2.01E+01	24.314	45592.2	18773.6
56	802.565	1.226	5.497	0.3512	401.352	2.714	1.38E+06	293.85	1.99E+01	24.092	9463.1	6234.0
57	802.564	0.640	2.869	0.7109	400.652	2.704	1.38E+06	292.96	1.99E+01	24.125	8299.0	5543.7
58	802.425	1.773	7.956	0.9480	400.466	2.712	1.38E+06	294.56	2.00E+01	24.071	10382.3	6654.1
59	802.374	2.438	10.941	2.6542	401.258	2.719	1.38E+06	295.21	2.00E+01	24.056	11521.6	7155.0
60	802.195	3.629	16.284	2.6340	601.949	4.095	2.08E+06	295.45	2.01E+01	24.164	25936.0	17515.7
61	802.28	2.726	12.234	1.9978	600.131	4.070	2.06E+06	295.28	2.01E+01	24.152	23355.5	15662.2
62	801.959	1.885	8.460	1.3898	600.271	4.069	2.06E+06	295.04	2.01E+01	24.159	21246.1	14359.6
63	801.375	0.956	4.293	0.7082	601.949	4.075	2.07E+06	294.33	2.01E+01	24.200	18759.4	12956.5
64	801.705	1.275	5.726	0.7091	801.763	5.448	2.78E+06	293.47	2.01E+01	24.283	34082.6	24028.8
65	801.861	2.420	10.866	1.3384	800.972	5.447	2.76E+06	295.21	2.02E+01	24.275	38438.5	27872.0
66	801.949	3.645	16.362	2.0051	799.668	5.443	2.75E+06	296.17	2.03E+01	24.304	43205.3	32068.8
67	801.997	3.035	13.624	1.4939	898.34	6.114	3.09E+06	296.14	2.03E+01	24.360	50430.6	37631.2
68	802.075	1.543	6.925	0.7252	947.967	6.428	3.25E+06	295.90	2.03E+01	24.329	48344.0	34323.6
69	801.908	0.631	2.831	0.6962	403.823	2.718	1.38E+06	295.07	2.00E+01	24.114	8347.1	5587.8
70	801.229	1.802	8.097	1.9777	401.305	2.720	1.38E+06	296.41	2.01E+01	24.078	10485.7	6722.8
71	800.587	1.797	8.080	1.3245	601.949	4.091	2.07E+06	296.14	2.01E+01	24.177	21264.0	14432.0
72	800.639	2.418	10.873	1.3334	804.558	5.483	2.77E+06	296.48	2.03E+01	24.291	38792.8	28152.4
73	800.988	2.965	13.327	1.4610	898.852	6.130	3.10E+06	296.95	2.04E+01	24.366	50333.6	37528.4
74	801.155	1.862	8.365	0.8893	932.279	6.337	3.20E+06	296.79	2.04E+01	24.347	48407.7	35099.3
75	801.137	1.202	5.400	0.5583	961.792	6.525	3.30E+06	296.38	2.03E+01	24.337	48129.1	32844.6

Point No.	Liquid Density	Liquid Mass Flowrate	Liquid Volume Flowrate	Liquid Volume Fraction	Gas Volume Flowrate	Gas Mass Flowrate	Gas Reynolds Number	Test Point Temperature	Test Point Pressure	Test Point Gas Density	ΔP_{tp}	ΔP_2
	kg/m³	kg/s	m³/hr		m³/hr	kg/s		K	N/m²	kg/m³	N/m²	N/m²
76	801.14	0.677	3.041	0.3039	997.679	6.749	3.42E+06	296.06	2.03E+01	24.306	483306.6	276191
77	800.843	0.414	1.861	0.1794	1035.84	6.996	3.54E+06	295.98	2.03E+01	24.279	496217	219401
78	799.959	0.562	2.530	0.2493	1012.2	6.855	3.47E+06	296.44	2.03E+01	24.325	488628	250712
79	799.687	0.797	3.589	0.3627	986.089	6.689	3.38E+06	296.81	2.04E+01	24.342	481363	295101

Table A3.2. The Nozzle Injector 20 Bar Wet Gas Test Data.

The ISA Controls Ltd. Venturi Meter was tested in wet gas flows at 40 Bar using an open pipe injector and then a Nozzle Injector. Table A3.3 presents the open pipe injector 40 Bar test data.

Point No.	Liquid Density	Liquid Mass Flowrate	Liquid Volume Flowrate	Liquid Volume Fraction	Gas Volume Flowrate	Gas Mass Flowrate	Gas Reynolds Number	Test Point Temperature	Test Point Pressure	Test Point Gas Density	ΔP_{tp}	ΔP_2
	kg/m³	kg/s	m³/hr		m³/hr	kg/s		K	N/m²	kg/m³	N/m²	N/m²
80	801.761	0.038	0.171	0.0424	404.15	5.126	2.53E+06	298.92	3.94E+01	45.744	12768.3	Not Read
81	802.604	0.029	0.129	0.0320	402.284	5.284	2.65E+06	291.75	3.97E+01	47.310	13073.3	Not Read
82	802.691	0.028	0.127	0.0210	601.949	7.886	3.95E+06	292.36	3.97E+01	47.201	29081.2	Not Read
83	802.724	0.028	0.124	0.0154	801.996	10.491	5.24E+06	293.58	3.99E+01	47.117	51146.6	Not Read
84	802.716	0.028	0.125	0.0125	1001.4	13.083	6.50E+06	295.57	4.01E+01	47.037	80532.3	Not Read
85	802.244	0.159	0.714	0.0713	1001.08	13.082	6.47E+06	297.10	4.03E+01	47.031	81597.9	Not Read
86	802.028	0.158	0.711	0.0887	801.065	10.476	5.19E+06	296.44	4.03E+01	47.080	52003.4	Not Read
87	801.819	0.159	0.713	0.1181	602.648	7.895	3.92E+06	295.32	4.02E+01	47.167	30219.7	Not Read
88	801.687	0.159	0.713	0.1778	400.606	5.259	2.62E+06	294.33	4.01E+01	47.241	13482.5	Not Read
89	801.509	0.320	1.437	0.3578	400.046	5.259	2.62E+06	293.90	4.00E+01	47.259	13924.7	Not Read
90	801.532	0.317	1.425	0.2372	599.525	7.870	3.92E+06	294.11	4.00E+01	47.234	30995.5	Not Read
91	801.598	0.316	1.420	0.1772	799.854	10.481	5.21E+06	295.00	4.01E+01	47.154	53057.8	Not Read
92	801.618	0.315	1.417	0.1415	999.68	13.083	6.48E+06	296.41	4.03E+01	47.091	82658.7	Not Read
93	802.313	0.033	0.149	0.0372	400.326	5.144	2.58E+06	292.30	3.89E+01	46.287	13001.1	4650.6
94	802.328	0.033	0.147	0.0242	604.465	7.916	3.96E+06	293.06	3.98E+01	47.185	29334.9	6294.5
95	802.335	0.032	0.145	0.0181	801.95	10.487	5.23E+06	294.14	3.99E+01	47.103	51146.9	8925.5
96	802.33	0.032	0.143	0.0143	1001.73	13.085	6.49E+06	295.91	4.01E+01	47.033	80643.8	12487.0
97	801.822	0.160	0.718	0.0716	1001.82	13.091	6.47E+06	297.62	4.04E+01	47.035	81766	13657.4
98	801.508	0.159	0.714	0.0890	801.903	10.493	5.20E+06	296.67	4.03E+01	47.106	52188.1	10564.6
99	801.246	0.159	0.714	0.1187	600.551	7.874	3.91E+06	295.64	4.02E+01	47.202	30092	10430.9
100	801.072	0.159	0.713	0.1775	400.699	5.265	2.62E+06	294.65	4.02E+01	47.277	13504.3	6584.8
101	800.899	0.318	1.430	0.3632	392.398	5.162	2.57E+06	294.23	4.01E+01	47.284	13418.1	7314.5
102	800.996	0.315	1.415	0.2339	603.487	7.926	3.95E+06	294.33	4.01E+01	47.253	31352.7	13465.3
103	801.227	0.315	1.415	0.1763	801.111	10.496	5.21E+06	295.51	4.02E+01	47.146	53274.5	13866.8
104	801.307	0.314	1.411	0.1409	1000.29	13.089	6.48E+06	296.91	4.03E+01	47.085	82821.6	15355.0
105	802.083	0.785	3.524	0.8742	399.58	5.263	2.63E+06	293.18	3.99E+01	47.218	150222	8642.4
106	802.175	1.272	5.709	1.4069	400.093	5.270	2.63E+06	294.15	4.00E+01	47.144	160626	9076.2
107	802.245	2.429	10.899	2.6442	401.305	5.291	2.63E+06	295.01	4.00E+01	47.069	184275	9934.4
108	802.406	2.421	10.864	1.3341	803.44	10.341	5.14E+06	295.91	3.94E+01	46.197	663451	38420.3
109	802.14	3.043	13.655	1.3645	987.113	13.011	6.43E+06	297.61	4.07E+01	47.402	101996	54160.4
110	803.403	3.677	16.476	3.9280	402.984	5.304	2.65E+06	293.93	3.98E+01	46.967	210156	11026.1

Table A3.3. The Open Pipe Injector 40 Bar Wet Gas Test Data.

Point No.	Liquid Density	Liquid Mass Flowrate	Liquid Volume Flowrate	Liquid Volume Fraction	Gas Volume Flowrate	Gas Mass Flowrate	Gas Reynolds Number	Test Point Temperature	Test Point Pressure	Test Point Gas Density	ΔP_{ip}	ΔP_2
	kg/m³	kg/s	m³/hr		m³/hr	kg/s		K	N/m²	kg/m³	N/m²	N/m²
111	803.682	3.649	16.346	2.6351	603.953	7.937	3.96E+06	294.16	3.99E+01	47.101	43002	26076.1
112	803.622	1.852	8.297	1.3636	600.178	7.871	3.92E+06	294.09	3.99E+01	47.082	36479.9	21321.5
113	803.24	1.830	8.202	0.8132	1000.38	13.132	6.51E+06	296.21	4.04E+01	47.230	96027.1	42889.1
114	802.252	2.547	11.429	1.1293	1000.56	13.149	6.49E+06	297.98	4.07E+01	47.302	101227	50603.4
115	801.994	0.798	3.582	0.3568	1000.24	13.078	6.45E+06	298.19	4.05E+01	47.068	87025.3	26001.4
116	801.572	0.801	3.597	0.4482	798.969	10.472	5.18E+06	296.92	4.04E+01	47.146	57136.3	24348.2
117	801.45	0.803	3.606	0.5970	600.411	7.877	3.91E+06	295.83	4.02E+01	47.150	33023.6	17393.2
118	801.469	0.809	3.634	0.8979	401.119	5.271	2.62E+06	295.00	4.01E+01	47.135	15116	8645.7
119	801.539	0.810	3.636	0.9019	399.533	5.254	2.62E+06	294.53	4.00E+01	47.155	15071.7	8650.7
120	801.562	4.878	21.907	5.1752	401.398	5.313	2.64E+06	295.15	4.00E+01	46.975	23946.6	12426.6
121	802.045	4.823	21.646	2.6041	809.588	10.674	5.30E+06	295.90	4.04E+01	47.324	79603.4	49978.6
122	801.389	7.224	32.453	3.8883	802.183	10.594	5.24E+06	296.84	4.06E+01	47.418	90211.9	57633.3
123	800.36	7.146	32.142	5.0556	603.626	7.978	3.94E+06	297.52	4.05E+01	47.186	56246.7	35093.0
124	785.07	5.402	24.771	3.9654	599.898	7.919	3.92E+06	297.08	4.04E+01	47.152	49346.8	30642.5

Table A3.4 presents the nozzle injector 40 Bar test data.

Point No.	Liquid Density	Liquid Mass Flowrate	Liquid Volume Flowrate	Liquid Volume Fraction	Gas Volume Flowrate	Gas Mass Flowrate	Gas Reynolds Number	Test Point Temperature	Test Point Pressure	Test Point Gas Density	ΔP_tp	ΔP_2
	kg/m³	kg/s	m³/hr		m³/hr	kg/s		K	N/m²	kg/m³	N/m²	N/m²
125	802.942	0.025	0.112	0.0278	402.564	5.295	2.65E+06	292.02	3.98E+01	47.404	13105.8	4571.3
126	802.939	0.027	0.123	0.0204	601.389	7.895	3.95E+06	292.53	3.98E+01	47.319	29121.8	6326.3
127	802.928	0.027	0.122	0.0152	801.391	10.507	5.25E+06	293.49	3.99E+01	47.251	51309.2	9041.1
128	802.915	0.028	0.124	0.0123	1003.264	13.140	6.53E+06	295.34	4.02E+01	47.181	81231.4	12605.7
129	802.663	0.158	0.708	0.0708	999.541	13.099	6.49E+06	296.73	4.04E+01	47.198	817037	13816.0
130	802.156	0.156	0.702	0.0878	798.550	10.479	5.19E+06	296.29	4.04E+01	47.267	519034	10907.7
131	801.686	0.156	0.699	0.1163	600.271	7.894	3.92E+06	295.39	4.03E+01	47.373	301892	10801.0
132	801.334	0.155	0.696	0.1731	401.585	5.294	2.64E+06	294.52	4.03E+01	47.458	13617	6613.0
133	800.871	C.317	1.424	0.3543	400.559	5.287	2.63E+06	294.21	4.02E+01	47.466	66130	7524.2
134	800.965	0.316	1.419	0.2357	600.737	7.917	3.94E+06	294.33	4.02E+01	47.435	140165	13692.0
135	801.108	0.315	1.414	0.1765	799.668	10.518	5.23E+06	295.26	4.03E+01	47.352	312953	14861.3
136	801.183	0.313	1.408	0.1404	1001.170	13.149	6.51E+06	296.74	4.05E+01	47.280	148613	15875.1
137	801.314	0.793	3.563	0.8823	400.279	5.289	2.63E+06	294.83	4.03E+01	47.398	15875.1	8726.7
138	801.378	1.265	5.683	1.3920	402.564	5.324	2.65E+06	295.19	4.03E+01	47.345	8726.7	9187.0
139	801.526	2.419	10.866	2.6425	400.326	5.299	2.63E+06	296.00	4.03E+01	47.254	9890.6	9890.6
140	801.805	2.379	10.680	1.3188	799.155	10.570	5.24E+06	296.27	4.06E+01	47.483	37904.2	37904.2
141	801.586	3.008	13.507	1.3396	994.785	13.157	6.49E+06	298.27	4.10E+01	47.599	545227	54522.7
142	800.773	3.672	16.508	3.9582	400.559	5.296	2.61E+06	298.04	4.06E+01	47.232	208685	10520.8
143	800.811	3.644	16.381	2.6631	598.733	7.930	3.92E+06	297.55	4.07E+01	47.385	428586	25700.5
144	801.031	1.840	8.269	1.3581	600.597	7.941	3.93E+06	296.71	4.06E+01	47.397	214212	21421.2
145	800.897	1.820	8.179	0.8112	1000.099	13.221	6.52E+06	298.30	4.09E+01	47.524	965582	42902.4
146	800.5	2.535	11.399	1.1265	1000.472	13.225	6.50E+06	299.84	4.12E+01	47.569	101563	50320.7
147	803.318	0.794	3.558	0.3540	1001.542	13.144	6.53E+06	295.18	4.02E+01	47.224	875222	26328.9
148	802.927	0.796	3.567	0.4435	800.692	10.515	5.23E+06	295.25	4.02E+01	47.253	572951	24789.5
149	802.64	0.799	3.584	0.5949	598.873	7.871	3.92E+06	294.49	4.01E+01	47.252	329323	17580.1
150	802.512	0.804	3.606	0.8919	400.745	5.276	2.63E+06	293.90	4.00E+01	47.238	15110	8683.9
151	803.273	4.958	22.220	5.2713	399.300	5.282	2.63E+06	294.60	3.99E+01	47.069	234579	11589.4
152	803.524	4.692	21.021	2.5305	809.681	10.702	5.32E+06	294.95	4.03E+01	47.446	79321	49641.5
153	802.14	7.208	32.349	3.8907	799.109	10.588	5.23E+06	297.31	4.08E+01	47.531	90159.6	57536.7
154	800.816	7.092	31.883	5.0354	601.296	7.972	3.93E+06	298.47	4.07E+01	47.299	552687	34206.0
155	800.897	5.453	24.511	3.9137	601.762	7.977	3.94E+06	297.72	4.06E+01	47.291	49430	30303.7
156	799.52	9.136	41.135	4.8632	804.698	10.747	5.27E+06	300.34	4.13E+01	47.633	103534	65887.8

Point No.	Liquid Density	Liquid Mass Flowrate	Liquid Volume Flowrate	Liquid Volume Fraction	Gas Volume Flowrate	Gas Mass Flowrate	Gas Reynolds Number	Test Point Temperature	Test Point Pressure	Test Point Gas Density	ΔP_{tp}	ΔP_2
	kg/m³	kg/s	m³/hr		m³/hr	kg/s		K	N/m²	kg/m³	N/m²	N/m²
157	799.885	5.966	26.850	2.7845	937.446	12.444	6.11E+06	300.19	4.13E+01	47.666	111647	68527.1
158	799.722	4.577	20.604	2.0995	960.768	12.723	6.24E+06	300.50	4.13E+01	47.609	107319	63292.0
159	798.358	9.229	41.616	4.3587	913.161	12.167	5.93E+06	302.73	4.18E+01	47.789	128208	79975.6

Table A3.4. The Nozzle Injector 40 Bar Wet Gas Test Data.

231

The ISA Controls Ltd. Venturi Meter was tested in wet gas flows at 60 Bar using an open pipe injector and then a Nozzle Injector.

Table A3.5 presents the open pipe 60 Bar test data.

Point No.	Liquid Density	Liquid Mass Flowrate	Liquid Volume Flowrate	Liquid Volume Fraction	Gas Volume Flowrate	Gas Mass Flowrate	Gas Reynolds Number	Test Point Temperature	Test Point Pressure	Test Point Gas Density	ΔP_{tp}	ΔP_2
	kg/m³	kg/s	m³/hr		m³/hr	kg/s		K	N/m²	kg/m³	N/m²	N/m²
160	804.062	0.029	0.130	0.0325	400.606	7.830	3.84E+06	290.35	5.93E+01	70.431	190721.1	4959.23
161	804.087	0.029	0.129	0.0215	600.644	11.713	5.74E+06	291.25	5.94E+01	70.276	427275	7401.46
162	804.094	0.029	0.132	0.0164	802.043	15.618	7.62E+06	292.65	5.96E+01	70.159	75528	111199
163	804.085	0.029	0.128	0.0128	999.541	19.437	9.44E+06	294.80	6.00E+01	70.040	117896	151551
164	804.014	0.158	0.708	0.0707	1000.24	19.450	9.41E+06	296.43	6.04E+01	70.023	119111	162792
165	803.646	0.158	0.707	0.0884	799.528	15.568	7.54E+06	295.68	6.03E+01	70.131	758476	120889
166	803.332	0.157	0.705	0.1175	599.619	11.694	5.68E+06	294.46	6.01E+01	70.244	432912	886183
167	803.135	0.158	0.707	0.1761	400.885	7.837	3.82E+06	293.16	5.99E+01	70.397	198191	7533.56
168	803.015	0.320	1.433	0.3564	400.699	7.841	3.83E+06	292.58	5.98E+01	70.424	202847	8628.5
169	803.082	0.318	1.426	0.2370	600.318	11.724	5.72E+06	292.99	5.98E+01	70.319	443291	11683.2
170	803.164	0.317	1.423	0.1771	802.136	15.641	7.61E+06	294.07	6.00E+01	70.212	77417	13550.3
171	803.158	0.316	1.417	0.1414	1000.56	19.481	9.43E+06	296.11	6.00E+01	70.102	120643	17327.5
172	802.996	0.796	3.569	0.8855	399.44	7.827	3.81E+06	293.22	6.00E+01	70.404	213888.2	102638
173	803.082	0.790	3.541	0.5858	600.923	11.755	5.72E+06	293.58	6.00E+01	70.364	473767	185673
174	803.153	0.790	3.541	0.4389	803.114	15.679	7.61E+06	294.72	6.02E+01	70.259	807981	197327
175	803.072	0.786	3.522	0.3513	999.122	19.476	9.42E+06	296.53	6.05E+01	70.171	124260	220743
176	801.781	4.472	20.080	1.9668	1000.84	19.592	9.40E+06	299.40	6.16E+01	70.568	154345	655807
177	800.804	3.676	16.525	1.6265	999.448	19.556	9.36E+06	300.73	6.18E+01	70.503	147735	585874
178	800.144	3.709	16.687	2.0467	798.643	15.656	7.50E+06	299.94	6.16E+01	70.490	983729	468101
179	800.096	3.754	16.889	2.7401	599.479	11.779	5.66E+06	298.64	6.13E+01	70.422	587859	308466
180	800.529	3.674	16.521	3.9532	401.398	7.902	3.81E+06	297.43	6.09E+01	70.303	28280.7	136391
181	801.155	1.849	8.308	2.0325	400.466	7.880	3.82E+06	295.70	6.06E+01	70.415	239914	115815
182	801.485	1.843	8.278	1.3553	602.555	11.830	5.73E+06	295.59	6.06E+01	70.439	521362	250192
183	801.736	1.833	8.230	1.0151	802.462	15.726	7.61E+06	296.32	6.07E+01	70.425	883894	34365
184	801.747	1.825	8.194	0.8115	1001.54	19.574	9.42E+06	298.25	6.11E+01	70.323	132233	355245
185	800.937	2.751	12.363	2.9910	400.979	7.887	3.81E+06	296.87	6.08E+01	70.343	261073	126213
186	801.138	2.733	12.282	2.0062	599.945	11.795	5.70E+06	296.38	6.07E+01	70.440	55156.2	28123
187	801.278	2.717	12.207	1.5014	800.879	15.723	7.59E+06	297.03	6.09E+01	70.486	936192	40789.1
188	801.157	2.701	12.138	1.1974	1001.59	19.611	9.42E+06	299.05	6.14E+01	70.436	140843	481689
189	784.596	5.342	24.511	5.7663	400.559	7.887	3.82E+06	295.59	6.04E+01	70.202	326665.6	15778
190	784.933	5.231	23.990	3.8655	596.636	11.729	5.69E+06	295.33	6.05E+01	70.404	646822	34942.4

Point No.	Liquid Density kg/m³	Liquid Mass Flowrate kg/s	Liquid Volume Flowrate m³/hr	Liquid Volume Fraction	Gas Volume Flowrate m³/hr	Gas Mass Flowrate kg/s	Gas Reynolds Number	Test Point Temperature K	Test Point Pressure N/m²	Test Point Gas Density kg/m³	ΔP_{tp} N/m²	ΔP_2 N/m²
191	784.937	7.866	36.075	8.2620	400.559	7.879	3.82E+06	295.57	6.03E+01	70.181	39177.3	18713.2
192	785.297	7.175	32.892	3.9216	805.843	15.849	7.67E+06	296.03	6.09E+01	70.672	120220	63083.3
193	805.497	5.298	23.678	5.5611	402.098	7.900	3.86E+06	292.53	5.97E+01	70.299	32434.8	15685.8
194	805.589	5.287	23.626	3.7789	601.576	11.816	5.77E+06	292.97	6.00E+01	70.518	650515	35163.5
195	804.885	7.395	33.074	7.5945	402.424	7.902	3.85E+06	293.38	5.99E+01	70.333	375239	179953
196	804.405	7.251	32.453	3.8766	804.698	15.839	7.70E+06	294.46	6.06E+01	70.851	119603	62756.7
197	803.2	8.118	36.385	5.7158	600.178	11.801	5.73E+06	294.91	6.05E+01	70.641	756339	40793
198	801.467	10.774	48.395	7.4474	601.436	11.861	5.75E+06	295.85	6.08E+01	70.738	87457.1	46440.9
199	801.534	10.638	47.778	5.6441	798.736	15.764	7.62E+06	296.88	6.14E+01	71.037	137564	72827.2
200	799.745	14.465	65.112	7.5382	798.643	15.798	7.60E+06	298.73	6.20E+01	71.204	160624	84796.3
201	798.631	5.380	24.251	2.3675	1000.05	19.693	9.44E+06	300.31	6.20E+01	70.878	162566	73747

Table A3.5. The Open Pipe Injector 60 Bar Wet Gas Test Data.

233

Table A3.6 presents the nozzle injector 60 Bar test data.

Point No.	Liquid Density	Liquid Mass Flowrate	Liquid Volume Flowrate	Liquid Volume Fraction	Gas Volume Flowrate	Gas Mass Flowrate	Gas Reynolds Number	Test Point Temperature	Test Point Pressure	Test Point Gas Density	ΔP_{tp}	ΔP_2
	kg/m³	kg/s	m³/hr		m³/hr	kg/s		K	N/m²	kg/m³	N/m²	N/m²
202	803.12	0.034	0.153	0.0381	401.212	7.814	3.83E+06	291.69	5.94E+01	70.191	190386	51726
203	803.124	0.034	0.151	0.0251	601.762	11.697	5.72E+06	292.19	5.94E+01	70.057	427504	75190
204	803.104	0.034	0.154	0.0192	802.695	15.575	7.59E+06	293.71	5.96E+01	69.919	753768	111753
205	803.095	0.036	0.161	0.0160	1002.98	19.435	9.43E+06	295.76	6.00E+01	69.804	1183358	151463
206	802.976	0.160	0.717	0.0717	999.913	19.373	9.34E+06	298.18	6.06E+01	69.785	118836	163423
207	802.575	0.159	0.715	0.0892	800.925	15.545	7.52E+06	297.21	6.04E+01	69.912	75998	122820
208	802.249	0.162	0.725	0.1206	600.457	11.677	5.67E+06	295.62	6.02E+01	70.050	433497	92990
209	802.064	0.160	0.717	0.1791	399.533	7.790	3.79E+06	294.21	6.00E+01	70.207	196389	75836
210	802.022	0.315	1.414	0.3499	402.751	7.859	3.83E+06	293.47	5.98E+01	70.223	203872	85833
211	802.174	0.312	1.401	0.2325	601.296	11.708	5.71E+06	293.82	5.98E+01	70.111	445159	125717
212	802.373	0.311	1.394	0.1739	800.366	15.554	7.56E+06	295.05	6.00E+01	69.985	768928	137474
213	802.385	0.309	1.388	0.1387	999.634	19.392	9.37E+06	297.48	6.05E+01	69.860	120132	175190
214	803.333	0.784	3.515	0.8691	400.885	7.817	3.82E+06	292.67	5.95E+01	70.079	213858	102675
215	803.414	0.780	3.494	0.5765	602.555	11.725	5.72E+06	293.23	5.96E+01	70.025	473813	188611
216	803.479	0.779	3.490	0.4337	801.298	15.561	7.57E+06	294.53	5.98E+01	69.918	801197	201615
217	803.347	0.771	3.455	0.3436	1001.96	19.422	9.40E+06	296.81	6.03E+01	69.815	124123	223736
218	801.929	3.672	16.484	1.6188	1001.77	19.486	9.37E+06	299.28	6.11E+01	70.160	147663	582374
219	800.177	3.724	16.753	2.0519	799.714	15.594	7.49E+06	299.84	6.13E+01	70.161	984756	464298
220	801.019	3.776	16.969	2.7436	601.529	11.789	5.71E+06	296.28	6.04E+01	70.125	595873	314032
221	801.52	3.686	16.555	3.9796	399.44	7.812	3.78E+06	296.41	6.03E+01	69.919	281326	132510
222	801.995	1.853	8.318	2.0355	400.326	7.820	3.80E+06	295.14	6.00E+01	70.007	239759	116267
223	802.116	1.840	8.258	1.3571	600.224	11.706	5.69E+06	295.28	6.01E+01	70.052	514222	247604
224	802.313	1.833	8.224	1.0174	800.087	15.578	7.55E+06	296.30	6.03E+01	70.049	875457	348064
225	802.184	1.823	8.183	0.8118	999.773	19.417	9.36E+06	298.45	6.08E+01	69.958	132150	365237
226	802.592	2.762	12.387	2.9971	400.932	7.831	3.81E+06	294.61	5.98E+01	69.918	261632	124958
227	802.814	2.700	12.106	1.1946	1001.31	19.481	9.42E+06	297.03	6.05E+01	70.074	140221	487773
228	801.787	2.746	12.329	2.0103	600.97	11.703	5.66E+06	297.06	6.05E+01	70.006	549834	280342
229	801.729	2.717	12.198	1.4997	801.158	15.604	7.54E+06	297.57	6.07E+01	70.083	930638	407134
230	802.602	4.326	19.403	1.9023	1000.61	19.457	9.37E+06	298.52	6.10E+01	70.177	153588	646632
231	800.865	5.383	24.199	57.108	399.533	7.809	3.77E+06	298.12	6.06E+01	69.841	320667	149461
232	801.199	5.281	23.730	37.981	601.063	11.751	5.68E+06	297.51	6.06E+01	70.048	648189	346755

Point No.	Liquid Density (kg/m³)	Liquid Mass Flowrate (kg/s)	Liquid Volume Flowrate (m³/hr)	Liquid Volume Fraction	Gas Volume Flowrate (m³/hr)	Gas Mass Flowrate (kg/s)	Gas Reynolds Number	Test Point Temperature (K)	Test Point Pressure (N/m²)	Test Point Gas Density (kg/m³)	ΔP_{tp} (N/m²)	ΔP_2 (N/m²)
233	800.199	8.099	36.437	8.3442	400.233	7.857	3.78E+06	299.27	6.08E+01	69.791	39476.7	18718.0
234	799.39	7.252	32.660	3.9241	799.621	15.680	7.52E+06	300.49	6.16E+01	70.325	119030	61987.0
235	799.423	5.420	24.407	5.7565	399.58	7.837	3.77E+06	299.52	6.09E+01	69.873	32349.3	15138.1
236	801.747	5.107	22.932	3.6823	599.821	11.728	5.68E+06	296.23	6.03E+01	69.991	63826.4	34248.3
237	801.369	7.247	32.556	7.5047	401.258	7.857	3.79E+06	297.70	6.05E+01	69.802	37128.8	17626.3
238	800.737	7.195	32.349	3.8742	802.648	15.724	7.57E+06	298.82	6.12E+01	70.304	119130	62255.3
239	799.256	7.929	35.713	5.5957	602.508	11.817	5.67E+06	300.55	6.14E+01	70.084	75561.2	40380.4
240	797.889	9.163	41.341	6.4480	599.805	11.836	5.66E+06	301.78	6.17E+01	70.120	81226.3	43022.0
241	797.865	9.162	41.341	4.9173	799.388	15.727	7.50E+06	302.56	6.21E+01	70.399	130918	69058.2
242	797.865	5.317	23.990	2.3411	1000.75	19.535	9.29E+06	303.77	6.23E+01	70.303	160823	70506.8
243	797.619	5.188	23.4177	3.7413	602.508	11.800	5.64E+06	302.05	6.17E+01	70.092	64821	343009

Table A3.6. The Nozzle Injector 60 Bar Wet Gas Test Data.

235

Appendix Four

In Chapter 5 the seven Differential Pressure Meter correlations that were chosen as potentially suitable for use with Venturi Meters metering wet gas flows were compared for the 20 Bar, 40 Bar and 60 Bar cases and for all the data combined. The values actually compared were the root mean square fractional deviations (d). The equation used was:

$$d = \sqrt{\frac{1}{n} \sum_{i=1}^{n} \left(\frac{\dot{m}_{g(predicted)i} - \dot{m}_{g(experimental)i}}{\dot{m}_{g(experimental)i}} \right)^2}$$

These results were listed in Table 5.1. The derivations of these stated values are given in Table A4.1 for the 20 Bar case, Table A4.2 for the 40 Bar case and Table A4.3 for the 60 Bar case. Table A4.4 summarises the case where all the data was used. In these tables the "residual" is the bracketed term in the above equation.

Point No	Actual Gas Mass Flowrate	Homo-geneous Equ (1 12)	Murdock (M 1 26) Equ (1 14)	Murdock Venturi (M=1.5) Equ(1 37)	Chisholm Equ.(1.24)	Smith and Leang Equ.(1.27)	Lin Equ.(1.31)	de Leeuw Equ.(1.32)
	(kg/s)	(kg/s)	(kg/s)	(kg/s)	(kg/s)	(kg/s)	(kg/s)	(kg/s)
1	2 764	2 833	2 847	2 845	2 847	2.999	2.719	2.839
2	2 763	2 833	2 847	2 845	2.846	2.999	2.719	2.839
3	4 135	4 233	4 247	4 245	4.246	4.476	4.064	4.237
4	4 130	4 230	4 244	4 242	4.244	4.474	4.062	4.235
5	5 495	5 580	5 594	5 592	5 593	5.898	5.364	5.580
6	5 493	5 579	5 593	5 591	5 592	5 897	5.363	5.580
7	6 878	6 999	7 013	7 011	7 012	7.396	6.740	6.996
8	6 888	7 007	7 020	7 018	7.020	7.403	6.747	7.004
9	2 753	2 814	2 979	2 951	2 972	3.074	2.847	2.888
10	2 765	2 758	3 049	2 995	3 038	3.120	2.917	2.888
11	2 769	2 683	3 080	3 002	3.068	3.149	2.948	2.859
12	2 775	2 599	3 101	2 994	3 090	3.191	2.971	2.821
13	4 198	3 954	4 709	4 548	4 690	4.841	4 522	4.206
14	4 186	4 031	4 636	4 517	4 617	4.740	4.449	4.230
15	4 181	4 138	4 589	4 506	4.571	4.692	4.400	4.282
16	4 171	4 259	4 507	4 465	4 495	4.650	4 318	4 336
17	5 560	5 698	6 026	5 971	6 010	6 217	5.787	5 705
18	5 553	5 688	6 019	5 963	6.003	6 208	5.780	5 695
19	5 572	5 570	6 149	6 043	6 125	6.289	5.910	5 594
20	5 567	5 451	6 251	6 094	6 222	6 387	6.013	5.499
21	5 566	5 447	6 258	6 098	6 229	6 395	6 020	5 497
22	6 211	6 200	6 918	6 784	6 889	7 069	6 658	6.159
23	6 565	6 769	7 168	7 101	7 149	7 392	6 896	6 710
24	6 557	6 765	7 164	7 097	7 145	7 387	6 892	6.705
25	2 759	2 819	2 981	2 954	2 974	3 077	2 850	2.892
26	2 767	2 676	3 079	2 999	3 066	3 148	2.947	2.855

Point No.	Actual Gas Mass Flowrate Equ.(1.12)	Homo-genous Equ.(1.12)	Murdock (M=1.26) Equ.(1.14)	Murdock Venturi (M=1.5) Equ(1.37)	Chisholm Equ.(1.24)	Smith and Leang Equ.(1.27)	Lin Equ.(1.31)	de Leeuw Equ.(1.32)
	(kg/s)	(kg/s)	(kg/s)	(kg/s)	(kg/s)	(kg/s)	(kg/s)	(kg/s)
27	4.167	4.137	4.572	4.492	4.554	4.676	4.383	4.277
28	5.550	5.552	6.137	6.031	6.113	6.276	5.899	5.579
29	6.192	6.186	6.903	6.770	6.874	7.053	6.644	6.147
30	6.440	6.595	7.066	6.985	7.043	7.263	6.797	6.538
31	6.662	6.905	7.224	7.171	7.208	7.477	6.949	6.850
32	6.910	7.181	7.365	7.335	7.355	7.681	7.083	7.141
33	7.177	7.420	7.531	7.513	7.524	7.891	7.244	7.391
34	7.011	7.277	7.432	7.407	7.423	7.765	7.148	7.241
35	6.828	7.109	7.324	7.289	7.313	7.625	7.045	7.064
36	2.768	2.843	2.930	2.916	2.925	3.051	2.799	2.882
37	4.136	4.267	4.354	4.340	4.350	4.553	4.169	4.295
38	5.537	5.724	5.812	5.798	5.807	6.089	5.576	5.725
39	6.887	7.098	7.185	7.172	7.181	7.538	6.908	7.079
40	6.985	7.128	7.171	7.164	7.169	7.546	6.893	7.118
41	5.499	5 651	5.694	5.687	5.692	5.988	5.461	5.652
42	4.125	4.245	4.288	4.281	4.286	4.505	4.104	4.259
43	2.758	2.826	2.868	2.862	2.866	3.007	2.740	2.845
44	2 689	2.741	2.756	2.754	2.755	2.902	2.631	2.748
45	4 026	4 121	4.136	4.133	4.135	4.359	3.957	4.126
46	5 372	5 454	5.468	5.466	5.467	5.765	5 243	5.454
47	6 708	6 827	6.841	6.839	6.840	7.214	6 573	6.824
48	6 714	6 865	6.908	6.901	6.906	7.269	6.638	6.856
49	5 364	5 512	5.555	5.549	5.553	5.841	5.327	5.514
50	4 035	4 152	4.195	4.188	4.193	4.406	4.014	4.167
51	2 694	2 764	2.806	2.799	2.804	2.941	2.680	2.783
52	2 698	2 766	2.852	2.839	2.848	2.969	2.725	2.805
53	4 065	4 188	4.275	4.261	4.270	4.469	4.092	4.217
54	5 417	5 603	5 690	5.677	5.685	5.961	5.458	5.605
55	6 771	6 993	7.082	7.068	7.077	7.428	6.807	6.975
56	2 714	2 703	2.998	2.944	2.986	3.063	2.867	2.834
57	2 704	2.755	2.921	2.894	2.914	3.011	2.792	2.830
58	2 712	2.631	3.029	2.952	3.016	3.093	2.898	2.807
59	2 719	2 556	3.061	2.955	3.048	3.145	2.931	2.778
60	4 095	3 846	4 597	4.440	4.577	4.721	4.412	4.106
61	4 070	3 914	4 521	4 402	4.500	4.617	4.336	4.123
62	4 069	4 025	4 475	4 394	4.457	4.571	4.289	4.176
63	4 075	4 142	4 390	4.349	4.378	4.526	4.205	4.223
64	5 448	5 587	5 918	5 863	5.901	6.101	5.681	5.597
65	5 447	5 459	6 042	5 937	6.016	6.173	5.804	5.489
66	5 443	5 346	6 159	6 001	6.129	6.288	5.922	5.401
67	6 114	6 136	6 854	6 723	6 823	6 997	6.594	6.096
68	6 428	6 624	7 023	6 957	7.003	7 237	6.754	6.569
69	2 718	2 764	2 928	2 901	2.920	3.019	2.798	2.838
70	2 720	2 638	3 041	2 962	3 027	3.106	2.910	2.816
71	4 091	4 070	4 503	4 425	4.485	4.603	4.316	4.212
72	5 483	5 496	6 078	5 973	6 053	6.212	5.840	5.523
73	6 130	6 166	6 869	6 741	6 839	7.015	6.609	6.123
74	6 337	6 492	6 964	6 884	6 941	7.154	6.698	6.437
75	6 525	6 768	7 086	7 034	7.069	7.331	6.814	6.717
76	6 749	7 024	7 208	7.179	7.198	7.515	6.931	6.986
77	6 996	7 245	7 360	7.342	7.353	7.708	7.078	7.217
78	6 855	7 126	7 280	7 256	7 271	7 605	7.000	7 091
79	6 689	6 962	7.177	7.143	7.166	7.469	6 901	6 920
Sum of Residual Squares	0 063995	0 535332	0 36174	0 496921	1.06126	0.16623	0.061683
Number of Points	79	79	79	79	79	79	79
R M S Fractional Deviation	0 0285	0 0823	0 0677	0 0793	0.1159	0.0449	0.0279

Table A4.1. The Root Mean Square Fractional Deviation Calculations at 20 Bar.

Point No.	Actual Gas Mass Flowrate	Homogenous Equ.(1.12)	Murdock (M−1.26) Equ.(1.14)	Murdock Venturi (M=1.5) Equ(1.37)	Chisholm Equ.(1.24)	Smith and Leang Equ.(1.27)	Lin Equ.(1.31)	de Leeuw Equ.(1.32)
	(kg/s)	(kg/s)	(kg/s)	(kg/s)	(kg/s)	(kg/s)	(kg/s)	(kg/s)
80	5.126	5.213	5.221	5.219	5.221	5.510	4.972	5.216
81	5.284	5.372	5.378	5.376	5.379	5.677	5.123	5.375
82	7.886	7.985	7.991	7.989	7.991	8.434	7.635	7.985
83	10.491	10.554	10.559	10.558	10.560	11.144	10.120	10.552
84	13.083	13.196	13.202	13.200	13.202	13.930	12.692	13.193
85	13.082	13.215	13.248	13.238	13.250	13.971	12.743	13.198
86	10.476	10.571	10.604	10.594	10.606	11.183	10.168	10.560
87	7.895	8.070	8.103	8.093	8.105	8.545	7.748	8.069
88	5.259	5.386	5.418	5.408	5.421	5.712	5.167	5.400
89	5.259	5.395	5.459	5.439	5.464	5.748	5.213	5.423
90	7.870	8.099	8.164	8.145	8.168	8.601	7.814	8.097
91	10.481	10.606	10.671	10.652	10.675	11.245	10.240	10.585
92	13.083	13.229	13.294	13.275	13.297	14.010	12.795	13.195
93	5.144	5.297	5.304	5.302	5.304	5.598	5.052	5.300
94	7.916	8.015	8.022	8.020	8.023	8.467	7.665	8.015
95	10 487	10.550	10.556	10.554	10.557	11.140	10.117	10.547
96	13.085	13.201	13.208	13.206	13.209	13.937	12.699	13.198
97	13.091	13 228	13.261	13.251	13.263	13.984	12.756	13.210
98	10 493	10.593	10.625	10.616	10.628	11.206	10.190	10.582
99	7.874	8 056	8.089	8.079	8.091	8.530	7.735	8.056
100	5 265	5 393	5.425	5.415	5.428	5.719	5.173	5.407
101	5.162	5 296	5.360	5.340	5.365	5.644	5.118	5.325
102	7 926	8 150	8.214	8.195	8.218	8.654	7.862	8.147
103	10 496	10 627	10.692	10.673	10.696	11.267	10.261	10.606
104	13 089	13 241	13 306	13 287	13.309	14.023	12.806	13.208
105	5 263	5 379	5.529	5.482	5.543	5.812	5.300	5.445
106	5 270	5 337	5.570	5.492	5.593	5.859	5.360	5.439
107	5 291	5 224	5 625	5.477	5.677	5.973	5.464	5.406
108	10 341	10 711	11 166	11.022	11.202	11.724	10.807	10.562
109	13 011	13 387	13 950	13.769	13.997	14.654	13.555	13.103
110	5 304	5.108	5 654	5.431	5.743	6.116	5.545	5.364
111	7 937	7.962	8.569	8 349	8.642	9.087	8.348	7.957
112	7 871	8 026	8.368	8.257	8.400	8.796	8.077	8.020
113	13 132	13 511	13.867	13.758	13.892	14.562	13.420	13.326
114	13 149	13 548	14.030	13 878	14.066	14.730	13.610	13.299
115	13 078	13 319	13 480	13 433	13 490	14.183	12.997	13.235
116	10 472	10 760	10 920	10 872	10 931	11.487	10.504	10.706
117	7 877	8 113	8 271	8 222	8 283	8 697	7.938	8.108
118	5 271	5 379	5 533	5 484	5 547	5.816	5.305	5.446
119	5 254	5 372	5 527	5 478	5.541	5.810	5.299	5.440
120	5 313	5 089	5 743	5 446	5.874	6.357	5.685	5.397
121	10 674	10 870	11 678	11 388	11.769	12.367	11.415	10.612
122	10 594	10 677	11 771	11 337	11.926	12 669	11.611	10.355
123	7 978	7 885	8 867	8 434	9 045	9 752	8.792	7.888
124	7 919	7 900	8 700	8 369	8 829	9.397	8.563	7.892
125	5 295	5 385	5 390	5 388	5.390	5 689	5.134	5 387
126	7 895	7 999	8 004	8 003	8 005	8.449	7.648	7.999
127	10 507	10 582	10 588	10 586	10 588	11.174	10.148	10.580
128	13 140	13 268	13 274	13 273	13.275	14.007	12.763	13.265
129	13 099	13 243	13 275	13 266	13.277	14.000	12.770	13.226
130	10 479	10 580	10 612	10.603	10.614	11.192	10.177	10.570
131	7 894	8 083	8 115	8 106	8.117	8.558	7.760	8 082
132	5 294	5 426	5 458	5 448	5.460	5.754	5.205	5 440
133	5 287	5 426	5 489	5 470	5 494	5 780	5.242	5.453
134	7 917	8 156	8 220	8 201	8 224	8 660	7.868	8 153
135	10 518	10 665	10 729	10.710	10.733	11.307	10.297	10 644
136	13 149	13 306	13 371	13 352	13 374	14 092	12 870	13.273
137	5 289	5 404	5 556	5 507	5 570	5 841	5.326	5 470
138	5 324	5 394	5 625	5 548	5 649	5 917	5.413	5.493
139	5 299	5 251	5 649	5 501	5 702	5 999	5 487	5.430
140	10 570	10 832	11 272	11.129	11 311	11 845	10.915	10 687
141	13 157	13 545	14 102	13 922	14.148	14.813	13.703	13.259
142	5 296	5 101	5 643	5 419	5 733	6 109	5 536	5.356

Point No.	Actual Gas Mass Flowrate	Homogenous Equ.(1.12)	Murdock (M=1.26) Equ.(1.14)	Murdock Venturi (M=1.5) Equ(1.37)	Chisholm Equ.(1.24)	Smith and Leang Equ.(1.27)	Lin Equ.(1.31)	de Leeuw Equ.(1.32)
	(kg/s)	(kg/s)	(kg/s)	(kg/s)	(kg/s)	(kg/s)	(kg/s)	(kg/s)
143	7.930	7.984	8.586	8.365	8.661	9.110	8.368	7.979
144	7.941	8.115	8.453	8.342	8.486	8.888	8.160	8.105
145	13.221	13.605	13.956	13.848	13.982	14.660	13.509	13.420
146	13.225	13.620	14.097	13.946	14.135	14.805	13.678	13.371
147	13.144	13.385	13.545	13.498	13.555	14.252	13.061	13.301
148	10.515	10.789	10.948	10.900	10.959	11.516	10.530	10.735
149	7.871	8.111	8.268	8.220	8.280	8.694	7.935	8.106
150	5.276	5.385	5.539	5.490	5.553	5.822	5.311	5.452
151	5.282	4.986	5.643	5.341	5.776	6.267	5.591	5.309
152	10.702	10.921	11.712	11.430	11.799	12.394	11.442	10.666
153	10.588	10.702	11.793	11.359	11.948	12.691	11.633	10.380
154	7.972	7.829	8.802	8.372	8.980	9.683	8.728	7.842
155	7.977	7.912	8.727	8.397	8.853	9.416	8.584	7.913
156	10.747	10.938	12.222	11.670	12.437	13.352	12.145	10.541
157	12.444	12.774	13.758	13.400	13.870	14.592	13.499	12.330
158	12.723	13.081	13.877	13.603	13.956	14.631	13.553	12.700
159	12.167	12.505	13.857	13.301	14.059	14.997	13.744	11.934
Sum of Residual Squares		0.038581	0.277169	0.13474	0.346428	1.150287	0.160392	0.02989
Number of Points		80	80	80	80	80	80	80
R M S Fractional Deviation		0.0220	0.0589	0.0410	0.0658	0.1199	0.0448	0.0193

Table A4.2. The Root Mean Square Fractional Deviation Calculations at 40 Bar.

Point No.	Actual Gas Mass Flowrate (kg/s)	Homo-genous Equ.(1.12) (kg/s)	Murdock (M=1.26) Equ.(1.14) (kg/s)	Murdock Venturi (M=1.5) Equ(1.37) (kg/s)	Chisholm Equ.(1.24) (kg/s)	Smith and Leang Equ.(1.27) (kg/s)	Lin Equ.(1.31) (kg/s)	de Leeuw Equ.(1.32) (kg/s)
160	7.830	7.956	7.960	7.958	7.961	8.405	7.551	7.957
161	11.713	11.861	11.866	11.864	11.867	12.526	11.293	11.860
162	15.618	15.710	15.714	15.712	15.715	16.586	15.006	15.707
163	19.437	19.551	19.556	19.554	19.557	20.636	18.738	19.548
164	19.450	19.581	19.605	19.593	19.611	20.690	18.797	19.563
165	15.568	15.674	15.697	15.686	15.703	16.570	15.001	15.660
166	11.694	11.870	11.894	11.882	11.900	12.558	11.331	11.863
167	7.837	8.041	8.064	8.053	8.071	8.517	7.661	8.046
168	7.841	8.053	8.099	8.075	8.112	8.558	7.708	8.063
169	11.724	11.934	11.981	11.957	11.993	12.653	11.428	11.920
170	15.641	15.759	15.807	15.784	15.819	16.688	15.120	15.732
171	19.481	19.633	19.681	19.658	19.692	20.772	18.884	19.598
172	7.827	8.027	8.138	8.079	8.171	8.619	7.785	8.053
173	11.755	12.099	12.212	12.154	12.244	12.912	11.691	12.064
174	15.679	15.858	15.974	15.916	16.004	16.875	15.322	15.790
175	19.476	19.686	19.803	19.746	19.831	20.909	19.042	19.601
176	19.592	20.111	20.698	20.372	20.874	22.065	20.227	19.674
177	19.556	20.026	20.520	20.252	20.663	21.815	19.987	19.659
178	15.656	16.063	16.541	16.269	16.695	17.658	16.120	15.776
179	11.779	12.043	12.499	12.220	12.665	13.451	12.219	11.904
180	7.902	7 886	8.287	8.012	8.463	9.082	8.173	7.990
181	7 880	8 004	8.238	8.100	8.321	8.806	7.971	8.059
182	11 830	12 184	12.433	12.297	12.510	13.203	11.993	12.105
183	15 726	16 084	16.340	16.205	16.412	17.307	15.765	15.931
184	19 574	19 872	20.132	19.999	20.201	21.294	19.451	19.679
185	7 887	7.943	8.267	8.062	8.395	8.935	8.076	8.024
186	11 795	12 116	12.467	12.264	12.584	13.311	12.101	12.007
187	15 723	16 138	16.503	16.303	16.613	17.537	15.999	15.919
188	19 611	20 017	20.391	20.194	20.495	21.614	19.779	19.739
189	7.887	7 838	8.335	7.932	8.611	9.425	8.374	7.970
190	11 729	12 011	12.584	12.193	12.830	13.747	12.439	11.827
191	7 879	7.722	8.320	7.726	8.749	9.907	8.579	7.902
192	15 849	16 284	17.075	16.542	17.401	18.646	16.949	15.784
193	7 900	7 819	8.334	7.939	8.597	9.386	8.351	7.963
194	11 816	12 026	12.625	12.234	12.864	13.769	12.466	11.847
195	7 902	7 684	8 293	7.742	8 680	9.744	8.489	7.876
196	15 839	16 215	17.036	16.503	17.354	18.582	16.898	15.719
197	11 801	11 876	12 667	12.066	13.059	14.264	12.749	11.647
198	11 861	11 914	12 831	12.031	13.376	14.931	13.138	11.637
199	15 764	16 111	17 164	16 381	17.660	19.250	17.317	15.468
200	15 798	16 149	17 392	16.324	18.101	20.189	17.872	15.367
201	19 693	20 307	20 987	20 593	21.205	22.460	20.592	19.794
202	7 814	7 932	7 937	7 935	7.939	8.381	7.529	7.934
203	11 697	11 843	11 848	11 845	11.849	12.508	11.277	11.841
204	15 575	15 664	15 669	15 667	15.671	16.539	14.963	15.661
205	19 435	19 551	19 557	19.554	19.558	20.638	18.740	19.547
206	19 373	19 523	19 547	19 535	19.553	20.629	18.740	19.505
207	15 545	15 663	15 687	15 675	15 693	16.559	14.991	15.649
208	11 677	11 859	11 883	11.871	11.890	12.547	11.321	11.852
209	7 790	7 992	8 016	8 004	8.023	8.467	7.615	7.998
210	7 859	8 064	8 110	8 086	8.123	8.570	7.718	8.074
211	11 708	11 944	11 990	11 967	12.002	12 662	11.436	11.930
212	15 554	15 683	15 730	15.707	15.742	16 606	15.045	15.656
213	19 392	19 560	19 607	19 584	19.618	20.693	18.811	19.526
214	7 817	8 012	8 122	8 064	8.155	8.601	7.768	8 037
215	11 725	12 073	12 185	12 128	12.216	12.882	11.663	12.038
216	15 561	15 754	15 869	15 812	15 899	16.764	15.219	15 688
217	19 422	19 628	19 743	19 687	19 771	20 846	18.982	19.544
218	19 486	19 961	20 458	20 191	20 599	21 744	19 922	19.593
219	15 594	16 019	16 502	16 229	16 655	17.614	16.080	15.731
220	11 789	12 109	12 569	12.290	12.735	13 524	12.287	11.965
221	7 812	7 826	8 231	7 957	8 406	9 021	8.118	7.934
222	7 820	7 967	8 204	8 067	8 286	8 768	7.937	8.024

Point No.	Actual Gas Mass Flowrate	Homo-genous Equ.(1.12)	Murdock (M=1.26) Equ.(1.14)	Murdock Venturi (M=1.5) Equ(1.37)	Chisholm Equ.(1.24)	Smith and Leang Equ.(1.27)	Lin Equ.(1.31)	de Leeuw Equ.(1.32)
	(kg/s)	(kg/s)	(kg/s)	(kg/s)	(kg/s)	(kg/s)	(kg/s)	(kg/s)
223	11.706	12.054	12.305	12.169	12.381	13.065	11.867	11.978
224	15.578	15.950	16.208	16.073	16.279	17.165	15.635	15.798
225	19.417	19.726	19.987	19.855	20.055	21.139	19.309	19.533
226	7.831	7.917	8.245	8.040	8.371	8.909	8.052	7.998
227	19.481	19.906	20.283	20.087	20.385	21.495	19.670	19.628
228	11.703	12.027	12.383	12.181	12.499	13.219	12.018	11.918
229	15.604	16.020	16.388	16.189	16.497	17.411	15.884	15.801
230	19.457	20.059	20.633	20.319	20.801	21.978	20.148	19.632
231	7.809	7.698	8.215	7.814	8.483	9.281	8.245	7.851
232	11.751	11.970	12.567	12.176	12.806	13.709	12.410	11.791
233	7.857	7.668	8.293	7.689	8.727	9.897	8.554	7.868
234	15.680	16.131	16.948	16.415	17.268	18.496	16.816	15.636
235	7.837	7.742	8.258	7.853	8.530	9.337	8.293	7.891
236	11.728	11.942	12.524	12.147	12.755	13.641	12.354	11.770
237	7.857	7.673	8.274	7.734	8.653	9.697	8.460	7.860
238	15.724	16.157	16.973	16.444	17.288	18.509	16.832	15.663
239	11.817	11.932	12.710	12.122	13.092	14.278	12.776	11.697
240	11.836	12.002	12.842	12.160	13.296	14.644	13.016	11.741
241	15.727	16.228	17.186	16.511	17.604	19.032	17.214	15.638
242	19.535	20.121	20.798	20.411	21.012	22.249	20.398	19.613
243	11.800	12.024	12.609	12.225	12.846	13.747	12.447	11.844
Sum of Residual Squares		0.03417	0.213074	0.068982	0.383275	1.649282	0.19234	0.016411
Number of Points		84	84	84	84	84	84	84
R.M.S. Fractional Deviation		0.0202	0.0504	0.0287	0.0675	0.1401	0.0479	0.0140

Table A4.3. The Root Mean Square Fractional Deviation Calculations at 60 Bar.

	Homo-genous Equ.(1.12)	Murdock (M=1.26) Equ.(1.14)	Murdock Venturi (M=1.5) Equ(1.37)	Chisholm Equ.(1.24)	Smith and Leang Equ.(1.27)	Lin Equ.(1.31)	de Leeuw Equ.(1.32)
Sum of 20 Bar Residual Squares	0.063995	0.535332	0.36174	0.496921	1.06126	0.16623	0.061683
Sum of 40 Bar Residual Squares	0.038581	0.277169	0.13474	0.346428	1.150287	0.160392	0.02989
Sum of 60 Bar Residual Squares	0.03417	0.213074	0.068982	0.383275	1.649282	0.19234	0.016411
Sum of Total Residual Squares	0.136747	1.025576	0.565463	1.226625	3.860829	0.518963	0.107984
Number of Points	243	243	243	243	243	243	243
R.M.S. Fractional Deviation	0.0237	0.0650	0.0482	0.0710	0.1260	0.0462	0.0211

Table A4.4. The Root Mean Square Fractional Deviation Calculations with All the Data.

Appendix Five ·

In Chapter 6 the four new correlations developed in this thesis (i.e. equations 6.1, 6.3, 6.5 and 6.6) were compared for the 20 Bar, 40 Bar and 60 Bar cases and for all the data combined. The values actually compared were the root mean square fractional deviations (d). The equation used was:

$$d = \sqrt{\frac{1}{n}\sum_{i=1}^{n}\left(\frac{\dot{m}_{g(predicted)i} - \dot{m}_{g(experimental)i}}{\dot{m}_{g(experimental)i}}\right)^2}$$

These results were listed in Table 6.10. The derivations of these stated values are given in Table A5.1 for the 20 Bar case, Table A5.2 for the 40 Bar case and Table A5.3 for the 60 Bar case. Table A5.4 summarises the case where all the data was used. In these tables the "residual" is the bracketed term in the above equation.

Point Number	Actual Gas Mass Flowrate	Equation 6.1	Equation 6.3	Equation 6.5	Equation 6.6
	(kg/s)	(kg/s)	(kg/s)	(kg/s)	(kg/s)
1	2.764	2.842	2.837	2.839	2.793
2	2.763	2.842	2.837	2.838	2.793
3	4.135	4.242	4.237	4.237	4.152
4	4.130	4.239	4.234	4.235	4.150
5	5.495	5.589	5.584	5.583	5.446
6	5.493	5.588	5.583	5.582	5.445
7	6.878	7.008	7.003	7.000	6.796
8	6.888	7.016	7.011	7.007	6.803
9	2.753	2.915	2.848	2.869	2.765
10	2.765	2.927	2.800	2.841	2.758
11	2.769	2.902	2.717	2.777	2.761
12	2.775	2.857	2.603	2.688	2.787
13	4.198	4.344	3.969	4.033	4.223
14	4.186	4.364	4.084	4.127	4.147
15	4.181	4.400	4.205	4.232	4.136
16	4.171	4.411	4.312	4.324	4.170
17	5.560	5.900	5.771	5.744	5.557
18	5.553	5.892	5.761	5.734	5.548
19	5.572	5.909	5.664	5.622	5.535
20	5.567	5.895	5.532	5.485	5.580
21	5.566	5.896	5.528	5.480	5.586
22	6.211	6.614	6.307	6.205	6.199
23	6.565	7.015	6.859	6.776	6.587
24	6.557	7.010	6.855	6.772	6.582
25	2.759	2.919	2.853	2.873	2.770
26	2.767	2.897	2.708	2.769	2.759
27	4.167	4.391	4.203	4.228	4.125
28	5.550	5.895	5.644	5.603	5.522
29	6.192	6.601	6.292	6.190	6.185

Point Number	Actual Gas Mass Flowrate	Equation 6.1	Equation 6.3	Equation 6.5	Equation 6.6
	(kg/s)	(kg/s)	(kg/s)	(kg/s)	(kg/s)
30	6.440	6.882	6.694	6.605	6.444
31	6.662	7.104	6.982	6.910	6.699
32	6.910	7.298	7.230	7.182	6.950
33	7.177	7.491	7.450	7.418	7.179
34	7.011	7.376	7.319	7.277	7.042
35	6.828	7.245	7.164	7.111	6.882
36	2.768	2.898	2.864	2.874	2.789
37	4.136	4.323	4.289	4.293	4.170
38	5.537	5.780	5.747	5.740	5.570
39	6.887	7.154	7.122	7.100	6.877
40	6.985	7.156	7.140	7.129	6.912
41	5.499	5.679	5.663	5.660	5.509
42	4.125	4.273	4.257	4.259	4.158
43	2.758	2.853	2.837	2.842	2.780
44	2.689	2.751	2.745	2.747	2.702
45	4.026	4.131	4.125	4.126	4.042
46	5.372	5.463	5.458	5.457	5.322
47	6.708	6.836	6.831	6.827	6.627
48	6.714	6.893	6.877	6.867	6.658
49	5.364	5.540	5.524	5.521	5.372
50	4.035	4.180	4.164	4.165	4.066
51	2.694	2.791	2.775	2.780	2.718
52	2.698	2.821	2.787	2.797	2.714
53	4.065	4.244	4.210	4.214	4.093
54	5.417	5.659	5.626	5.619	5.452
55	6.771	7.051	7.017	6.996	6.775
56	2.714	2.876	2.745	2.785	2.707
57	2.704	2.858	2.789	2.810	2.708
58	2.712	2.853	2.663	2.722	2.713
59	2.719	2.819	2.559	2.641	2.749
60	4.095	4.238	3.855	3.919	4.122
61	4.070	4.252	3.963	4.007	4.041
62	4.069	4.289	4.090	4.116	4.029
63	4.075	4.296	4.195	4.206	4.057
64	5.448	5.792	5.658	5.631	5.450
65	5.447	5.803	5.550	5.509	5.433
66	5.443	5.800	5.422	5.374	5.495
67	6.114	6.556	6.243	6.135	6.139
68	6.428	6.872	6.713	6.631	6.448
69	2.718	2.866	2.799	2.819	2.718
70	2.720	2.862	2.671	2.731	2.724
71	4.091	4.325	4.136	4.161	4.061
72	5.483	5.840	5.589	5.546	5.468
73	6.130	6.578	6.273	6.166	6.157
74	6.337	6.782	6.590	6.501	6.347
75	6.525	6.968	6.844	6.774	6.567
76	6.749	7.142	7.072	7.026	6.799
77	6.996	7.319	7.277	7.244	7.011
78	6.855	7.225	7.167	7.126	6.896
79	6.689	7.099	7.017	6.965	6.741
Sum of Residual Squares		0.201159	0.083158	0.063006	0.003163
Number of Points		79	79	79	79
R.M.S. Fractional Deviation		0.0505	0.0324	0.0282	0.0063

Table A5.1. The Root Mean Square Fractional Deviation Calculations at 20 Bar.

Point Number	Actual Gas Mass Flowrate	Equation 6.1	Equation 6.3	Equation 6.5	Equation 6.6
	(kg/s)	(kg/s)	(kg/s)	(kg/s)	(kg/s)
80	5.126	5.216	5.215	5.217	5.179
81	5.284	5.374	5.374	5.375	5.338
82	7.886	7.987	7.986	7.987	7.908
83	10.491	10.556	10.555	10.554	10.416
84	13.083	13.198	13.197	13.195	12.975
85	13.082	13.226	13.224	13.210	12.980
86	10.476	10.582	10.580	10.575	10.424
87	7.895	8.081	8.079	8.081	7.985
88	5.259	5.396	5.394	5.400	5.347
89	5.259	5.415	5.410	5.423	5.350
90	7.870	8.120	8.116	8.120	8.002
91	10.481	10.628	10.623	10.614	10.442
92	13.083	13.251	13.247	13.218	12.975
93	5.144	5.299	5.298	5.300	5.261
94	7.916	8.018	8.017	8.018	7.938
95	10.487	10.552	10.551	10.551	10.412
96	13.085	13.204	13.203	13.201	12.981
97	13.091	13.239	13.237	13.223	12.994
98	10.493	10.604	10.602	10.597	10.445
99	7.874	8.067	8.065	8.067	7.972
100	5.265	5.403	5.401	5.407	5.354
101	5.162	5.316	5.312	5.324	5.253
102	7.926	8.170	8.166	8.170	8.052
103	10.496	10.649	10.645	10.635	10.464
104	13.089	13.263	13.259	13.231	12.988
105	5.263	5.421	5.409	5.441	5.324
106	5.270	5.394	5.376	5.427	5.286
107	5.291	5.289	5.256	5.354	5.225
108	10.341	10.839	10.801	10.717	10.433
109	13.011	13.538	13.505	13.234	12.945
110	5.304	5.146	5.092	5.244	5.211
111	7.937	8.069	8.018	8.065	7.875
112	7.871	8.114	8.088	8.111	7.887
113	13.132	13.619	13.597	13.423	13.112
114	13.149	13.685	13.657	13.415	13.113
115	13.078	13.372	13.363	13.289	13.015
116	10.472	10.811	10.802	10.775	10.558
117	7.877	8.161	8.150	8.160	7.993
118	5.271	5.422	5.411	5.443	5.325
119	5.254	5.415	5.404	5.436	5.318
120	5.313	5.067	4.998	5.202	5.313
121	10.674	11.020	10.961	10.806	10.622
122	10.594	10.784	10.703	10.513	10.582
123	7.978	7.882	7.799	7.908	8.078
124	7.919	7.949	7.883	7.962	7.920
125	5.295	5.386	5.386	5.387	5.351
126	7.895	8.001	8.000	8.001	7.922
127	10.507	10.584	10.584	10.583	10.445
128	13.140	13.270	13.270	13.268	13.046
129	13.099	13.254	13.252	13.238	13.009
130	10.479	10.591	10.589	10.585	10.434
131	7.894	8.094	8.092	8.094	7.999
132	5.294	5.436	5.434	5.440	5.387
133	5.287	5.445	5.441	5.454	5.381
134	7.917	8.176	8.172	8.176	8.059
135	10.518	10.686	10.682	10.673	10.502
136	13.149	13.328	13.324	13.296	13.052
137	5.289	5.446	5.435	5.467	5.351
138	5.324	5.449	5.433	5.483	5.343
139	5.299	5.313	5.283	5.381	5.251
140	10.570	10.946	10.919	10.842	10.561
141	13.157	13.693	13.664	13.386	13.097
142	5.296	5.133	5.092	5.242	5.207
143	7.930	8.083	8.043	8.090	7.900

Point Number	Actual Gas Mass Flowrate	Equation 6.1	Equation 6.3	Equation 6.5	Equation 6.6
	(kg/s)	(kg/s)	(kg/s)	(kg/s)	(kg/s)
144	7.941	8.200	8.179	8.200	7.978
145	13.221	13.709	13.691	13.516	13.210
146	13.225	13.753	13.730	13.488	13.190
147	13.144	13.437	13.427	13.353	13.072
148	10.515	10.840	10.829	10.803	10.583
149	7.871	8.158	8.148	8.157	7.990
150	5.276	5.428	5.417	5.449	5.331
151	5.282	4.956	4.886	5.097	5.229
152	10.702	11.071	11.013	10.860	10.663
153	10.588	10.806	10.729	10.540	10.603
154	7.972	7.823	7.746	7.859	8.023
155	7.977	7.975	7.913	7.992	7.950
156	10.747	10.966	10.888	10.640	10.957
157	12.444	12.944	12.894	12.485	12.400
158	12.723	13.254	13.215	12.856	12.653
159	12.167	12.593	12.533	12.009	12.333
Sum of Residual Squares		0.0571294	0.0564288	0.0367618	0.0080418
Number of Points		80	80	80	80
R.M.S. Fractional Deviation		0.0267	0.0266	0.0214	0.0100

Table A5.2. The Root Mean Square Fractional Deviation Calculations at 40 Bar.

Point Number	Actual Gas Mass Flowrate	Equation 6.1	Equation 6.3	Equation 6.5	Equation 6.6
	(kg/s)	(kg/s)	(kg/s)	(kg/s)	(kg/s)
160	7.830	7.955	7.957	7.958	7.918
161	11.713	11.861	11.862	11.862	11.776
162	15.618	15.709	15.711	15.709	15.556
163	19.437	19.551	19.553	19.549	19.303
164	19.450	19.579	19.588	19.567	19.315
165	15.568	15.671	15.680	15.671	15.505
166	11.694	11.867	11.876	11.876	11.774
167	7.837	8.038	8.047	8.051	7.995
168	7.841	8.045	8.063	8.072	7.999
169	11.724	11.927	11.945	11.944	11.826
170	15.641	15.754	15.772	15.754	15.576
171	19.481	19.629	19.646	19.605	19.349
172	7.827	8.003	8.048	8.071	7.953
173	11.755	12.080	12.124	12.120	11.957
174	15.679	15.842	15.886	15.842	15.632
175	19.476	19.673	19.717	19.616	19.351
176	19.592	19.957	20.222	19.644	19.516
177	19.556	19.911	20.131	19.653	19.474
178	15.656	15.921	16.144	15.928	15.679
179	11.779	11.866	12.090	12.068	11.815
180	7.902	7.663	7.879	7.984	7.817
181	7.880	7.924	8.031	8.084	7.906
182	11.830	12.123	12.229	12.217	11.987
183	15.726	16.034	16.139	16.031	15.777
184	19.574	19.830	19.936	19.697	19.437
185	7.887	7.800	7.962	8.039	7.850
186	11.795	12.006	12.165	12.149	11.894
187	15.723	16.049	16.207	16.047	15.782
188	19.611	19.943	20.102	19.748	19.514
189	7.887	7.418	7.729	7.888	7.831
190	11.729	11.694	11.997	11.977	11.770
191	7.879	6.969	7.426	7.671	7.912
192	15.849	15.863	16.284	15.879	15.821
193	7.900	7.437	7.731	7.890	7.826
194	11.816	11.737	12.032	12.012	11.807
195	7.902	7 041	7.456	7.685	7.852
196	15.839	15.825	16.240	15.843	15.785
197	11.801	11.300	11.768	11.755	11.779
198	11.861	11.012	11.643	11.640	11.993
199	15.764	15.381	16.014	15.488	15.820
200	15.798	14.962	15.847	15.194	16.130
201	19.693	20.092	20.419	19.722	19.674
202	7.814	7.932	7.933	7.934	7.895
203	11.697	11.842	11.844	11.844	11.758
204	15.575	15.664	15.665	15.664	15.510
205	19.435	19.551	19.553	19.548	19.302
206	19.373	19.521	19.530	19.509	19.257
207	15.545	15.660	15.669	15.661	15.494
208	11.677	11.856	11.865	11.865	11.762
209	7.790	7.989	7.998	8.003	7.947
210	7.859	8.057	8.074	8.083	8.010
211	11.708	11.938	11.955	11.954	11.836
212	15.554	15.678	15.695	15.679	15.502
213	19.392	19.556	19.573	19.533	19.277
214	7.817	7.989	8.033	8.055	7.940
215	11.725	12.055	12.097	12.093	11.933
216	15.561	15.740	15.782	15.739	15.533
217	19.422	19.616	19.659	19.559	19.297
218	19.486	19.851	20.064	19.587	19.404
219	15.594	15.881	16.100	15.883	15.636
220	11.789	11.934	12.150	12.128	11.875
221	7.812	7.607	7.818	7.925	7.761
222	7.820	7.891	7.996	8.048	7.873
223	11.706	11.996	12.099	12.089	11.863

Point Number	Actual Gas Mass Flowrate	Equation 6.1	Equation 6.3	Equation 6.5	Equation 6.6
	(kg/s)	(kg/s)	(kg/s)	(kg/s)	(kg/s)
224	15.578	15.903	16.006	15.899	15.648
225	19.417	19.686	19.790	19.554	19.296
226	7.831	7.778	7.932	8.012	7.827
227	19.481	19.837	19.989	19.637	19.402
228	11.703	11.923	12.080	12.063	11.812
229	15.604	15.936	16.091	15.932	15.670
230	19.457	19.919	20.168	19.605	19.463
231	7.809	7.303	7.615	7.775	7.725
232	11.751	11.679	11.984	11.960	11.760
233	7.857	6.918	7.394	7.641	7.910
234	15.680	15.735	16.170	15.767	15.732
235	7.837	7.337	7.658	7.816	7.768
236	11.728	11.666	11.956	11.936	11.726
237	7.857	7.046	7.464	7.684	7.836
238	15.724	15.771	16.193	15.793	15.745
239	11.817	11.373	11.848	11.822	11.836
240	11.836	11.291	11.849	11.823	11.979
241	15.727	15.650	16.213	15.714	15.893
242	19.535	19.917	20.243	19.555	19.514
243	11.800	11.735	12.050	12.019	11.818
Sum of Residual Squares		0.096795	0.052141	0.026902	0.005905
Number of Points		84	84	84	80
R.M.S. Fractional Deviation		0.0340	0.0250	0.0181	0.0086

Table A5.3. The Root Mean Square Fractional Deviation Calculations at 60 Bar.

	Equation 6.1	Equation 6.3	Equation 6.5	Equation 6.6
Sum of 20 Bar Residual Squares	0.201159	0.083158	0.063006	0.003163
Sum of 40 Bar Residual Squares	0.057129	0.056429	0.036762	0.008042
Sum of 60 Bar Residual Squares	0.096795	0.052141	0.026902	0.005905
Sum of Total Residual Squares	0.355084	0.191728	0.126669	0.01711
Number of Points	243	243	243	243
R.M.S. Fractional Deviation	0.0383	0.0281	0.0229	0.0084

Table A5.4. The Root Mean Square Fractional Deviation Calculations with All the Data.

In Chapter 7 equation 7.3 is offered as a Venturi Meter wet gas correlation which uses the throat to downstream differential pressure to predict the gas mass flowrate provided the liquid mass flowrate is known. The performance of this correlation was discussed in terms of the root mean square fractional deviation (d). The equation used was:

$$d = \sqrt{\frac{1}{n}\sum_{i=1}^{n}\left(\frac{\dot{m}_{g(predicted)i} - \dot{m}_{g(experimental)i}}{\dot{m}_{g(experimental)i}}\right)^2}$$

These results were given in Table 7.2. The derivations of these stated values are given in Table A6.1 for the 20 Bar, 40 Bar and 60 Bar cases. Table A6.2 summarises the case where all the data was used. In these tables the "residual" is the bracketed term in the above equation.

20 Bar Point Number	20 Bar Actual Gas Mass Flowrate (kg/s)	20 Bar Equ. 7.3 Gas Mass Flowrate (kg/s)	40 Bar Point Number	40 Bar Actual Gas Mass Flowrate (kg/s)	40 Bar Equ. 7.3 Gas Mass Flowrate (kg/s)	60 Bar Point Number	60 Bar Actual Gas Mass Flowrate (kg/s)	60 Bar Equ. 7.3 Gas Mass Flowrate (kg/s)
1	2.764	2.741	80	5.126	Not Read	160	7.830	7.850
2	2.763	2.740	81	5.284	Not Read	161	11.713	11.577
3	4.135	4.137	82	7.886	Not Read	162	15.618	15.455
4	4.130	4.130	83	10.491	Not Read	163	19.437	20.239
5	5.495	5.548	84	13.083	Not Read	164	19.450	18.593
6	5.493	5.545	85	13.082	Not Read	165	15.568	15.154
7	6.878	6.709	86	10.476	Not Read	166	11.694	11.768
8	6.888	6.714	87	7.895	Not Read	167	7.837	7.774
9	2.753	2.771	88	5.259	Not Read	168	7.841	7.822
10	2.765	2.753	89	5.259	Not Read	169	11.724	11.941
11	2.769	2.709	90	7.870	Not Read	170	15.641	15.632
12	2.775	2.633	91	10.481	Not Read	171	19.481	19.023
13	4.198	3.978	92	13.083	Not Read	172	7.827	7.752
14	4.186	4.225	93	5.144	5.168	173	11.755	11.855
15	4.181	4.241	94	7.916	7.827	174	15.679	16.042
16	4.171	4.103	95	10.487	10.214	175	19.476	19.663
17	5.560	5.404	96	13.085	12.894	176	19.592	19.269
18	5.553	5.392	97	13.091	12.591	177	19.556	19.371
19	5.572	5.510	98	10.493	10.399	178	15.656	15.392
20	5.567	5.412	99	7.874	7.812	179	11.779	11.503
21	5.566	5.421	100	5.265	5.235	180	7.902	7.741
22	6.211	6.064	101	5.162	5.117	181	7.880	7.832
23	6.565	6.407	102	7.926	7.878	182	11.830	11.725
24	6.557	6.393	103	10.496	10.589	183	15.726	15.734
25	2.759	2.777	104	13.089	12.925	184	19.574	19.917
26	2.767	2.705	105	5.263	5.193	185	7.887	7.779
27	4.167	4.233	106	5.270	5.228	186	11.795	11.575
28	5.550	5.483	107	5.291	5.228	187	15.723	15.641
29	6.192	6.037	108	10.341	10.178	188	19.611	19.661
30	6.440	6.283	109	13.011	12.736	189	7.887	7.775
31	6.662	6.522	110	5.304	5.145	190	11.729	11.448
32	6.910	6.878	111	7.937	7.826	191	7.879	7.916
33	7.177	7.176	112	7.871	7.796	192	15.849	15.442
34	7.011	7.050	113	13.132	13.047	193	7.900	7.750
35	6.828	6.734	114	13.149	12.951	194	11.816	11.486
36	2.768	2.784	115	13.078	13.121	195	7.902	7.785
37	4.136	3.955	116	10.472	10.473	196	15.839	15.433
38	5.537	5.462	117	7.877	7.848	197	11.801	11.670
39	6.887	6.890	118	5.271	5.212	198	11.861	12.140
40	6.985	6.929	119	5.254	5.194	199	15.764	15.744
41	5.499	5.515	120	5.313	5.136	200	15.798	16.304
42	4.125	4.039	121	10.674	10.283	201	19.693	19.244
43	2.758	2.746	122	10.594	10.335	202	7.814	7.783
44	2.689	2.639	123	7.978	7.820	203	11.697	11.498
45	4.026	3.998	124	7.919	7.724	204	15.575	15.234
46	5.372	5.392	125	5.295	5.235	205	19.435	19.567
47	6.708	6.551	126	7.895	7.809	206	19.373	18.524
48	6.714	6.644	127	10.507	10.325	207	15.545	15.128
49	5.364	5.342	128	13.140	13.184	208	11.677	11.712
50	4.035	3.898	129	13.099	12.587	209	7.790	7.707
51	2.694	2.689	130	10.479	10.344	210	7.859	7.850
52	2.698	2.717	131	7.894	7.773	211	11.708	11.807
53	4.065	3.892	132	5.294	5.261	212	15.554	15.518
54	5.417	5.254	133	5.287	5.261	213	19.392	18.915
55	6.771	6.753	134	7.917	7.843	214	7.817	7.743
56	2.714	2.713	135	10.518	10.525	215	11.725	11.772
57	2.704	2.731	136	13.149	12.949	216	15.561	15.874
58	2.712	2.671	137	5.289	5.196	217	19.422	19.562
59	2.719	2.622	138	5.324	5.287	218	19.486	19.309
60	4.095	3.985	139	5.299	5.287	219	15.594	15.404

61	4.070	4.126	140	10.570	10.236	220	11.789	11.542
62	4.069	4.143	141	13.157	12.871	221	7.812	7.822
63	4.075	3.965	142	5.296	5.316	222	7.820	7.794
64	5.448	5.289	143	7.930	7.878	223	11.706	11.601
65	5.447	5.413	144	7.941	7.875	224	15.578	15.526
66	5.443	5.314	145	13.221	13.116	225	19.417	19.681
67	6.114	6.049	146	13.225	13.021	226	7.831	7.846
68	6.428	6.218	147	13.144	13.155	227	19.481	19.463
69	2.718	2.729	148	10.515	10.450	228	11.703	11.503
70	2.720	2.667	149	7.871	7.800	229	15.604	15.517
71	4.091	4.154	150	5.276	5.202	230	19.457	19.205
72	5.483	5.437	151	5.282	5.273	231	7.809	7.804
73	6.130	6.057	152	10.702	10.333	232	11.751	11.505
74	6.337	6.142	153	10.588	10.351	233	7.857	7.894
75	6.525	6.320	154	7.972	7.809	234	15.680	15.448
76	6.749	6.670	155	7.977	7.837	235	7.837	7.823
77	6.996	6.986	156	10.747	10.793	236	11.728	11.440
78	6.855	6.862	157	12.444	12.053	237	7.857	7.817
79	6.689	6.544	158	12.723	12.283	238	15.724	15.421
			159	12.167	12.212	239	11.817	11.772
Sum of Residual Squares	0.033063					240	11.836	12.050
Number of Points	79		Sum of Residual Squares		0.019961	241	15.727	15.697
R.M.S. Fractional Deviation	0.0205		Number of Points		67	242	19.535	19.321
			R.M.S. Fractional Deviation		0.0173	243	11.800	11.614
						Sum of Residual Squares		0.023392
						Number of Points		84
						R.M.S. Fractional Deviation		0.0167

Table A6.1. The Root Mean Square Fractional Deviation Calculations at 20 Bar, 40 Bar and 60 Bar for Equation 7.3.

Pressure	Sum of Residual Squares
20 Bar	0.033063
40 Bar	0.019961
60 Bar	0.023392
All Pressures	0.076416
Number of Data Points	230
R.M.S. Fractional Deviation	0.0182

Table A6.2. The Root Mean Square Fractional Deviation Calculation for Equation 7.3 using All Data.

In Chapter 7 the equations 6.11 and 7.3 are graphically combined to obtain a prediction of the gas mass flowrate without prior knowledge of the liquid flowrate. The result of combining these equations for each of the tests carried out is shown in Table A6.3 for 20 Bar, Table A6.4 for 40 Bar and Table A6.5 for 60 Bar. The end column noting problems lists three types.

"2 Soltns" denotes cases where two distinct solutions where observed.

"StpGrad" denotes cases where the two lines have relatively steep gradients.

"Ext." denotes cases where the upper limit of the equations have been exceeded to obtain a solution.

Point No.	Actual Gas Mass Flow (kg/s)	Predict Gas Mass Flow (kg/s)	Actual Liquid Mass Flow (kg/s)	Predict Liquid Mass Flow (kg/s)	Actual X	Predict X	% error Gas Mass Flow	% error Liquid Mass Flow	% error X	Problem
1	2.764	2.815	0.051	0.066	0.0034	0.0043	1.8469	30.336	27.962	
2	2.763	2.817	0.051	0.067	0.0034	0.0043	1.9624	31.661	29.116	
3	4.135	4.195	0.050	0.065	0.0022	0.0028	1.4557	28.994	27.127	
4	4.130	4.189	0.050	0.065	0.0022	0.0028	1.4248	29.202	27.375	
5	5.495	5.452	0.050	0.039	0.0017	0.0013	-0.7893	-20.970	-20.336	
6	5.493	5.495	0.050	0.040	0.0017	0.0013	0.0315	-20.838	-20.863	
7	6.878	6.826	0.050	0.106	0.0013	0.0028	-0.7610	113.06	114.71	
8	6.888	6.831	0.050	0.106	0.0013	0.0028	-0.8370	113.91	115.73	
9	2.753	2.778	0.641	0.612	0.0430	0.0407	0.9260	-4.571	-5.450	2 Soltns
10	2.765	2.773	1.217	1.180	0.0813	0.0786	0.2901	-3.028	-3.310	
11	2.769	2.806	1.778	1.610	0.1185	0.1059	1.3360	-9.434	-10.633	2 Soltns
12	2.775	2.862	2.442	2.043	0.1624	0.1317	3.1098	-16.357	-18.890	2 Soltns
13	4.198	4.337	3.654	3.036	0.1605	0.1290	3.3116	-16.918	-19.598	2 Soltns
14	4.186	4.122	2.728	2.920	0.1200	0.1304	-1.5202	7.049	8.712	2 Soltns
15	4.181	4.020	1.894	2.383	0.0833	0.1091	-3.8509	25.844	30.917	2 Soltns
16	4.171	4.048	0.958	1.263	0.0422	0.0574	-2.9495	31.923	35.958	
17	5.560	5.437	1.269	1.613	0.0419	0.0545	-2.2024	27.118	30.005	2 Soltns
18	5.553	5.420	1.282	1.564	0.0424	0.0530	-2.3968	21.972	24.993	2 Soltns
19	5.572	5.405	2.417	2.949	0.0797	0.1003	-3.0121	22.016	25.837	
20	5.567	5.484	3.583	3.354	0.1184	0.1125	-1.4925	-6.404	-4.974	
21	5.566	5.539	3.645	3.256	0.1205	0.1081	-0.4904	-10.680	-10.236	StpGrad
22	6.211	5.951	3.060	3.198	0.0906	0.1205	-4.1720	4.534	33.008	StpGrad
23	6.565	6.476	1.551	1.823	0.0434	0.0517	-1.3500	17.563	19.187	
24	6.557	6.460	1.553	1.819	0.0435	0.0517	-1.4696	17.111	18.875	
25	2.759	2.669	0.625	0.894	0.0417	0.0617	-3.2744	42.929	47.788	
26	2.767	2.789	1.812	1.667	0.1207	0.1102	0.7764	-7.996	-8.707	2 Soltns
27	4.167	3.976	1.811	2.384	0.0799	0.1103	-4.6012	31.622	38.011	2 Soltns
28	5.550	5.363	2.446	3.007	0.0810	0.1031	-3.3848	22.929	27.272	
29	6.192	5.940	3.052	3.836	0.0906	0.1187	-4.0725	25.687	31.073	StpGrad
30	6.440	6.328	1.861	2.201	0.0530	0.0638	-1.7263	18.269	20.367	
31	6.662	6.613	1.212	1.422	0.0333	0.0394	-0.7337	17.309	18.185	
32	6.910	6.917	0.676	0.740	0.0179	0.0196	0.1037	9.418	9.304	
33	7.177	7.188	0.402	0.410	0.0102	0.0104	0.1661	1.958	1.787	
34	7.011	7.067	0.565	0.579	0.0148	0.0150	0.7920	2.384	1.571	
35	6.828	6.857	0.800	0.961	0.0215	0.0257	0.4308	20.011	19.491	

Point No.	Actual Gas Mass Flow (kg/s)	Predict Gas Mass Flow (kg/s)	Actual Liquid Mass Flow (kg/s)	Predict Liquid Mass Flow (kg/s)	Actual X	Predict X	% error Gas Mass Flow	% error Liquid Mass Flow	% error X	Problem
36	2.768	2.783	0.321	0.318	0.0213	0.0210	0.5248	-0.856	-1.376	2 Soltns
37	4.136	4.084	0.319	0.534	0.0142	0.0240	-1.2468	67.468	69.596	2 Soltns
38	5.537	5.522	0.318	0.362	0.0105	0.0120	-0.2798	13.895	14.217	
39	6.887	6.928	0.317	0.341	0.0084	0.0090	0.6024	7.715	7.063	
40	6.985	6.959	0.155	0.153	0.0040	0.0040	-0.3776	-1.410	-1.032	
41	5.499	5.578	0.154	0.180	0.0051	0.0059	1.4309	17.009	15.344	
42	4.125	4.132	0.153	0.200	0.0068	0.0089	0.1706	30.636	30.412	
43	2.758	2.778	0.153	0.180	0.0102	0.0119	0.7285	17.462	16.609	
44	2.689	2.695	0.053	0.064	0.0036	0.0043	0.2202	21.042	20.775	
45	4.026	4.046	0.052	0.063	0.0024	0.0028	0.4953	19.537	18.944	
46	5.372	5.381	0.052	0.040	0.0017	0.0014	0.1690	-22.692	-22.824	
47	6.708	6.665	0.052	0.104	0.0014	0.0028	-0.6468	99.053	100.36	
48	6.714	6.661	0.154	0.160	0.0041	0.0043	-0.7868	3.944	4.777	
49	5.364	5.394	0.153	0.173	0.0052	0.0058	0.5546	12.784	12.157	
50	4.035	4.037	0.153	0.229	0.0069	0.0103	0.0549	49.885	49.802	
51	2.694	2.722	0.152	0.176	0.0103	0.0118	1.0241	15.865	14.686	
52	2.698	2.720	0.319	0.332	0.0216	0.0223	0.8325	4.131	3.268	
53	4.065	4.005	0.315	0.512	0.0141	0.0233	-1.4657	62.341	64.771	2 Soltns
54	5.417	5.415	0.316	0.440	0.0106	0.0148	-0.0299	39.524	39.566	
55	6.771	6.778	0.316	0.328	0.0085	0.0088	0.1037	3.780	3.671	
56	2.714	2.705	1.226	1.240	0.0824	0.0836	-0.3468	1.137	1.490	2 Soltns
57	2.704	2.760	0.640	0.518	0.0431	0.0342	2.0730	-19.006	-20.657	2 Soltns
58	2.712	2.735	1.773	1.657	0.1194	0.1106	0.8645	-6.562	-7.366	2 Soltns
59	2.719	2.812	2.438	2.097	0.1638	0.1362	3.4025	-13.997	-16.838	2 Soltns
60	4.095	4.182	3.629	3.298	0.1618	0.1440	2.1267	-9.115	-11.020	2 Soltns
61	4.070	3.985	2.726	2.360	0.1222	0.1080	-2.0788	-13.435	-11.586	2 Soltns
62	4.069	3.901	1.885	2.404	0.0845	0.1124	-4.1221	27.563	33.081	2 Soltns
63	4.075	3.904	0.956	1.250	0.0428	0.0584	-4.1994	30.833	36.604	StpGrad
64	5.448	5.316	1.275	1.616	0.0426	0.0554	-2.4153	26.736	29.899	2 Soltns
65	5.447	5.395	2.420	2.534	0.0810	0.0856	-0.9565	4.684	5.704	StpGrad
66	5.443	5.482	3.645	3.079	0.1221	0.1024	0.7206	-15.529	-16.138	StpGrad
67	6.114	5.935	3.035	3.782	0.0904	0.1161	-2.9351	24.613	28.417	
68	6.428	6.315	1.543	1.988	0.0436	0.0572	-1.7571	28.826	31.153	
69	2.718	2.746	0.631	0.563	0.0422	0.0373	1.0310	-10.794	-11.709	2 Soltns
70	2.720	2.762	1.802	1.632	0.1211	0.1080	1.5451	-9.432	-10.816	2 Soltns
71	4.091	3.945	1.797	2.271	0.0803	0.1052	-3.5683	26.375	31.081	2 Soltns
72	5.483	5.329	2.418	2.947	0.0805	0.1010	-2.8151	21.871	25.431	
73	6.130	5.897	2.965	3.955	0.0882	0.1224	-3.8051	33.378	38.704	
74	6.337	6.190	1.862	2.308	0.0535	0.0679	-2.3237	23.992	26.970	
75	6.525	6.453	1.202	1.547	0.0335	0.0436	-1.0965	28.753	30.194	
76	6.749	6.768	0.677	0.779	0.0182	0.0209	0.2752	15.164	14.845	
77	6.996	7.061	0.414	0.463	0.0107	0.0119	0.9352	11.940	10.891	
78	6.855	6.864	0.562	0.563	0.0149	0.0149	0.1279	0.125	-0.004	
79	6.689	6.689	0.797	0.993	0.0217	0.0270	0.0022	24.500	24.498	

Table A6.3. The Performance of the Simultaneous Gas and Liquid Mass Flowrate Prediction Method at 20 Bar.

Point No.	Actual Gas Mass Flow (kg/s)	Predict Gas Mass Flow (kg/s)	Actual Liquid Mass Flow (kg/s)	Predict Liquid Mass Flow (kg/s)	Actual X	Predict X	% error Gas Mass Flow	% error Liquid Mass Flow	% error X	Problem
80	5.126	N/A	0.038	N/A	0.0019	N/A	N/A	N/A	N/A	
81	5.284	N/A	0.029	N/A	0.0014	N/A	N/A	N/A	N/A	
82	7.886	N/A	0.028	N/A	0.0009	N/A	N/A	N/A	N/A	
83	10.491	N/A	0.028	N/A	0.0007	N/A	N/A	N/A	N/A	
84	13.083	N/A	0.028	N/A	0.0005	N/A	N/A	N/A	N/A	
85	13.082	N/A	0.159	N/A	0.0031	N/A	N/A	N/A	N/A	
86	10.476	N/A	0.158	N/A	0.0038	N/A	N/A	N/A	N/A	
87	7.895	N/A	0.159	N/A	0.0051	N/A	N/A	N/A	N/A	
88	5.259	N/A	0.159	N/A	0.0077	N/A	N/A	N/A	N/A	
89	5.259	N/A	0.320	N/A	0.0155	N/A	N/A	N/A	N/A	
90	7.870	N/A	0.317	N/A	0.0103	N/A	N/A	N/A	N/A	
91	10.481	N/A	0.316	N/A	0.0076	N/A	N/A	N/A	N/A	
92	13.083	N/A	0.315	N/A	0.0061	N/A	N/A	N/A	N/A	
93	5.144	5.215	0.033	0.058	0.0016	0.0028	1.3893	75.311	71.772	
94	7.916	7.965	0.033	0.032	0.0010	0.0010	0.6207	-3.164	-4.477	
95	10.487	10.295	0.032	0.115	0.0008	0.0028	-1.8333	256.06	259.84	
96	13.085	13.094	0.032	0.026	0.0006	0.0005	0.0677	-17.918	-18.718	
97	13.091	13.124	0.160	0.026	0.0031	0.0005	0.2521	-83.571	-83.762	
98	10.493	10.411	0.159	0.021	0.0038	0.0005	-0.7846	-86.958	-86.961	
99	7.874	7.898	0.159	0.194	0.0051	0.0062	0.3025	22.233	20.964	
100	5.265	5.292	0.159	0.200	0.0077	0.0096	0.5185	26.365	24.890	
101	5.162	5.141	0.318	0.466	0.0157	0.0230	-0.3979	46.450	46.087	2 Soltns
102	7.926	7.956	0.315	0.372	0.0101	0.0118	0.3783	18.143	16.824	2 Soltns
103	10.496	10.567	0.315	0.307	0.0076	0.0073	0.6807	-2.465	-3.930	
104	13.089	13.064	0.314	0.026	0.0061	0.0005	-0.1877	-91.681	-91.741	
105	5.263	5.176	0.785	1.017	0.0381	0.0499	-1.6385	29.567	30.885	StpGrad
106	5.270	5.347	1.272	1.054	0.0616	0.0500	1.4604	-17.146	-18.880	
107	5.291	5.168	2.429	2.529	0.1173	0.1242	-2.3257	4.111	5.916	2 Soltns
108	10.341	10.171	2.421	2.841	0.0587	0.0695	-1.6389	17.316	18.328	
109	13.011	12.747	3.043	3.379	0.0592	0.0665	-2.0329	11.047	12.373	
110	5.304	5.172	3.677	3.665	0.1768	0.1796	-2.4874	-0.317	1.579	2 Soltns
111	7.937	7.964	3.649	3.206	0.1168	0.1015	0.3372	-12.134	-13.078	
112	7.871	7.782	1.852	1.956	0.0597	0.0633	-1.1310	5.618	6.055	2 Soltns
113	13.132	13.032	1.830	1.793	0.0352	0.0344	-0.7649	-2.044	-2.169	
114	13.149	12.956	2.547	2.613	0.0489	0.0505	-1.4649	2.597	3.208	
115	13.078	13.057	0.798	0.737	0.0154	0.0141	-0.1612	-7.629	-8.314	
116	10.472	10.449	0.801	0.774	0.0194	0.0186	-0.2191	-3.376	-3.955	
117	7.877	7.885	0.803	0.935	0.0259	0.0299	0.0981	16.401	15.430	
118	5.271	5.122	0.809	1.010	0.0392	0.0500	-2.8315	24.832	27.663	
119	5.254	5.164	0.810	1.018	0.0393	0.0500	-1.7303	25.683	27.082	StpGrad
120	5.313	5.317	4.878	4.657	0.2351	0.2228	0.0743	-4.528	-5.222	2 Soltns
121	10.674	10.141	4.823	5.663	0.1147	0.1407	-4.9934	17.435	22.686	
122	10.594	10.170	7.224	8.076	0.1733	0.2003	-3.9992	11.791	15.564	
123	7.978	8.232	7.146	5.984	0.2286	0.1841	3.1781	-16.260	-19.471	StpGrad
124	7.919	7.887	5.402	4.969	0.1757	0.1611	-0.4026	-8.005	-8.309	StpGrad
125	5.295	5.299	0.025	0.059	0.0012	0.0028	0.0797	134.43	132.72	
126	7.895	7.938	0.027	0.019	0.0009	0.0006	0.5496	-30.935	-31.823	
127	10.507	10.313	0.027	0.115	0.0007	0.0028	-1.8425	321.53	326.04	
128	13.140	13.156	0.028	0.026	0.0005	0.0005	0.1199	-4.673	-5.654	
129	13.099	13.120	0.158	0.026	0.0030	0.0005	0.1600	-83.379	-83.557	
130	10.479	10.323	0.156	0.210	0.0038	0.0051	-1.4870	34.002	34.942	
131	7.894	7.962	0.156	0.230	0.0050	0.0073	0.8586	47.847	45.494	
132	5.294	5.327	0.155	0.201	0.0075	0.0096	0.6231	29.963	28.310	
133	5.287	5.294	0.317	0.434	0.0153	0.0208	0.1307	36.929	35.858	2 Soltns
134	7.917	7.969	0.316	0.372	0.0102	0.0118	0.6574	17.772	16.131	
135	10.518	10.499	0.315	0.305	0.0076	0.0073	-0.1780	-3.217	-3.839	
136	13.149	12.823	0.313	0.261	0.0060	0.0051	-2.4842	-16.698	-15.308	
137	5.289	5.121	0.793	0.965	0.0384	0.0479	-3.1868	21.623	24.840	StpGrad
138	5.324	5.352	1.265	1.151	0.0608	0.0547	0.5184	-8.995	-10.060	
139	5.299	5.131	2.419	2.652	0.1169	0.1315	-3.1632	9.614	12.485	2 Soltns

Point No.	Actual Gas Mass Flow (kg/s)	Predict Gas Mass Flow (kg/s)	Actual Liquid Mass Flow (kg/s)	Predict Liquid Mass Flow (kg/s)	Actual X	Predict X	% error Gas Mass Flow	% error Liquid Mass Flow	% error X	Problem
140	10.570	10.214	2.379	2.959	0.0572	0.0731	-3.3646	24.397	27.738	
141	13.157	12.878	3.008	3.187	0.0580	0.0622	-2.1191	5.966	7.323	
142	5.296	5.112	3.672	3.978	0.1775	0.1980	-3.4685	8.342	11.534	2 Soltns
143	7.930	8.039	3.644	3.114	0.1174	0.0982	1.3684	-14.549	-16.338	
144	7.941	7.855	1.840	1.984	0.0591	0.0640	-1.0893	7.844	8.242	2 Soltns
145	13.221	13.109	1.820	1.810	0.0349	0.0347	-0.8456	-0.520	-0.568	
146	13.225	13.031	2.535	2.640	0.0486	0.0509	-1.4692	4.159	4.781	
147	13.144	13.091	0.794	0.736	0.0152	0.0141	-0.4074	-7.333	-7.791	
148	10.515	10.497	0.796	0.870	0.0192	0.0208	-0.1638	9.382	8.664	
149	7.871	7.850	0.799	0.996	0.0258	0.0320	-0.2638	24.713	24.127	
150	5.276	5.151	0.804	1.014	0.0389	0.0499	-2.3712	26.168	28.415	StpGrad
151	5.282	5.277	4.958	4.985	0.2400	0.2400	-0.0898	0.555	-0.010	Ext.
152	10.702	10.168	4.692	5.671	0.1113	0.1406	-4.9839	20.872	26.263	
153	10.588	10.144	7.208	8.247	0.1732	0.2053	-4.1879	14.414	18.511	
154	7.972	8.321	7.092	5.615	0.2274	0.1711	4.3733	-20.827	-24.745	
155	7.977	8.035	5.453	4.904	0.1747	0.1548	0.7315	-10.058	-11.379	
156	10.747	10.811	9.136	9.123	0.2175	0.2141	0.5928	-0.135	-1.556	
157	12.444	11.957	5.966	6.769	0.1220	0.1429	-3.9183	13.455	17.125	
158	12.723	12.218	4.577	5.366	0.0914	0.1107	-3.9745	17.238	21.093	
159	12.167	12.289	9.229	8.796	0.1936	0.1811	0.9983	-4.693	-6.479	

Table A6.4. The Performance of the Simultaneous Gas and Liquid Mass Flowrate Prediction Method at 40 Bar.

Point No.	Actual Gas Mass Flow (kg/s)	Predict Gas Mass Flow (kg/s)	Actual Liquid Mass Flow (kg/s)	Predict Liquid Mass Flow (kg/s)	Actual X	Predict X	% error Gas Mass Flow	% error Liquid Mass Flow	% error X	Problem
160	7.830	7.815	0.029	0.010	0.0012	0.0004	-0.1905	-65.019	-65.462	
161	11.713	11.588	0.029	0.015	0.0008	0.0004	-1.0707	-47.480	-47.807	
162	15.618	15.268	0.029	0.171	0.0006	0.0034	-2.2421	481.13	483.13	
163	19.437	18.727	0.029	0.211	0.0005	0.0034	-3.6508	638.79	650.68	
164	19.450	18.719	0.158	0.217	0.0025	0.0035	-3.7572	37.392	39.761	
165	15.568	15.193	0.158	0.175	0.0031	0.0035	-2.4135	11.000	11.585	
166	11.694	11.667	0.157	0.130	0.0042	0.0034	-0.2319	-17.495	-18.711	
167	7.837	7.834	0.158	0.242	0.0063	0.0095	-0.0440	53.293	51.125	
168	7.841	7.870	0.320	0.396	0.0127	0.0155	0.3659	23.886	21.630	2 Soltns
169	11.724	11.778	0.318	0.247	0.0084	0.0064	0.4539	-22.497	-24.171	
170	15.641	15.466	0.317	0.329	0.0063	0.0065	-1.1177	3.641	2.785	
171	19.481	18.885	0.316	0.406	0.0050	0.0065	-3.0610	28.436	29.682	
172	7.827	7.687	0.796	1.065	0.0318	0.0427	-1.7875	33.831	34.310	2 Soltns
173	11.755	11.802	0.790	0.716	0.0209	0.0186	0.4024	-9.388	-11.300	
174	15.679	15.513	0.790	0.485	0.0156	0.0095	-1.0564	-38.594	-39.141	
175	19.476	19.125	0.786	0.412	0.0124	0.0065	-1.8035	-47.594	-47.783	
176	19.592	19.316	4.472	3.964	0.0706	0.0621	-1.4078	-11.362	-12.053	
177	19.556	19.382	3.676	3.197	0.0582	0.0500	-0.8910	-13.019	-14.159	
178	15.656	15.413	3.709	3.608	0.0737	0.0714	-1.5518	-2.713	-3.082	
179	11.779	11.387	3.754	4.227	0.0996	0.1141	-3.3230	12.609	14.555	
180	7.902	7.567	3.674	4.048	0.1459	0.1655	-4.2385	10.189	13.442	
181	7.880	8.079	1.849	1.284	0.0736	0.0491	2.5283	-30.552	-33.274	
182	11.830	11.715	1.843	1.993	0.0486	0.0522	-0.9741	8.146	7.357	
183	15.726	15.638	1.833	1.431	0.0362	0.0279	-0.5625	-21.937	-23.029	
184	19.574	19.524	1.825	1.017	0.0288	0.0158	-0.2596	-44.273	-45.362	
185	7.887	7.513	2.751	3.273	0.1094	0.1347	-4.7473	18.996	23.172	2 Soltns
186	11.795	11.502	2.733	3.100	0.0724	0.0828	-2.4827	13.432	14.380	
187	15.723	15.644	2.717	2.375	0.0538	0.0463	-0.5006	-12.586	-13.864	
188	19.611	19.513	2.701	1.811	0.0426	0.0281	-0.5009	-32.955	-34.103	
189	7.887	7.545	5.342	5.874	0.2147	0.2433	-4.3409	9.953	13.323	2 Soltns
190	11.729	11.193	5.231	6.153	0.1407	0.1707	-4.5682	17.626	21.252	
191	7.879	7.875	7.866	8.074	0.3162	0.3200	-0.0423	2.647	1.191	Ext.
192	15.849	15.520	7.175	6.940	0.1424	0.1379	-2.0778	-3.281	-3.129	
193	7.900	7.523	5.298	5.814	0.2096	0.2381	-4.7663	9.735	13.608	
194	11.816	11.347	5.287	5.836	0.1393	0.1575	-3.9618	10.383	13.049	StpGrad
195	7.902	7.583	7.395	7.936	0.2925	0.3225	-4.0444	7.326	10.268	Ext.
196	15.839	15.544	7.251	6.854	0.1423	0.1344	-1.8612	-5.485	-5.550	
197	11.801	12.253	8.118	6.222	0.2146	0.1556	3.8288	-23.360	-27.501	
198	11.861	13.485	10.774	5.796	0.2841	0.1318	13.690	-46.207	-53.612	
199	15.764	16.314	10.638	8.072	0.2104	0.1511	3.4928	-24.115	-28.181	
200	15.798	17.358	14.465	7.183	0.2861	0.1265	9.8743	-50.340	-55.801	
201	19.693	19.286	5.380	5.141	0.0849	0.0811	-2.0666	-4.430	-4.524	
202	7.814	7.754	0.034	0.086	0.0014	0.0034	-0.7740	151.46	149.75	
203	11.697	11.759	0.034	0.131	0.0009	0.0034	0.5282	288.97	280.29	
204	15.575	15.219	0.034	0.171	0.0007	0.0034	-2.2892	397.07	399.04	
205	19.435	18.732	0.036	0.211	0.0006	0.0034	-3.6174	489.84	499.12	
206	19.373	18.650	0.160	0.217	0.0025	0.0035	-3.7328	35.405	37.710	
207	15.545	15.161	0.159	0.175	0.0032	0.0035	-2.4689	9.744	10.388	
208	11.677	11.595	0.162	0.131	0.0043	0.0035	-0.7035	-18.884	-19.692	
209	7.790	7.833	0.160	0.242	0.0064	0.0095	0.5535	51.514	48.478	2 Soltns
210	7.859	7.848	0.315	0.318	0.0125	0.0125	-0.1345	0.992	-0.346	2 Soltns
211	11.708	11.651	0.312	0.244	0.0083	0.0064	-0.4851	-21.800	-22.753	
212	15.554	15.116	0.311	0.169	0.0062	0.0034	-2.8146	-45.509	-44.990	
213	19.392	18.812	0.309	0.406	0.0049	0.0065	-2.9872	31.104	32.280	
214	7.817	7.679	0.784	1.060	0.0313	0.0424	-1.7642	35.097	35.549	2 Soltns
215	11.725	11.721	0.780	0.709	0.0206	0.0185	-0.0376	-9.090	-10.608	2 Soltns
216	15.561	15.413	0.779	0.483	0.0155	0.0095	-0.9485	-37.965	-38.581	
217	19.422	19.043	0.771	0.411	0.0122	0.0065	-1.9543	-46.667	-46.773	
218	19.486	19.318	3.672	2.973	0.0581	0.0464	-0.8637	-19.041	-20.121	
219	15.594	15.444	3.724	3.453	0.0741	0.0680	-0.9605	-7.271	-8.183	

220	11.789	11.381	3.776	4.411	0.0999	0.1189	-3.4650	16.815	19.011	
221	7.812	7.452	3.686	4.406	0.1475	0.1823	-4.6161	19.548	23.615	
222	7.820	8.019	1.853	1.350	0.0740	0.0518	2.5386	-27.143	-30.003	
223	11.706	11.592	1.840	1.966	0.0489	0.0519	-0.9743	6.854	6.083	
224	15.578	15.471	1.833	1.568	0.0364	0.0308	-0.6850	-14.448	-15.530	
225	19.417	19.288	1.823	1.003	0.0289	0.0157	-0.6656	-44.977	-45.820	
226	7.831	7.423	2.762	3.583	0.1101	0.1481	-5.2140	29.756	34.560	2 Soltns
227	19.481	19.371	2.700	1.982	0.0427	0.0309	-0.5642	-26.593	-27.797	
228	11.703	11.410	2.746	3.194	0.0729	0.0856	-2.5076	16.320	17.329	
229	15.604	15.522	2.717	2.514	0.0539	0.0492	-0.5277	-7.463	-8.782	
230	19.457	19.241	4.326	3.932	0.0685	0.0616	-1.1125	-9.104	-10.082	
231	7.809	7.412	5.383	6.254	0.2155	0.2592	-5.0834	16.184	20.288	2 Soltns
232	11.751	11.529	5.281	5.290	0.1400	0.1406	-1.8893	0.173	0.391	
233	7.857	7.680	8.099	8.700	0.3231	0.3500	-2.2613	7.424	8.335	Ext.
234	15.680	15.602	7.252	6.644	0.1440	0.1300	-0.5013	-8.386	-9.722	
235	7.837	7.410	5.420	6.346	0.2168	0.2635	-5.4519	17.093	21.557	2 Soltns
236	11.728	11.432	5.107	5.223	0.1356	0.1399	-2.5248	2.271	3.175	
237	7.857	7.583	7.247	7.854	0.2885	0.3194	-3.4811	8.377	10.694	2 Soltns
238	15.724	15.512	7.195	6.891	0.1422	0.1354	-1.3476	-4.234	-4.804	
239	11.817	12.427	7.929	5.775	0.2096	0.1419	5.1576	-27.165	-32.281	
240	11.836	13.075	9.163	5.533	0.2428	0.1302	10.467	-39.618	-46.379	
241	15.727	16.043	9.162	7.676	0.1818	0.1463	2.0097	-16.218	-19.524	
242	19.535	19.410	5.317	4.617	0.0843	0.0721	-0.6387	-13.161	-14.522	
243	11.800	11.766	5.188	4.752	0.1374	0.1241	-0.2886	-8.409	-9.712	

Table A6.5. The Performance of the Simultaneous Gas and Liquid Mass Flowrate Prediction Method at 60 Bar.

Appendix Six (C)

In Chapter 7 the root mean square fractional deviations (d) for the simultaneous gas and liquid measurement method at 20 Bar, 40 Bar, 60 Bar and all pressures was given in Table 7.4. The equation used was:

$$d = \sqrt{\frac{1}{n}\sum_{i=1}^{n}\left(\frac{\dot{m}_{g(predicted)i} - \dot{m}_{g(experimental)i}}{\dot{m}_{g(experimental)i}}\right)^2}$$

These results were given in Table 7.4. The derivations of these stated values are given in Table A6.6 for the 20 Bar, 40 Bar and 60 Bar cases. Table A6.7 summarises the case where all the data was used. In these tables the "residual" is the bracketed term in the above equation.

20 Bar Point Number	20 Bar Actual Gas Mass Flowrate (kg/s)	20 Bar Prediction Gas Mass Flowrate (kg/s)	40 Bar Point Number	40 Bar Actual Gas Mass Flowrate (kg/s)	40 Bar Prediction Gas Mass Flowrate (kg/s)	60 Bar Point Number	60 Bar Actual Gas Mass Flowrate (kg/s)	60 Bar Prediction Gas Mass Flowrate (kg/s)
1	2.764	2.815	80	5.126	Not Read	160	7.830	7.815
2	2.763	2.817	81	5.284	Not Read	161	11.713	11.588
3	4.135	4.195	82	7.886	Not Read	162	15.618	15.268
4	4.130	4.189	83	10.491	Not Read	163	19.437	18.727
5	5.495	5.452	84	13.083	Not Read	164	19.450	18.719
6	5.493	5.495	85	13.082	Not Read	165	15.568	15.193
7	6.878	6.826	86	10.476	Not Read	166	11.694	11.667
8	6.888	6.831	87	7.895	Not Read	167	7.837	7.834
9	2.753	2.778	88	5.259	Not Read	168	7.841	7.870
10	2.765	2.773	89	5.259	Not Read	169	11.724	11.778
11	2.769	2.806	90	7.870	Not Read	170	15.641	15.466
12	2.775	2.862	91	10.481	Not Read	171	19.481	18.885
13	4.198	4.337	92	13.083	Not Read	172	7.827	7.687
14	4.186	4.122	93	5.144	5.215	173	11.755	11.802
15	4.181	4.020	94	7.916	7.965	174	15.679	15.513
16	4.171	4.048	95	10.487	10.295	175	19.476	19.125
17	5.560	5.437	96	13.085	13.094	176	19.592	19.316
18	5.553	5.420	97	13.091	13.124	177	19.556	19.382
19	5.572	5.405	98	10.493	10.411	178	15.656	15.413
20	5.567	5.484	99	7.874	7.898	179	11.779	11.387
21	5.566	5.539	100	5.265	5.292	180	7.902	7.567
22	6.211	5.951	101	5.162	5.141	181	7.880	8.079
23	6.565	6.476	102	7.926	7.956	182	11.830	11.715
24	6.557	6.460	103	10.496	10.567	183	15.726	15.638
25	2.759	2.669	104	13.089	13.064	184	19.574	19.524
26	2.767	2.789	105	5.263	5.176	185	7.887	7.513
27	4.167	3.976	106	5.270	5.347	186	11.795	11.502
28	5.550	5.363	107	5.291	5.168	187	15.723	15.644
29	6.192	5.940	108	10.341	10.171	188	19.611	19.513
30	6.440	6.328	109	13.011	12.747	189	7.887	7.545
31	6.662	6.613	110	5.304	5.172	190	11.729	11.193
32	6.910	6.917	111	7.937	7.964	191	7.879	7.875
33	7.177	7.188	112	7.871	7.782	192	15.849	15.520
34	7.011	7.067	113	13.132	13.032	193	7.900	7.523
35	6.828	6.857	114	13.149	12.956	194	11.816	11.347
36	2.768	2.783	115	13.078	13.057	195	7.902	7.583
37	4.136	4.084	116	10.472	10.449	196	15.839	15.544
38	5.537	5.522	117	7.877	7.885	197	11.801	12.253
39	6.887	6.928	118	5.271	5.122	198	11.861	13.485
40	6.985	6.959	119	5.254	5.164	199	15.764	16.314
41	5.499	5.578	120	5.313	5.317	200	15.798	17.358
42	4.125	4.132	121	10.674	10.141	201	19.693	19.286
43	2.758	2.778	122	10.594	10.170	202	7.814	7.754
44	2.689	2.695	123	7.978	8.232	203	11.697	11.759
45	4.026	4.046	124	7.919	7.887	204	15.575	15.219
46	5.372	5.381	125	5.295	5.299	205	19.435	18.732
47	6.708	6.665	126	7.895	7.938	206	19.373	18.650
48	6.714	6.661	127	10.507	10.313	207	15.545	15.161
49	5.364	5.394	128	13.140	13.156	208	11.677	11.595
50	4.035	4.037	129	13.099	13.120	209	7.790	7.833
51	2.694	2.722	130	10.479	10.323	210	7.859	7.848
52	2.698	2.720	131	7.894	7.962	211	11.708	11.651
53	4.065	4.005	132	5.294	5.327	212	15.554	15.116
54	5.417	5.415	133	5.287	5.294	213	19.392	18.812
55	6.771	6.778	134	7.917	7.969	214	7.817	7.679
56	2.714	2.705	135	10.518	10.499	215	11.725	11.721
57	2.704	2.760	136	13.149	12.823	216	15.561	15.413
58	2.712	2.735	137	5.289	5.121	217	19.422	19.043
59	2.719	2.812	138	5.324	5.352	218	19.486	19.318
60	4.095	4.182	139	5.299	5.131	219	15.594	15.444

61	4.070	3.985	140	10.570	10.214	220	11.789	11.381
62	4.069	3.901	141	13.157	12.878	221	7.812	7.452
63	4.075	3.904	142	5.296	5.112	222	7.820	8.019
64	5.448	5.316	143	7.930	8.039	223	11.706	11.592
65	5.447	5.395	144	7.941	7.855	224	15.578	15.471
66	5.443	5.482	145	13.221	13.109	225	19.417	19.288
67	6.114	5.935	146	13.225	13.031	226	7.831	7.423
68	6.428	6.315	147	13.144	13.091	227	19.481	19.371
69	2.718	2.746	148	10.515	10.497	228	11.703	11.410
70	2.720	2.762	149	7.871	7.850	229	15.604	15.522
71	4.091	3.945	150	5.276	5.151	230	19.457	19.241
72	5.483	5.329	151	5.282	5.277	231	7.809	7.412
73	6.130	5.897	152	10.702	10.168	232	11.751	11.529
74	6.337	6.190	153	10.588	10.144	233	7.857	7.680
75	6.525	6.453	154	7.972	8.321	234	15.680	15.602
76	6.749	6.768	155	7.977	8.035	235	7.837	7.410
77	6.996	7.061	156	10.747	10.811	236	11.728	11.432
78	6.855	6.864	157	12.444	11.957	237	7.857	7.583
79	6.689	6.689	158	12.723	12.218	238	15.724	15.512
			159	12.167	12.289	239	12.289	12.427
Sum of Residual Squares	0.030688					240	11.836	13.075
Number of Points	79	Sum of Residual Squares		0.026553		241	15.727	16.043
R.M.S. Fractional Deviation	0.01970	Number of Points		67		242	19.535	19.410
		R.M.S. Fractional Deviation		0.0199		243	11.800	11.766

Sum of Residual Squares		0.09167
Number of Points		84
R.M.S. Fractional Deviation		0.033

Table A6.6. The Root Mean Square Fractional Deviation Calculations at 20 Bar, 40 Bar and 60 Bar for the Simultaneous Gas and Liquid Flowrate Prediction Method.

Pressure	Sum of Residual Squares
20 Bar	0.030688
40 Bar	0.026553
60 Bar	0.09167
All Pressures	0.148911
Number of Data Points	230
R.M.S. Fractional Deviation	0.0254

Table A6.7. The Root Mean Square Fractional Deviation Calculation for the Simultaneous Gas and Liquid Flowrate Prediction Method Using All Data.

Appendix 7

<u>The Calculation of the NEL Wet Gas Loop Parameter Uncertainties</u>

As with all experimental apparatus there is a level of uncertainty in the stated values of individual parameters measured by the NEL Wet Gas Loop. However, as the NEL Wet Gas Loop is part of the United Kingdom Accreditation Service (UKAS) this research benefited from the extremely high calibre of measurement offered by this equipment. That is, this systems primary measurement uncertainties are considerably less than would be encountered in many other test rigs. These primary measurements are stated in Chapter 4 (Section 4.3.7) and are repeated below for the readers convenience.

From the NEL quality document [50] the following primary measurement uncertainties were stated:

The Yokogawa Pressure Transducers have an uncertainty of 0.1%.

The PRT (PT100) Temperature readings have an uncertainty of 0.05%.

The gas mass flow reference turbine meter reading has an uncertainty of 0.322%.

The liquid mass flow reference turbine reading has an uncertainty of 0.2%.

The compressibility factor (Z) in the equation of state has an uncertainty of 0.02%.

It is known from ISA Controls Ltd. that the Venturi Meter has an inside bore uncertainty of 0.9% and a throat diameter uncertainty of 0.1%.

All the Yokogawa Differential Pressure Transducers are held in calibration by the NEL to within 0.1%.

The liquid flow coefficient, K_l, (i.e. the product of the liquid compressibility factor and the discharge coefficient) is stated to have an uncertainty of 1% for flows with a Reynolds Number less than one million [9]. (All superficial liquid flows in this research are within this limit.)

From these primary uncertainties it was necessary to calculate the resulting uncertainties of the parameters required by this research. Namely, these were the eight parameters listed in Chapter 4 (Section 4.3.7), i.e.,

1) The gas density.

2) The liquid density.

3) The dry gas flow coefficient, K_g, (i.e. the product of the gas compressibility factor and the gas discharge coefficient).

4) The ratio of the square roots of the actual two-phase differential pressure between the upstream and throat pressure tappings and the differential pressure between these points that would be read if the gas phase flowed alone.

5) The Modified Lockhart Martinelli Parameter. That is, the ratio of the square roots of the differential pressure between the upstream and throat pressure tappings for when the liquid phase flows alone and when the gas phase flows alone.

6) The Gas Densiometric Froude Number. That is, the square root of the Inertial to Gravity Forces on a liquid drop in a gas flow.

7) The dry gas flow coefficient, K_g^*, (i.e. the flow coefficient which is defined as the product of the gas compressibility factor, the discharge coefficient and the velocity of approach for when the flow expansion between the throat and the downstream pressure tapping is used to meter the flow).

8) The ratio of the square roots of the actual two-phase differential pressure between the throat pressure tapping and the downstream pressure tapping and the differential pressure that would be read if the gas phase flowed alone.

In Chapter 4 (Section 4.3.7) these parameters had their percentage uncertainties stated. In this Appendix these values will now be derived. The standard analytical uncertainty calculation method was used here. For the case of the gas density at 20 Bar the method is worked through as an example. The remaining calculations are summarised in tables.

263

A7.1)An Example of the Gas Density Percentage Expanded Uncertainty Calculation

From the equation of state the density of nitrogen can be found (see equation A7.1)

$$\rho_g = \frac{P_g}{ZRT_g} \qquad \text{(A7.1)}$$

Taking a sample point (say point one in Appendix 3) the stated gas density was found to be 24.7073 kg/m^3. The absolute pressure measured was 2124161 N/m^2 and the temperature was 290.963 K. The product of the compressibility factor, Z, and the nitrogen gas constant, R (which is assumed to have effectively no uncertainty as it is an order of magnitude less than the uncertainties being dealt with here), was stated to be 295.477 J/KgK. On applying these values to equation A7.1 the above stated gas density is obtained.

In order to find the percentage expanded uncertainty in this gas density statement the following procedure was used. Each parameter required in the calculation of the gas density (i.e. the right hand side of equation A7.1) had the percentage expanded uncertainty stated and then the absolute expanded uncertainty calculated. The standard uncertainty (i.e. defined as half the expanded uncertainty and denoted as U_i) was then calculated. That is:

Step One

1) The Pressure measured was 2124161 N/m^2 and the percentage expanded uncertainty was stated to be 0.1%. The expanded uncertainty is therefore 2124.161 N/m^2. Therefore, the standard uncertainty, U_P, is half of this value, i.e., 1062.08 N/m^2.

2) The Temperature measured was 290.963 K and the percentage expanded uncertainty was stated to be 0.05%. The expanded uncertainty is therefore 0.145481 K. Therefore, the standard uncertainty, U_T, is half of this value, i.e., 0.072741 K.

3) The measured value of the product of the nitrogen compressibility factor and gas constant (denoted as ZR) was 295.477 J/Kg K and the percentage expanded uncertainty was stated to be 0.02%. The expanded uncertainty is therefore

0.059096 J/Kg K. Therefore, the standard uncertainty, U_{ZR}, is half of this value, i.e., 0.029548 J/Kg K.

It is now possible to add each parameters actual read value to its standard uncertainty and obtain that parameters maximum value. That is,

Step Two

1) The maximum pressure is the sum of the read pressure and the standard uncertainty of the pressure (U_p). That is, 2125223 N/m^2.

2) The maximum temperature is the sum of the read temperature and the standard uncertainty of the temperature (U_T). That is, 291.0354 K.

3) The maximum ZR value is the sum of the read ZR value and the standard uncertainty of the ZR (U_{ZR}). That is,295.5071 J/KgK).

The individual influence of each parameter on the gas density is now examined. By holding the other parameters constant the maximum gas density is calculated for each maximum parameter value by use of equation A7.1. That is,

Step 3

1) The gas density is calculated by equation A7.1 with the read pressure replaced by the maximum pressure calculated in Step 2. The resulting "maximum" gas density is 24.71968 kg/m^3.

2) The gas density is calculated by equation A7.1 with the read temperature replaced by the maximum temperature calculated in Step 2. The resulting "maximum" gas density is 24.70115 kg/m^3.

3) The gas density is calculated by equation A7.1 with the read value of ZR replaced by the maximum value of ZR calculated in Step 2. The resulting "maximum" gas density is 24.70485 kg/m^3.

It is now possible to calculate the difference in these three "maximum" gas densities to that which was read by the Wet Gas Loop. Denoting these differences as $\Delta \rho_P$,

$\Delta\rho_T$ and $\Delta\rho_{ZR}$ respectively the sensitivity coefficients C_i are defined as the ratio of the density differences $\Delta\rho_i$ to the standard uncertainty U_i That is,

<u>Step 4</u>

1) The difference between the "maximum" gas density when the maximum pressure is used and the read gas density is $\Delta\rho_p$. Here this value is 0.012354 kg/m^3. The pressure sensitivity coefficient, C_p, is defined as the ratio of this density difference and the standard uncertainty of the pressure (i.e. U_p) which was found in Step 2 to be 1062.08 N/m^2. Therefore, C_p is 1.16E-05.

2) The difference between the "maximum" gas density when the maximum temperature is used and the read gas density is $\Delta\rho_T$. Here this value is -0.00618 kg/m^3 (where the negative sign simply indicates that the increase in the temperature leads to a reduction in the gas density). The temperature sensitivity coefficient ,C_T, is defined as the ratio of this density difference and the standard uncertainty of the temperature (i.e. U_T) which was found in Step 2 to be 0.072741 K. Therefore, C_T is –0.08489.

3) The difference between the "maximum" gas density when the maximum value of ZR is used and the read gas density is $\Delta\rho_{ZR}$. Here this value is –0.00247 J/KgK. The pressure sensitivity coefficient, C_{ZR}, is defined as the ratio of this density difference and the standard uncertainty of the ZR value (i.e. U_{ZR}) which was found in Step 2 to be -0.00247 J/KgK. Therefore, C_{ZR} is –0.08361.

In order to find the percentage expanded uncertainty of the gas density the standard method now requires the use of equation A7.2

$$\% \ Expanded \ Uncertainty = \frac{2\sqrt{\sum_{i=1}^{n}(U_i * C_i)^2}}{\rho_g} * 100\% \qquad (A7.2)$$

266

Therefore the percentage expanded uncertainty of the gas density for this 20 Bar case is found to be 0.113572 %. Table A7.1 shows a summary of this calculation.

Gas Density	24.7073	kg/m³					
		Expanded	Standard	Parameter	Maximum	Sensitivity	Expanded
Parameter	Value	Uncertainty	Uncertainty	Maximum	Gas	Coefficient	Uncertainty
	Read	%	Ui	Value	Density	Ci	%
Pressure	2124161	0.1	1062.08	2125223	24.71968	1.16E-05	0.113572
Temperature	290.963	0.05	0.072741	291.0354	24.70115	-0.08489	
ZR	295.477	0.02	0.029548	295.5071	24.70485	-0.08361	

Table A7.1. A summary of the gas density percentage expanded uncertainty calculation for 20 Bar.

The same calculation was carried out for 40 Bar and 60 Bar. The results are shown in Table A7.2 and Table A7.3 below.

Gas Density	45.6602	kg/m³					
		Expanded	Standard	Parameter	Maximum	Sensitivity	Expanded
Parameter	Value	Uncertainty	Uncertainty	Maximum	Gas	Coefficient	Uncertainty
	Read	%	Ui	Value	Density	Ci	%
Pressure	4042375	0.1	2021.19	4044396	45.68299	1.13E-05	0.113572
Temperature	298.918	0.05	0.074729	298.99252	45.64875	-0.15271	
ZR	296.174	0.02	0.029617	296.2040	45.65560	-0.15415	

Table A7.2. A summary of the gas density percentage expanded uncertainty calculation for 40 Bar.

Gas Density		kg/m³					
		Expanded	Standard	Parameter	Maximum	Sensitivity	Expanded
Parameter	Value	Uncertainty	Uncertainty	Maximum	Gas	Coefficient	Uncertainty
	Read	%	Ui	Value	Density	Ci	%
Pressure	6026897	0.1	3013.45	6029911	70.46610	1.17E-05	0.113572
Temperature	290.354	0.05	0.072589	290.42661	70.41328	-0.24251	
ZR	294.715	0.02	0.029472	294.74486	70.42384	-0.23896	

Table A7.3. A summary of the gas density percentage expanded uncertainty calculation for 60 Bar.

A7.2) The Liquid Density Percentage Expanded Uncertainty

It was found by the Physical Properties Department of the NEL that the Kerosene substitute used varied linearly with temperature. The resulting linear line fit had an uncertainty of an order of magnitude less than the temperature measurement of the Wet Gas Loop. The expanded uncertainty of the liquid phase is therefore that of the temperature measurement, 0.05%.

A7.3) <u>The Dry Gas Flow Coefficient, K_g, Percentage Expanded Uncertainty</u>

In order to calculate the percentage expanded uncertainty of the dry gas flow coefficient a problem arises that did not exist in the worked example of section A7.1. This is the uncertainty in the K_g value itself when it is estimated from the dry gas flow equation (A7.3) is not the only uncertainty. In addition to this the uncertainty due to the gas mass flow reference turbine meter uncertainty and the line fit uncertainty needs to be established and then these uncertainties need to be combined to give an overall uncertainty. These uncertainties will now be looked at in turn.

A.7.3.1) <u>The Percentage Expanded Uncertainty of the Dry Gas Flow Coefficient K_g with Respect to the Primary Measurement Uncertainties of the NEL Wet Gas Loop</u>

The value of K_g was calculated for each dry gas test point shown in Appendix 2 at 20 Bar and 60 Bar using the Venturi gas mass flow equation (equation A7.3).

$$K_g = \frac{\dot{m}_g \sqrt{1 - \left(\frac{D_t}{D}\right)^4}}{\left(\frac{\pi}{4}\right) D_t^2 \sqrt{2\rho_g \Delta P_g}}$$

(A7.3)

As all the parameters in the right hand side of equation A7.3 have their uncertainties known the percentage expanded uncertainty of K_g could be calculated. The same method as used in section A7.1 was followed and Tables A7.4 and A7.5 summarise these uncertainty calculations for the 20 and 60 Bar cases respectively.

Kg	1.0186						
		Expanded	Standard	Parameter	Maximum	Sensitivity	Expanded
Parameter	Value	Uncertainty	Uncertainty	Maximum	Kg	Coefficient	Uncertainty
	Read	%	Ui	Value		Ci	%o
Gas Flowrate	4.07631	0.322	0.006563	4.082876	1.020266	0.249889	0.431194
Throat Diameter	0.07584	0.1	3.79E-05	0.075878	1.017511	-29.3962	
Pipe Diameter	0.13971	0.9	0.000629	0.140339	1.019487	1.370557	
Gas Density	24.3711	0.113572	0.013839	24.38497	1.018337	-0.02089	
Diff Prerssure	14702.0	0.1	7.351016	14709.38	1.018371	-3.5E-05	

Table A7.4 A summary of the K_g percentage expanded uncertainty calculation for 20 Bar.

Kg	1.03090						
		Expanded	Standard	Parameter	Maximum	Sensitivity	Expanded
Parameter	Value	Uncertainty	Uncertainty	Maximum	Kg	Coefficient	Uncertainty
	Read	%	Ui	Value		Ci	%
Gas Flowrate	6.79764	0.322	0.010944	6.808582	1.032556	0.151655	0.431194
Throat Diameter	0.07584	0.1	3.79E-05	0.075878	1.029768	-29.7503	
Pipe Diameter	0.13971	0.9	0.000629	0.140339	1.031768	1.387067	
Gas Density	70.0021	0.113572	0.039752	70.04188	1.030604	-0.00736	
Diff. Pressure	13897.0	0.1	6.948515	13903.98	1.030639	-3.7E-05	

Table A7.5. A summary of the K_g percentage expanded uncertainty calculation for 60 Bar.

The percentage expanded uncertainty for the gas flow coefficient is therefore 0.431194%. However, the practical use of these gas flow coefficients calculated from the dry gas tests was the creation of graphs of the gas flow coefficient, K_g, vs. the gas mass flow in order to fit a linear line to the data. Hence, each data point in these graphs has an uncertainty of 0.431194% with respect to the ordinate and 0.322% with respect to the abscissa. The next stage of the uncertainty analysis however was to calculate the maximum expanded uncertainty for the linear line fit for the 20 Bar and 60 Bar cases assuming the data points to have no uncertainty.

A7.3.2) <u>The Uncertainty in the Gas Flow Coefficient vs. Gas Mass Flowrate Linear Line Fit</u>

For both the 20 Bar and the 60 Bar case graphs of the gas flow coefficient vs. the gas mass flow were plotted and shown in Chapter 4 (Section 4.3.3) as Figures 4.6 and 4.7. These graphs show the best linear fit to the data assuming the calculated values of K_g and the read values of the gas mass flowrate have no uncertainty associated with them. The following calculation is the standard method for predicting the maximum uncertainty in the line fits.

The confidence level of the linear fit is found by the standard equation presented here as equation A7.4. This is the equation offered in the lecture notes of the British Statistics Company "Statistics for Industry".

$$(a + bX) \pm t(RSD)\sqrt{1 + \frac{1}{n} + \frac{\left(X - \bar{X}\right)^2}{(n-1)(SD(X))^2}} \qquad (A7.4)$$

Where $(a+bX)$ is the line fit.

t is the t-student value

a and b are the linear line fit constants.

n is the number of points in the data set.

X is the particular value on the abscissa in question (i.e. m_g).

$\bar{X}$ (or X_m) is the data set mean value of X (i.e. m_g here).

RSD is the Residual Standard Deviation.

$$RSD = \sqrt{\frac{Residual\ Sum\ of\ Squares}{Degrees\ of\ Freedom}} \qquad (A7.5)$$

i.e.

$SD(X)$ is the standard deviation of the data sets X values, i.e.:

$$SD(X) = \sqrt{\frac{\sum(X_i - X_m)^2}{(n-1)}} \qquad (A7.6)$$

Naturally in this case the value of X is the gas mass flowrate. From Appendix 2 it can be seen that at 20 bar there are 29 data points (i.e. $n = 29$) and therefore the value of the student-t test to get 95% confidence in the fit is 2.06 (i.e. $t = 2.06$). For 20 Bar the value of the Residual Standard Deviation was found to be 0.002491648 and the mean value of the gas mass flowrate was 5.064215 kg/s. The Standard Deviation $(SD(X))$ of the gas mass flowrate was 1.05912 kg/s. Therefore, with the line fit for 20 Bar being:

$$K_g = 1.046513 + \left(-1.58381 * 10^{-3}\right) m_g$$

Equation A7.4 can be applied across the gas mass flow range and confidence bands can then be plotted as in Figure A7.1.
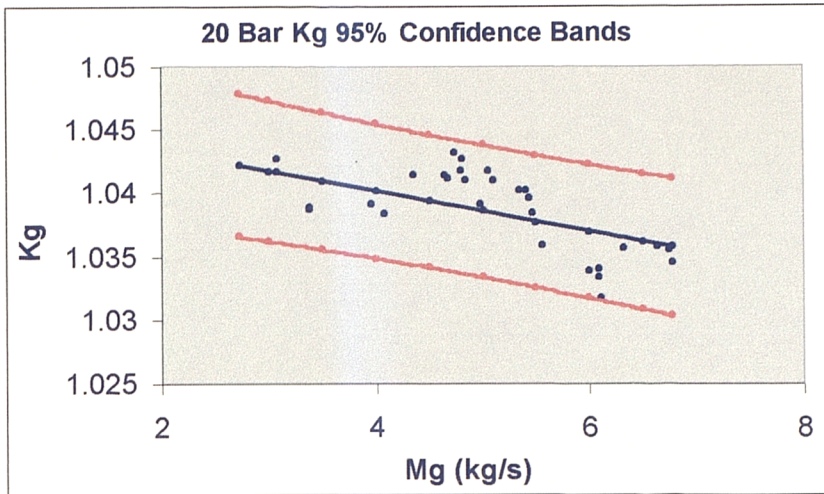
Figure A7.1 The Dry Gas Flow Coefficient 95% Confidence Bands associated with the linear line fitted to the data points.

For 20 Bar the maximum difference in the value of K_g between the linear fitted equation and the 95% confidence bands was found to be 0.0056436. As the equations predicted value of K_g was 1.04219985 the uncertainty is predicted to be 0.54151231 %.

Similarly for the 60 Bar case Appendix 2 shows that at 60 bar there are 24 data points (i.e. n = 24) and therefore the value of the student-t test to get 95% confidence in the fit is 2.08 (i.e. t = 2.08). For 60 Bar the value of the Residual Standard Deviation was found to be 0.00321918 and the mean value of the gas mass flowrate was 12.67107 kg/s. The Standard Deviation ($SD(X)$) of the gas mass flowrate was 3.458682 kg/s. Therefore, with the line fit for 60 Bar being:

$$K_g = 1.056648 + \left(-9.251689 * 10^{-4}\right)\dot{m}_g$$

Equation A7.4 can be applied across the gas mass flow range and confidence bands can then be plotted as in Figure A7.2.
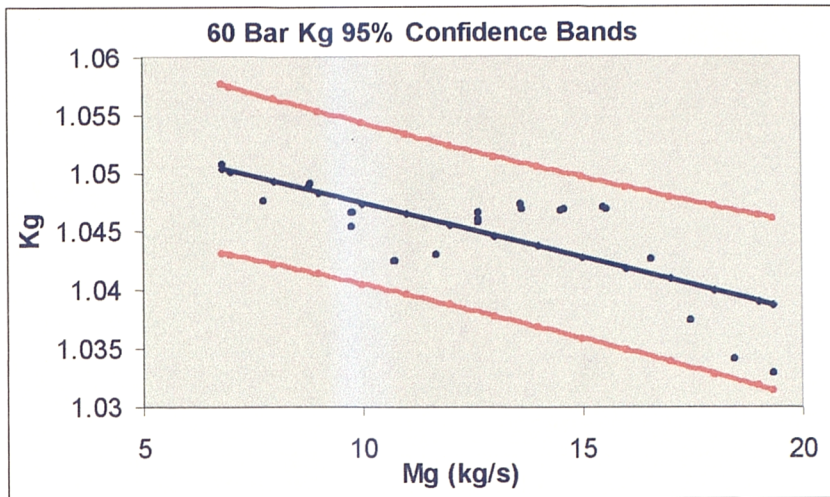
Figure A7.2. The Dry Gas Flow Coefficient 95% Confidence Bands associated with the linear line fitted to the data points.

For 60 Bar the maximum difference in the value of K_g between the linear fitted equation and the 95% confidence bands was found to be 0.00736387. As the equations predicted value of K_g was 1.03877697 the uncertainty is predicted to be 0.70889761%.

A7.3.3) The Total Uncertainty in the Predicted Values of the Gas Flow Coefficient

So far in this analysis the uncertainties for the data points and the linear line fit have been separately considered. In reality the magnitude of the actual uncertainty is a combination of these uncertainties. The maximum uncertainty is now calculated by use of equation A7.7.

$$U_{total} = \sqrt{\left(U_{m_g} + U_{K_g}\right)^2 + U_{lf}^2} \qquad \text{(A7.7)}$$

Where U_{total} is the total uncertainty in the K_g prediction

U_{m_g} is the uncertainty in the K_g prediction due to the uncertainty in the gas mass flowrate measurement.

U_{K_g} is the uncertainty in the K_g prediction due to the uncertainty in the parameters used to calculate K_g.

U_{lf} is the uncertainty in the K_g prediction due to the uncertainty in the line fit.

For both the 20 Bar and 60 Bar cases the value of U_{m_g} is 0.161%. This can be found from examination of Tables A7.4 and A7.5. It will be seen that for the 20 Bar case the read value of K_g is 1.018626 while the value predicted if the gas mass flowrate is 0.322% higher than read is 1.020266. For the 60 Bar case the read value of K_g is 1.030896 while the value predicted if the gas mass flowrate is 0.322% higher than read is 1.03256. For both cases the percentage difference is 0.161%. The value of U_{K_g} is as calculated in Tables A7.4 and A7.5, i.e. 0.431194%. The value of U_{lf} is predicted to be 0.54151231 % at 20 Bar and 0.70889761% at 60 Bar as previously discussed.

For 20 Bar the read value of K_g is 1.018626 and therefore the value of U_{m_g} is 0.001639987, the value of U_{K_g} is 0.00439225 and the value of U_{lf} is 0.005516 which means the value of U_{total} is 0.008174. This is a total uncertainty of 0.802452 %. For 60 Bar the read value of K_g is 1.030896 and therefore the value of U_{m_g} is 0.00165974, the value of U_{K_g} is 0.004445 and the value of U_{lf} is 0.007308 which means the value of U_{total} is 0.009522. This is a total uncertainty of 0.92370426 %. As no dry gas data was taken at 40 Bar the uncertainty is assumed to be 0.86307816 % by interpolation of the 20 Bar and 40 Bar results.

A7.4) The Uncertainty Calculation of the Ratio of the Square Roots of the Actual Wet Gas Differential Pressure between the Upstream and Throat Pressure Tappings and the Differential Pressure that would be Read if the Gas Phase Flowed Alone.

The uncertainty in the Yokogawa Transducers is 0.1% which means the uncertainty in the square root of the actual wet gas differential pressure read between the upstream and throat pressure tappings is 0.05%. The uncertainty of the differential pressure read between the upstream and throat pressure tappings if the

gas flow flowed alone has to be calculated. The Venturi mass flow equation is used to predict this differential pressure. This is given as equation A7.8.

$$\sqrt{\Delta P_g} = \frac{\dot{m}_g \sqrt{1 - \left(\frac{D_t}{D}\right)^4}}{\left(\frac{\pi}{4}\right) D_t^2 K_g \sqrt{2\rho_g}}$$

(A7.8)

The uncertainties of all the parameters on the right side of the equation were known so a summary of the standard calculation to find the percentage expanded uncertainty of point one in Appendix 3 is given in Table A7.6.

$\sqrt{\Delta P_g}$	79.8177						
		Expanded	Standard	Parameter	Maximum	Sensitivity	Expanded
Parameter	Value	Uncertainty	Uncertainty	Maximum	Sqr.Rt.DPg	Coefficient	Uncertainty
	Read	%	Ui	Value		Ci	%
Gas Flowrate	2.76415	0.322	0.00445	2.768599	79.94618	28.87604	0.906778
Flow Coefficient	1.04213	0.802452	0.004181	1.046314	79.4987	-76.2846	
Gas Density	24.7073	0.114	0.014083	24.72141	79.79493	-1.61457	
Throat Diameter	0.07584	0.1	3.79E-05	0.075878	79.73032	-2303.43	
Pipe Diameter	0.13971	0.9	0.000629	0.140339	79.88519	107.3944	

Table A7.6. The 20 Bar sample calculation for the percentage expanded uncertainty on the prediction of the square root of the differential pressure between the upstream and throat pressure tappings read if the gas phase flows alone.

Similar calculations were carried out for 40 Bar (point 80 of Appendix 3) and 60 Bar (point 160 of Appendix 3). Tables A7.7 and A7.8 summaries these calculations.

$\sqrt{\Delta P_g}$	109.174						
		Expanded	Standard	Parameter	Maximum	Sensitivity	Expanded
Parameter	Value	Uncertainty	Uncertainty	Maximum	Sqr.Rt.DPg	Coefficient	Uncertainty
	Read	%	Ui	Value		Ci	%
Gas Flowrate	5.12598	0.322	0.008253	5.134236	109.3502	21.29825	0.960193
Flow Coefficient	1.03839	0.863078	0.004481	1.042874	108.7054	-104.686	
Gas Density	45.7442	0.114	0.026074	45.77032	109.1434	-1.1928	
Throat Diameter	0.07584	0.1	3.79E-05	0.075878	109.055	-3150.63	
Pipe Diameter	0.13971	0.9	0.000629	0.140339	109.2668	146.8938	

Table A7.7. The 40 Bar sample calculation for the percentage expanded uncertainty on the prediction of the square root of the differential pressure between the upstream and throat pressure tappings read if the gas phase flows alone.

$\sqrt{\Delta P_g}$	134.958						
		Expanded	Standard	Parameter	Maximum	Sensitivity	Expanded
Parameter	Value	Uncertainty	Uncertainty	Maximum	Sqr.Rt.DPg	Coefficient	Uncertainty
	Read	%	Ui	Value		Ci	%
Gas Flowrate	7.83022	0.322	0.012607	7.842825	135.1755	17.23557	1.014325
Flow Coefficient	1.03411	0.923704	0.004776	1.038886	134.3378	-129.907	
Gas Density	70.4309	0.114	0.040146	70.47103	134.9198	-0.95768	
Throat Diameter	0.07584	0.1	3.79E-05	0.075878	134.8106	-3894.72	
Pipe Diameter	0.13971	0.9	0.000629	0.140339	135.0724	181.5858	

Table A7.8. The 60 Bar sample calculation for the percentage expanded uncertainty on the prediction of the square root of the differential pressure between the upstream and throat pressure tappings read if the gas phase flows alone.

With these percentage expanded uncertainties known it was possible to calculate the percentage expanded uncertainties of the ratio of the square roots of the actual wet gas differential pressure between the upstream and throat pressure tappings and the differential pressure that would be read if the gas phase flowed alone (i.e. $\sqrt{\Delta P_{tp} / \Delta P_g}$). The summaries of these calculations are given for 20 Bar (point 1 in Appendix 3) in Table A7.9, for 40 Bar (point 80 in Appendix 3) in Table A7.10 and for 60 Bar (point 160 in Appendix 3) in Table A7.11.

$\sqrt{\Delta P_{tp} / \Delta P_g}$	1.05438						
		Expanded	Standard	Parameter	Maximum	Sensitivity	Expanded
Parameter	Value	Uncertainty	Uncertainty	Maximum	Sqr.RtRatio	Coefficient	Uncertainty
	Read	%	Ui	Value		Ci	%
$\sqrt{\Delta P_{tp}}$	84.1579	0.05	0.021039	84.17895	1.054641	0.012529	0.904069
$\sqrt{\Delta P_g}$	79.8177	0.906778	0.361885	80.17955	1.049618	-0.01315	

Table A7.9. The 20 Bar sample calculation of the percentage expanded uncertainty for the ratio of the square roots of the differential pressure between the upstream and throat tappings of the actual wet gas and that which would be read if the gas flowed alone.

$\sqrt{\Delta P_{tp}/\Delta P_g}$	1.03501						
		Expanded	Standard	Parameter	Maximum	Sensitivity	Expanded
Parameter	Value	Uncertainty	Uncertainty	Maximum	Sqr.RtRatio	Coefficient	Uncertainty
	Read	%	Ui	Value		Ci	%
$\sqrt{\Delta P_{tp}}$	112.997	0.05	0.028249	113.025	1.035269	0.00916	0.956912
$\sqrt{\Delta P_g}$	109.175	0.960193	0.524143	109.6986	1.030065	-0.00944	

Table A7.10. The 40 Bar sample calculation of the percentage expanded uncertainty for the ratio of the square roots of the differential pressure between the upstream and throat tappings of the actual wet gas and that which would be read if the gas flowed alone.

$\sqrt{\Delta P_{tp}/\Delta P_g}$	1.02329						
		Expanded	Standard	Parameter	Maximum	Sensitivity	Expanded
Parameter	Value	Uncertainty	Uncertainty	Maximum	Sqr.RtRatio	Coefficient	Uncertainty
	Read	%	Ui	Value		Ci	%
$\sqrt{\Delta P_{tp}}$	138.101	0.05	0.034525	138.1364	1.023549	0.00741	1.010445
$\sqrt{\Delta P_g}$	134.958	1.014325	0.684458	135.6427	1.01813	-0.00754	

Table A7.11. The 60 Bar sample calculation of the percentage expanded uncertainty for the ratio of the square roots of the differential pressure between the upstream and throat tappings of the actual wet gas and that which would be read if the gas flowed alone.

A7.5) The Uncertainty of the Modified Lockhart Martinelli Parameter

The Modified Lockhart Martinelli Parameter is calculated from equation A7.9.

$$X = \left(\frac{\dot{m}_l}{\dot{m}_g}\right)\left(\frac{K_g}{K_l}\right)\sqrt{\frac{\rho_g}{\rho_l}} \qquad (A7.9)$$

As all the uncertainties of the parameters on the right hand side of the equation A7.6 are known standard uncertainty calculations could be made for the Modified

276

Lockhart Martinelli Parameter at each test pressure. Tables A7.12, A7.13 and A7.14 show a summary of these calculations for 20 Bar, 40 Bar and 60 Bar respectively.

X	0.00339						
		Expanded	Standard	Parameter	Maximum	Sensitivity	Expanded
Parameter	Value	Uncertainty	Uncertainty	Maximum	X	Coefficient	Uncertainty
	Read	%	Ui	Value		Ci	%
Gas Mass Flow	2.76415	0.322	0.00445	2.768599	0.003386	-0.00122	1.237006
Liq. Mass Flow	0.05101	0.2	5.1E-05	0.051058	0.003394	0.066481	
K_g	1.04213	0.626805	0.003266	1.045399	0.003402	0.003254	
K_l	0.995	1	0.004975	0.999975	0.003374	-0.00339	
Gas Density	24.7073	0.114	0.014083	24.72141	0.003392	6.86E-05	
Liquid Density	802.607	0.05	0.200652	802.808	0.003391	-2.1E-06	

Table A7.12. The 20 Bar Modified Lockhart Martinelli Uncertainty Calculation.

X	0.00189						
		Expanded	Standard	Parameter	Maximum	Sensitivity	Expanded
Parameter	Value	Uncertainty	Uncertainty	Maximum	X	Coefficient	Uncertainty
	Read	%	Ui	Value		Ci	%
Gas Mass Flow	5.12598	0.322	0.008253	5.134236	0.001889	-0.00037	1.237006
Liq. Mass Flow	0.03819	0.2	3.82E-05	0.038232	0.001894	0.049549	
K_g	1.05801	0.626805	0.003316	1.061325	0.001898	0.001789	
K_l	0.995	1	0.004975	0.999975	0.001883	-0.00189	
Gas Density	45.7442	0.114	0.026074	45.77032	0.001893	2.07E-05	
Liquid Density	801.760	0.05	0.20044	801.961	0.001892	-1.2E-06	

Table A7.13. The 40 Bar Modified Lockhart Martinelli Uncertainty Calculation.

X	0.00117						
		Expanded	Standard	Parameter	Maximum	Sensitivity	Expanded
Parameter	Value	Uncertainty	Uncertainty	Maximum	X	Coefficient	Uncertainty
	Read	%	Ui	Value		Ci	%
Gas Mass Flow	7.83022	0.322	0.012607	7.842825	0.001173	-0.00015	1.237006
Liq. Mass Flow	0.02907	0.2	2.91E-05	0.029095	0.001176	0.040414	
K_g	1.06389	0.626805	0.003334	1.067225	0.001178	0.001104	
K_l	0.995	1	0.004975	0.999975	0.001169	-0.00117	
Gas Density	70.4309	0.114	0.040146	70.47103	0.001175	8.34E-06	
Liquid Density	804.061	0.05	0.201015	804.2625	0.001175	-7.3E-07	

Table A7.14. The 60 Bar Modified Lockhart Martinelli Uncertainty Calculation.

A7.6) The Uncertainty of the Gas Densiometric Froude Number Parameter

The Gas Densiometric Froude Number is calculated from equation A7.10.

$$Fr_g = \frac{m_g}{\left(\frac{\pi}{4}\right)D^{2.5}\sqrt{g}}\sqrt{\frac{1}{\rho_g\left(\rho_l - \rho_g\right)}} \qquad (A7.10)$$

As all the uncertainties of the parameters on the right hand side of the equation A7.10 are known standard uncertainty calculations could be made for the Gas Densiometric Froude Number at each test pressure. Tables A7.15, A7.16 and A7.17 show a summary of these calculations for 20 Bar (point 1 of Appendix 3), 40 Bar (point 80 of Appendix 3) and 60 Bar (point 160 of Appendix 3) respectively.

Frg	1.11099						
		Expanded	Standard	Parameter	Maximum	Sensitivity	Expanded
Parameter	Value	Uncertainty	Uncertainty	Maximum	Frg	Coefficient	Uncertainty
	Read	%	Ui	Value		Ci	%
Gas Mass Flow	2.76415	0.322	0.00445	2.768599	1.112547	0.359327	2.296913
Pipe Diameter	0.13971	0.9	0.000629	0.140339	1.09836	-20.0216	
Gas Density	24.7160	0.113572	0.014035	24.73005	1.112241	0.092153	
Liquid Density	802.607	0.05	0.200652	802.808	1.110615	-0.00166	

Table A7.15. The 20 Bar Gas Densiometric Froude Number Uncertainty Calculation.

Frg	1.53585						
		Expanded	Standard	Parameter	Maximum	Sensitivity	Expanded
Parameter	Value	Uncertainty	Uncertainty	Maximum	Frg	Coefficient	Uncertainty
	Read	%	Ui	Value		Ci	%
Gas Mass Flow	5.12598	0.322	0.008253	5.134236	1.538328	0.299622	2.271593
Pipe Diameter	0.13971	0.9	0.000629	0.140339	1.518712	-27.2679	
Gas Density	45.7442	0.113572	0.025976	45.77022	1.537918	0.079401	
Liquid Density	801.760	0.05	0.20044	801.961	1.535652	-0.00102	

Table A7.16. The 40 Bar Gas Densiometric Froude Number Uncertainty Calculation.

Frg	1.91938						
		Expanded	Standard	Parameter	Maximum	Sensitivity	Expanded
Parameter	Value	Uncertainty	Uncertainty	Maximum	Frg	Coefficient	Uncertainty
	Read	%	Ui	Value		Ci	%
Gas Mass Flow	7.83029	0.322	0.012607	7.842825	1.922468	0.245124	2.271843
Pipe Diameter	0.13971	0.9	0.000629	0.140339	1.897954	-34.0771	
Gas Density	70.4309	0.113572	0.039995	70.47088	1.921975	0.064932	
Liquid Density	804.061	0.05	0.201015	804.2625	1.919115	-0.00131	

Table A7.17. The 60 Bar Gas Densiometric Froude Number Uncertainty Calculation.

A7.7) The Dry Gas Flow Coefficient, K_g^*, Percentage Expanded Uncertainty

The dry gas flow coefficient K_g^* is defined as the product of the gas compressibility factor, the discharge coefficient and the velocity of approach for when the flow expansion between the throat and the downstream pressure tapping is used to meter the flow. The percentage expanded uncertainty calculation was carried out using the same method as described in A7.3. That is, the uncertainty in the K_g^* value itself when it was calculated from the dry gas flow equation A7.11, the uncertainty caused by the gas mass reference meter reading and the uncertainty of the

line fit needs to be established separately and then these uncertainties need to be combined to give an overall uncertainty. These uncertainties will now be looked at in turn.

A7.7.1) The Percentage Expanded Uncertainty of the Dry Gas Flow Coefficient K_g^* with Respect to the Primary Measurement Uncertainties of the NEL Wet Gas Loop

The value of K_g^* was calculated for each dry gas test point shown in Appendix 2 at 20 Bar and 60 Bar using the Venturi gas mass flow equation for the throat to downstream expansion (equation A7.11).

$$K_g^* = \frac{m_g}{\left(\frac{\pi}{4}\right) D_t^2 \sqrt{2\rho_g \Delta P_g^*}}$$
(A7.11)

where all the percentage expanded uncertainties in the right hand side of the equation are known with the exception of the ΔP_g^* value. This is found by subtracting the upstream to downstream differential pressure from the upstream to the throat differential pressure. Both measurements have a percentage expanded uncertainty of 0.1%. The calculation of the uncertainty in the 20 Bar (point 1 in the 20 Bar data of Appendix 2) and 60 Bar (point 1 in the 60 Bar data of Appendix 2) ΔP_g^* values is summarised in Tables A7.18 and A7.19.

ΔP_g^*	13022.8						
		Expanded	Standard	Parameter	Maximum	Sensitivity	Expanded
Parameter	Value	Uncertainty	Uncertainty	Maximum	ΔP_g^*	Coefficient	Uncertainty
	Read	%	Ui	Value		Ci	%
ΔP_t	14702.0	0.1	7.351016	14709.38	13030.14	1	0.113629
ΔP_2	1679.24	0.1	0.839623	1680.085	13021.95	-1	

Table A7.18. The 20 Bar ΔP_g^* percentage expanded uncertainty calculation.

279

ΔP_g^*	12424.4						
		Expanded Uncertainty	Standard Uncertainty	Parameter Maximum	Maximum ΔP_g^*	Sensitivity Coefficient	Expanded Uncertainty
Parameter	Value	Read	%	Value		Ci	%
		%	Ui	Value			
ΔP_t	13897.0	0.1	6.948515	13903.98	12431.4	1	0.112478
ΔP_2	1472.58	0.1	0.73629	1473.316	12423.71	-1	

Table A7.19. The 60 Bar ΔP_g^* percentage expanded uncertainty calculation.

As all the parameters in the right hand side of equation A7.11 now have their uncertainties known the percentage expanded uncertainty of K_g^* can be calculated. The same method as used in section A7.1 was followed and Tables A7.20 and A7.21 summarise these uncertainty calculations for the 20 and 60 Bar cases respectively.

Kg *	1.13260						
		Expanded Uncertainty	Standard Uncertainty	Parameter Maximum	Maximum Kg *	Sensitivity Coefficient	Expanded Uncertainty
Parameter	Value	Read	%	Value		Ci	%
		%	Ui	Value			
Gas Mass Flow	4.07631	0.322	0.006563	4.082876	1.134423	0.277849	0.38739
Throat Diameter	0.07584	0.1	3.79E-05	0.075878	1.131467	-29.8457	
Gas Density	24.3711	0.113572	0.013839	24.38497	1.132278	-0.02323	
ΔP_g^*	13022.8	0.113629	7.398811	13030.19	1.132277	-4.3E-05	

Table A7.20. The 20 Bar K_g^* Percentage Expanded Uncertainty Calculation.

Kg *	1.14094						
		Expanded Uncertainty	Standard Uncertainty	Parameter Maximum	Maximum Kg *	Sensitivity Coefficient	Expanded Uncertainty
Parameter	Value	Read	%	Value		Ci	%
		%	Ui	Value			
Gas Mass Flow	6.79764	0.322	0.010944	6.808582	1.142775	0.167843	0.387306
Throat Diameter	0.07584	0.1	3.79E-05	0.075878	1.139798	-30.0655	
Gas Density	70.0021	0.113572	0.039752	70.04188	1.140615	-0.00815	
ΔP_g^*	12424.5	0.112478	6.987416	12431.44	1.140618	-4.6E-05	

Table A7.21. The 60 Bar K_g^* Percentage Expanded Uncertainty Calculation.

Therefore with the percentage expanded uncertainty in 20 Bar calculated to 0.38739 % and 60 Bar calculated to 0.38731 % all three test pressures had their percentage expanded uncertainty estimated as 0.38739 %. However, the practical use of these gas flow coefficients calculated from the dry gas tests was the creation of graphs of the throat pressure tapping to downstream pressure tapping flow coefficient, K_g^*, vs. the gas mass flow, m_g, in order to fit a linear line to the data. Hence, each data point in these graphs has an uncertainty of 0.38739 % with respect

to the ordinate and 0.322% with respect to the abscissa. The next stage of the uncertainty analysis however was to calculate the maximum expanded uncertainty for the linear line fit for the 20 Bar and 60 Bar cases assuming the data points to have no uncertainty.

A7.7.2) <u>The Uncertainty in the Gas Flow Coefficient, K_g^* vs. Gas Mass Flowrate Linear Line Fit</u>

For both the 20 Bar and the 60 Bar case graphs of the gas flow coefficient, K_g^* vs. the gas mass flow, m_g, were plotted and shown in Chapter 7 (Section 7.2.1) as Figures 7.6 and 7.7. These graphs show the best linear fit to the data assuming the calculated values of K_g^* and the read values of the gas mass flowrate have no uncertainty associated with them. The following calculation is the standard method for predicting the maximum uncertainty in line fits as in Section A7.3.2

From Appendix 2 as before it can be seen that at 20 bar there are 29 data points (i.e. $n = 29$) and therefore the value of the student-t test to get 95% confidence in the fit is 2.06 (i.e. $t = 2.06$). For 20 Bar the value of the Residual Standard Deviation was found to be 0.004487 and the mean value of the gas mass flowrate was 5.064215 kg/s. The Standard Deviation ($SD(X)$) of the gas mass flowrate was 1.05912 kg/s. Therefore, with the line fit for 20 Bar being:

$$K_g^* = 1.1158 + (-0.0027) m_g$$

Equation A7.4 can be applied across the gas mass flow range and confidence bands can then be plotted as in Figure A7.3.
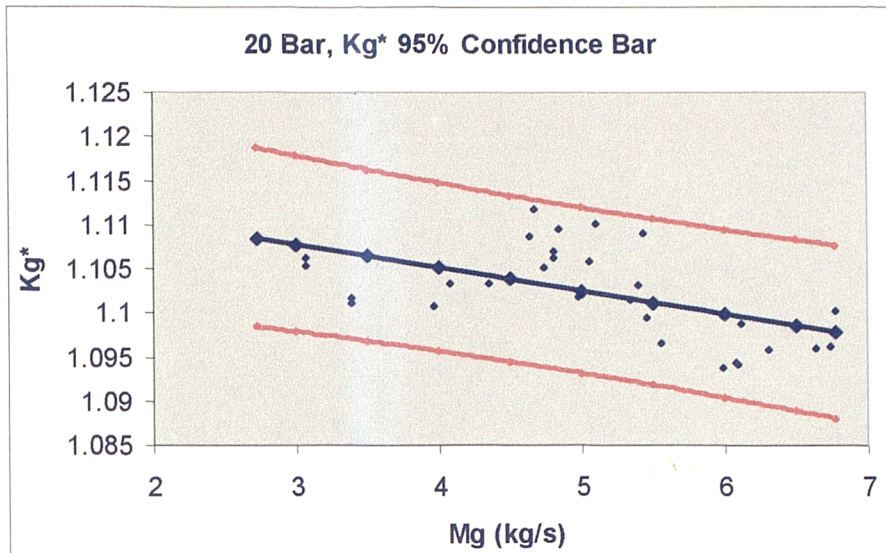
Figure A7.3. The 20 Bar Dry Gas Flow Coefficient, K_g^*, 95% Confidence Bands associated with the linear line fitted to the data points.

For 20 Bar the maximum difference in the value of K_g^* between the linear fitted equation and the 95% confidence bands was found to be 0.010163. As the equations predicted value of K_g^* was 1.10854 the uncertainty is predicted to be 0.916752 %.

Similarly for the 60 Bar case Appendix 2 shows that at 60 bar there are 24 data points (i.e. n = 24) and therefore the value of the student-t test to get 95% confidence in the fit is 2.08 (i.e. t = 2.08). For 60 Bar the value of the Residual Standard Deviation was found to be 0.003150 and the mean value of the gas mass flowrate was 12.67107 kg/s. The Standard Deviation ($SD(X)$) of the gas mass flowrate was 3.458682 kg/s. Therefore, with the line fit for 60 Bar being:

$$K_g^* = 1.1179 + (-0.0009)\dot{m}_g$$

Equation A7.4 can be applied across the gas mass flow range and confidence bands can then be plotted as in Figure A7.4.

60 Bar, Kg* 95% Confidence
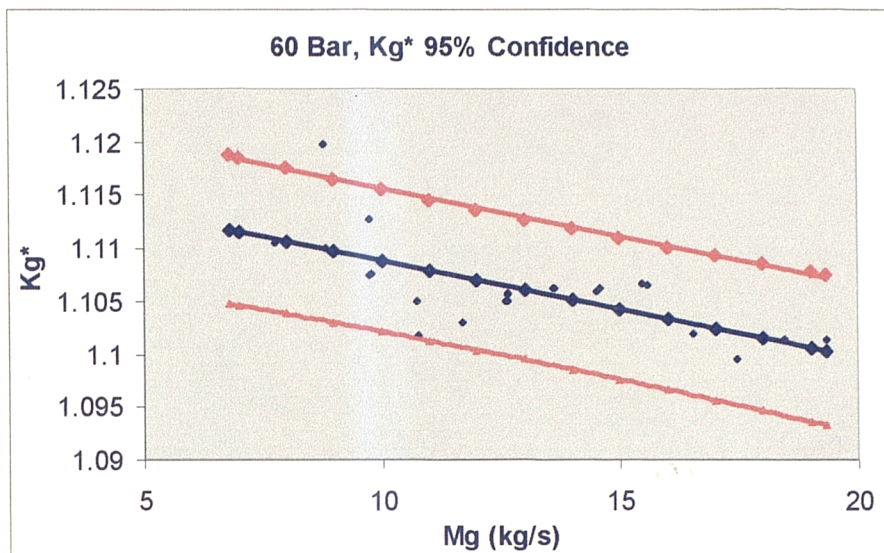
Figure A7.4. The 60 Bar Dry Gas Flow Coefficient, K_g^*, 95% Confidence Bands associated with the linear line fitted to the data points.

For 60 Bar the maximum difference in the value of K_g^* between the linear fitted equation and the 95% confidence bands was found to be 0.0071252. As the equations predicted value of K_g^* was 1.100292 the uncertainty is predicted to be 0.64757 %.

A7.7.3) The Total Uncertainty in the Predicted Values of the Gas Flow Coefficient, K_g^*

So far, as in Section A7.3, in this analysis of K_g^* the uncertainties for the data points and the linear line fit have been separately considered. In reality the magnitude of the actual uncertainty is a combination of these uncertainties. The maximum uncertainty is now calculated by use of equation A7.7.

Both the 20 Bar and 60 Bar cases for K_g^* the value of U_{m_g} was again 0.161%.

This can be found from examination of Tables A7.20 and A7.21. It will be seen that for the 20 Bar case the read value of K_g^* is 1.13260 while the value predicted if the gas mass flowrate is 0.322% higher than read is 1.13442. For the 60 Bar case the read value of K_g^* is 1.14094 while the value predicted if the gas mass flowrate is 0.322% higher than read is 1.14278. For both cases the percentage difference is

0.161%. The value of U_{K_g} is as calculated in Tables A7.20 and A7.21, i.e.

0.38739%. The value of U_{lf} is predicted to be 0.916752 % at 20 Bar and

0.64757% at 60 Bar as previously discussed. For 20 Bar the read value of K_g^* is

1.10854 and therefore the value of U_{m_g} is 0.001785, the value of U_{K_g} is 0.004294

and the value of U_{lf} is 0.010163 which means the value of U_{total} is 0.011842. This is

a total uncertainty of 1.068254 %. For 60 Bar the read value of K_g^* is 1.100292 and

therefore the value of U_{m_g} is 0.0017715, the value of U_{K_g} is 0.004262 and the value

of U_{lf} is 0.007125 which means the value of U_{total} is 0.009336. This is a total

uncertainty of 0.8485228 %. As no dry gas data was taken at 40 Bar the uncertainty

is assumed to be 0.9583883 % by interpolation of the 20 Bar and 40 Bar results.

A7.8) The Ratio of the Square Roots of the Actual Two-Phase Differential Pressure
between the Throat Pressure Tapping and the Downstream Pressure Tapping and the
Differential Pressure that would be Read if the Gas Phase Flowed Alone.

The uncertainty in the Yokogawa Differential Pressure Transducers is 0.1% The

uncertainties in the throat to downstream differential pressure reading were found to

be 0.202795% for 20 Bar (for point 1 of Appendix 3), 0.165353 % for 40 Bar (for

point 93 of Appendix 3) and 0.139634% for 60 Bar (for point 160 of Appendix 3)

from examination of the uncertainties of the parameters in equation A7.12.

$$\Delta P_{tp}^* = \Delta P_{tp} - \Delta P2 \qquad\qquad A7.12$$

These calculations are summarised in Tables A7.22 to A7.24.

ΔP_{tp}^*	3840.90	N/m^2					
		Expanded	Standard	Parameter	Maximum	Sensitivity	Expanded
Parameter	Value	Uncertainty	Uncertainty	Maximum		Coefficient	Uncertainty
	Read	%	Ui	Value		Ci	%
ΔP_{tp}	7082.55	0.1	3.541277	7086.095	3844.445	1	0.202795
$\Delta P2$	3241.65	0.1	1.620825	3243.271	3839.283	-1	

Table A7.22. The 20 Bar ΔP_{tp}^* calculation summary.

284

$\Delta P_{tp}{}^*$	8350.48	N/m²					
		Expanded	Standard	Parameter	Maximum	Sensitivity	Expanded
Parameter	Value	Uncertainty	Uncertainty	Maximum		Coefficient	Uncertainty
	Read	%	Ui	Value		Ci	%
ΔP_{tp}	13001.1	0.1	6.500534	13007.57	8356.984	1	0.165353
$\Delta P2$	4650.58	0.1	2.325292	4652.91	8348.158	-1	

Table A7.23. The 40 Bar $\Delta P_{tp}{}^*$ calculation summary.

$\Delta P_{tp}{}^*$	14112.9	N/m²					
		Expanded	Standard	Parameter	Maximum	Sensitivity	Expanded
Parameter	Value	Uncertainty	Uncertainty	Maximum		Coefficient	Uncertainty
	Read	%	Ui	Value		Ci	%
ΔP_{tp}	19072.1	0.1	9.536066	19081.67	14122.44	1	0.139634
$\Delta P2$	4959.23	0.1	2.479616	4961.712	14110.42	-1	

Table A7.24. The 60 Bar $\Delta P_{tp}{}^*$ calculation summary.

The percentage expanded uncertainty of the prediction of the square root of the differential pressure between the throat and downstream tappings for when the gas flows alone needs to be calculated. That is, the uncertainty in $\sqrt{\Delta P_g{}^*}$ when it is being predicted by equation A7.13 and not when it is being read off a dry gas flow as in Section A7.7.1.

$$\sqrt{\Delta P_g{}^*} = \frac{\dot{m}_g}{K_g{}^* \left(\frac{\pi}{4}\right) D_t{}^2 \sqrt{2\rho_g}}$$
(A7.13)

As all the uncertainties of the parameters on the right hand side of equation A7.13 are known the standard procedure for calculating the percentage expanded uncertainty of $\sqrt{\Delta P_g{}^*}$ could be carried out. Tables A7.25, A7.26 and A7.27 show summaries of these calculations.

$\sqrt{\Delta P_g^{\ *}}$	78.5305						
		Expanded	Standard	Parameter	Maximum	Sensitivity	Expanded
Parameter	Value	Uncertainty	Uncertainty	Maximum		Coefficient	Uncertainty
	Read	%	Ui	Value		Ci	%
Gas Mass Flow	2.76415	0.322	0.00445	2.768599	78.65691	28.41036	0.927289
Kg*	1.10843	0.84797	0.0047	1.113131	78.19893	-70.5492	
Gas Density	24.7073	0.114	0.014083	24.72141	78.50811	-1.58854	
Throat Diameter	0.07584	0.1	3.79E-05	0.075878	78.45201	-2069.4	

Table A7.25. The 20 Bar $\sqrt{\Delta P_g^{\ *}}$ calculation summary.

$\sqrt{\Delta P_g^{\ *}}$	106.184						
		Expanded	Standard	Parameter	Maximum	Sensitivity	Expanded
Parameter	Value	Uncertainty	Uncertainty	Maximum		Coefficient	Uncertainty
	Read	%	Ui	Value		Ci	%
Gas Mass Flow	5.14354	0.322	0.008281	5.151823	106.3552	20.64419	1.027454
Kg*	1.11447	0.957871	0.005338	1.119811	105.6782	-94.8234	
Gas Density	46.2873	0.114	0.026384	46.31365	106.154	-1.14652	
Throat Diameter	0.07584	0.1	3.79E-05	0.075878	106.0782	-2798.12	

Table A7.26. The 40 Bar $\sqrt{\Delta P_g^{\ *}}$ calculation summary.

$\sqrt{\Delta P_g^{\ *}}$	131.485						
		Expanded	Standard	Parameter	Maximum	Sensitivity	Expanded
Parameter	Value	Uncertainty	Uncertainty	Maximum		Coefficient	Uncertainty
	Read	%	Ui	Value		Ci	%
Gas Mass Flow	7.83022	0.322	0.012607	7.842825	131.6968	16.79201	1.129128
Kg*	1.11075	1.067772	0.00593	1.116675	130.7869	-117.747	
Gas Density	70.4309	0.114	0.040146	70.47103	131.4477	-0.93303	
Throat Diameter	0.07584	0.1	3.79E-05	0.075878	131.3537	-3464.84	

Table A7.27. The 60 Bar $\sqrt{\Delta P_g^{\ *}}$ calculation summary.

Therefore, the percentage expanded uncertainty of the ratio of the square roots of the actual two-phase differential pressure between the throat pressure tapping and the downstream pressure tapping and the differential pressure that would be read if the gas phase flowed alone can be calculated. Tables A7.28, A7.29 and A7.30 show summaries of these calculations.

$\sqrt{\Delta P_{tp}^* / \Delta P_g^*}$	0.82585						
		Expanded	Standard	Parameter	Maximum	Sensitivity	Expanded
Parameter	Value	Uncertainty	Uncertainty	Maximum		Coefficient	Uncertainty
	Read	%	Ui	Value		Ci	%
$\sqrt{\Delta P_{tp}^*}$	61.9750	0.165353	0.051239	62.02627	0.826537	0.013326	0.937704
$\sqrt{\Delta P_g^*}$	75.0436	0.927289	0.347935	75.3915	0.822043	-0.01095	

Table A7.28. The 20 Bar $\sqrt{\Delta P_{tp}^* / \Delta P_g^*}$ calculation summary.

$\sqrt{\Delta P_{tp}^* / \Delta P_g^*}$	0.90058						
		Expanded	Standard	Parameter	Maximum	Sensitivity	Expanded
Parameter	Value	Uncertainty	Uncertainty	Maximum		Coefficient	Uncertainty
	Read	%	Ui	Value		Ci	%
$\sqrt{\Delta P_{tp}^*}$	91.3810	0.139634	0.063799	91.44478	0.901205	0.009855	1.031696
$\sqrt{\Delta P_g^*}$	101.470	1.027454	0.521276	101.9908	0.895973	-0.00883	

Table A7.29. The 40 Bar $\sqrt{\Delta P_{tp}^* / \Delta P_g^*}$ calculation summary.

$\sqrt{\Delta P_{tp}^* / \Delta P_g^*}$	0.94549						
		Expanded	Standard	Parameter	Maximum	Sensitivity	Expanded
Parameter	Value	Uncertainty	Uncertainty	Maximum		Coefficient	Uncertainty
	Read	%	Ui	Value		Ci	%
$\sqrt{\Delta P_{tp}^*}$	118.798	0.069817	0.04147	118.8392	0.945819	0.007959	1.124958
$\sqrt{\Delta P_g^*}$	125.647	1.129128	0.709357	126.3563	0.940181	-0.00748	

Table A7.30. The 60 Bar $\sqrt{\Delta P_{tp}^* / \Delta P_g^*}$ calculation summary.

Hence, the percentage expanded uncertainty of $\sqrt{\Delta P_{tp}^* / \Delta P_g^*}$ for 20 Bar is 0.937704%, for 40 Bar is 1.031696% and for 60 Bar is 1.124958%.

A7.9) A Discussion on the Uncertainty Associated with the Gas Mass Flowrate Predictions of Equations 6.11 and 7.3.

When presenting a new correlation it is desirable to include an uncertainty analysis in order to indicate to the reader the confidence a user should have in the correlation. However, one of the problems often encountered by engineers during uncertainty analysis procedures is the fact that there is a lot of uncertainty about uncertainty. For the cases of this documents equations 6.11 and 7.3 it was found that no standard uncertainty analysis method existed in the literature. That is, such an uncertainty analysis is a PhD subject in its one right and hence the analysis is beyond the scope of this research. All that can be done here is to look at the standard deviation of the plotted points with respect to the equations predicted points for each of the surface fits (i.e. Figure 6.21, 6.22 and 6.23 for equation 6.11 and Figures 7.8, 7.9 and 7.10 for equation 7.3) to assess the closeness of the equation fit to the data points. These calculations are shown in Tabular form below (see Tables A7.31 to A7.36).

The Standard Deviations of the $\sqrt{\Delta P_{tp} / \Delta P_g}$ measured to predicted values of Figure 6.21, 6.22 and 6.23 for equation 6.11 and the Standard Deviations of the $\sqrt{\Delta P_{tp}^* / \Delta P_g^*}$ measured to predicted values of Figures 7.8, 7.9 and 7.10 for equation 7.3 are calculated by equation A7.14.

$$SD(Z) = \sqrt{\frac{\sum_{i=1}^{n}\left[\left(Z_{measured} - Z_{predicted}\right)^2\right]}{n-1}}$$

A7.14

where $Z_{measured}$ and $Z_{predicted}$ are the appropriate values of $\sqrt{\Delta P_{tp} / \Delta P_g}$ or $\sqrt{\Delta P_{tp}^* / \Delta P_g^*}$ and n is the number of data points. (In Tables A7.31 to A7.36 the values of $Z_{measured}$ - $Z_{predicted}$ are called the Residual.)

Point Number	X	Fr_g	Measured $\sqrt{\Delta P_{tp}/\Delta P_g}$	Predicted $\sqrt{\Delta P_{tp}/\Delta P_g}$	Residual
1	0.003391	1.110948	1.05437695	1.02382075	0.0305562
2	0.003361	1.110414	1.0549234	1.02371604	0.03120736
3	0.002226	1.662304	1.0500311	1.02590433	0.02412677
4	0.002222	1.66024	1.05080785	1.02586829	0.02493956
5	0.001657	2.209816	1.04004465	1.02987094	0.01017371
6	0.001668	2.209224	1.04031727	1.0299004	0.01041687
7	0.001318	2.766959	1.04112997	1.03463557	0.0064944
8	0.001312	2.771174	1.04067608	1.03465966	0.00601642
9	0.042757	1.111923	1.15252337	1.13239665	0.02012672
10	0.080718	1.115651	1.22085997	1.20848995	0.01237002
11	0.117707	1.116281	1.27826656	1.26524389	0.01302267
12	0.161277	1.11845	1.33920808	1.3172819	0.02192617
13	0.159607	1.686888	1.34324255	1.31767199	0.02557056
14	0.119441	1.682864	1.27817024	1.27023521	0.00793503
15	0.08298	1.681869	1.22141688	1.21567909	0.00573779
16	0.042083	1.679221	1.1524233	1.13521845	0.01720485
17	0.041811	2.233028	1.15633395	1.13882996	0.01750398
18	0.042301	2.23043	1.15711163	1.13991837	0.01719326
19	0.0795	2.234818	1.22473682	1.21299397	0.01174285
20	0.11809	2.229995	1.29441423	1.27098857	0.02342565
21	0.120157	2.229627	1.29875509	1.27370724	0.02504785
22	0.090393	2.486343	1.25022727	1.23227577	0.0179515
23	0.043295	2.630858	1.1678306	1.14515067	0.02267993
24	0.043413	2.627956	1.16868975	1.14539184	0.02329791
25	0.041537	1.11485	1.1497353	1.12958006	0.02015524
26	0.119893	1.116741	1.28085167	1.26819199	0.01265968
27	0.079532	1.678424	1.21543684	1.2097744	0.00566243
28	0.080701	2.228615	1.2274254	1.21500014	0.01242526
29	0.090314	2.481324	1.25061421	1.23212366	0.01849055
30	0.052915	2.582759	1.18549739	1.16536766	0.02012973
31	0.033291	2.67371	1.14758933	1.12237461	0.02521472
32	0.017886	2.77686	1.10904453	1.08372074	0.02532378
33	0.010237	2.889907	1.08238844	1.0631269	0.01926154
34	0.014744	2.823828	1.09833639	1.0754308	0.02290559
35	0.021464	2.746813	1.11972854	1.09310284	0.02662571
36	0.021263	1.113528	1.10479045	1.07787531	0.02691514
37	0.014141	1.66222	1.09105115	1.06272824	0.02832291
38	0.010501	2.22482	1.08329145	1.05745482	0.02583663
39	0.008402	2.766963	1.07441295	1.05650858	0.01790436
40	0.004041	2.810026	1.05174987	1.04365571	0.00809416
41	0.005115	2.211255	1.0623166	1.04088656	0.02143004
42	0.006823	1.658215	1.06844259	1.04056365	0.02787895
43	0.010199	1.108589	1.07279728	1.04545008	0.02734719
44	0.003561	1.091584	1.04970842	1.02417273	0.02553569
45	0.002355	1.634149	1.05080376	1.02602457	0.02477918
46	0.00175	2.181231	1.04054438	1.02986927	0.01067511
47	0.001398	2.724962	1.04195784	1.03445274	0.00750509
48	0.004133	2.725648	1.05460825	1.04308235	0.0115259
49	0.005172	2.177278	1.06276891	1.04071768	0.02205123
50	0.006876	1.637638	1.06895875	1.04051821	0.02844053
51	0.010284	1.093676	1.0745152	1.04556351	0.02895169

Point Number	X	Fr_g	Measured $\sqrt{\Delta P_{tp}/\Delta P_g}$	Predicted $\sqrt{\Delta P_{tp}/\Delta P_g}$	Residual
52	0.021549	1.09566	1.10360496	1.07850548	0.02509948
53	0.014123	1.649776	1.08927265	1.0625556	0.02671705
54	0.010595	2.197663	1.08397412	1.05746678	0.02650734
55	0.008482	2.74739	1.07674917	1.05655492	0.02019425
56	0.081939	1.104395	1.22562919	1.21053317	0.01509602
57	0.042953	1.099401	1.15303064	1.13275182	0.02027881
58	0.118647	1.103791	1.28458503	1.26645677	0.01812826
59	0.162624	1.10739	1.34884846	1.31865097	0.03019749
60	0.160754	1.664052	1.34420012	1.31878644	0.02541368
61	0.121499	1.654096	1.28322298	1.27281716	0.01040582
62	0.084038	1.653844	1.22434929	1.21729668	0.00705262
63	0.042601	1.655697	1.14963318	1.13622349	0.01340969
64	0.042494	2.209187	1.15874349	1.14019265	0.01855084
65	0.080637	2.209129	1.23046712	1.21477801	0.01568911
66	0.121609	2.205965	1.30636347	1.27548906	0.03087441
67	0.090145	2.475353	1.25649556	1.23182496	0.02467061
68	0.04354	2.60372	1.16893362	1.14549328	0.02344034
69	0.042145	1.105829	1.15009393	1.13092838	0.01916555
70	0.120296	1.107922	1.28713207	1.26868916	0.0184429
71	0.07978	1.663747	1.21862387	1.21011487	0.008509
72	0.08012	2.224871	1.22828784	1.21399231	0.01429553
73	0.08791	2.483068	1.25217318	1.22831403	0.02385915
74	0.053342	2.567594	1.18704118	1.16613909	0.02090209
75	0.033431	2.644042	1.14907519	1.12247278	0.02660241
76	0.01818	2.736864	1.11174137	1.084165	0.02757638
77	0.010724	2.838751	1.08611101	1.06405684	0.02205417
78	0.014883	2.78085	1.10111017	1.07542407	0.0256861
79	0.021653	2.7129	1.1207609	1.09330445	0.02745645
				Sum of Residual Squares	0.034978281
				Standard Deviation	0.02117639

Table A7.31. The Standard Deviation Calculation for equation 6.11 at 20 Bar.

Point Number	X	Fr_g	Measured $\sqrt{\Delta P_{tp}/\Delta P_g}$	Predicted $\sqrt{\Delta P_{tp}/\Delta P_g}$	Residual
1	0.001892	1.535855	1.03501057	1.01011595	0.02489462
2	0.001405	1.557435	1.03303561	1.00910811	0.0239275
3	0.000925	2.326957	1.02698956	1.01149724	0.01549231
4	0.000681	3.098023	1.01883076	1.01474266	0.00408809
5	0.000554	3.866642	1.02017348	1.0186528	0.00152068
6	0.003161	3.867603	1.02696444	1.0254812	0.00148323
7	0.003923	3.096087	1.02844382	1.02277488	0.00566894
8	0.005202	2.331705	1.04533217	1.02159982	0.02373235
9	0.007799	1.552021	1.05337062	1.02338494	0.02998567
10	0.015706	1.551958	1.07068529	1.04060785	0.03007744
11	0.010442	2.323251	1.06280867	1.03367414	0.02913453
12	0.007828	3.096226	1.03911004	1.03232532	0.00678472
13	0.006272	3.867422	1.03413336	1.03351938	0.00061398
14	0.001651	1.53204	1.04696995	1.00955353	0.03741642
15	0.001067	2.33662	1.02738294	1.01188056	0.01550238
16	0.000798	3.098153	1.01904991	1.01503535	0.00401456
17	0.000635	3.868353	1.02068286	1.01887559	0.00180727
18	0.003177	3.871302	1.02731469	1.02554412	0.00177056
19	0.003932	3.101559	1.02879579	1.0228292	0.00596659
20	0.005223	2.325588	1.04632185	1.02161575	0.0247061
21	0.007782	1.553916	1.05337881	1.02335722	0.03002159
22	0.015927	1.523598	1.07119999	1.04090692	0.03029307
23	0.01029	2.340215	1.0614656	1.03342847	0.02803714
24	0.00779	3.101604	1.0396506	1.03226547	0.00738513
25	0.006245	3.870038	1.03465314	1.03346585	0.00118729
26	0.038496	1.553172	1.11075077	1.08760285	0.02314791
27	0.062236	1.556408	1.14604534	1.13276549	0.01327985
28	0.118257	1.563712	1.22162476	1.22636832	-0.0047436
29	0.060113	3.082721	1.16593902	1.14675043	0.01918859
30	0.061012	3.832953	1.15904592	1.15867952	0.0003664
31	0.178276	1.567881	1.30001767	1.3103176	-0.0102999
32	0.118738	2.342851	1.23936889	1.23911333	0.00025556
33	0.060763	2.323717	1.1510659	1.13869767	0.01236823
34	0.036272	3.872242	1.11206362	1.10589058	0.00617304
35	0.050486	3.877036	1.14113641	1.13724018	0.00389623
36	0.015866	3.865771	1.06127907	1.05763001	0.00364906
37	0.019848	3.093783	1.07918801	1.06076144	0.01842657
38	0.026372	2.327406	1.09505587	1.06908891	0.02596696
39	0.039588	1.557647	1.11138933	1.08979952	0.02158982
40	0.039745	1.552288	1.11358373	1.09006149	0.02352224
41	0.236384	1.572339	1.38545368	1.37916801	0.00628566
42	0.117469	3.146941	1.25166445	1.25055479	0.00110966
43	0.177531	3.121749	1.34404718	1.33865015	0.00539703
44	0.232038	2.358004	1.41142398	1.38990913	0.02151485
45	0.178354	2.365462	1.33152818	1.32491531	0.00661287
46	0.001219	1.558908	1.03315615	1.00869439	0.02446176
47	0.000897	2.326321	1.02788542	1.01142778	0.01645763
48	0.000672	3.098178	1.02032592	1.01472027	0.00560565
49	0.000547	3.877425	1.02161503	1.01869764	0.00291739
50	0.003138	3.865356	1.02802792	1.02540599	0.00262193
51	0.003876	3.090984	1.02918735	1.02263123	0.00655612

Point Number	X	Fr_g	Measured $\sqrt{\Delta P_{tp}/\Delta P_g}$	Predicted $\sqrt{\Delta P_{tp}/\Delta P_g}$	Residual
52	0.005114	2.326934	1.04718366	1.02136963	0.02581403
53	0.007577	1.559359	1.05397132	1.02293258	0.03103873
54	0.015519	1.557739	1.07077852	1.04024157	0.03053695
55	0.010354	2.333313	1.06379581	1.03353193	0.03026388
56	0.007784	3.102115	1.04126909	1.0322558	0.0090133
57	0.006214	3.880759	1.03505513	1.03345934	0.00159579
58	0.038786	1.559056	1.1110351	1.08822716	0.02280794
59	0.061421	1.57017	1.14463072	1.13142486	0.01320586
60	0.1179	1.563838	1.22424106	1.22582483	-0.0015838
61	0.058606	3.111983	1.15034917	1.14413202	0.00621715
62	0.059796	3.869655	1.15755599	1.15669937	0.00085662
63	0.179088	1.564201	1.30101248	1.31129094	-0.0102785
64	0.119244	2.338658	1.24212367	1.23983869	0.00228498
65	0.06013	2.341143	1.15076239	1.13769573	0.01306667
66	0.035992	3.893188	1.11092196	1.10549312	0.00542884
67	0.050155	3.893664	1.13953584	1.13674921	0.00278663
68	0.015719	3.875925	1.06058734	1.05735271	0.00323463
69	0.019642	3.100385	1.07742275	1.06033893	0.01708382
70	0.026276	2.321393	1.09559499	1.06883306	0.02676193
71	0.039317	1.556308	1.11142408	1.08925339	0.02217068
72	0.241659	1.559905	1.38075962	1.38466098	-0.0039014
73	0.114031	3.148293	1.24773184	1.24496536	0.00276648
74	0.177354	3.115025	1.346001	1.33827512	0.00772588
75	0.23068	2.352894	1.40183219	1.38827342	0.01355877
76	0.177229	2.354364	1.32480475	1.32323237	0.00157238
77	0.222097	3.164181	1.42219311	1.39550097	0.02669214
78	0.125523	3.66178	1.27256476	1.2729668	-0.000402
79	0.094171	3.746443	1.21902121	1.22106319	-0.002042
80	0.19898	3.579618	1.39711237	1.37635301	0.02075936
				Sum of Residual Squares	0.022259187
				Standard Deviation	0.016785764

Table A7.32. The Standard Deviation Calculation for equation 6.11 at 40 Bar.

Point Number	X	Fr_g	Measured $\sqrt{\Delta P_{tp}/\Delta P_g}$	Predicted $\sqrt{\Delta P_{tp}/\Delta P_g}$	Residual
1	0.001175	1.919378	1.02329341	1.00686911	0.0164243
2	0.000783	2.874031	1.01666877	1.00874257	0.0079262
3	0.000599	3.834915	1.00683461	1.0112228	-0.0043882
4	0.000469	4.776308	1.00393562	1.01396574	-0.0100301
5	0.002591	4.780321	1.00826475	1.01853841	-0.0102737
6	0.003224	3.824641	1.01204016	1.01660245	-0.0045623
7	0.00427	2.871379	1.0248334	1.0156453	0.0091881
8	0.006374	1.922758	1.04192933	1.01678084	0.02514849
9	0.012909	1.9235	1.05379116	1.02906633	0.02472483
10	0.008616	2.877902	1.03487647	1.02419863	0.01067784
11	0.00646	3.841738	1.01818316	1.02328757	-0.0051044
12	0.005179	4.78836	1.01362146	1.02409182	-0.0104704
13	0.032199	1.920394	1.08384535	1.06426754	0.01957781
14	0.02134	2.88456	1.0673712	1.04871578	0.01865541
15	0.016042	3.849891	1.03795722	1.0426429	-0.0046857
16	0.012879	4.785248	1.02949216	1.04030801	-0.0108159
17	0.07315	4.805634	1.14361152	1.15727613	-0.0136646
18	0.060243	4.802053	1.12045244	1.13364544	-0.013193
19	0.075695	3.846525	1.14887724	1.15346266	-0.0045854
20	0.101437	2.895202	1.1870222	1.18775869	-0.0007365
21	0.147331	1.943181	1.23354615	1.24692203	-0.0133759
22	0.074386	1.935538	1.14027919	1.13637823	0.00390096
23	0.049556	2.904766	1.11305609	1.10065406	0.01240203
24	0.037186	3.86116	1.08354457	1.0837987	-0.0002541
25	0.029824	4.809079	1.06163907	1.07505573	-0.0134167
26	0.110514	1.938524	1.18777449	1.19316876	-0.0053943
27	0.073726	2.896813	1.14831791	1.1424493	0.00586861
28	0.055178	3.860092	1.11584988	1.11717551	-0.0013256
29	0.044116	4.816591	1.09029415	1.10320655	-0.0129124
30	0.216628	1.962437	1.32721788	1.33838756	-0.0111697
31	0.143297	2.913754	1.25034056	1.25156634	-0.0012258
32	0.319201	1.960084	1.45489323	1.45390384	0.00098938
33	0.146226	3.929543	1.25585522	1.2675444	-0.0116892
34	0.211858	1.936133	1.32136275	1.33214994	-0.0107872
35	0.142042	2.89165	1.24554389	1.24949499	-0.0039511
36	0.295792	1.937151	1.42112174	1.4289926	-0.0078709
37	0.14629	3.871232	1.25500626	1.26694362	-0.0119374
38	0.218881	2.890538	1.3458877	1.35336842	-0.0074807
39	0.289563	2.906855	1.44080869	1.43666486	0.00414384
40	0.21629	3.855757	1.35433085	1.36354876	-0.0092179
41	0.294144	3.864772	1.46191395	1.45684781	0.00506614
42	0.087915	4.831442	1.16999194	1.18366072	-0.0136688
43	0.001381	1.919685	1.0227442	1.00726479	0.01547942
44	0.000913	2.875965	1.01679878	1.0090076	0.00779118
45	0.0007	3.832943	1.00692513	1.01142569	-0.0045006
46	0.000587	4.78646	1.0042857	1.01425513	-0.0099694
47	0.00263	4.772237	1.00947578	1.01859232	-0.0091165
48	0.003259	3.827097	1.01301749	1.01668254	-0.003665
49	0.004386	2.872982	1.02560194	1.01587865	0.00972329
50	0.006487	1.914855	1.04216288	1.01697076	0.02519212
51	0.012685	1.931619	1.05254817	1.02867542	0.02387276

Point Number	X	Fr_g	Measured $\sqrt{\Delta P_{tp}/\Delta P_g}$	Predicted $\sqrt{\Delta P_{tp}/\Delta P_g}$	Residual
52	0.008458	2.879436	1.03702419	1.02389521	0.01312898
53	0.006352	3.828078	1.01888024	1.023019	-0.0041388
54	0.005084	4.77634	1.01452501	1.02384629	-0.0093213
55	0.031685	1.92134	1.0827784	1.0633543	0.0194241
56	0.021063	2.882949	1.06758038	1.04818486	0.01939552
57	0.015896	3.82845	1.03909647	1.04225866	-0.0031622
58	0.012637	4.782187	1.02922567	1.03978887	-0.0105632
59	0.060201	4.791748	1.12158304	1.13348362	-0.0119006
60	0.076113	3.839297	1.15146623	1.15412529	-0.0026591
61	0.10167	2.901561	1.19145221	1.18818682	0.00326538
62	0.148993	1.924649	1.24116149	1.24906001	-0.0078985
63	0.074855	1.924857	1.14536397	1.1370652	0.00829877
64	0.049833	2.880256	1.11425347	1.10099189	0.01326158
65	0.037423	3.832507	1.08596596	1.08407681	0.00188915
66	0.02995	4.78024	1.06337255	1.0751397	-0.0117672
67	0.111298	1.927818	1.19405244	1.19425851	-0.0002061
68	0.04422	4.790366	1.0925532	1.10322649	-0.0106733
69	0.074379	2.881141	1.15206378	1.14342825	0.00863553
70	0.055406	3.839697	1.11799714	1.11744349	0.00055365
71	0.071003	4.782058	1.14571892	1.15319433	-0.0074754
72	0.217658	1.92574	1.32488138	1.33919008	-0.0143087
73	0.142574	2.89322	1.24609129	1.25028785	-0.0041966
74	0.325491	1.939114	1.46038061	1.46002812	0.0003525
75	0.14768	3.858543	1.26028454	1.26885196	-0.0085674
76	0.218611	1.934095	1.3262404	1.34046707	-0.0142267
77	0.138036	2.887538	1.23847855	1.24358506	-0.0051065
78	0.291079	1.937323	1.41647258	1.42392915	-0.0074566
79	0.145975	3.866234	1.25704222	1.26641569	-0.0093735
80	0.213172	2.912751	1.33804481	1.34647046	-0.0084256
81	0.246235	2.919408	1.38542679	1.38720591	-0.0017791
82	0.186304	3.872308	1.3183739	1.32398402	-0.0056101
83	0.087268	4.812698	1.16867622	1.18234992	-0.0136737
84	0.13985	2.91158	1.24123992	1.24650892	-0.005269
				Sum of Residual Squares	0.009948696
				Standard Deviation	0.010948233

Table A7.33. The Standard Deviation Calculation for equation 6.11 at 60 Bar.

Point Number	X	Fr_g	Measured $\sqrt{\Delta P_{tp}^* / \Delta P_g^*}$	Predicted $\sqrt{\Delta P_{tp}^* / \Delta P_g^*}$	Residual
1	0.003391	1.110948	0.825854	0.819233	0.006621
2	0.003361	1.110414	0.826889	0.820066	0.006824
3	0.002226	1.662304	0.877979	0.860576	0.017402
4	0.002222	1.66024	0.877573	0.86057	0.017002
5	0.001657	2.209816	0.94745	0.91677	0.030681
6	0.001668	2.209224	0.947203	0.916579	0.030624
7	0.001318	2.766959	0.981987	0.99836	-0.01637
8	0.001312	2.771174	0.981529	0.999035	-0.01751
9	0.042757	1.111923	0.706057	0.689902	0.016155
10	0.080718	1.115651	0.760089	0.749369	0.010719
11	0.117707	1.116281	0.817362	0.814282	0.00308
12	0.161277	1.11845	0.876892	0.887886	-0.01099
13	0.159607	1.686888	0.802472	0.80674	-0.00427
14	0.119441	1.682864	0.777661	0.759265	0.018396
15	0.08298	1.681869	0.738087	0.717442	0.020646
16	0.042083	1.679221	0.687537	0.685815	0.001723
17	0.041811	2.233028	0.672405	0.679976	-0.00757
18	0.042301	2.23043	0.67164	0.679561	-0.00792
19	0.0795	2.234818	0.684155	0.67632	0.007835
20	0.11809	2.229995	0.700911	0.697749	0.003162
21	0.120157	2.229627	0.703443	0.699188	0.004256
22	0.090393	2.486343	0.668327	0.666027	0.0023
23	0.043295	2.630858	0.678031	0.683013	-0.00498
24	0.043413	2.627956	0.677182	0.682775	-0.00559
25	0.041537	1.11485	0.704255	0.688627	0.015628
26	0.119893	1.116741	0.819846	0.818062	0.001785
27	0.079532	1.678424	0.734399	0.714054	0.020346
28	0.080701	2.228615	0.68312	0.677104	0.006016
29	0.090314	2.481324	0.66671	0.66627	0.00044
30	0.052915	2.582759	0.667643	0.671416	-0.00377
31	0.033291	2.67371	0.699652	0.704253	-0.0046
32	0.017886	2.77686	0.786075	0.77565	0.010425
33	0.010237	2.889907	0.873793	0.85724	0.016553
34	0.014744	2.823828	0.825976	0.803574	0.022402
35	0.021464	2.746813	0.751879	0.752245	-0.00037
36	0.021263	1.113528	0.700197	0.682695	0.017502
37	0.014141	1.66222	0.69916	0.723291	-0.02413
38	0.010501	2.22482	0.784285	0.783517	0.000767
39	0.008402	2.766963	0.884118	0.866114	0.018004
40	0.004041	2.810026	0.958384	0.951685	0.006699
41	0.005115	2.211255	0.87178	0.850597	0.021184
42	0.006823	1.658215	0.774656	0.779511	-0.00486
43	0.010199	1.108589	0.730099	0.720517	0.009581
44	0.003561	1.091584	0.814566	0.814454	0.000112
45	0.002355	1.634149	0.866043	0.856281	0.009763
46	0.00175	2.181231	0.935086	0.912348	0.022738
47	0.001398	2.724962	0.977815	0.99159	-0.01378
48	0.004133	2.725648	0.940718	0.936729	0.003988
49	0.005172	2.177278	0.857817	0.845963	0.011855
50	0.006876	1.637638	0.759752	0.777664	-0.01791
51	0.010284	1.093676	0.730838	0.718925	0.011913

Point Number	X	Fr_g	Measured $\sqrt{\Delta P_{tp}^{*} / \Delta P_g^{*}}$	Predicted $\sqrt{\Delta P_{tp}^{*} / \Delta P_g^{*}}$	Residual
52	0.021549	1.09566	0.698372	0.681178	0.017194
53	0.014123	1.649776	0.698581	0.722857	-0.02428
54	0.010595	2.197663	0.762164	0.780339	-0.01818
55	0.008482	2.74739	0.875274	0.862506	0.012769
56	0.081939	1.104395	0.761524	0.751574	0.00995
57	0.042953	1.099401	0.706672	0.689607	0.017064
58	0.118647	1.103791	0.81879	0.816465	0.002325
59	0.162624	1.10739	0.883244	0.891004	-0.00776
60	0.160754	1.664052	0.81364	0.811682	0.001958
61	0.121499	1.654096	0.782442	0.76526	0.017181
62	0.084038	1.653844	0.740549	0.720902	0.019648
63	0.042601	1.655697	0.679299	0.686437	-0.00714
64	0.042494	2.209187	0.667808	0.679391	-0.01158
65	0.080637	2.209129	0.68457	0.678179	0.006391
66	0.121609	2.205965	0.703777	0.702524	0.001253
67	0.090145	2.475353	0.671301	0.666544	0.004757
68	0.04354	2.60372	0.667403	0.682099	-0.0147
69	0.042145	1.105829	0.703335	0.68894	0.014395
70	0.120296	1.107922	0.820144	0.819169	0.000975
71	0.07978	1.663747	0.733844	0.715452	0.018392
72	0.08012	2.224871	0.682579	0.677092	0.005487
73	0.08791	2.483068	0.669777	0.665706	0.00407
74	0.053342	2.567594	0.659926	0.67104	-0.01111
75	0.033431	2.644042	0.68647	0.702633	-0.01616
76	0.01818	2.736864	0.771115	0.770218	0.000897
77	0.010724	2.838751	0.859615	0.845098	0.014517
78	0.014883	2.78085	0.814287	0.79805	0.016236
79	0.021653	2.7129	0.738969	0.74871	-0.00974
				Sum of Residual Squares	0.014093758
				Standard Deviation	0.013442069

Table A7.34. The Standard Deviation Calculation for equation 7.3 at 20 Bar.

Point Number	X	Fr_g	Measured $\sqrt{\Delta P_{tp}^{*} / \Delta P_{g}^{*}}$	Predicted $\sqrt{\Delta P_{tp}^{*} / \Delta P_{g}^{*}}$	Residual
1	0.001651	1.53204	0.900576	0.871626	0.02895
2	0.001067	2.33662	0.980288	0.965777	0.014511
3	0.000798	3.098153	0.999718	0.998412	0.001306
4	0.000635	3.868353	1.01616	1.000502	0.015658
5	0.003177	3.871302	1.015367	1.031661	-0.01629
6	0.003932	3.101559	0.992067	0.972083	0.019984
7	0.005223	2.325588	0.910525	0.893067	0.017459
8	0.007782	1.553916	0.809399	0.79441	0.014989
9	0.015927	1.523598	0.775435	0.764312	0.011123
10	0.01029	2.340215	0.863208	0.84515	0.018058
11	0.00779	3.101604	0.96549	0.923408	0.042082
12	0.006245	3.870038	1.011279	0.993189	0.01809
13	0.038496	1.553172	0.777018	0.770388	0.00663
14	0.062236	1.556408	0.811337	0.800258	0.011079
15	0.118257	1.563712	0.890284	0.879922	0.010362
16	0.060113	3.082721	0.81662	0.813178	0.003442
17	0.061012	3.832953	0.859511	0.853952	0.005559
18	0.178276	1.567881	0.962161	0.959375	0.002786
19	0.118738	2.342851	0.837166	0.829415	0.007751
20	0.060763	2.323717	0.798814	0.787742	0.011072
21	0.036272	3.872242	0.895901	0.872926	0.022975
22	0.050486	3.877036	0.873978	0.860764	0.013214
23	0.015866	3.865771	0.962399	0.92401	0.03839
24	0.019848	3.093783	0.882708	0.85428	0.028428
25	0.026372	2.327406	0.81107	0.792335	0.018734
26	0.039588	1.557647	0.780538	0.771462	0.009076
27	0.039745	1.552288	0.78022	0.7717	0.00852
28	0.236384	1.572339	1.031568	1.028327	0.003242
29	0.117469	3.146941	0.824644	0.834774	-0.01013
30	0.177531	3.121749	0.872221	0.869213	0.003008
31	0.232038	2.358004	0.931967	0.924005	0.007961
32	0.178354	2.365462	0.882596	0.879158	0.003438
33	0.001219	1.558908	0.894988	0.884287	0.010702
34	0.000897	2.326321	0.97908	0.964004	0.015076
35	0.000672	3.098178	0.99996	0.988744	0.011216
36	0.000547	3.877425	1.016946	0.984535	0.03241
37	0.003138	3.865356	1.014819	1.031834	-0.01701
38	0.003876	3.090984	0.987614	0.972242	0.015372
39	0.005114	2.326934	0.90349	0.894685	0.008804
40	0.007577	1.559359	0.811436	0.796352	0.015084
41	0.015519	1.557739	0.782293	0.767028	0.015264
42	0.010354	2.333313	0.858983	0.844191	0.014792
43	0.007784	3.102115	0.955305	0.923498	0.031807
44	0.006214	3.880759	1.008558	0.994239	0.014319
45	0.038786	1.559056	0.775757	0.770619	0.005139
46	0.061421	1.57017	0.811356	0.798351	0.013004
47	0.1179	1.563838	0.896185	0.879404	0.016781
48	0.058606	3.111983	0.807956	0.814616	-0.00666
49	0.059796	3.869655	0.863022	0.856508	0.006514
50	0.179088	1.564201	0.983447	0.961071	0.022376
51	0.119244	2.338658	0.846166	0.829919	0.016247

Point Number	X	Fr_g	Measured $\sqrt{\Delta P_{tp}^{*}/\Delta P_{g}^{*}}$	Predicted $\sqrt{\Delta P_{tp}^{*}/\Delta P_{g}^{*}}$	Residual
52	0.06013	2.341143	0.802086	0.787757	0.014328
53	0.035992	3.893188	0.896946	0.874702	0.022243
54	0.050155	3.893664	0.876688	0.862014	0.014675
55	0.015719	3.875925	0.96044	0.925413	0.035027
56	0.019642	3.100385	0.876285	0.855398	0.020887
57	0.026276	2.321393	0.805324	0.792146	0.013177
58	0.039317	1.556308	0.778048	0.771197	0.006851
59	0.241659	1.559905	1.054286	1.037103	0.017182
60	0.114031	3.148293	0.8243	0.833059	-0.00876
61	0.177354	3.115025	0.87433	0.869025	0.005305
62	0.23068	2.352894	0.93177	0.923221	0.00855
63	0.177229	2.354364	0.887301	0.878693	0.008608
64	0.222097	3.164181	0.926252	0.8972	0.029052
65	0.125523	3.66178	0.855821	0.857088	-0.00127
66	0.094171	3.746443	0.845195	0.850442	-0.00525
67	0.19898	3.579618	0.927031	0.890678	0.036353
				Sum of Residual Squares	0.020119909
				Standard Deviation	0.017459871

Table A7.35. The Standard Deviation Calculation for equation 7.3 at 40 Bar.

Point Number	X	Fr_g	Measured $\sqrt{\Delta P_{tp}^* / \Delta P_g^*}$	Predicted $\sqrt{\Delta P_{tp}^* / \Delta P_g^*}$	Residual
1	0.001175	1.919378	0.945488713	0.924121819	0.021366894
2	0.000783	2.874031	0.995698004	0.992205412	0.003492592
3	0.000599	3.834915	1.004276484	1.003108645	0.001167839
4	0.000469	4.776308	1.015116022	0.975693697	0.039422325
5	0.002591	4.780321	1.014738597	1.050885749	-0.03614715
6	0.003224	3.824641	1.002212515	1.017405742	-0.01519323
7	0.00427	2.871379	0.984388223	0.959320671	0.025067552
8	0.006374	1.922758	0.881136834	0.873783777	0.007353058
9	0.012909	1.9235	0.858025163	0.845695751	0.012329412
10	0.008616	2.877902	0.956569541	0.918482699	0.038086842
11	0.00646	3.841738	0.99892117	0.982735613	0.016185557
12	0.005179	4.78836	1.01603667	1.028469036	-0.01243237
13	0.032199	1.920394	0.839585377	0.834720759	0.004864619
14	0.02134	2.88456	0.896534948	0.872631407	0.023903541
15	0.016042	3.849891	0.974708641	0.931255077	0.043453564
16	0.012879	4.785248	1.01123682	0.983126401	0.028110418
17	0.07315	4.805634	0.939481096	0.94808144	-0.00860034
18	0.060243	4.802053	0.942827395	0.943926088	-0.00109869
19	0.075695	3.846525	0.898452942	0.90543022	-0.00697728
20	0.101437	2.895202	0.881464822	0.890424779	-0.00895996
21	0.147331	1.943181	0.953398016	0.953563778	-0.00016576
22	0.074386	1.935538	0.880906977	0.872702305	0.008204672
23	0.049556	2.904766	0.864686279	0.860765562	0.003920717
24	0.037186	3.86116	0.915071376	0.901297566	0.01377381
25	0.029824	4.809079	0.984847166	0.950069728	0.034777438
26	0.110514	1.938524	0.916980034	0.913272723	0.003707311
27	0.073726	2.896813	0.865951313	0.871476762	-0.00552545
28	0.055178	3.860092	0.905474779	0.899441188	0.006033591
29	0.044116	4.816591	0.958072455	0.943670665	0.01440179
30	0.216628	1.962437	1.025051744	1.022366671	0.002685072
31	0.143297	2.913754	0.913196839	0.922909486	-0.00971265
32	0.319201	1.960084	1.129464612	1.114472392	0.014992219
33	0.146226	3.929543	0.9353186	0.950749051	-0.01543045
34	0.211858	1.936133	1.019952462	1.020570764	-0.0006183
35	0.142042	2.89165	0.909421963	0.921748887	-0.01232692
36	0.295792	1.937151	1.101243163	1.09767754	0.003565624
37	0.14629	3.871232	0.934706133	0.948641511	-0.01393538
38	0.218881	2.890538	0.983958714	0.981442564	0.00251615
39	0.289563	2.906855	1.062886846	1.03282137	0.030065476
40	0.21629	3.855757	1.003630152	0.995035645	0.008594508
41	0.294144	3.864772	1.085091182	1.045518907	0.039572275
42	0.087915	4.831442	0.936894551	0.955805472	-0.01891092
43	0.001381	1.919685	0.937493542	0.923893794	0.013599748
44	0.000913	2.875965	0.994211717	0.996671154	-0.00245944
45	0.0007	3.832943	1.003729217	1.013800117	-0.0100709
46	0.000587	4.78646	1.015804649	1.00090914	0.014895509
47	0.00263	4.772237	1.01540184	1.050442734	-0.03504089
48	0.003259	3.827097	1.001834723	1.017049321	-0.0152146
49	0.004386	2.872982	0.979021049	0.957938779	0.02108227
50	0.006487	1.914855	0.8770019	0.872398841	0.004603059
51	0.012685	1.931619	0.860263238	0.846673046	0.013590192

Point Number	X	Fr_g	Measured $\sqrt{\Delta P_{tp}^{*}/\Delta P_{g}^{*}}$	Predicted $\sqrt{\Delta P_{tp}^{*}/\Delta P_{g}^{*}}$	Residual
52	0.008458	2.879436	0.946192761	0.919667258	0.026525503
53	0.006352	3.828078	0.997263946	0.983123784	0.014140162
54	0.005084	4.77634	1.015565306	1.028909137	-0.01334383
55	0.031685	1.92134	0.838570931	0.834520467	0.004050464
56	0.021063	2.882949	0.892136497	0.87304484	0.019091657
57	0.015896	3.82845	0.97089311	0.930730186	0.040162925
58	0.012637	4.782187	1.009331212	0.98395369	0.025377522
59	0.060201	4.791748	0.945430358	0.94342606	0.002004298
60	0.076113	3.839297	0.904172295	0.9053132	-0.0011409
61	0.10167	2.901561	0.882632668	0.890702833	-0.00807016
62	0.148993	1.924649	0.969594933	0.95692321	0.012671723
63	0.074855	1.924857	0.882917946	0.873651081	0.009266865
64	0.049833	2.880256	0.86418361	0.860042416	0.004141194
65	0.037423	3.832507	0.910400834	0.899881879	0.010518955
66	0.02995	4.78024	0.979765978	0.948642855	0.031123122
67	0.111298	1.927818	0.926977454	0.91485328	0.012124174
68	0.04422	4.790366	0.955684542	0.942422664	0.013261878
69	0.074379	2.881141	0.868729879	0.871501872	-0.00277199
70	0.055406	3.839697	0.90570131	0.898579404	0.007121905
71	0.071003	4.782058	0.944289453	0.946159848	-0.0018704
72	0.217658	1.92574	1.039802402	1.027393631	0.01240877
73	0.142574	2.89322	0.915295132	0.922179813	-0.00688468
74	0.325491	1.939114	1.13750065	1.122610948	0.014889702
75	0.14768	3.858543	0.942411291	0.94910831	-0.00669702
76	0.218611	1.934095	1.039068765	1.027376252	0.011692514
77	0.138036	2.887538	0.908098117	0.918561056	-0.01046294
78	0.291079	1.937323	1.102690849	1.093560607	0.009130242
79	0.145975	3.866234	0.938234961	0.948249879	-0.01001492
80	0.213172	2.912751	0.98346992	0.977032323	0.006437597
81	0.246235	2.919408	1.023490964	1.001614234	0.02187673
82	0.186304	3.872308	0.97894181	0.975535697	0.003406113
83	0.087268	4.812698	0.948683868	0.954593704	-0.00590984
84	0.13985	2.91158	0.917428184	0.920189927	-0.00276174
				Sum of Residual Squares	0.024955896
				Standard Deviation	0.017339938

Table A7.36. The Standard Deviation Calculation for equation 7.3 at 60 Bar.

Table A7.37 summaries the Standard Deviations of equations 6.11 and 7.3 at 20 Bar, 40 Bar and 60 Bar.

	20 Bar	40 Bar	60 Bar
Equation 6.11	0.0212	0.0168	0.0109
Equation 7.3	0.0134	0.0175	0.0173

Table A7.37 Summary of Standard Deviation Results.

It can be seen from Table A7.37 that the Standard Deviation of the equations 6.11 and 7.3 are small indicating that the equations fit the data points well in most cases. However, no method could be found in the literature that would calculate the percentage expanded uncertainty of these equations prediction of the gas mass flow. Nevertheless, when considering the uncertainty in these equations two facts should be noted. Firstly, equations 6.11 and 7.3 are offered here specifically for the popular 6" Venturi Meter with a beta ratio of 0.55, while the other existing correlations were formed with data from different sized meters. Secondly, the equations were created from the data obtained from the UKAS accredited NEL Wet Gas Loop and as such the data set is likely to be at least as accurate as any in existence. Hence, the author is confident that when applied to a 6" Venturi Meter with a beta ratio of 0.55 metering a wet gas flow these equations will be more accurate than any that existed previous to this research.